# Saltmarsh restoration and blue carbon dynamics in a Scottish estuary

Benjamin Taylor

A thesis submitted for the degree of PhD
at the
University of St Andrews

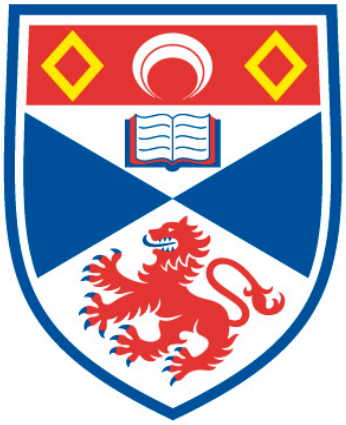

2019



Identifier to use to cite or link to this thesis:

DOI: https://doi.org/10.17630/10023-20891

# Declaration

## Candidate's declaration

I, Benjamin Taylor, do hereby certify that this thesis, submitted for the degree of PhD, which is approximately 53,000 words in length, has been written by me, and that it is the record of work carried out by me, or principally by myself in collaboration with others as acknowledged, and that it has not been submitted in any previous application for any degree.

I was admitted as a research student at the University of St Andrews in September 2014.

I received funding from an organisation or institution and have acknowledged the funder(s) in the full text of my thesis.

Date 22/08/2019 Signature of candidate

## Supervisor's declaration

I hereby certify that the candidate has fulfilled the conditions of the Resolution and Regulations appropriate for the degree of PhD in the University of St Andrews and that the candidate is qualified to submit this thesis in application for that degree.

Date 22/08/2019 Signature of supervisor

## Permission for publication

In submitting this thesis to the University of St Andrews we understand that we are giving permission for it to be made available for use in accordance with the regulations of the University Library for the time being in force, subject to any copyright vested in the work not being affected thereby. We also understand, unless exempt by an award of an embargo as requested below, that the title and the abstract will be published, and that a copy of the work may be made and supplied to any bona fide library or research worker, that this thesis will be electronically accessible for personal or research use

and that the library has the right to migrate this thesis into new electronic forms as required to ensure continued access to the thesis.

I, Benjamin Taylor, confirm that my thesis does not contain any third-party material that requires copyright clearance.

The following is an agreed request by candidate and supervisor regarding the publication of this thesis:

**Printed copy**

No embargo on print copy.

**Electronic copy**

Embargo on all of electronic copy for a period of 1 year on the following ground(s):

- Publication would preclude future publication

**Supporting statement for electronic embargo request**

Various research outputs and data contained within the thesis are related to future publications.

**Title and Abstract**

- I agree to the title and abstract being published.

Date 22/08/2019 Signature of candidate

Date 22/08/2019 Signature of supervisor

**Underpinning Research Data or Digital Outputs**

**Candidate's declaration**

I, Benjamin Taylor, understand that by declaring that I have original research data or digital outputs, I should make every effort in meeting the University's and research funders' requirements on the deposit and sharing of research data or research digital outputs.

Date 22/08/2019 Signature of candidate

**Permission for publication of underpinning research data or digital outputs**

We understand that for any original research data or digital outputs which are deposited, we are giving permission for them to be made available for use in accordance with the requirements of the University and research funders, for the time being in force.

We also understand that the title and the description will be published, and that the underpinning research data or digital outputs will be electronically accessible for use in accordance with the license specified at the point of deposit, unless exempt by award of an embargo as requested below.

The following is an agreed request by candidate and supervisor regarding the publication of underpinning research data or digital outputs:

Embargo on all of electronic files for a period of 1 year on the following ground(s):

- Publication would preclude future publication

**Supporting statement for embargo request**

Various data which have been used towards the completion of this thesis may inform on future planned publications.

Date 22/08/2019 Signature of candidate

Date 22/08/2019 Signature of supervisor

# Acknowledgments

Firstly, my thanks go to Prof. David Paterson, my primary Supervisor. Thank you for the initial opportunity to take on the PhD and then for the following 4 years of unending support. I am grateful for all your input throughout my research and appreciate your allowing me to take ownership of the project, knowing your office was only a couple of doors away when I needed clarification or extra guidance. A special thank you for the rapid feedback and advice towards the completion of the thesis, without which it is unlikely it would have been completed on time.

A huge thank you goes to the Irv Davidson and Jack Maunder without whom the collection of all the field data would have been far less enjoyable and, likely not even achievable. Thanks also for all the input and design support relating to how best to carry out the field campaigns, your experience and knowledge were invaluable.

Thanks also goes to Dr Clare Maynard for her past and continuing efforts to restore the saltmarshes of the Eden Estuary, on which this study is based. Thanks also to Clare to the countless valuable pieces of information and insight she provided on every aspect of saltmarsh restoration and the Eden Estuary in general.

Thank you to SNH and Fife Coast and Countryside Trust for their helpful input and permissions to carry out the research. To the MoD (RAF and Army) and to the Links Trust golf course for facilitating this research by permitting access to the field sites through their land on the north and south shores of the Estuary.

To SERG, thank you for endless tea breaks, probably far too many biscuits and for amusing my occasional ‘big’ questions, these distractions definitely added to my PhD experience. Thanks to all past and present PhD students, for being in the same boat and providing useful and enlightening discussions on a whole variety of topics.

Thank you to friends old and new for providing distractions from PhD life, from drinking companions to climbing partners to house mates to cycling buddies; some of you feature in more than one group and all helped keep a good balance between work and life.

Thank you to my family for the continued support throughout the PhD, and the rest of my life, which has enabled me to reach this point. Thank you for opportunities you have given me, from exploring rock pools in Cornwall on family holidays to travelling around Madagascar’s natural parks; all of these have driven my love for the natural world and led to the PhD in the first place.

Finally, thank you to Tam for putting up with me moving away to Scotland and the inevitably colder conditions it comes with when visiting. Thanks for the holidays and distractions, which were well needed breaks during the project. I promise I will have more free time now.

## Funding

The work was primarily supported 50/50 by two organisations, the first was MASTS (The Marine Alliance for Science and Technology for Scotland) pooling initiative; MASTS is funded by the Scottish Funding Council (grant reference HR09011) and contributing institutions. The other was Scottish Natural Heritage (SNH).

Funding was also received from British Society for Geomorphology towards the completion of sediment carbon stock research. Support was received in kind from the NERC Geophysical Equipment Facility with the loan of remote sensing equipment (reference: 1044).

## Research Data/Digital Outputs access statement

Research data underpinning this thesis are available at [DOI]

OR

Digital outputs underpinning this thesis are available at [DOI]

# Contents

# Abstract

Saltmarshes are biogeomorphic intertidal systems of halophytic plant communities, typically found on low-energy temperate coasts. These provide valuable ecosystem services, such as biodiversity provision, coastal protection and climate change mitigation. They are sites of extensive carbon sequestration and storage, termed *Blue Carbon*, largely attributed to their deep organic rich sediments which continue to build with marsh development. Saltmarshes are amongst the most threatened ecosystems globally, estimated to have lost over 25 % since 1800s. Their past and future losses require action to be taken to conserve and restore this valuable ecosystem.

Restoration can be achieved through direct-transplantation of existing vegetation onto potential saltmarsh habitat within an estuary. This approach has been carried out on the Eden Estuary, Scotland since the start of the millennium. Restoration aimed to enhance the degraded saltmarsh of the estuary. These areas are likely to increase carbon sequestration and storage capacity of the ecosystem; this capacity was investigated during this study.

The *Blue carbon* benefit afforded by restored saltmarsh areas was compared to the 'business as usual' mudflat and the possible end point state of a 'natural' saltmarsh extent. The study assessed the influence of vegetation structure, sediment dynamics and buried sediments on the area's carbon sink.

Restoration activities have increased the current total amount of carbon stored in sediment and vegetation by over 0.5 t, and furthermore, contain the largest sedimentary carbon store per unit area, of 23.48 kgC $m^2$. Areas of restoration exhibited, on average, higher rates of carbon burial than found on mudflats, being 14 gC $m^2$ $yr^{-1}$. At present their relatively small extent limits their added value to both store significant quantities of carbon and provide a monetary self-subsidisation. In the future it is likely their value will increase as a function of their increased spatial extent and temporal development.

# Chapter 1: Saltmarshes, carbon storage and restoration

This thesis assesses the influence of saltmarsh restoration in the Eden Estuary, Scotland, on the area's carbon sequestration and storage capability. Informing on the potential for 'self-subsidisation' of conservation through *Blue carbon* payments for their possibly increased natural capital value.

## 1.1 Unsettled systems: Saltmarshes

Saltmarsh systems can be broadly described as a group of halophytic higher plants (Burd, 1989) which are found high in the intertidal frame of, typically, low energy coasts (such as estuaries), growing on and supported by muddy sediments (Allen and Pye, 1992; Burd, 1989).

These areas are distributed along temperate coasts, being located in at least 99 countries, with extent estimates ranging broadly from 400,000 $km^2$ (Duarte et al., 2005) to 55, 000 $km^2$ (Mcowen et al., 2017) up to high estimates of 40,000,000 $km^2$ (Pendleton et al., 2012). Within Europe their presence is widely distributed, with examples found in most countries with a coastline. The United Kingdom features saltmarshes along many stretches of its coast (Figure 1.1), being most abundant in England, with approximately 40 different plant species represented and usually 10 – 20 featured on any specific marsh (Boorman, 2003). Saltmarshes feature along 3 % of Scotland's coast and are estimated to cover 67 $km^2$ (Burrows et al., 2014; Haynes, 2016) (Figure 1.2), far less than that estimated to be found along the coast of England, at 325 $km^2$ (Boorman, 2003).

These are 'biogeomorphic' environments (Baptist et al., 2016; Thorne et al., 2014), their biological components (i.e. vegetative structures, stem density)(Van Proosdij et al., 2006) modify the physical environment (Kirwan and Mudd, 2012), affecting properties such as sediment deposition and erosion thresholds. These biological factors contribute to the maintenance and succession of saltmarshes (Pethick, 1992). Van Proosdij et al. (2006) surmised that "sediment deposition is hypothesized to be a complex function of variables controlling the availability of sediment and those controlling the opportunity for this sediment to be deposited".


*Figure 1.1: Distribution map of saltmarshes within the UK, taken from Boorman (2003), after Burd (1992).*

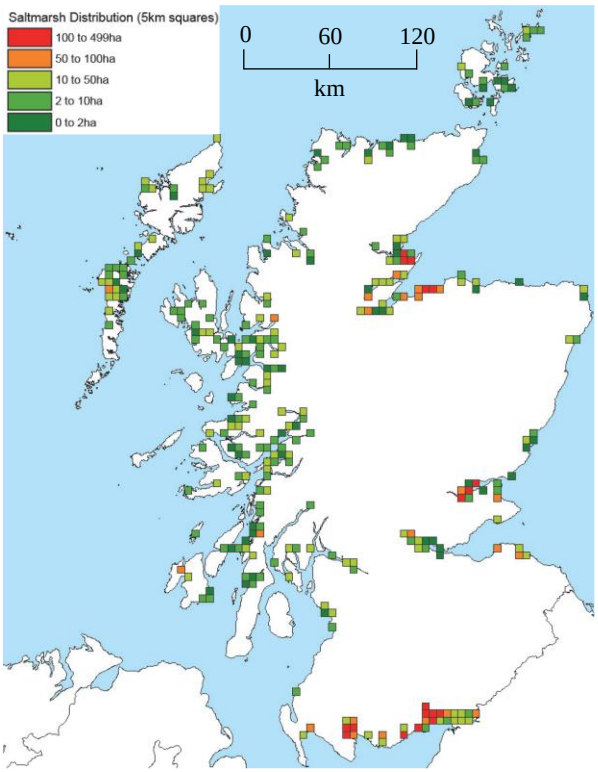


*Figure 1.2: Distribution map of saltmarshes in Scotland defined by their extents along the coast. After T. Haynes (2017).*

Saltmarshes exist as part of the dynamic intertidal environment meaning there is significant interaction between their vegetated area and other areas in the tidal frame. For example, mudflats (Figure 1.3) and marshes exchange material (Pethick, 1992) both acting intermittently as sources and sinks of material. Further inputs and exchange are likely to occur from sources out-with their immediate vicinity, coming from alluvial processes and fluxes between the marine environment and the coast (Dame et al., 1991). Perhaps the most influential interaction is that of sediment and factors that alter this dynamics, such as the presence of vegetation, typically leads to an increased consolidation of material (Boorman et al., 1998) which becomes incorporated into a long-term store. Though generally retained, this may be released by higher-magnitude events (Pethick, 1992) or due to chronic degradation/pressure. The development and long-term persistence of saltmarshes within the dynamic intertidal frame is generally reliant upon enhanced deposition/retention and stabilisation of sediment (Adam, 2002) which allow vertical accretion to take place (Boorman, 1999). However, the development of a saltmarsh is tied to sediment supply and therefore to tidal influence. If supply is good and accretion takes place, the marsh rises in the tidal frame and if supply is poor it may erode, thus changing the prevailing environmental dynamics such as tidal inundation frequency and sediment accretion (J. S.

Pethick, 1981). This constant exchange leads to saltmarshes being in a near constant state of flux, with the varying forces of inundation, deposition, erosion, stabilisation etc always progressing towards an equilibrium state and never quite reaching it.

### *1.1.1 Saltmarsh development process*

The presence of vegetation in intertidal areas, such as saltmarshes, is part of a succession and each stage owes their success to the initial pioneers which were able to establish in this dynamic environment.

Due to the strong influence of successional processes and the effective vertical range on which tidal influence is exerted there is a tendency for saltmarshes to exhibit a strongly spatial arrangements (Figure 1.3). Typically there is a parallel zonation to the coast of vegetation (Gray, 1992); with distinct separation of species and communities along the tidal gradient.

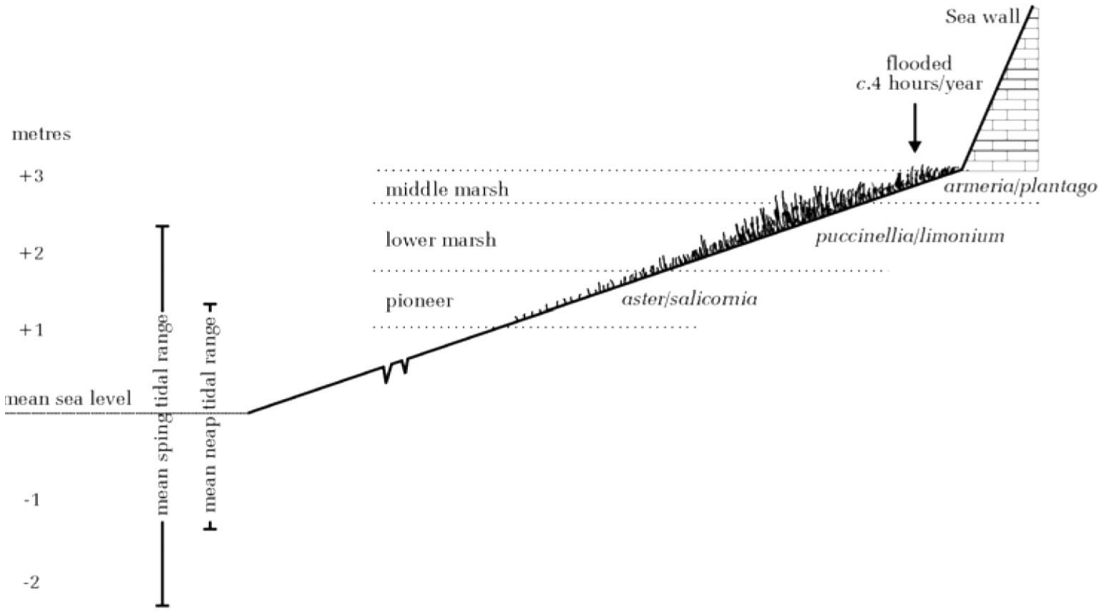


*Figure 1.3: Typical saltmarsh vegetation zonation and its relation to its location within the tidal frame. Taken from Boorman (2003).*

Initially bare mudflat environments are colonised by pioneer species when site and situation allow. This requires the environmental and ecological conditions to be tolerable to a given vegetation type. This condition can be met through a balance of physical processes, or assisted through the action of organisms such as biofilm producing diatoms or filamentous algal growth (Boorman, 2003). Furthermore, these conditions need to be coupled with a vegetation source, such that there is sufficient supply of vegetative material (e.g. seeds) to allow transport to a given area; thus allowing it to settle, grow and persist. Boorman (2003)

postulated that there are four elements necessary for saltmarsh development, these being; stable sediment which is covered by the tide less than it is not, a suitable sediment supply, water velocities which allow settlement of sediment (Davy, 2000) and a supply of seeds or propagules to provide establishment of vegetation.

The vertical zonation within a saltmarsh is assumed, for each vegetation type/species, to broadly be governed by tolerance of tidal influence at lower limits and restrained by interspecific competition at upper limits (Gray, 1992).

Pioneer vegetation is typically associated with being lower in the tidal frame than are other 'zones' of vegetation (Figure 1.3). Thus, pioneer species are characterised by being tolerant/requiring frequent inundation and likely higher salinity than other vegetation types. These species will occupy the full range of their functional niche in the absence of other vegetation, which they eventually come into competition with (Gray, 1992). The lower limit of pioneer species usually occurs at the mean neap high tide line (Burd, 1989), where they are covered by most tides (Boorman, 2003). For establishment it is considered a requirement that there are periods in which germinating seedlings will be free from tidal influence over a number of consecutive days (Ranwell, 1972). Pioneer species found in the UK would be considered as examples such as *Spartina* spp. and *Salicornia* spp. (Boorman, 2003; Gray, 1992); in the Eden Estuary *Bolboschoenus maritimus* is considered to fill the effective pioneer species niche.

The establishment of vegetation leads to a shift in the hydrodynamics due to increased surface roughness and so encourages the retention and deposition of sediments (Boorman et al., 1998; J.Court Stevenson et al., 1988). The cover of vegetation also acts to consolidate those deposited sediments and reduce resuspension/erosion (Allen and Pye, 1992); so leading to the vertical accretion of sediment (Boorman et al., 1998). The vegetation may also promote/protect microbial growth on the sediment further enhancing stability.

As sediments accumulate and raise sections within the tidal frame, the influence of inundation is altered and so provides an environment in which species which are less tolerant to tidal processes can colonise (Boorman, 2003). Thus, the diversity of the saltmarsh increases, as the environment becomes less harsh. This increased diversity leads to interspecies competition, serving to restrict the fundamental niche space of each species, down to a realised niche space (Gray, 1992). The specific locality in the tidal frame of the each marsh type means it is exposed to different dynamics (Childers et al., 2000), such as altered sediment regimes as aligned to tidal inundation. For example, establishing immature

pioneer marshes experience increased sedimentation (Maynard et al., 2011), due to the longer inundation periods being located lower in the tidal frame (Kirwan et al., 2010; van Wijnen and Bakker, 2001) as compared to those 'developed' mid to high marsh areas. This successional process continues to occur, where eventually an area reaches a relatively stable condition in which all available niche space is occupied under the prevailing environmental conditions.

The continued development of the marsh leads to an increased accumulation of organic matter both in the form of above ground biomass (AGB) and below ground biomass (BGB), with BGB productivity suggested to be four times that of AGB (Boorman, 2003). The developing system also experiences vertical loss through subsidence, or compaction, of surface sediment (Cahoon et al., 1995; van Wijnen and Bakker, 2001). The degree of subsidence is a product of a number of factors, including the organic matter content, bulk density through the sediment (Cahoon et al. 1995), the annual drying period, and depth of 'clay' soil. Developed marsh areas experience more compaction than do new marsh with relatively thin surface sediment layers (van Wijnen and Bakker, 2001). Another important process within the ecosystem are rates of decomposition which change along the salinity gradient (Craft, 2007; Weston et al., 2006) and with sediment depth (Mudd et al., 2009).

These factors – accretion, sedimentation, decomposition and compaction – are integrated in the net rate of relative vertical elevation change and reflect the persistence of the ecosystem (Chmura, 2013). The resultant balance between abiotic and biotic factors produce areas in which a given species or community exists and typically ensures the maintenance of the marsh surface in equilibrium with changing sea-levels (Crooks et al., 2014), and so optimally placed within the tidal frame (Mudd et al., 2009). The balance of these factors act to influence the development towards a mature saltmarsh state, which typically takes between 80 and 100 years (Boorman, 2003).

## 1.2 Saltmarsh benefits and services

Ecosystem services are broadly categorised into provisioning, regulating, cultural and supporting (Reid et al., 2005). Tidal wetlands offer a variety of valuable ecosystem service of benefit to the natural world and society (Christie et al., 2014; Jones et al., 2011), being amongst the highest value ecosystems on earth (Costanza et al., 1997). Ecosystem services afforded by saltmarshes include the protection of coasts, water purification, maintenance of fisheries, recreational use (Barbier et al., 2013), for grazing livestock (Davidson et al.,

2017) and biodiversity provision. These services are delivered through a variety of functions, for example their coastal protection capacity (I. Möller et al., 2001; Morgan et al., 2009; Shepard et al., 2011) mitigat wave impact and flooding due to flow attenuation that occurs as water travels over the relatively rough surface of the marsh (Boorman, 2003; Morgan et al., 2009); this reduces the size requirement (and so the cost) of 'hard' sea defences significantly (Boorman, 1999; King and Lester, 1995).

## 1.3 Carbon storage in wetlands

Intertidal vegetated ecosystems, such as saltmarshes (Table 1.1), mangroves and seagrasses, have been recognised for their carbon sequestration potential (Beaumont et al., 2014; Burden et al., 2013; Burrows et al., 2014; Chmura et al., 2003; Craft et al., 2003; Howard et al., 2017; Kirwan and Mudd, 2012; McLeod et al., 2011; Rogers et al., 2018; Van de Broek et al., 2018), often termed *Blue carbon* (Grimsditch et al., 2013; Herr et al., 2012). In Scotland it is estimated that intertidal saltmarshes have an average sequestration potential of 14,200 tC/yr (Burrows et al., 2014).

These systems hold increased benefit over other vegetated carbon sinks, such as tropical rain forests or peat lands, as their sediments do not become saturated with carbon, due to their vertical accretion (McLeod et al., 2011). Furthermore, the rates of carbon burial are greater at intertidal vegetated areas than terrestrial systems which, on average, range from 4 to 5.1 gC $m^{-2}$ $yr^{-1}$ across forest types (McLeod et al., 2011), lower than all estimates for saltmarsh areas (Table 1.1).

*Table 1.1: Example carbon sequestration rates and storage within saltmarshes recorded in the literature*

| **Carbon burial rate (gC $m^{-2}$ $yr^{-1}$)** | **Global carbon burial rate (TgC $yr^{-1}$)** | **Estimated global stock** | *Source* |
|---|---|---|---|
| 18 – 1713 | 4.8 ± 0.5<br>87.2 ± 9.6 | | *(McLeod et al., 2011)* |
| | | 570 – 10,360 MgC | *(Howard et al., 2017)* |
| 151.0 | 60.4 | | *(Duarte et al., 2005)* |
| 210 ± 20 | 42.6 ± 4.0 | 430 ± 30 TgC | *(Chmura et al., 2003)* |

However, it is also possible they are net sources of carbon to the atmosphere, with air-water carbon fluxes over areas occupied by saltmarshes presenting a net emission of carbon (Borges, 2005). It has been shown that there is much reduced $CH_4$ (methane) production in saltmarsh areas (Chmura et al., 2003), compared with their terrestrial counterparts peat-bogs, due to increased salinity (Bartlett et al., 1987). The lower methanogenesis values offers increased climate change mitigation benefit as methane has a 25 times higher warming potential than carbon dioxide (Crooks et al., 2014).

Generally it can be assumed that within coastal ecosystem there are broadly four carbon pools; AGB, BGB, non-living biomass and sedimentary stores (McLeod et al., 2011), each of which are influenced by different factors. AGB and BGB store carbon on a short timescale (Duarte et al., 2005). The primary drivers of carbon sequestration are not clear; for example, Chmura et al. (2003), suggests sediment supply contributes most to carbon sequestration, Jones et al. (2013) found it to be productivity and Dame et al. (1991) proposes tidal flow to be most influential. However, carbon stored within sediments which are deposited and buried within these areas is perhaps the most important and facilitates their long-term large storage capacity (Crooks et al., 2014; Duarte et al., 2005; McLeod et al., 2011). This capacity is a predominantly due to the presence of waterlogged anaerobic conditions which reduce decomposition (Chmura et al., 2003), continued accretion of these sediments and organic matter (Duarte et al., 2005; Howard et al., 2017; McLeod et al., 2011) and high bulk density values (Chmura et al., 2003; Chmura, 2013). The prolific carbon storage capacity of sediments is suggested to account for approximately 50 % of total oceanic sedimentary carbon, despite only covering 2 % of the total area (Duarte et al., 2005). Being located within dynamic transitional zones of estuaries, saltmarshes gain both autochthonous and allochthonous carbon (Dame et al., 1991), resulting in the potential to mitigate carbon emissions from a range of sources, thus "represent a C [carbon] sink for a larger area" (McLeod et al., 2011, p. 3). The rates of flux (e.g. sediment dynamics) within the system are important when evaluating carbon sequestration potential as they signify the rate at which carbon can accumulate within the ecosystem. These rates vary significantly between and within area type, being a product of the dynamic situation of intertidal vegetated areas (Christiansen et al., 2000).

The total capacity of saltmarshes to sequester and store carbon varies widely, with suggested ranges of between 5 and 87 TgC $yr^{-1}$ (McLeod et al., 2011). These differences have many drivers, however, the carbon content of sediments will play a significant role. These values vary broadly, with reported carbon content ranges of in a single estuary

between 0.51 % and 45.78 % (Crooks et al., 2014); a near 100 fold difference. These values are combined with sediment bulk density to produce a carbon density value which indicates the actual amount of carbon within a given quantity of sediment (Burden et al., 2013). These two factors play an important role in the resulting carbon storage of different areas, as different elevation (Bouma et al., 2016), vegetation, tidal regime etc alter both of these variables; for example Chmura et al. (2003) found that highest carbon density occurred at high elevations and Crooks et al. (2014) found high elevations to have low density.

### *1.3.1 Value of blue carbon*

The foundation of all Payment for Ecosystem Service (PES) schemes is to integrate 'unpriced' ecosystem services into economic markets by assigning a 'tradable value' to these services (Hanley et al., 2013). This is not a trivial task and requires correct valuation to ensure created markets function effectively (Hanley et al., 2013); either as an incentive to maintain existing areas (avoided emissions) or to restore areas (sequester carbon). As an example, Pendleton et al. (2012) suggests that, globally, coastal wetlands annually release between 0.15 and 1.02 $PgCO_2\ yr^{-1}$ due to land-use change; with an estimated cost of between 6.1 and 42 Billion US$ $yr^{-1}$, based on the *Social Cost of Carbon*, which refers to the environmental damages that could be avoided by reducing emissions. If used correctly economic markets are a powerful tool which can be used to work for the environment (Hanley et al., 2013).

There are various methodologies which outline how *Blue carbon* can be used and integrated into a PES style systems, such as *Verified Carbon Standard*'s 'Methodology for Coastal Wetland Creation, v1.0' (VCS 2014) or *The Blue Carbon Initiative*'s 'Coastal Blue Carbon' manual (Howard et al., 2014). Information and data on 'additionality' are important for such PES schemes to illustrate the change (increase) in carbon sequestration and storage of an area due to undertaken activities (Murray and Vegh, 2012). As such it is crucial schemes are measurable, reportable and verifiable (Murray and Vegh, 2012), in order to deliver robust total carbon values with minimal ambiguity. These requirements influence the sampling necessary to ensure data are reliable, for example, information on aspects of current sediment dynamics, sedimentary carbon store (Saintilan et al., 2013) and vegetation stocks are required to accurate estimate the ecosystem's total value (Chmura, 2013).

At present, the most widely available option for taking *Blue carbon* to markets is through various voluntary schemes which have developed, however these are generally smaller and lower in price than regulated markets would be (Ullman et al., 2013). Existing prices of

carbon dioxide equivalents ($CO_2e$) are on average 3 times lower in voluntary markets than they are in regulated settings, being 6 US$ per tonne and 18.52 US$ per tonne, respectively (Peters-Stanley et al., 2011; Ullman et al., 2013). Presently regulated markets and policy frameworks are under-developed, key questions which need urgent evaluation include; quantifying the rate of natural carbon sequestration, quantifying the stocks of carbon, understanding the natural variation in these values, and the agents of change (Ullman et al., 2013). These questions are subjects of emerging academic and social interest to facilitate an increased adoption of carbon payment type schemes which successfully access these funds and applies them effectively to provide climate change mitigation benefits and ecosystem enhancement.

## 1.4 Threats and losses of Saltmarsh

Coastal ecosystems are some of the most threatened in the world (Murray et al., 2010) but experiencing greater degrees of long-term loss (Davidson, 2014; Saintilan et al., 2014) than are found in other terrestrial systems, such as tropical forests (Pendleton et al., 2012). Estimates for historical saltmarsh losses in particular range from a 25 % reduction since the 1800s (McLeod et al., 2011) to annual loss of 1 to 2 % from 1980-2000 (Murray et al., 2010).

Losses of these ecosystems have various drivers, both natural and anthropogenic. A major predicted driver of loss in the future is climate change, and the associated alterations it will bring to the environment; such as changes in productivity, decomposition and a changing sea level (Craft et al., 2009; Jones et al., 2013; Kirwan and Blum, 2011; Kirwan et al., 2016, 2010; Mudd et al., 2009; van Wijnen and Bakker, 2001). As discussed, tidal processes play a key role in determining saltmarsh development and structure, and their survival generally relies on the maintenance of their place in the tidal frame. Previously saltmarsh areas have accreted vertically at sufficient pace to have kept pace with historic sea level rises (Crooks et al., 2014). In the UK rate of saltmarshes sediment accretion has been found to be equal to, or greater than, the current rate of sea level rise (Cahoon et al., 2000). However, the maintenance of this equilibrium may be lost under predicted increased climate change related relative sea level rise (RSLR) (Craft et al., 2009; Kirwan and Blum, 2011; van Wijnen and Bakker, 2001). If rates of RSLR increase sufficiently it could lead to significant losses of global coastal wetland within the century (Craft et al., 2009; Crooks et al., 2014; Pendleton et al., 2012); Kirwan et al. 2010 concluded there will be a 20 – 80 % loss dependent upon RSLR and specific marsh situation. Saltmarshes areas which currently sit

within or along macro and meso tidal coasts are likely to be the most resilient to RSLR (Craft et al., 2009), placing the UK in relatively 'strong' position for the future; due to its prevalence of such tidal ranges (Allen and Pye, 1992). Scottish coastlines have previously been characterised by falling RSLR due to the process of glacio-isostatic uplift, however this trend has recently altered to indicate RSLR is now increasing (Teasdale et al., 2011). The increasingly engineered coastal environment due to anthropogenic activity also lead to losses of saltmarshes, adding to the cumulative impacts of changes to natural processes (Pendleton et al., 2012). These could be 'direct' impacts from converted land-use or 'in-direct' as a result of coastal squeeze arising from RSLR and developed land behind coastal systems preventing natural retreat of the saltmarsh system (Burden et al., 2013; Doody, 2004).

These losses lead to a reduction in the valuable services they provide; such as reduced carbon sequestration and increased emissions during degradation (Pendleton et al., 2012); thus reducing their climate change mitigation potential. Such trends could serve to undermine the application of payments for ecosystem service approaches in regards to their carbon storage capacity as it brings into question the 'permanence' of sequestered carbon (Chmura et al., 2003). Climate change will affect many of the factors which driver carbon sequestration and storage in saltmarshes. These changes could lead to an increased rate of sequestration due to enhanced productivity (Kirwan and Mudd, 2012), however this rate may be negated by increased decomposition, of up to 19 % per 1°C, thus, removing (or reducing) carbon storage in these areas (Kirwan and Blum, 2011; Kirwan and Mudd, 2012).

## 1.5 Saltmarsh restoration approaches

Generally, the aim of restoration is to create or enhance the ecologically functionality of an area to replicate and contribute to the natural system, and help restore the ecological health of an ecosystem under recognised threat (Duarte et al., 2005). The restoration or creation of new saltmarshes are not only important for the conservation of species, but also the maintenance of the valuable ecosystem servcies which they deliver (Boorman, 2003). The continued development of restoration strategies to achieve a diverse range of efficient and economical approaches is crucial. The requirment to conserve such threatened areas will become increasingly important as future pressures add further risk to their loss. There is also direction from governments in the form of a '25 Year Plan for the Environment' to

strive to improve our natural environment and leave it “in a better state than we found it”, thus conserving ecosystems and enhancing natural capital (HM Government, 2018).

### *1.5.1 Managed realignment*

The restoration of saltmarshes has historically been approached through managed realignment. This is the practice of allowing land, which had possibly been previous drained and ‘claimed’ from the intertidal zone, to return to an intertidal environment. The intentional flooding of such coastal areas comes with associated conflicts (i.e. social) and risks (i.e. failure); such as the loss of productive (valuable) agricultural land and the risk of failure due to altered soil properties (e.g. compaction).

Various schemes and approaches have been used to enable this approach, including managed tidal regimes (Maris et al., 2007; Masselink et al., 2017), channel network design (Zeff, 1999) and sediment subsidisation (Schrift et al., 2008). The success of realignment projects is likely to be influenced by many factors, all of which require consideration prior to commencement. However, successful realignment has been shown to quickly result in the growth of new saltmarsh area which begin to mirror their natural counterparts (Garbutt and Wolters, 2008).

In the UK there are various examples of managed realignment which have shown varying degrees of success. On the south coast of England, at Medmerry, old sea defences were breached creating a large lagoon/saltmarsh area, with new defences constructed around the realignment (Lewis, 2013). This area has experienced a rapid evolution of sedimentary processes, that have led to significant accretion, however it highlighted discrepancies in this development across the site, illustrating the need for design considerations when implementing such schemes (Dale et al., 2017). Another example can be found at Skinflats, on the banks of the Firth of Forth, at which a more involved scheme has been applied, with the application of regulated tidal regimes and the addition of shingle material to optimise the resulting 10 hectares of intertidal habitat which has been created (IFLI, 2018). These examples, both aimed to create relatively large areas of new intertidal habitat, incurred costs in loss of land and capital costs for the heavy engineering required to complete the project, such as the construction of new defences and the breaching of existing defences.

### *1.5.2 Direct-transplantation*

The restoration approach which has been employed on the Eden Estuary, and studied here, was achieved through the direct transplanting of a local species (as desribed in Sullivan, 2001), in this case *B. maritimus*. Such restoration is designed to encourage the spread of

new swards and confer protection and repair to existing marshes. This restoration is still being carried out (2018-19) on the Eden Estuary (East coast of Scotland) and has been taking place since the start of the millennium (Maynard, 2014). *B. maritimus* plants were harvested from donor stands within the estuary and transplanted onto selected restoration sites (see Maynard, 2014 for details). It was found that the transplantation of this species was best suited to restoration activities on the Eden Estuary, giving better returns than other vegetation types (Maynard, 2014).

Direct transplantation activity has benefit that it removes (or reduces) likely conflicts and costs that occur in managed realignment as it takes place on existing intertidal areas (mudflats) which, typically, stakeholder groups will have lower vested interests and potential conflicts. However, these projects are generally more labour intensive, with direct human action required during all stages, from obtaining vegetation material to planting it. The relatively high effort cost along with the typically limited available space means that restoration through transplantation are usually completed on a smaller scale than managed realignment projects. It is important to optimise transplantation approaches, to deliver successful restoration and also maximise the area which can be restored with a given amount of vegetation, for example; employing the most efficient planting densities to deliver natural system functionality (Broome et al., 1986), or planting during 'windows of opportunity' which provide optimal conditions for vegetation survival (Hu et al., 2015). Restoration through transplantation requires careful site selection, to provide both the highest chance of success and deliver desired services or benefits, such as enhanced protection to existing marsh extents (Maynard, 2014). Site selection will largely determine the success of a restoration project, requiring continual new information to best inform on this. On the Eden Estuary, restoration success has ranged from areas rapidly reaching equivalent growth to natural areas, to vegetation failing to grow. Such issues are important to consider when estimating possible future ecosystem service delivery and evaluating altered natural capital values for restored areas.

## 1.6 Research aim

The current research focussed on improving our understanding of the impacts of saltmarsh restoration, through direct-transplantation, on carbon sequestration and storage potential within the Eden Estuary. This was achieved through directed studies on vegetation components, sediment dynamics and sediment carbon stores. Briefly, these were; a measurement of carbon present within different vegetative structures and their relationship

with season; a prolonged study of sediment deposition, settlement and accretion rates and their resulting carbon input (or removal) from different areas of the estuary over four seasons; and finally the sampling of deep, buried sediment and measurement of their characteristics to evaluate total carbon sedimentary carbon store.

Together, these data inform on the total carbon situation (cycle, sequestration, and storage) in the estuary area, and further, describes this situation in each area type; specifically, how saltmarsh restoration areas differ from mudflats and natural stands of vegetation. Ultimately this information helps develop an understanding to the limitations and possibilities of conservation 'self-subsidisation' through leveraging the increased natural capital value due to the delivery of enhanced ecosystem services through *Blue carbon* payments.

## 1.7 Study site

Research was conducted on the Eden Estuary, which was selected as it afforded an ideal model system in which the effects of saltmarsh restoration, which has been subject to long-term efforts, could be readily examined and evaluated.

The research was conducted on the Eden Estuary (56°21'52" N, 2°50'32" W), Fife, on the east coast of Scotland (Figure 1.5), sitting between the larger estuaries of the Tay to the

*Figure 1.4: Image of the Eden Estuary looking due east along its longitudinal axis*

north and the Firth of Forth to the south. The Eden Estuary is a small 'pocket' estuary, being approximately 11 $km^2$ and spanning 2 km at its widest point (Figure 1.4), receiving a typically meso-tidal range. The River Eden drains approximately 400 $km^2$, of which 76 % comprises agricultural land. The kingdom of Fife typically experiences an average annual temperature of 9°C, with the lowest mean daily temperature occurring in January of 2°C and the highest being in July of approximately 15°C. Sea surface temperatures around the East Fife coast range from approximately 7°C in February to 15°C in August. The East coast of Fife, receives an average of around 1,500 hours of sunshine per year, being one of the sunniest places in Scotland. The region is mostly sheltered from weather systems carrying rain from the Atlantic, meaning it receives an annual average of 700 mm of rainfall. The annual mean wind-speed, recorded at Leuchars on the north shore of the Eden Estuary, is approximately 10 knots (11.5 mph).

The saltmarshes of the estuary are considered to be in an "unfavourable condition as a result of coastal erosion, and the impacts of the extensive coastal defences" (SNH, 2011). However, the Eden Estuary remains an important and valuable ecosystem reflected in the many designations it holds, which help to strengthen its protection and conservation status. The list of designations includes:

- SSSI (596) – designated for the nationally and internationally important role the intertidal mud and sand flats play in supporting population of waders. It is also the site of the largest saltmarsh extent in Fife and where nationally scarce types of eelgrass can be found *Zostera angustifolia* and *Z. nolte*.
- NATURA 2000 site – designated as an SPA (UK9004121) for supporting populations of both migratory and non-species of European importance (Article 4.1 & 4.2 of the Directive (79/409/EEC), for example Marsh Harrier (*Circus aeruginosus*); and is a wetland of international importance. It is also an SAC (UK0030311) due to being a high-quality estuarine area such as its intertidal mud and sand flats and sustaining populations of Harbour Seals (*Phoca vitulina*).
- Local Nature Reserve.
- Ramsar Wetland area (UK13018).

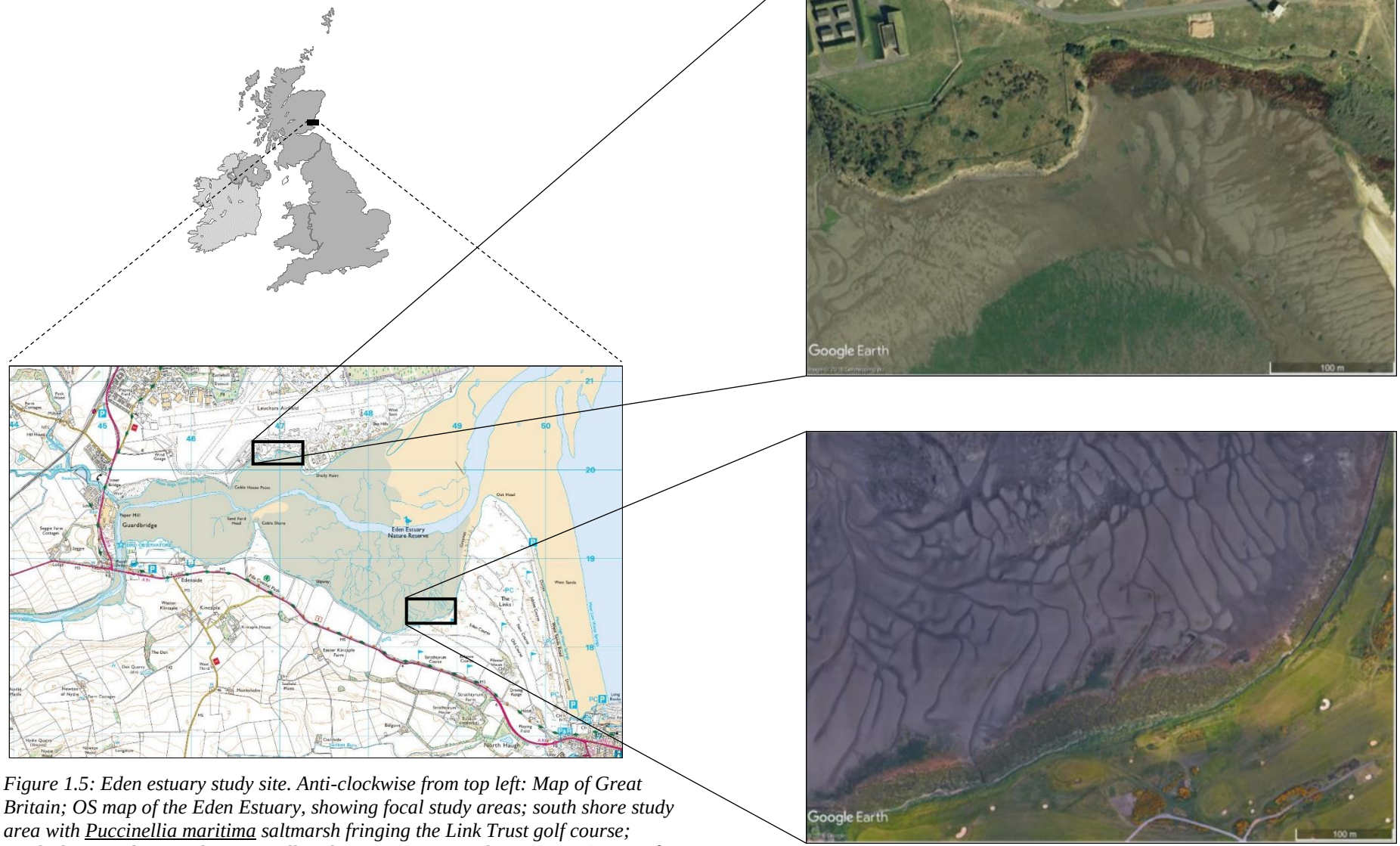


*Figure 1.5: Eden estuary study site. Anti-clockwise from top left: Map of Great Britain; OS map of the Eden Estuary, showing focal study areas; south shore study area with <u>Puccinellia maritima</u> saltmarsh fringing the Link Trust golf course; north shore study area showing <u>Bolboschoenus maritimus</u> (brown-green) area of MoD Army camp (Leuchars).*

### *1.7.1 Specific study areas*

Study areas within the Eden Estuary were determined through initial scoping visits, the use of aerial imagery and discussion with individuals who had specific knowledge of the area; for example, Dr Maynard provided background information as to the locations, ages, and states of restoration activities. Area were selected to provide a meaningful range across habitat types, encompassing existing 'natural' extents and bare mudflat – providing a baseline or 'business-as-usual' measure – through to young and older restored areas – being approximately 5 years and 12 years old at the commencement of this research. These chosen areas were distributed across adjacent shores of the estuary (Figure 1.5), which each contained examples of similar aged sites of restoration, mudflats and extents of natural vegetation, being *Bolboschoenus maritimus* on the north shore and a community dominated by *Puccinellia maritima* on the south shore (section 1.8).

The two shores were assumed to be broadly exposed to similar environmental inputs, stresses and fluxes. However, there were slight differences found in their overall elevations, with the north shore sitting generally lower in the tidal frame than the south; whose average elevations were 1.51 m and 1.76 m above ordnance datum respectively (16 points on each shore, measured in September 2016). The total extent of the areas on each shore also differed (Table 1.2; the area assigned as mudflat was calculated as the being the length across each shore and 20 m wide), with the north shore measuring approximately 480 m across and the south being approximately 640 m across.

*Table 1.2: The size of each area type which was included during the study. calculated using various data input from ground collected GPS tracks and remote sensed image processing*

| Shore | Area type | Areal extent ($m^2$) |
|---|---|---|
| North | Natural | 3,503 |
| | Old Restored | 100 |
| | Young Restored | 2,294 |
| | Mudflat | 9,680 |
| South | Natural | 15,289 |
| | Old Restored | 368 |
| | Young Restored | 611 |
| | Mudflat | 16,972 |

## 1.8 Vegetation of the Eden Estuary

The Eden Estuary is home to the largest single extent of saltmarsh in the Kingdom of Fife (seen in the foreground of Figure 1.4), which a complex community, dominated by *Puccinellia maritima*. The same community marsh type is located in the study area of the south shore (Figure 1.5), being an example of 'natural' saltmarsh. The other vegetation type studied were mono-specific stands of *Bolboschoenus maritimus* which was located on the north shore (Figure 1.5), being an example of 'natural' saltmarsh. This species was employed in restoration activities.

The structure and characteristics of the two studied vegetation types are as follows:

### *1.8.1 Puccinellia maritima (Common saltmarsh grass)*

*Figure 1.6: Example of typical vegetation found in the natural area on the south shore of the Eden Estuary. Right show patch dominated solely by P. maritima. Left shows a patch of complex community vegetation.*

*Puccinellia maritima* is a type of perennial 'alkali grass'(Figure 1.6) restricted to saline soils (Gray and Scott, 1977) and colloquially known as Common saltmarsh grass. It is distributed widely within the UK, being present along most coastline (Figure 1.7). It is typically classified as an indicator of a low to mid marsh area, although it can be found in pioneer communities on the fallen edges of saltmarshes and recently disturbed areas of saltmarsh. In the mid marsh area it is usual to encounter this vegetation as a community assemblage in which it is the dominant vegetation (Tyler-Walters, 2004). The structure of

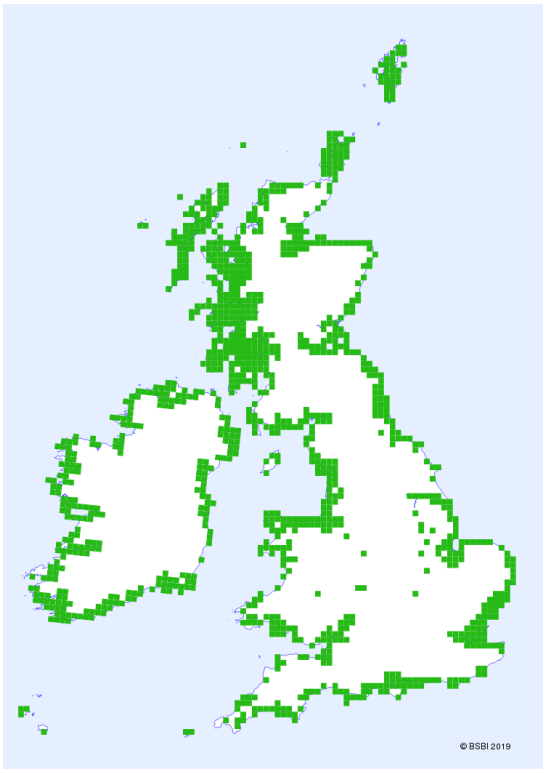


*Figure 1.7: Distribution map of P. maritima taken from the Botanical Society of Britain and Ireland records. Green squares are 10 km$^2$ indicating presence of P. maritima.*

communities varies, with up -to six sub-communities being recognised (Pigott et al., 2000), typical co-species include *Plantago maritima* (common name = sea plantain), and *Aster tripolium* (common name = sea aster).

Common saltmarsh grass exhibits limited seasonal structural changes, during summer there is notable growth, which begins in April and leads to flowering by August (Gray and Scott, 1977; Tyler-Walters, 2004). The vegetation creates an extremely dense covering for the sediment on which it grows, during the winter stems remain green and retain much of this vegetative complexity. The stems of *P. maritima* are between 3 and 80 cm long, and can produce a caespitose plant (Gray and Scott, 1977); as typically found in the Eden Estuary.

The extent of *P. maritima* found within the Eden Estuary is notably higher in the tidal frame than all other vegetation studied with an average elevation of 2.36 m above mean sea level. There is generally a steep step between the sediment surface of the mudflat (or fringing vegetation of *B. maritimus* or *S. anglica*) and the level of the *P. maritima* community.

The *P. maritima* dominated community is classified in the National Vegetation Classification (NVC) as SM13 - Sub-community with *Puccinellia maritima* dominant (Pigott et al., 2000); described as SM13a in Haynes (2016). There was no clear difference of community structure within the extent of vegetation, with all sub-species represented uniformly. Other species present

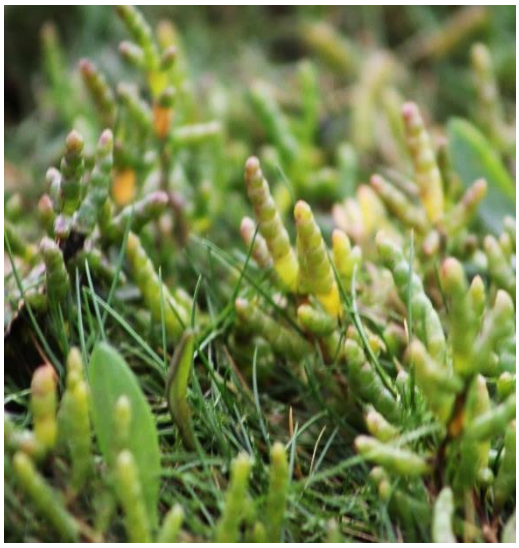

*Figure 1.8: Typical pioneer type vegetation Salicornia sp. growing within the complex community dominated by the grass P. maritima.*

included *A. tripolium*, *Cochlearia officinalis* (common scurvy grass), *Festuca rubra* (red fescue), and during summer examples of *Salicornia* sp. limited to the fringing edge of the extent (Figure 1.8).

### *1.8.2 Bolboschoenus maritimus (Sea club-rush)*

*Figure 1.9: B. maritimus vegetation of the north shore natural vegetation, also the vegetation with which restoration activities took place.*

*Bolboschoenus maritimus* (sea club-rush) is typically associated with saline environments, however, can be considered a brackish water species due to is prevalence along rivers some distance from the full influence of tidal activity. It is found around much of the UK coastline with extensive examples in-land from coastal locations (Figure 1.10), typically along the courses of rivers following tidal intrusion up these water courses.

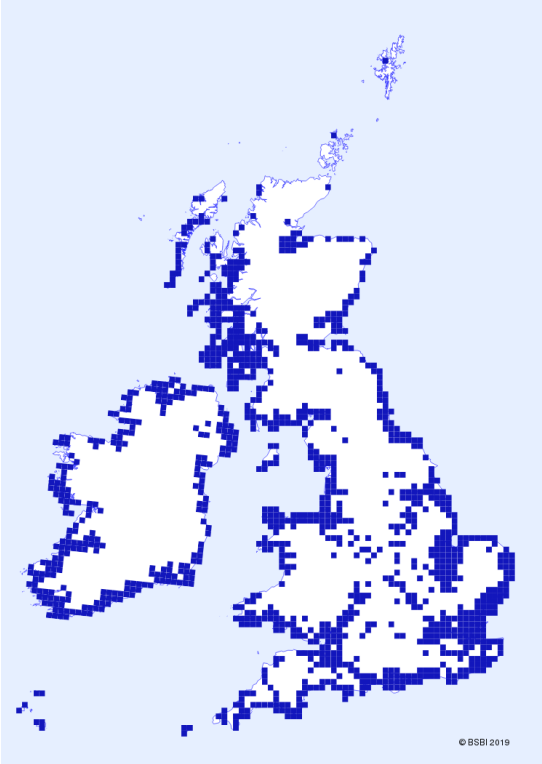


*Figure 1.10: Distribution map of B. maritimus taken from the Botanical Society of Britain and Ireland records. Green squares are 10 km$^2$ indicating presence of B. maritimus.*

Sea club-rush exhibits a relatively simple above ground structure of vertical erect stems, which reach between 50 and 150 cm tall (Koch and Koch, 1846). *B. maritimus* produces seeds during summer but also spreads vegetatively through the growth of rhizomes. This vegetation displays a strong seasonal trend, with impressive green growth during spring and summer, increasing in both height and density through the production of new shoots and leaves. During winter there is significant die back, where much of the above ground vegetative material is lost leaving only

relatively short stems of low density. This trend is more pronounced at the fringing edge of vegetation which fronted tidal and wave action.

*B. maritimus* was found as mono-specific stands and was classified as NVC S21 - *Scirpus maritimus* swamp communities (Rodwell, 1995), the previously classified genus *Scirpus* is now *Bolboschoenus* (Marhold et al., 2006). This classification is found within the context of 'Aquatic communities, Swamps and Tall-fen herbs', indicating its tendency for appearance outwith 'coastal' settings. However, it is considered as saltmarsh vegetation on the Eden Estuary due to its location low in the tidal frame. These vegetation stands were typically found at similar elevations to those of the bare mudflat at an average elevation of 1.62 m above mean sea level.

### *1.8.3 Other vegetation types*

*Figure 1.11: Mudflat area of the Eden Estuary during summer, showing the presence of Salicornia sp. and an established permanent sampling point.*

Although this study defined areas of vegetation as areas of *P. maritima* and *B. maritimus*, there were other types of vegetation present. Predominantly during the summer months there was the growth of *Salicornia* sp. across areas of the 'bare' mudflat. The seasonal growth of this herb is unpredictable, whose distribution and density on the Eden Estuary fluctuates year-to-year. Generally, the individual plants encountered during the course of this study were small in stature and only found in low densities (Figure 1.11); further, they were rarely located within direct sampling areas on the mudflat. During the study, occasionally there were dense growth of *Ulva intestinalis* (Enteromorpha), a green filamentous alga which forms mats on the mudflat and in areas of vegetation (Figure 1.12).

There were also examples, of predominantly discreet, clumps of the invasive non-native *Spartina anglica* (common cord-grass) found fringing the seaward edge of the *P. maritima* extent of the south shore. During the course of the study there appeared to be a general increase in the quantity of *S. anglica*.

*Figure 1.12: A sward of dead macro-algae deposited on the south shore P. maritima saltmarsh area during summer.*

## 1.9 Restoration activity on the Eden Estuary

Saltmarsh restoration activity, in the form of direct transplantation, on the Eden Estuary has been taking place since the turn of the millennium (Maynard, 2014). *B. maritimus* plants were first harvested from various donor stands within the estuary, involving the removal of approximately 30 $cm^2$ sections of the marsh; ensuring the retention of the rooting structures in each section (approximately 30 cm deep). These sections were then broken down into individual vegetative 'plugs' which incorporated the above ground and blow ground structure of separate stems into a single unit. These plugs become the planting units, which were planted into the specified area designated for restoration. Planting densities were lower than that found naturally to increase the effective area of restoration and planted at 10 stems per $m^2$ (see Maynard, 2014 for further details).

### *1.9.1 Old restored areas*

The areas in the study classified as 'old restored' were planted in 2000 and 2003 on the north and south shore of the Eden Estuary, respectively. They were characterised as being

'successful' examples of restoration initiatives, that is they had persisted, expanded and developed structurally. This development included an increase in plant density towards (or possibly exceeding) that found in the natural area of *B. maritimus* (Maynard, 2014; Maynard et al., 2011) and the lateral expansion of vegetation, which generates a 'natural' edge to the stands as appose to the angular lines created during planting (Figure 1.13).

*Figure 1.13: Typical area of old restored saltmarsh area (here on the south shore in winter), showing increased density and complexity as the original planting of B. maritimus has developed.*

### *1.9.2 Young restored areas*

The areas in the study classified as 'young restored' were planted in 2010 and 2013 on the north and south shore, respectively. These areas, on both the north and south shore, exhibited a still fragmented and low-density community structure (Figure 1.14). During the study, some parts of these areas appeared devoid of any vegetation, suggesting there had been reduced success in establishment by the planted *B. maritimus*. This trend was important to consider when assessing the behaviour within 'young' restoration sites.

*Figure 1.14: Typical area of young restored saltmarsh area (here on the south shore in winter), showing low density planting arrangement of B. maritimus with limited expansion having taken place.*

## 1.10 Thesis structure

The thesis is structured as individual chapters, each containing the relevant methodology and concerning a specific aspect of carbon storage potential within the saltmarsh ecosystem and assesses the influence restoration activities. The chapters address each of the following:

### *1.10.1 Chapter 2: Vegetation assessment and carbon stock*

An assessment of the carbon stored in vegetative components was made, which included a comparison between vegetation types (both natural and restored) and seasons (i.e. the difference between retained vegetation in winter and summer growth). Vegetation structure data were collected using a Terrestrial Laser Scanner (TLS), producing high-resolution-high-precision 3D models of the estuary (Figure 1.15); from which relevant information was extracted (i.e. vegetation height), to which allometric scaling was applied to estimate carbon stores. The success of this methodology was evaluated in chapter 2.

These data allowed the testing of the hypotheses that:

- TLS will be able to effectively acquire sediment and vegetation structure information.
- Restoration activity increased the carbon storage of an area due to vegetation presence.
- Different vegetation structures will display different carbon storage and cyclic components.

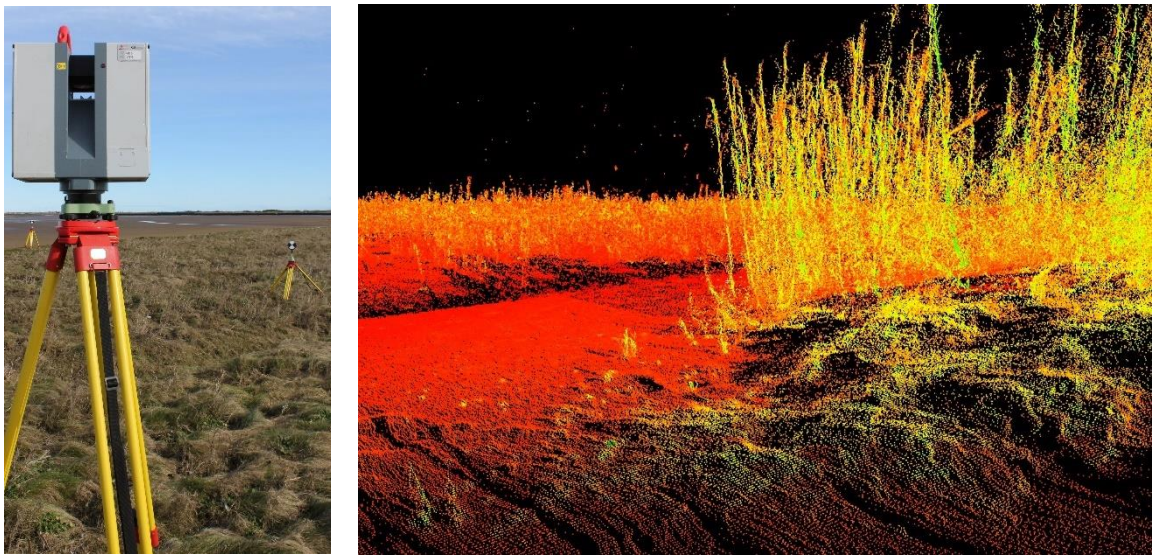

*Figure 1.15: Left image shows data being collected with Terrestrial Laser Scanner (TLS) and the right image shows raw output of 3D point-cloud from the TLS.*

### *1.10.2 Chapter 3: Sediment dynamics and carbon sequestration*

An investigation into sediment deposition and settlement rates were measured seasonally over a year, across natural extents of saltmarsh, different age restored saltmarsh areas and bare mudflats (Figure 1.16); gathering data on the varying relationship between potential deposits and actual deposition in each area type. Data were collected on vegetation structure and sediment elevation changes (Figure 1.16) to further understand the dynamics within each area. Samples also provided carbon content data which were used to inform on the carbon sequestration potential of each area.

These data allowed the testing of the hypotheses that:

- There would be significant variation in carbon deposition and accretion between area types.
- Restored areas will experience an increased carbon accretion rate than bare mudflats.
- Vegetated areas will experience higher content carbon deposits than bare mudflats.

*Figure 1.16: Example of a permanent sampling point on the Eden Estuary at which data of sediment settlement, deposition and accretion were collected.*

### *1.10.3 Chapter 4: Sedimentary carbon store*

A study of current sedimentary carbon stores at three area types, being natural mid-marsh, restored-established marsh and bare mudflat, through sediment coring. The extracted sediment cores were sectioned (Figure 1.17) to generate depth profiles of various characteristics including carbon content, bulk density and particle size composition. These

data allowed total carbon stock estimates to be made for each are type and how storage changes with depth.

These data allowed the testing of the hypotheses that:

- There would be significant difference in carbon stores between vegetated and non-vegetated areas
- Restoration activities will have increased sedimentary carbon storage
- Older stands of restored marsh would store or carbon than younger stands

*Figure 1.17: Left image of sediment core retrieved from core tube and right image shows top of core being sectioned into 1 cm layers.*

### *1.10.4 Chapter 5: Research discussion*

This deals with the findings of the research as a whole in-order to construct an understanding of the way in which saltmarsh restoration on the Eden Estuary has altered the carbon sequestration and storage state therein. Furthermore, it uses this information to comment on the economic potential for such initiatives to access payments for ecosystem services and thus subsidise (to some degree) conservation projects in the future.

# Chapter 2: Seasonal change in vegetative carbon storage assessed by terrestrial laser scanning (TLS)

The role of vegetation, both as a direct carbon storage pool and through its role in biogeomorphic-sedimentary interactions, is important for the functional capacity of saltmarshes to both sequester and store carbon. In this chapter, focus is given to quantifying the role vegetation plays in directly storing carbon within the saltmarsh system. Specifically, the investigation aimed assess the efficacy of remote sensing technology, namely Terrestrial Laser Scanning (TLS), to capture relevant information, such as vegetative structure, across an entire marsh area. In this case study, TLS was used to compare the 'natural' and 'restored' areas contribution to the vegetative carbon pool and capture the "additionality" of restoration efforts above the reclaimed mudflat. Furthermore, the study also assessed the seasonal variation in these areas, highlighting the retained and cyclic components of vegetation. This investigation was made possible through a loan of the necessary equipment (a Leica HDS6100 laser scanner, two Leica GNSS receivers, and various ancillary equipment) from the NERC Geophysical Equipment Facility.

*Figure 2.1: Example images of the vegetation types surveyed in the laser scan. (A) Typical Puccinellia maritima marsh, (B) Typical stand of Bolboschoenus maritimus.*

## 2.1 Saltmarsh vegetation growth and measurement

Saltmarshes, in their various forms, are comprised of halophytic macrophytes, having some degree of tolerance to salt. The type, structure and distribution of this vegetation is a function of the various abiotic and biotic features of a given area (Silvestri et al., 2005). During marsh development, typically, a 'pioneer' species will first establish when conditions (e.g. sufficient sediment elevation within the tidal frame) (Allen and Pye, 1992) and seeding material availability (e.g. arrival of seeds) (Zhu et al., 2014) coincide. This

‘Pioneer zone’ is usually confined between mudflat areas that are covered for 6 hours per day and the mean high water mark (Boorman, 1999). The presence of established vegetation alters the immediate environment, for example, roots bind unconsolidated sediments and their above ground structures influence water column dynamics (Boorman et al., 1998). The result of successful establishment is a series of biogeomorphic feedback loops, whereby sediment accretion and vegetative structures interact. The resultant trajectory of a healthy marsh establishment is either towards a state of equilibrium, retaining its given community structure, or leading to successional development and the colonisation of higher marsh plants as features, such as surface elevation, are altered. This progression frequently results in a strong spatial structure, usually forming parallel bands of zonation along the elevation gradients (Gray, 1992); comprised of pioneers to low-marsh through mid-marsh to high-marsh. The resultant zones are characterised by different plant species, communities and structure, for example; the pioneer zone is characterised by open communities featuring *Spartina* spp. and *Salicornia spp*. (Boorman, 2003) (Figure 2.2), low-marsh is characterised by closed communities with the addition of *Puccinellia maritima* and *Atriplex portulacoides*, mid-marsh areas are, again, closed communities with the addition of species such as *Plantago* spp., and high-marsh areas, with examples of *Festuca rubra* / *Armeria maritima* / *Elytrigia* spp., beyond which communities transition to terrestrial non-halophytic plants (Boorman, 2003). These assemblages result in differing structural mosaics dependent upon their morphologies. Pioneer species such as *Spartina* spp. are generally tall and erect stands, whereas *Puccinellia maritima*, a low-marsh species, is a herbaceous graminoid (grass), typically lower in stature and more flexible, but creates dense coverage. These two vegetation types exhibit different growth modes, both because of their differing vegetation type and their specific situations within the estuary. Stands of the rush *B. maritimus* (as used in restoration here) typically has a growing season between April and September, after which those active photosynthetic parts of the plant are lost and predominantly only below-ground structures are retained (Lillebø et al., 2003). Furthermore, as stands of vegetation develop, they are liable to expand (or contract) depending upon prevailing site conditions. In the case of the grass *P. maritima* community, there is likely to be lower variation in vegetation height between seasons and less opportunity for annual expansion or contraction due to its position on a sediment platform higher in the tidal frame.

These morphological differences also reflect differing biomass distribution and production, and so affect the size of the given vegetative carbon pool (Radabaugh et al., 2017). The contribution to the carbon pool is a function of morphology, density and cover. The quantification of biomass and carbon content can be achieved in two ways. The first of

which employs destructive sampling taking material directly from the environment and removing both above and below ground components of vegetation. This approach can provide site specific information regarding biomass allocation and carbon content data for all the species or communities being studied. However, the need to remove large amounts of vegetation is not ideal, particularly within a restoration/conservation context. The second approach utilises previous destructive sampling studies and applies allometric relationships developed therein; linking physical (field measurable) structure to aspects such as above-ground biomass or organic content. Such scaling relationships for saltmarsh species are increasingly available in the literature, so facilitating rapid, non-destructive assessments to be made as to the biomass contribution of different vegetation. Trilla et al. (2013) for example, found that for species of *Spartina* they achieved strong predictive relationships between tiller height and biomass with $R^2$ values ranging between 0.88 and 0.97. These relationships have further been shown to have satisfactory predictive power beyond their origin sample area (Trilla et al., 2013), allowing their application at a broad spatial-temporal scale. In this study biomass allometric relationships for *B. maritimus* were taken from a previous study within the Eden Estuary (David, 2012) and for *P. maritima* from a study by Engels and Jensen (2010).

*Figure 2.2: Examples of 'typical' saltmarsh pioneer species. Left - Spartina spp.; Right - Salicornia spp.*

The conversion of biomass values to carbon content again can be achieved via different routes, one is a destructive approach taking samples of vegetation and directly quantify their carbon content values, secondly a generic conversion factor can be applied. Howard et al. (2014) suggest the using a conversion factor of 45 % (from Fang et al. (1996)), however a study by Radabaugh et al. (2017) found a range of 23 – 47 % across 18 saltmarsh species,

with an average of 41 %. Consideration should, therefore, be paid to variation in carbon content between species and specifically species type, for example succulent versus graminoid forms (Radabaugh et al., 2017). Species-specific carbon conversion factors are, therefore, to be preferred. In this study conversion factors have been generated from measurements taken during a summer and winter sampling campaign for other associated research on the Estuary.

### *2.1.1 Study site detail*

This study considers the contributions made to the vegetative carbon pool of the Eden Estuary by two different types of 'natural' saltmarsh areas and 'restored' stands of vegetation. The 'natural' areas are comprised of a low to mid-marsh *Puccinellia maritima* (Common saltmarsh-grass) complex (Maynard, 2014) (NVC SM13; Sub-community with *Puccinellia maritima* dominant (Pigott et al., 2000); described as SM13a in Haynes (2016)); with an average elevation of 2.36 m above mean sea level, and low-marsh, mono-culture of well-developed *Bolboschoenus maritimus* (Sea Club-rush) (NVC S21; *Scirpus maritimus* swamp communities (Rodwell, 1995)), previously classified as the genus *Scirpus*, now *Bolboschoenus* (Marhold et al., 2006); with an average elevation of 1.64 m above mean sea level. The 'restored' areas consist of mono-culture transplanted stands of *B. maritimus*, planted in 5 m x 2 m plots, at a density of 10 plugs/$m^2$; where natural density ranged between 120 and 550 stems/$m^2$ depending upon location within a marsh stand (Maynard, 2014). Examples of restoration are present on the north and south shores of the Eden Estuary, with the north shore site being planted in the spring of 2000, with a current average elevation of 1.76 m, and the south shore being planted in the spring of 2003, with a current average elevation of 1.67 m.

## 2.2 Remote sensing opportunities

As detailed, this study applied allometric scaling relationships to capture vegetative biomass, using plant height as a defining measurement. The rapidly evolving field of remote sensing perhaps offers an opportunity to utilise and develop new approaches to obtaining various structural information across a large study area; specifically, Terrestrial Laser Scanning (TLS) technology may hold promise. However, though other remote sensing technologies have been previously utilised (e.g. Belluco et al., 2006; Hardisky et al., 1984), including TLS (Loudermilk et al., 2009), in characterisation of vegetation applications in an

inter-tidal are is uncommon (Owers et al., 2018); and its ability to deliver useful data on above-ground vegetative structure is largely untested.

### *2.2.1 Laser scanning approaches*

Light Detecting and Ranging (LiDAR) remote sensing utilise laser light to make distance measurements from the environment (with additional information extraction possible from the laser return data). Static TLS, or ground-based LiDAR technology, comes in two major variants; being time-of-flight (TOF) and phase-based systems. Both approaches employ emitting laser light and measure the returning reflected portion. Simplistically, in the case of TOF systems, distances are calculated using the speed of light as a known constant and the time taken for the laser reflection to return (Equation 1)

$$D = \frac{t * c}{2}$$

*Equation 1*

Where *D* is the distance to an object from a static scanner, *t* is the time taken for the laser reflection to return and the constant, *c*, being the speed of light (299,792,458 $m.s^{-1}$).

In a phase-based system, such as used in this study, laser-light is emitted at alternating frequencies and the difference between emitted and reflected signals is measured to determine distance. These systems offer a higher range of measurement accuracy, although have a more limited functional range (Bienert et al., 2006).

Typically, LiDAR surveys are carried out from an aircraft, historically solely on aeroplanes, however drone deployment is becoming increasingly accessible. Typical resolution achievable from an aircraft are horizontally up to 25 cm with a vertical accuracy of ±15 cm RMSE (specification of Environment Agency Lidar dataset). Although this approach facilitates large spatial coverage, this introduces possible issues around total accuracy. The system relies upon at least three components – a GPS sensor, an INS (inertial navigation system) and the laser scanner setup (such as beam divergence or laser footprint) – which must all be calibrated correctly. Therefore, the total accuracy is a product of error propagation from the various components of the system and additionally movement of the aircraft (both direction, angle and height) (May and Toth, 2007). This approach has various useful high-level applications which demand large spatial coverage at 'lower' accuracy and are not overly impeded by complex surface structures, although perhaps is limited in its

applicability to finer scale information gathering. Static TLS technology is deployed manually ‘on the ground’, which naturally limits the spatial coverage realistically achievable, but allows higher-resolution, higher-accuracy data to be collected. The interactive static nature of TLS allows a more considered and tailored approach to be taken during surveying, for example manually determined scanner positioning to minimise data shadowing (where the laser is intercepted by a foreground object leaving the background data-void – ‘in shadow’). This approach facilitates the collection of all necessary information, where each scan can provide sub-centimetre resolution and accuracy in the order of millimetres.

This technology has seen increasing use in fields such as engineering (Mukupa et al., 2016) and crash scene investigation (Cavagnini et al., 2007). There are, however, fewer examples of its deployment in an ecological research context; those that exist typically focus on forest inventory applications (for example see Andersen et al., 2006; Bauwens et al., 2016; Liang et al., 2016; Thies and Spiecker, 2004). The technology lends itself well to questions related to the structural components of ecosystems, such as, the quantification of forest canopy cover, habitat complexity of rocky shores (Hollenbeck et al., 2014) or in the present case the vegetative structure of a saltmarsh. Its application within the context of this study holds similarity to those concerning forest canopy cover and gap structure investigations, in that the 3D model should provide information of the above-ground vegetation (“canopy”) and through to the sediment surface (“gaps”); thus, allowing such analysis as, structure, height and density. The capacity of TLS technology is demonstrated (Figure 1.3), showing a section taken through the saltmarsh-mudflat continuum surveyed with points coloured by intensity of return values. This technology can be integrated with high-accuracy location information to contextualise the 3D information in space. This additional data layer extends the possible applications of such data, for example understanding of tidal inundation or spatially-specific temporal changes.

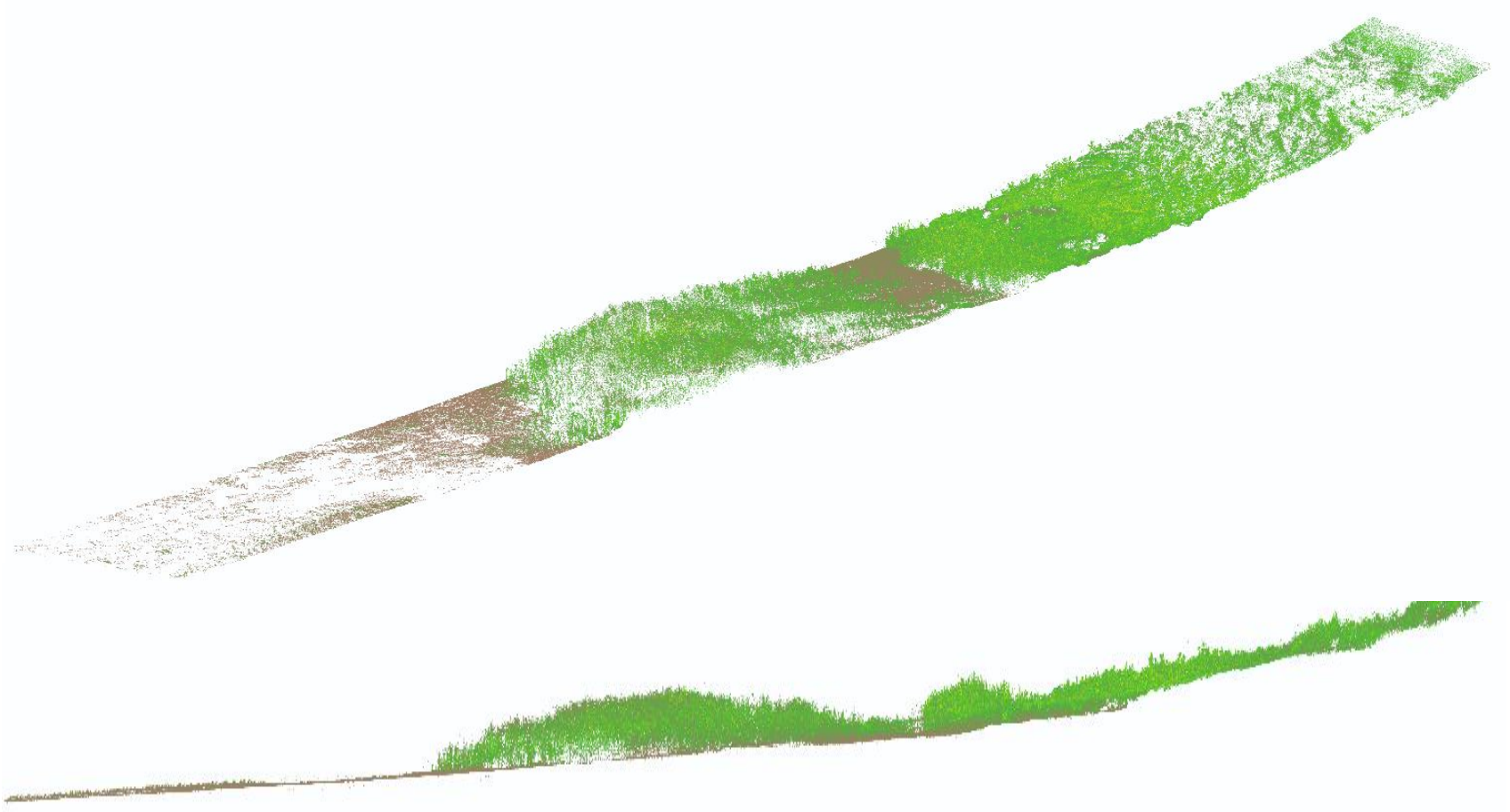

*Figure 2.3: Example sections of TLS of the studied saltmarsh, extending from the terrestrial zone (right) through to the mudflat (left). The upper panel shows an elevated-skew view and the lower panel, a transverse view, looking through the point cloud section. Scalar has been applied to colour points by their scanner intensity return value.*

### *2.2.2 High-accuracy location data*

The relative location of points provided by satellite signal receivers, typically known as GPS (Global-Positioning System), is determined through evaluation of their distance from a group of satellites. The system utilises the shift in satellites' signal frequencies - due to the Doppler Effect – to assess their own movement and so calculate its position. This was originally developed by the US Government creating a network of 24 satellites known as the GPS, providing multi-use access positioning service typically used at present. Improvements to positioning system capabilities are constantly being made, for example, Russia's GLONASS program and the European Union's Galileo satellites. These systems can be known collectively as the global navigation satellite system (GNSS). Handheld GPS units may use more than one satellite system and have a typical maximum accuracy in the order of meters in the horizontal and vertical planes. Higher accuracy location data can be attained using improved sensors and applying a 'relative carrier phase positioning' (relative -GPS) correction approach; such accuracy is useful when combining data with extremely accurate TLS information. Relative-GPS uses data collected simultaneously from two locations, one as a static Base station and the other a Rover point, and post-processing of short-term Rover location against longer-term Base location. In the case of user-established Base stations (as used here), the unit is located to minimise distance from the survey site. The more data collected, the more accurate its averaged location becomes. The Base station location is processed against a 'fixed reference' point, which are known locations that are deemed to have an accuracy error of 'zero'. These points continually collect data from satellites, allowing calculation of error difference corrections between its fixed known location and the calculated location from satellite data. Satellite trajectories at time of surveying are predicted and therefore calculated locations are less accurate. As such post-processed 'precise ephemeris' information is used which provides actual satellite positions from their tracked trajectories; which allow more accurate locations to be calculated.

The current study used a pair a Leica VIVA GS10 GNSS receivers, collecting location data at 15 second intervals. The Base station was established 30 minutes prior to surveying and retrieved 30 minutes after survey completion having a maximum 3-mile baseline distance for the entire survey. These data were processed in Lecia *Geo Office 8.4* where the corrected survey locations resulted in ~ 5 mm horizontal and ~ 10 mm vertical accuracy.

## 2.3 TLS surveying

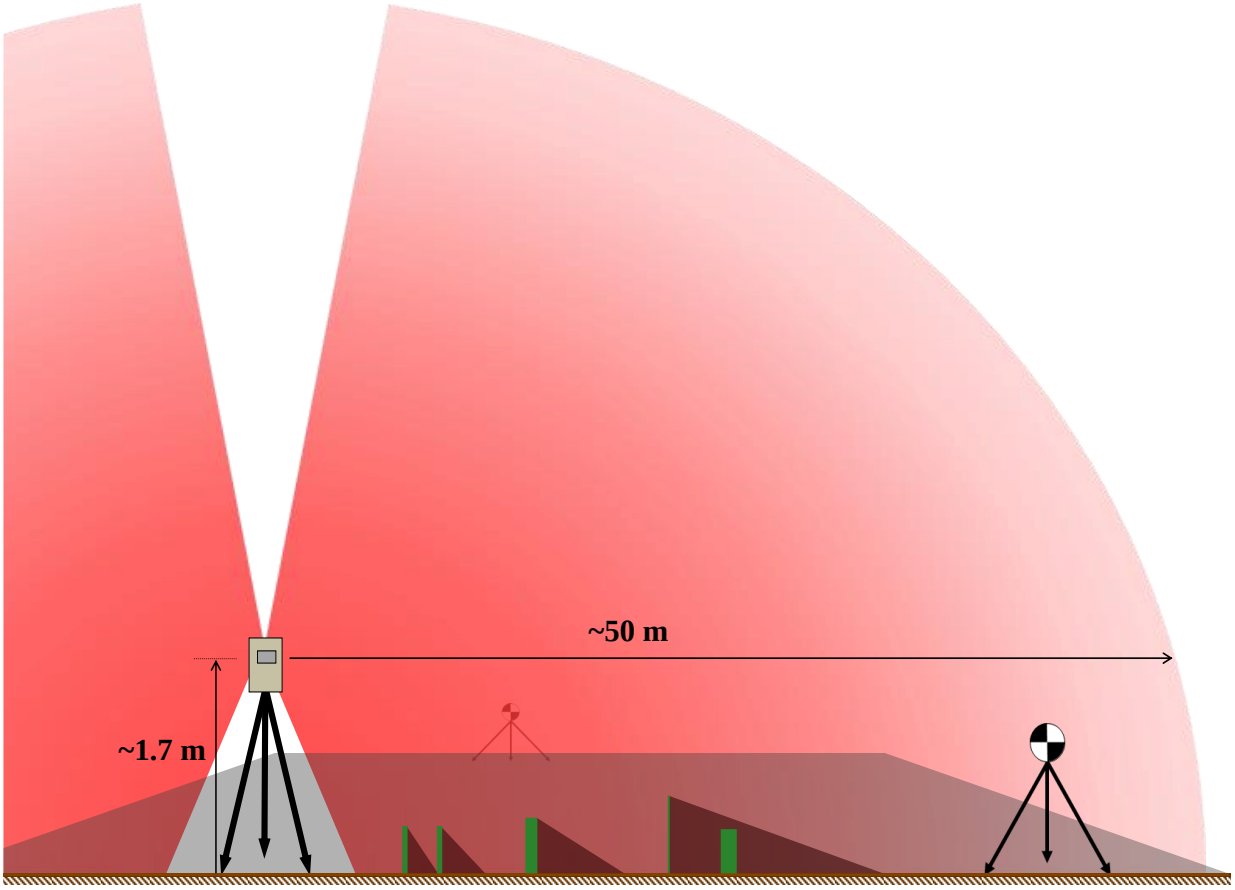


*Figure 2.4: Typical setup of the terrestrial laser scanning (TLS) equipment. The Scanner (beige box) sits on a tripod and scans vertically between 25º - 135º and 225º – 345, rotating through 180º. Six 6 inch Black & White Tilt and Turn targets were distributed within each scan vicinity. Vertical green lines represent vegetation illustrating its potential shadowing effect on the laser.*

High accuracy terrestrial laser scans, generating detailed 3D point cloud data, were obtained using a Leica HDS6100 scanner. The scanner has a maximal view range of ≈50 m at which it had an accuracy of 9 mm, with an optimal accuracy within 25 m of 5 mm. To facilitate the easy and accurate registration of multiple scans into a single unit, Leica Black & White "Tilt and Turn Targets" were used to provide cross-scan anchor points (see Figure 2.4 for illustration of survey set up). The system relies on line-of-sight, so producing 'shadowing' behind objects which intercept the laser, by topographic features or vegetation for example; a limitation which was considered whilst scanning. The scanners' elevation was restricted to approximately 170 cm, limited by the maximum safe working height of its tripod, ensuring safety of the equipment and allowing access to controls on the unit. An increased height was desirable to minimise the impacts of shadowing across each scans viewshed, by reducing the effective laser-ground angle. Consideration of this factor was applied to the semi-random logical scan distribution, working along the primary shore-parallel axis and

adjustment made on the shore-perpendicular to minimise data deficient space. Surveys were completed during neap tides affording the longest exposure period (Figure 2.5). A logical survey approach was employed, traversing along the length of the shore.

The use of TLS survey equipment in the inter-tidal zone holds some difficulties and restrictions, further to those typically associated with fieldwork in such location. The most dominant restriction here was the tide. The technology does not work very effectively in wet environments, due to the altered reflection and refraction of the laser generating inaccurate return information. This restriction is compounded by the requirements of optimal weather conditions, which include; low humidity, no precipitation and minimal wind speed. In general surveying, low wind speeds are desired to minimise potential disturbance of the TLS unit during acquisition (in the study here a period of approximately seven minutes); here however, it was critical for low wind speed to minimise vegetation movement which could degrade scan quality (Dassot et al., 2011), influencing predicted vegetation heights or increasing occlusion of the sediment surface. Such meteorological conditions are uncommon for, typically exposed, inter-tidal estuarine environment, potentially impacting the opportunity and ability to acquire data.

## 2.4 Survey methodology

Given the discussed limitations and requirements of TLS surveying in the inter-tidal zone careful consideration was given to the design of surveys towards the collection of accurate 3D spatial data.

The first consideration for survey design was centred around tidally restricted site accessibility. Surveys conducted in the current study were carried out during neap tides, where low tide fell in the middle of the day; maximising accessibility within the tidal frame, allowing surveying to begin earlier as the tide ebbed and continue later as it flooded (Figure 2.5). The requirements of tides are relatively amenable, as its timing and amplitude are largely governed by predictable forces, with some influences from prevailing meteorological conditions. This allowed several survey dates to be chosen, providing sufficient redundancy to accommodate possible restrictions due to weather. On pre-selected survey days, weather forecasts were consulted over the days leading up to it and on the actual day, including real-time information from a local weather station (Location: Leuchars; WMO ID: 03171; 56° 22' 39" N, 2° 51' 45" W). The decision to survey was made based on available information suggesting favourable conditions. During the survey,

conditions were constantly re-assessed and, if necessary, the survey was terminated; for example, due to increasing wind-speeds or precipitation.

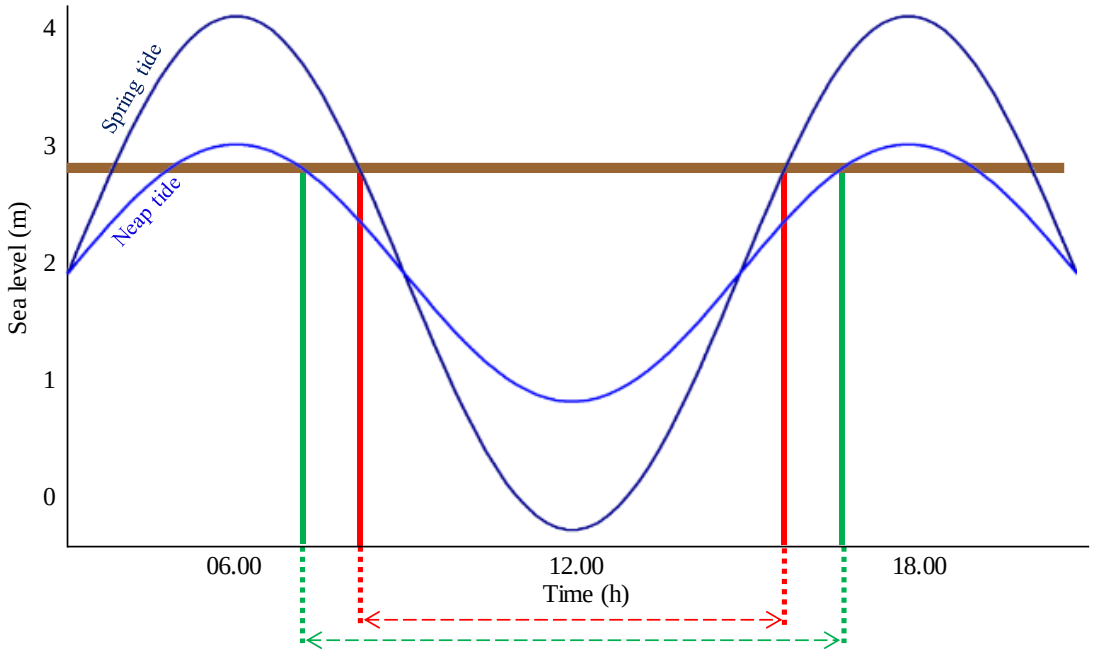


*Figure 2.5: Example of a spring (dark blue) and neap (light blue) tidal cycle. Brown line indicates example sediment surface. Vertical lines and dashed arrows highlight exposure (accessible) period, green lines during neap tide and red lines during spring tide.*

On a given survey day, the first step was to establish the GNSS Base station to maximise location data collection period. The height of the unit was taken using a height hook with data being collected at 15 s intervals from the start, with its clock time remotely set.

The surveys themselves followed a workflow as follows:

- Begin at one end of the survey area and work longitudinally along the shore
- Scanner positioned on a tripod at approximately 1.8 m high;
- Six Tilt and Turn Black and White targets arranged around the scanner position at varying heights and distances with faces aligned towards the scanner;
- One tripod was set with the Rover unit attached. The height was taken with a height hook and input into the unit, along with its unique ID and set recording for a minimum of 7 mins.
- The scanner was set running at High scan setting (6.3 mm point spacing), vertically scanning 20° - 170° 190° - 340° and rotating through 180°; all personnel and equipment was kept out of scan view-field.

- The scanner was then relocated, progressing along the long axis of the survey area and moved on the perpendicular axis to ensure full scan coverage. In topographically complex areas a more scans were acquired.
- Any given target was retained within at least three scans to provide common tie-points for post-registration processing. Faces were realigned towards scanner.
- GNSS unit was moved to different target locations as they became redundant as the scanner progressed along the shore. Not all target locations were acquired, to maintain workflow efficiency.
- This process was repeated along the length of the survey area. Maps were made onto aerial imagery of scanner and target locations.
- In case of the area being too large to cover in a single day (e.g. the south shore studied here) it was necessary to break the survey in an area with enough in-cloud registration points; for example, ridged posts or large immovable debris. Once the area was selected, at least three overlapping scans were acquired at the end of one day and the beginning of the next, in which cloud-to-cloud registration could be used.

All survey data were collected over a total of seven days, four days in summer and three days in winter (Table 3). 146 scans were taken; 59 in winter and 87 in summer. The additional scans were taken at both sites in summer, with an increase of 30 % and 50 % for the north and south shores, respectively. Additional scans were taken to reduce point cloud shadowing resulting from the increased summer vegetation height and density.

*Table 3: Summary information of the TLS/GNSS surveying carried out during the study.*

| Survey name | Total number of scans | Total number of targets | Total number of targets GPS-located |
|---|---|---|---|
| **Winter north shore** | 23 | 37 | 17 |
| **Summer north shore** | 30 | 40 | 19 |
| **Winter south shore** | 36 | 55 | 29 |
| **Summer south shore** | 57 | 74 | 40 |

## 2.5 Survey data processing

After data collection all data were processed through Lecia software, namely *Geo Office 8.4* and Cyclone 9.1, for GNSS and TLS data respectively.

### *2.5.1 GNSS data processing*

Data from the Base station and Rover station were imported into the *Leica Geo Office 8.4*, with each day processed separately. The software was updated with the type of antennae and the mount being used, which provides the relevant accurate height offsets to be automatically incorporated into the processing. Once imported, points were assigned as 'Reference' (Base) or 'Rover'. Processing parameters were set with a satellite cut-off angle of 15° and to use 'Precise ephemeris' information; acquired from the NASA Crustal Dynamics Data Information System (CDDIS). Precise RINEX data for the Dundee reference station were acquired from the NERC British Isles continuous GNSS Facility (BIGF). RINEX reference data were used to improve the location accuracy of the Base station, through re-processing with the RINEX as 'Reference' and the Base station as a 'Rover', this subsequently re-corrected the location of the survey points.

Data were then exported as '.csv' files and elevation information altered to reflect the height of the target centre, through the addition of the specific measured height offset and the constant antenna height offset. These data were used in geo-referencing the registered point clouds from the TLS.

### *2.5.2 TLS data processing*

Data was downloaded from the TLS unit daily and imported into *Leica Cyclone 9.1*, with each day held in its own database. Each scan was first cleaned, to remove erroneous returns, using the 'segment cloud' and 'fence' functions. Firstly, a point was selected on the mudflat then the cloud segmented based on elevation from this point, retaining points within -5cm and 250 cm, further discrete cleaning was carried out manually. Within each scan, targets were labelled with their unique ID from that mapped during survey and matching that used in geo-referencing. Targets were automatically recognised by the software and vertices generated at their centre.

Individual scans were combined to create a single point-cloud for each survey using the registration function. Scans from a single day were registered first using targets as constraints then auto-adding cloud constraints to further align all scans (Table 4). Surveys

conducted over multiple days were registered together using the overlapping scans as a base to which the surrounding scans were added. For cloud-to-cloud registration, at least three constraint-pairs were picked for each coupling of scans. Average absolute error across all the registered scans was 3 – 5 mm.

*Table 4: Summary information of registered point-clouds and the constraints used in their alignment.*

| Survey name | Number of target constraints | Number of non-target constraints | Total number of constraints | Mean absolute error (m) |
|---|---|---|---|---|
| **Winter north shore** | 192 | 53 | 245 | 0.004 |
| **Summer north shore** | 315 | 61 | 376 | 0.003 |
| **Winter south shore** | 335 | 14 | 349 | 0.005 |
| **Summer south shore** | 606 | 215 | 821 | 0.003 |

The location data layer was added to these registered scans. The GNSS information was imported as a set of points, with common target ID labels. As previously, a new registration was created for each survey, in which the GNSS layer was applied as the primary cloud. This registration best aligns the entire fixed laser point-cloud onto the framework of the GNSS points using target IDs as constraints (Table 5). This process has a higher error rate than linking TLS clouds, to minimise the impact of this on the total accuracy those constraints with errors of $\geq 0.1$ m were removed from the registration.

*Table 5: Summary information of the GNSS target location use in registration with the TLS surveys.*

| Survey name | Number of targets located | Number of target locations constraints | Mean absolute error (m) |
|---|---|---|---|
| **Winter north shore** | 17 | 17 | 0.037 |
| **Summer north shore** | 19 | 17 | 0.029 |
| **Winter south shore** | 29 | 28 | 0.061 |
| **Summer south shore** | 40 | 23 | 0.025 |

Finally, the created point clouds were ‘unified’, which combines the individual scans used in the registration into a single cloud which can be exported as one unit. In this process cloud reduction was set with a minimum point distance of 5 mm to remove unnecessary point overlaps. The result was high-resolution 3D point cloud maps with high-accuracy against a real-world coordinate system.

## 2.6 Point cloud processing

Analysis was carried out to compare the difference in vegetation between winter and summer of restored and natural areas of saltmarsh. Point cloud data were sectioned into four discrete areas comprising two established restored areas (one each on the north and south shores), one natural stand of *B. maritimus* on the north shore, and a natural *P. maritima* marsh on the south shore. Data were exported from *Cyclone 9.1* in ‘.pts’ format and then converted to ‘.las/.laz’ format using *pointzip 1.0*, providing far smaller and manageable file sizes for further analysis. Clouds were imported into *CloudCompare v2.10*, were ‘cleaned’ of obviously erroneous points which were missed during initial processing, for example the removal of returns from below the surface of the sediment. Within *CloudCompare* various approaches were tested to acquire separate information on the sediment surface and vegetation layer. Initial tests were carried out on a restored area (*B. maritimus*) from the south shore.

### *2.6.1 Cloud classification*

#### *2.6.1.1 Cloth Simulator Filter (CSF)*

This algorithm was developed to separate ground from non-ground points within LiDAR data sets (Zhang et al., 2016). This simulates a ‘cloth’ which is placed on the underside of a given point cloud creating an effective Digital Terrain Model (DTM). The CSF plugin was tested on various cloud types (full resolution, re-sampled and cleaned), however it was not effective at separating out solely sediment surface return points with significant retention of vegetative structures.

#### *2.6.1.2 CANUPO*

CAractérisation de NUages de POints (CANUPO) is a plugin designed to allow “classification of the scene elements based uniquely on their 3D geometrical properties across multiple scales” (Brodu and Lague, 2011). Briefly the process asses the local geometry of a given point at varying scales (diameter spheres, Figure 2.6) and determines

its likely environmental class based upon defined feature signatures contained within specific classifier algorithms; either pre-existing or user created.

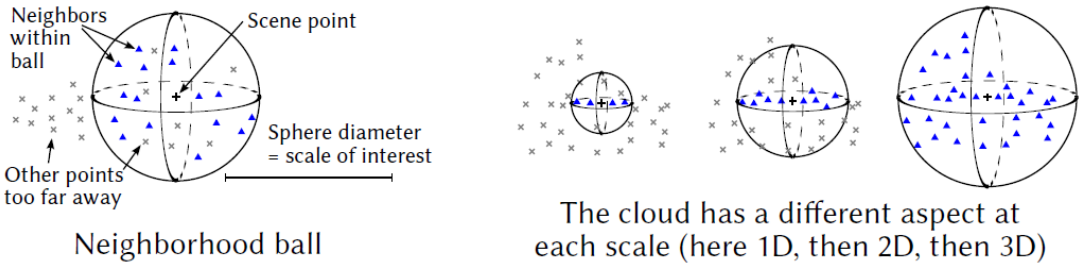


*Figure 2.6: Illustration of the way in which CANUPO assess a given point's dimensionality at varying scales to determine its classification. Blue triangles are neighbouring points being considered, grey crosses are outwith the sphere of interest. Taken from Brodu and Langue, 2011.*

Here, specific classifiers were created for use in separation of different vegetation types from sediment surfaces and the removal of tripod structures. Classifiers are created through a process of 'training' on a sub-sample of the data which provide discrete examples of the structures wishing to be classified; in this case sediment (which included bare mudflat and sections from within vegetation if possible), vegetation (of varying heights and densities) and tripods. The CANUPO trainer tool is loaded with two example sections and instructed at which scales it should evaluate a points dimensionality (set as 0.03, 0.05, 0.1, 0.25, 0.5 and 1 m). The trainer automatically evaluates each point and its neighbourhood within varying size (scale) spheres, applying a PCA within each, determining the ratio of

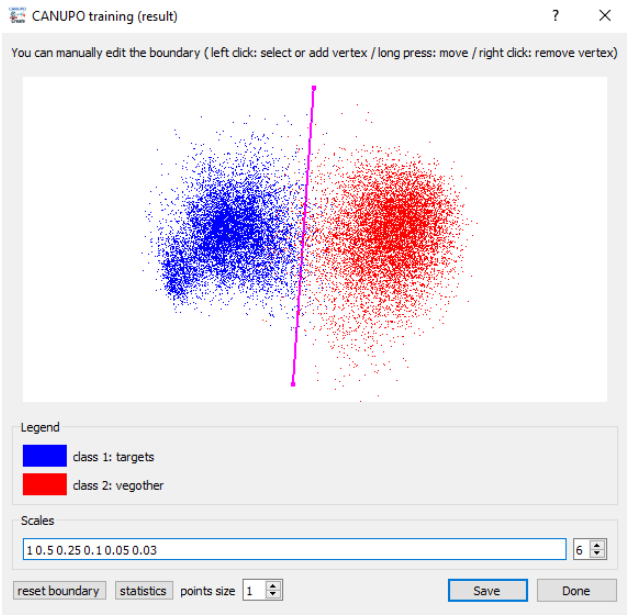


*Figure 2.7: Example output from the CANUPO classifier trainer, showing the data represented in a 2D plane with classes seperated by a movable pink spline.*

1D/2D/3D structures which best describes that class scale (Brodu and Lague, 2011). This constructs feature signatures for each class which best separate them, the trainer allows the user to manually alter the boundary of separation though the manipulation of their separation boundary on a 2D plot in the plane of maximum separability (Brodu and Lague, 2011). The trainer provides statistical information of its effectiveness in the form of:

- 'Balanced accuracy' (*ba*) values quantify the classifiers performance through assessment of falsely and truly classified points; where 50 % would indicate random class assignment (Brodu and Lague, 2011);
- 'Fisher Discriminant Ratio' (*fdr*) assesses the separability of the two classes, where the larger the value, the further the separation, and further, informs on the robustness of the balanced accuracy value to be *actually* distinguish between the classes (Brodu and Lague, 2011).

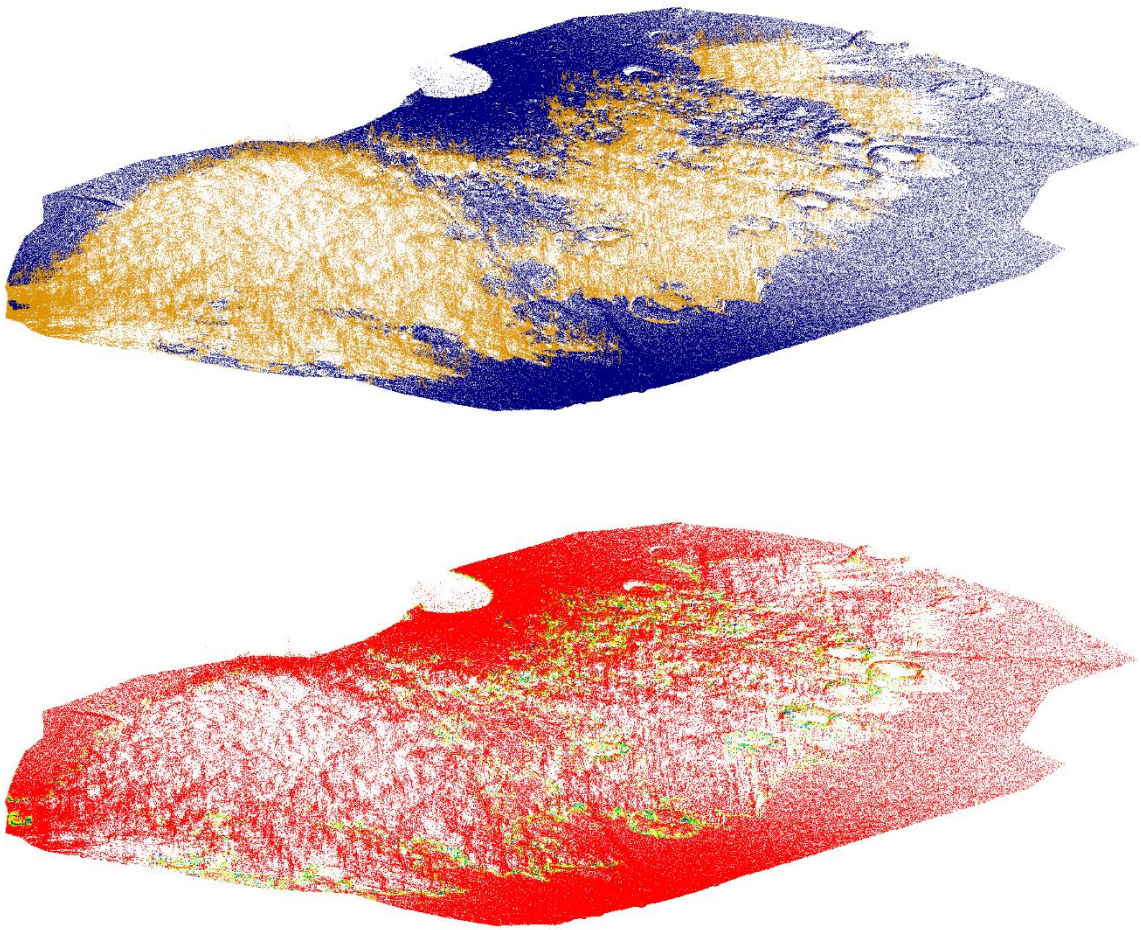

*Figure 2.8: Example of point cloud classification effectiveness on a different stand of B. maritimus vegetation to that used in CANUPO classifier training. Top image shows the 'classification' output from CANUPO, with blue classed as sediment and yellow as vegetation. Bottom image shows the 'confidence' of the classification on a typical 'heat' scalar from red (fully confident) through to blue (not confident) White space within the cloud section are were no data is present.*

Separate classifiers were created for the rush-type vegetation of *B. maritimus* and the grass-type marsh of *P. maritima* (*ba* = 95.2 %, *fdr* = 4.01). The *B. maritimus* classifier was trained using data of a restored stand on the south shore (*ba* = 99.7 %, *fdr* = 14.78), the classifier had satisfactory effectiveness for all areas of *B. maritimus* (for example, see Figure 2.8); indicating its broad spatial applicability of specific classifiers, as was found by Brodu and Lague (2011). Final classifiers were developed to remove tripod and targets that were present in the 'natural vegetation' sections. This was trained using classes of vegetation, sediment structures and tripod and target examples, being applied to the vegetation classified cloud in a second-level classification. The benefit of unsupervised classification in this fashion is that it should produce un-biased outputs on which analysis of vegetative carbon measurement can be based.

#### *2.6.1.1 LAStools*

*Lastools* is an independent set of software tools designed specifically for the fast and efficient processing of large LIDAR datasets. A useful feature is one which allows the classification of ground-points to generate a Digital Elevation/Terrain Model (DEM/DTM), or the extraction of the lowest points in user defined grid processing. These processes were evaluated on this data, to facilitate the extraction of accurate ground points. It was found that due to point-cloud shadowing, these approaches were not effective, with the resulting cloud containing many points with far higher elevation than expected for the sediment surface.

The separation of vegetation and sediment laser returns for all data was carried out using CANUPO which in testing proved to be the most effective at successful separation of these two structures.

## 2.7 Physical measurement conversions

As described previously the application of allometric scaling relationships to translate physical characteristics into data on the biomass and carbon content of vegetation can be highly useful and effective. In the current setting this is a preferable approach to minimise disturbance on the already degraded system. As such information from previous studies are used to provide biomass and carbon values from the extracted point cloud data.

### *2.7.1 Vegetative biomass*

A study of the allometric relationship between *B. maritimus* stem heights and biomass found a robust relationship ($R^2 = 0.686$), detailed in Equation 2, the study used 171 individual stems from the Eden Estuary (David, 2012).

$$Bm.dB\ (grams) = 0.026 \times\ l^{1.402}$$

*Equation 2*

Where *Bm.dB* is the dry biomass of a *B. maritimus* stem (g) and *l* is the length of the stem (cm). Stem density is also required to be known when calculating biomass. A density range of 324 - 736 stems/$m^2$ (1 stem per 30.68 - 13.57 $cm^2$) is used, based on previous research of *B. maritimus* marshes of the Eden Estuary (Maynard, 2014 and personal observations).

In the case of the *P. maritima* vegetation complex, no such local studies were available, therefore information from a different area was used, applying the assumption of their broad-scale applicability (Trilla et al., 2013). Engels and Jensen (2010) found that a second-order polynomial regression best represented the relationship of shoot length to dry biomass, explaining 58 % of the variance through Equation 3.

$$Pm.dB(grams) = (0.0001 \times l^2) + (0.0011 \times l)$$

*Equation 3*

Where *Pm.dB* is the dry biomass of a *P. maritima* tiller (g) and *l* is the length (cm). Density of tillers is calculated from work by Bos et al. (2005) who found an average density on un-grazed marsh of 3000 tillers/$m^2$.

### *2.7.2 Vegetation carbon content*

The carbon content correction factors of the two vegetation types studied are calculated from samples of vegetation taken in winter and summer and analysed through Elemental Analysis using a gas chromatography approach. Samples of above-ground vegetation were taken randomly from across the site in winter and summer 2017, for each species samples were taken from various locations within the site and processed together. Vegetation was freeze dried and finely-ground for analysis. No significant difference in carbon content of

dry biomass was found between seasons. A conversion factor of 0.35 was used for *B. maritimus* and 0.36 for the *P. maritima* complex (NVC SM13). Both values are lower than that suggested by Howard et al. (2014), but are within the 21 – 47 % range suggested by Radabaugh et al. (2017).

## 2.8 Point cloud analysis

Various approaches were taken during comparison and analysis of the processed point cloud data to best extract information of use in quantification of the vegetative carbon pool, and how this varies between vegetation types and with seasonal cycles.

### *2.8.1 Vegetation layer data*

Structural data on the heights of vegetation were extracted using the classification process of CANUPO in *CloudCompare* described previously. Once the clouds had been classified the resulting points classes were split into two separate clouds. These points retain their geographic information, specifically both location and elevation. The point data was converted to a raster format within *CloudCompare*. Briefly, this takes the objectively

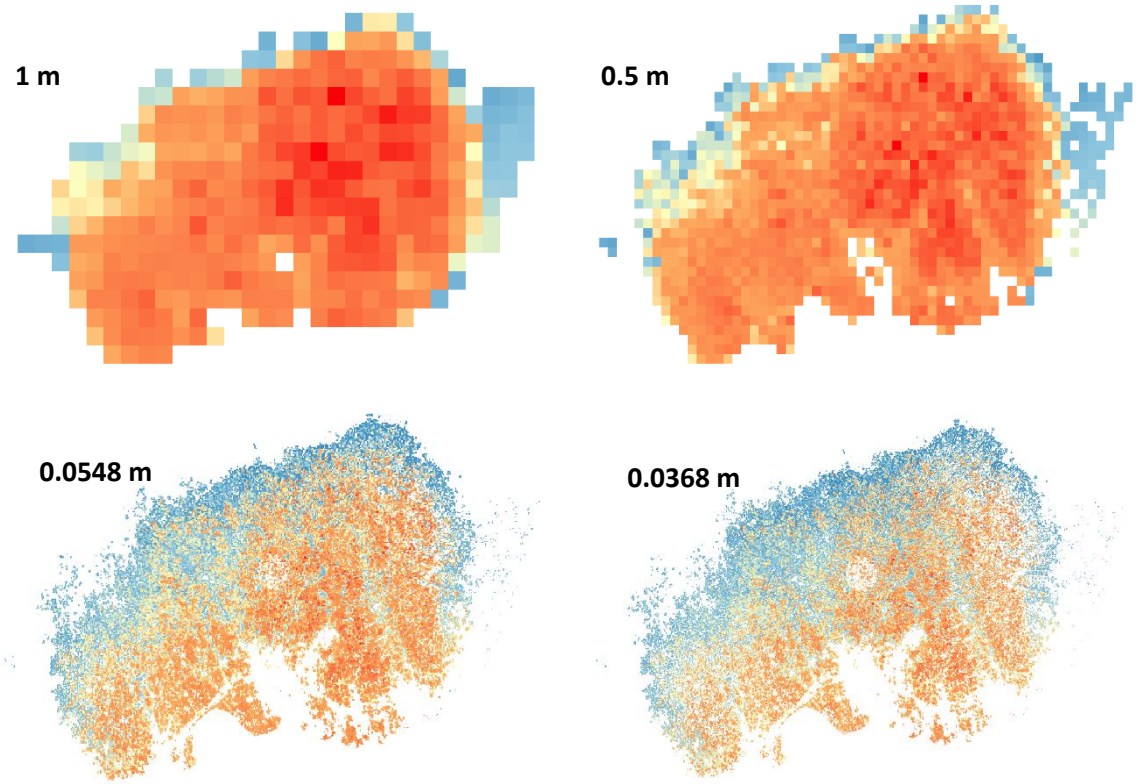


*Figure 2.9: Images of vegetation layer raster surfaces generated in CloudCompare from classified and separated vegetation point clouds. The variety of scales (pixel size in meters is shown), illustrates the way in which the resulting data differ. Larger pixel values take their value from more points, with finer scale rasters showing data gaps as white pixels. Pixels coloured based on absolute elevation value.*

classified 3D point cloud information and presents it as a 2D surface of pixels which contain information relating to the discreet ground point they cover, here being elevation in meters. The raster layer is populated with data pixels where any point is found to be within the defined grid square of the raster, if no points are present a 'no-value' pixel is generated (white). The total number of pixels which contain data can therefore also provide insight into the total area covered by vegetation at each site in each season.

Each raster was generated with a grid-cell (pixel) size range of 1 m, 0.5 m, 0.0548 m and 0.0368 m (1 and 0.5 m only in the case of *P. maritima*) (Figure 2.9), using maximum elevation of points to define the value of each pixel. 0.0548 and 0.0368 m pixels were used so that each cell represents the area which a single stem would occupy when applying measured natural density values of *B. maritimus*; 324 to 736 stems/$m^2$ or 1 stem per 30.68 and 13.57 $cm^2$, which gives squares with lengths of 5.48 cm and 3.68 cm, respectively. The approach of generating fine versus coarse scale raster layers hold different possible limitations; specifically, the resulting effective area being quantified (Table 6). In creating coarse, 1 m and 0.5 m, raster layers, there is the potential to expand the area being quantified as a pixel will be generated from the presence of a single laser return point within the given grid square, this is most likely to occur at the fringing edge of the vegetation. Under fine scale raster creation, 0.0548 m and 0.0368 m, issues could arise through the multiple pixel generation of a single stem due to movement beyond the vertical of a stem during scanning, placing points in multiple grid squares. On average, coarse scale raster layers (1 m and 0.5 m) are 81 % larger than their fine scale (0.0548 m and 0.0368 m) counterparts; this will have subsequent influence on the calculation of biomass and carbon content.

*Table 6: Area coverage ($m^2$) of each raster layer created from point cloud data in CloudCompare. Areas are calculated based on the number of pixels in each raster and their known size.*

| ***Site*** | **Raster scale** | | | |
|---|---|---|---|---|
| | **1 m** | **0.5 m** | **0.0548 m** | **0.0368 m** |
| ***Winter north shore restored area*** | 135 | 109.75 | 52.53 | 44.92 |
| ***Winter north shore natural area*** | 5907 | 5489.75 | 3363.71 | 2805.52 |
| ***Winter south shore restored area*** | 367 | 323.50 | 226.89 | 200.27 |
| ***Winter south shore natural area*** | 22292 | 21421 | | |
| ***Summer north shore restored area*** | 147 | 130.25 | 84.71 | 78.05 |
| ***Summer north shore natural area*** | 6243 | 5874.75 | 3931.13 | 3339.70 |
| ***Summer south shore restored area*** | 406 | 368.25 | 275.78 | 244.81 |
| ***Summer south shore natural area*** | 22384 | 21437.25 | | |

At the different scales each cell (pixel) of the raster utilises a different number of points to define its' value, in general the larger the pixel, the higher number of points there are which fall within it. The balance between averaging over a 'large' area and the production of 'no-data' pixels at finer scale due to lack of points is important to consider; where the former will possibly reduce over estimation of height from erroneous points, however the latter perhaps provides a more accurate representation of the actual vegetation present. These raster layers were exported for further processing in *QGIS 3.2.1 Bonn*.

### *2.8.2 Sediment surface data*

It is necessary to extract structural information of the sediment surface layer to later compute actual vegetation heights above this surface; as detailed above, and all points retain their elevation value, which is their height above sea-level. A similar approach was taken as used to extract a vegetation data layer. The classified cloud output from CANUPO was separated and the sediment layer used to generate a raster surface. The classified sediment

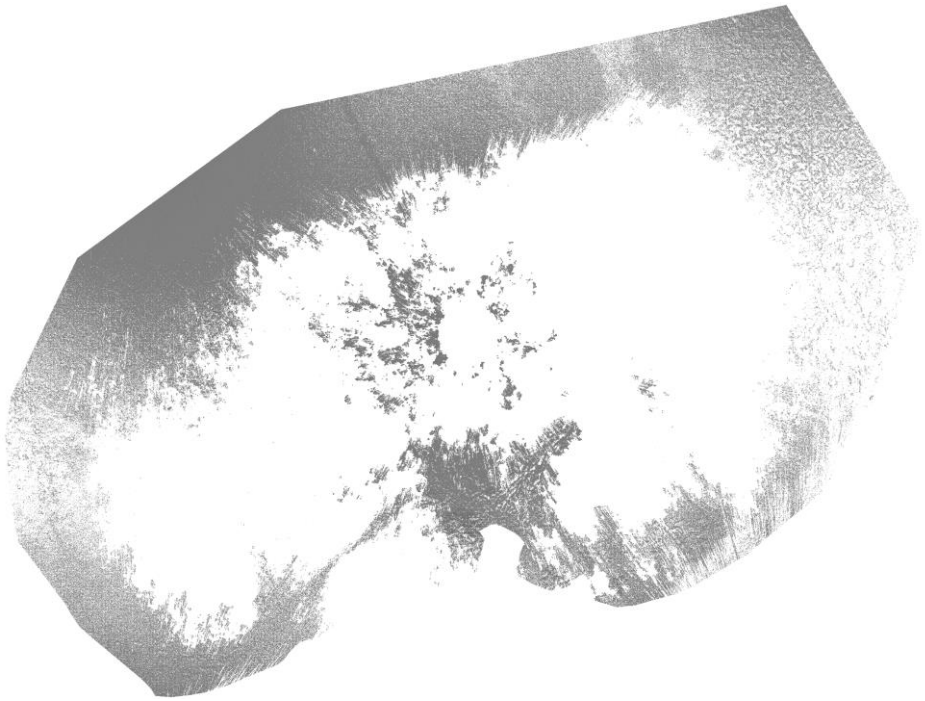

*Figure 2.10: Example output of separated point cloud classified as sediment using CANUPO in CloudCompare, illustrating the gaps in data primarily where vegetation was present. Approximately 25 m across, containing 23,218,427 points.*

surface layers typically ended up being point sparse (Figure 2.10), a result of either, a lack of actual laser returns from the sediment within vegetation due to shadowing or loss through false classification when applying the CANUPO algorithm. Raster layers with a grid (pixel)

size of 0.5 m were generated from this point-sparse data. Values were calculated using an average of all points within each cell. To address this during the rasterization process, the software was instructed to interpolate the values for missing cells, using nearest neighbour elevation averages to compute their value; giving full-unbroken raster surface, as required in further processing.

### *2.8.3 Vegetation height extraction*

The two raster surfaces (sediment and vegetation layers) for each area in each season were used to create a new layer whose information relates to the absolute heights of vegetation above the mapped sediment. Raster files were analysed in the *QGIS 3.2.1 Bonn* (QGIS Development Team (2018). QGIS Geographic Information System. Open Source Geospatial Foundation Project). In general, a season specific 0.5 m resolution sediment raster was used to as the 'ground' layer; however, this was not possible for the natural (*B. maritimus*) stand on the north shore in summer due to insufficient data points, as such the winter sediment layer was used. To attain vegetation height information the 'Raster Calculator' function was employed, to create a new raster of the difference between the two layers (Figure 2.11); furthermore, a mask was applied to ensure no negative values were included in the new raster (Equation 4). Such values could be generated through errors in classification of 'sediment' and 'vegetation' points, and although these are typically small, negative values cannot be considered during further biomass and carbon calculations.

$$Vegetation\_height\_raster\ (m) = \big((Vegetation\_raster\_Sm - Sediment\_raster\_5m) \geq 0\big) \times (Vegetation\_raster\_Sm - Sediment\_raster\_5m)$$

*Equation 4*

In the above equation, vegetation and sediment raster layers of the same site were used, where '*Sm*' was the scale of a given vegetation raster layer. During calculation, the extent of the resulting raster was set to follow that of the input vegetation layer, so maintaining the correct area.

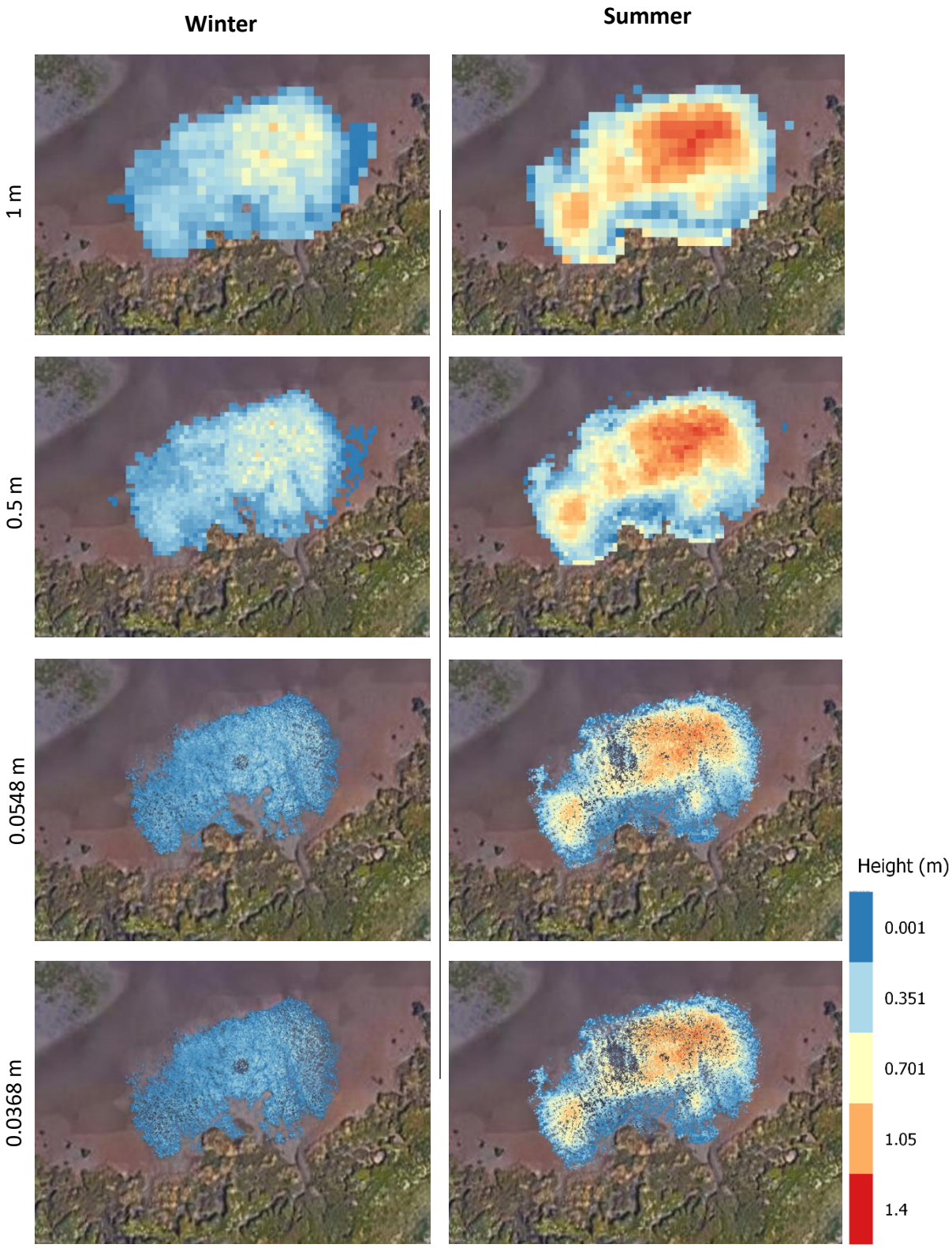


*Figure 2.11: Example of mapped raster images showing actual vegetation heights in winter and summer for an area of restored marsh on the south shore of the Eden Estuary. Rasters were calculated at different scales from 0.0368 m to 1 m.*

### *2.8.4 Biomass and carbon content conversion*

The new vegetation height raster data allowed calculation of carbon content through the application of allometric scaling relationships to biomass, as described Equation 2 and Equation 3. These were coupled with relevant species-specific shoot density multiplication (in the case of 1 m and 0.5 m pixels) and the respective carbon content values; together shown in Equation 6 and Equation 9.

$$(B.maritimus)\ 1\ m\ Biomass\_content\_raster\ (g/C/pixel) = (530 \times (0.0026 \times (Vegetation\_height\_raster \times 100)^{1.042}))$$

*Equation 5*

$$(B.maritimus)\ 5\ m\ Biomass\_content\_raster\ (g/C/pixel) = ((530/4) \times (0.0026 \times (Vegetation\_height\_raster \times 100)^{1.042}))$$

*Equation 6*

$$(B.maritimus)\ Finescale\ Biomass\_content\_raster\ (g/C/pixel) = 0.0026 \times (Vegetation\_height\_raster \times 100)^{1.042})$$

*Equation 7*

Where *530* (Equation 5 & Equation 6) is the average stem density of *B. maritimus* per $m^2$ (Section 2.7.1); Equation 5 is used to calculate biomass for 1 m resolution raster data, Equation 6 'density' is quartered for calculating biomass for 0.5 m (0.25 $m^2$) resolution raster data. Equation 7 is applied to both fine scale raster layer data, where density is not included as each 'value' pixel is assumed to represent a single stem. The vegetation height raster layers are multiplied by 100 to transform from meters to centimetres.

$$(P.maritima)\ 1\ m\ Biomass\_content\_raster(g/C/pixel) = 3000 \times (0.0001 \times (Vegetation\_height\_raster \times 100)^2) + \left(0.0011 \times (Vegetation\_height\_raster \times 100)\right)$$

*Equation 8*

$$(P.maritima)\ 0.5\ m\ Biomass\_content\_raster(g/C/pixel) = (3000/4) \times (0.0001 \times (Vegetation\_height\_raster \times 100)^2) + \left(0.0011 \times (Vegetation\_height\_raster \times 100)\right)$$

*Equation 9*

Where 3000 is the number of tillers per $m^2$ (Bos et al., 2005), Equation 8 is used when calculating biomass for the 1 m resolution ratser data and Equation 9 when applying to 0.5 m (0.25 $m^2$) raster. The vegetation height raster is multiplied by 100 to transform from meters to centimetres.

The biomass quantity raster layers are converted to a carbon content value through the application of a specific conversion factor; 0.35 (35 %) for *B. maritimus* and 0.36 (36 %) for *P. maritima.*

## 2.9 Statistical analysis

Analysis of seasonal influence on vegetation height was made. A series of unpaired t-tests were compared winter and summer data, applying the tests to data from the two rasters of the same area as generated at the same resolution, for example *winter* and *summer* of the *North Shore*, *Restored* area at *1m* raster scale. Further unpaired t-tests were run in the same fashion, however these compared winter data to masked summer data, which restricted comparison of vegetation height changes across the same areal extent. Data for the tests were the average height values of each pixel within a raster. Analysis was also carried out on the differences of seasonal change in vegetation height between the north and south shore restored sites using a Wilcoxon test.

## 2.10 Hypotheses – vegetative carbon

Data in this chapter assess how the vegetative carbon component of the study area differs between area types and the influence of season on this. The study held the following hypotheses:

- Different vegetation area types (*P. maritima* and *B.maritimus*) would hold different amounts of carbon.

- Restored vegetation would display different carbon storage capacity than its natural counterpart.
- Different vegetation area types would display different carbon store relationships with season.

## 2.11 Vegetation analysis results

### *2.11.1 Seasonal difference in height*

The seasonal changes in vegetation height of *B. maritimus* and *P. maritima* were extracted from 3D point cloud data which were converted to raster format for analysis and further processed using the statistical analysis software R (R Core Team, 2016) and the packages 'ggplot2' (Wickham, 2016), 'raster' (Hijmans and Etten, 2012) and 'dplyr' (Wickham et al., 2017). All sites presented changes in vegetation heights between seasons, with increases in height in summer compared to winter. Data were analysed using a series of unpaired t-tests since although seasonal raster layers were spatially aligned, their individual grid layout were not – where necessary non-normal data were transformed to assess the difference between winter and summer vegetation heights, and further, to compare vegetation heights between sites. Data were extracted from the raster data to create data frames where pixel values were stored in individual rows within a column.

#### *2.11.1.1 Seasonal difference in vegetation heights – Restored sites*

The restored site of *B. maritimus* on the north shore had an average vegetation height (across raster data scales) of 0.086 m in winter and 0.156 m in summer, a significant difference of 0.07 m; $t(d.f. = 79225) = 116.53$, $p < 0.001$ (transformed: sqrt(x+0.0005)). In winter vegetation heights were skewed to the left (shorter); with a large proportion of values falling very close to zero, especially visible in the fine scale raster data (Figure 2.13). In summer, data was more distributed across the range, with maximum vegetation heights also increasing for all sites. The difference in vegetation height, as measured using different raster scales was assessed, full extent data for each scale in each season. Secondly, initial winter extent data was used to mask summer data and compare just those common areas (excluding the influence of summer expansion) (Figure 2.12). Analysis of vegetation height data using each full raster layer's extent were:

- 1 m raster gives a mean height of 0.187 m in winter and 0.321 m in summer, a significant growth of 0.133 m; $t(d.f. = 272.03) = 116.53$, $p < 0.001$.

- 0.5 m raster gives a mean height of 0.145 m in winter and 0.254 m in summer, a significant growth of 0.109 m; t(d.f. = 910.8) = 14.552, p < 0.001.
- 0.0548 m raster gives a mean height of 0.087 m in winter and 0.164 m in summer, a significant growth of 0.076 m; t(d.f. = 29155) = 74.775, p < 0.001 (transformed: sqrt(x+0.0005)).
- 0.0368 m raster gives a mean height of 0.083 m in winter and 0.15 m in summer, a significant growth of 0.068 m; t(d.f. = 48949) = 91.315, p <0.001 (transformed: sqrt(x+0.0005)).

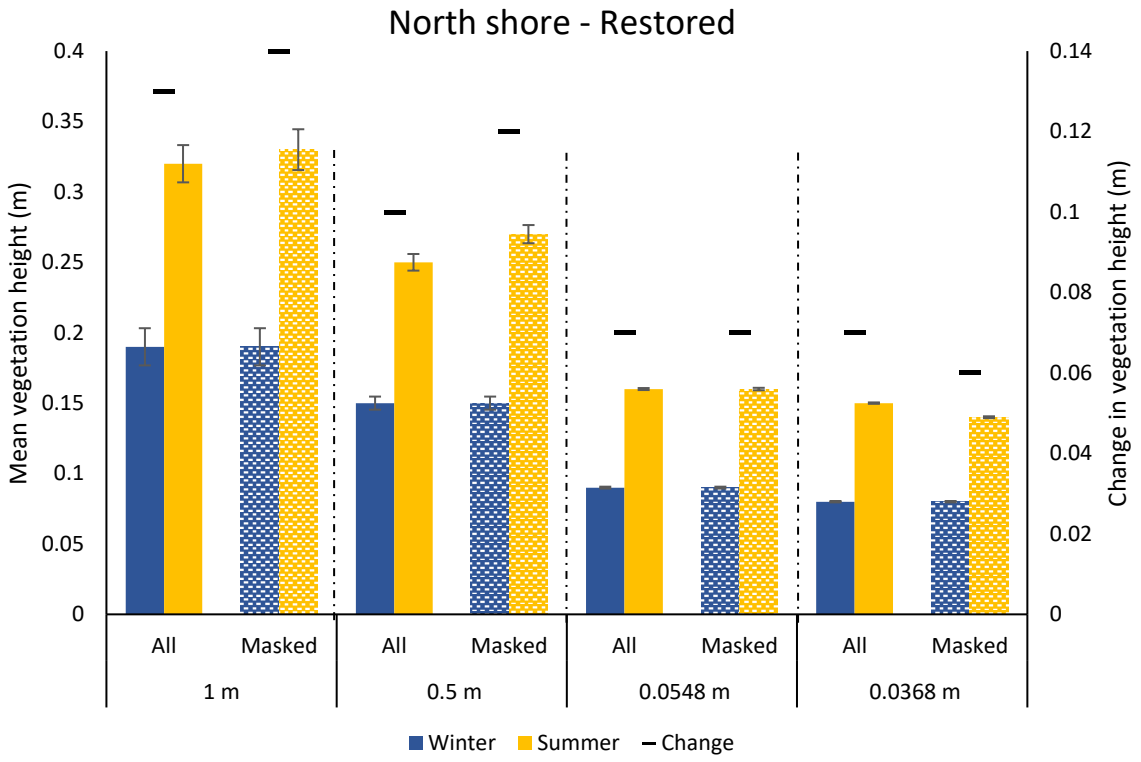


*Figure 2.12: Mean vegetation heights of restored (B. maritimus) vegetation of the* ***north shore*** *as measured at different raster scales; using both full datasets (solid) and with a mask applied to the summer data generated from the winter extent (dotted). Also showing change in vegetation height between winter and summer (short black lines). Error bars show standard error of the mean.*

When applying a mask to the summer data of the corresponding winter raster, the results were as follows:

- 1 m raster gives a mean height of 0.187 m in winter and 0.325 m in summer, a significant growth of 0.138 m; t(d.f. = 250.29) = 7.0192, p < 0.001.
- 0.5 m raster gives a mean height of 0.145 m in winter and 0.265 m in summer, a significant growth of 0.12 m; t(d.f. = 764.08) = 15.122, p < 0.001.

- 0.0548 m raster gives a mean height of 0.087 m in winter and 0.158 m in summer, a significant growth of 0.071 m; t(d.f. = 28764) = 51.204, p < 0.001 (transformed: sqrt(x+0.0005)).
- 0.0368 m raster gives a mean height of 0.083 m in winter and 0.143 m in summer, a significant growth of 0.061 m; t(d.f. = 50932) = 58.175, p < 0.001 (transformed: sqrt(x+0.0005)).

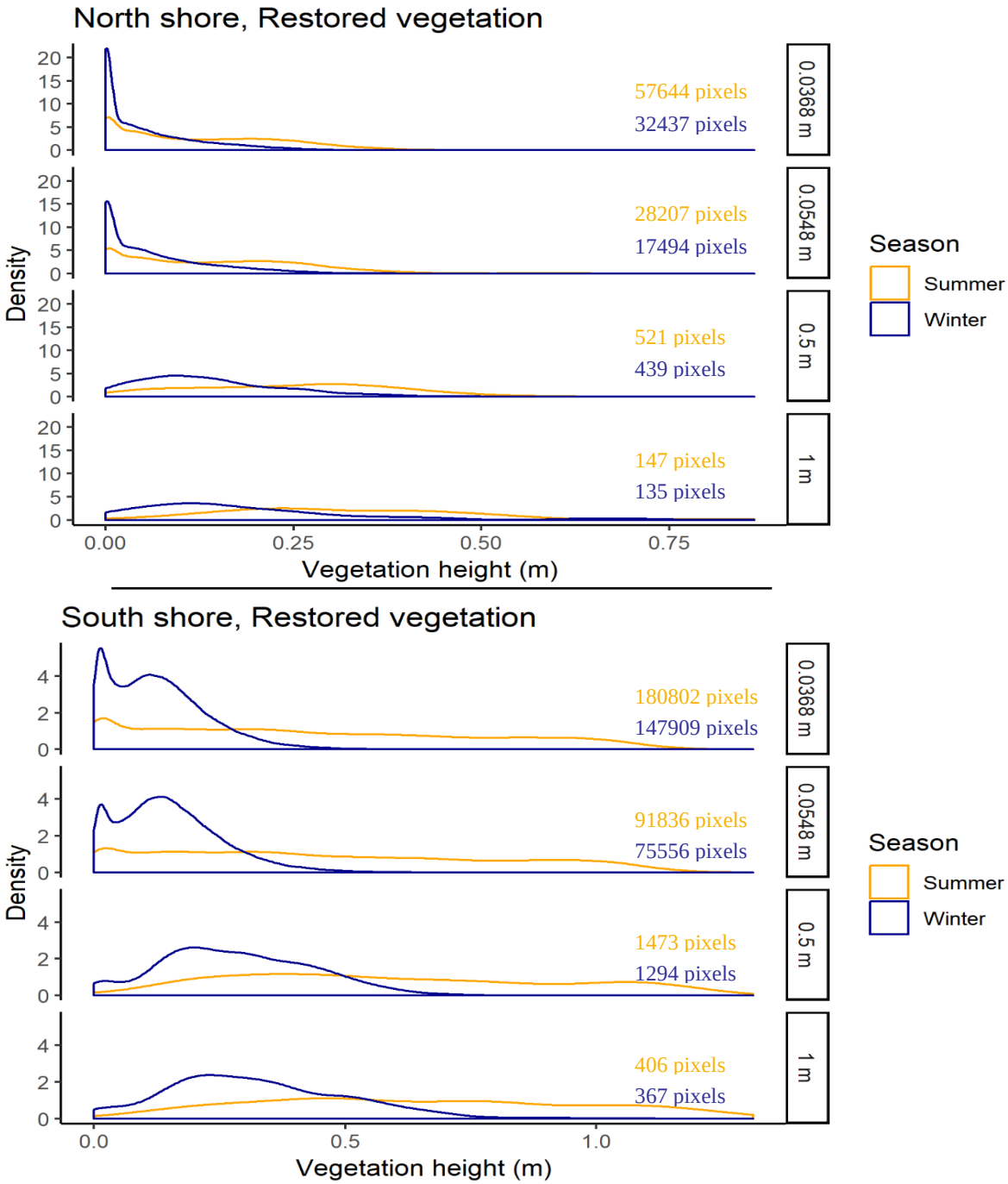


*Figure 2.13: Seasonal density curves for both restored sites (top = north shore, bottom = **south shore**) plotting the frequency of pixels within vegetation height (cm) bins; where widths are defined by the 'height range'/30. Each season showing data extracted when using four different scales - 1 m, 0.5 m, 0.0548 m and 0.0368 m; the number of pixels present in each raster are also shown.*

For the south shore restored site of *B. maritimus* there was an average vegetation height of 0.141 m in winter and 0.466 m in winter; a significant average increase of 0.325 m; t(d.f. = 423110) = 474.15, $p < 0.001$. Vegetation height distribution alters between winter and summer, displaying a similar trend to that seen at the north shore restored site (Figure 2.13). The difference in vegetation height as measured using different scale raster was assessed, full extent data for each scale in each season. Secondly, initial winter extent data was used to mask summer data and compare just those common areas (excluding the influence of summer expansion) (Figure 2.14). Analysis of vegetation height data using each full raster layer's extent were:

- 1 m raster gives a mean height of 0.321 m in winter and 0.649 m in summer, a significant growth of 0.327 m; t(d.f. = 631) = 17.91, $p < 0.001$.
- 0.5 m raster gives a mean height of 0.288 m in winter and 0.649 m in summer, a significant growth of 0.313 m; t(d.f. = 2132.2) = 33.32, $p < 0.001$.
- 0.0548 m raster gives a mean height of 0.154 m in winter and 0.47 m in summer, a significant growth of 0.324 m; t(d.f. = 141560) = 272.08, $p < 0.001$ (transformed: sqrt(x+0.0005)).
- 0.0368 m raster gives a mean height of 0.132 m in winter and 0.46 m in summer, a significant growth of 0.327 m; t(d.f. = 275990) = 393.65, $p < 0.001$ (transformed: sqrt(x+0.0005)).

When applying a mask to the summer data of the corresponding winter raster, the results were as follows:

- 1 m raster gives a mean height of 0.321 m in winter and 0.686 m in summer, a significant growth of 0.365 m; t(d.f. = 537.69) = 19.146, $p < 0.001$.
- 0.5 m raster gives a mean height of 0.288 m in winter and 0.654 m in summer, a significant growth of 0.366 m; t(d.f. = 1729.1) = 36.626, $p < 0.001$.
- 0.0548 m raster gives a mean height of 0.154 m in winter and 0.559 m in summer, a significant growth of 0.405 m; t(d.f. = 100770) = 324.59, $p < 0.001$ (transformed: sqrt(x+0.0005)).
- 0.0368 m raster gives a mean height of 0. 132 m in winter and 0.544 m in summer, a significant growth of 0.412 m; t(d.f. = 170610) = 452.16, $p < 0.001$ (transformed: sqrt(x+0.0005)).

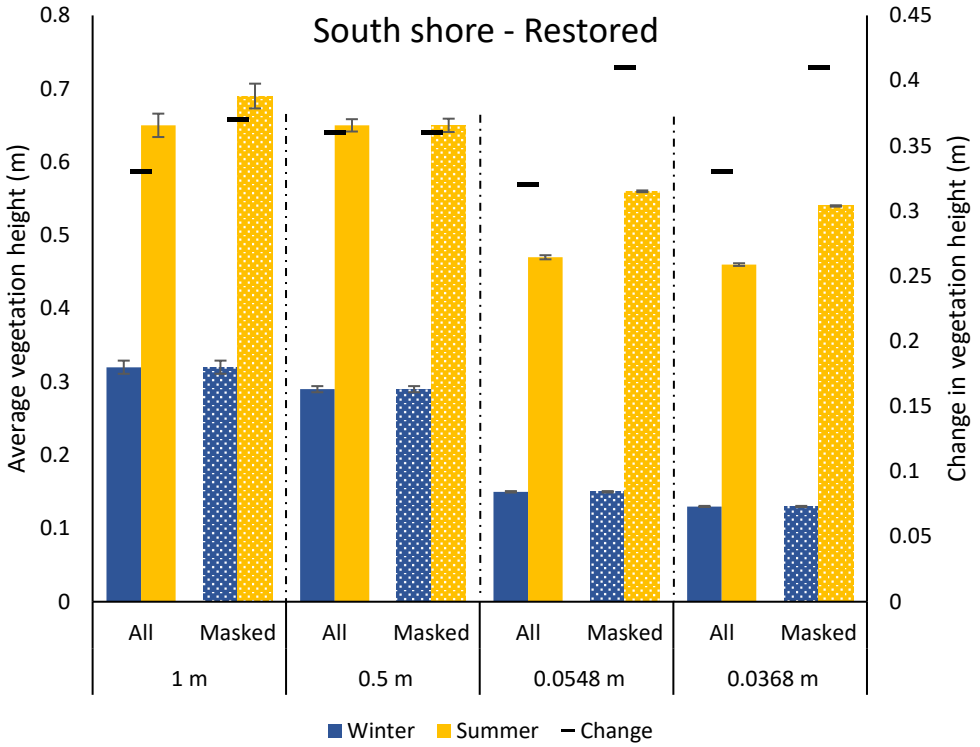


*Figure 2.14: Mean vegetation heights of restored (B. maritimus) vegetation of the **south shore** as measured at different raster scales; using both full datasets (solid) and with a mask applied to the summer data generated from the winter extent (dotted). Also showing change in vegetation height between winter and summer (short black lines). Error bars show standard error of the mean.*

#### *2.11.1.2 Seasonal difference in vegetation heights – Natural areas*

Natural areas studied comprised a mono-culture sward of the rush *B. maritimus* on the north shore of the estuary and a complex community of *P. maritima* (NVC SM13) to the south. The distribution of vegetation height values follows similar trends to those occurring in restored areas (Figure 2.16); whereby height distributions move to the right, illustrating an increased number of taller plants. As occurred at the restored sites, there was an expansion of the effective area of vegetation being quantified, as determined by pixel count and their known size, though proportionally this difference was negligible.

The average height of *B. maritimus* vegetation was 0.103 m in winter and 2.052 m in summer, a significant positive change of 1.949 m; t(d.f. =5161300) = 10670, $p < 0.001$. The distribution of height values transition between being dominated by short vegetation to taller stems (Figure 2.16, Upper chart). When assessing the change in vegetation height between seasons using the full extent of the raster layers at the four scales all data indicate a significant difference between winter and summer (Figure 2.15), as follows:

- 1 m raster data had an average height of 0.369 m in winter and 2.364 m in summer, a significant growth of 1.978 m; t(d.f. = 11205) = 402.59, $p < 0.001$.

- 0.5 m raster data had an average height of 0.277 m in winter and 2.286 m in summer, a significant growth of 1.984 m; t(d.f. = 39423) = 789.03, p < 0.001.
- 0.0548 m raster data had an average height of 0.111 m in winter and 2.073 m in summer, a significant growth of 1.918 m; t(d.f. = 1907500) = 5984.8, p < 0.001.
- 0.0368 m raster data had an average height of 0.096 m in winter and 2.039 m in summer, a significant growth of 1.899 m; t(d.f. = 3542700) = 8165.9, p < 0.001.

The average height of *P. maritima* vegetation was 0.192 m in winter and 0.289 m in summer, a significant average increase of 0.097 m; t(d.f. = 204800) = 130.86, p < 0.001. The distribution of vegetation heights (Figure 2.16, Lower chart) do not show as drastic a shift as found with *B. maritimus* vegetation, however there is still an increase in the proportion of taller vegetation. Comparing the heights of vegetation between winter and summer within scale data all present significant differences, as follows:

- 1 m raster data had an average vegetation height of 0.267 m in winter and 0.374 m in summer, a significant difference of 0.107 m; t(d.f. = 42942) = 50.034, p < 0.001 (transformed: sqrt(x+0.0005)).
- 0.5 m raster data had an average vegetation height of 0.182 m in winter and 0.278 m in summer, a significant difference of 0.095 m; t(d.f. = 58900) = 87.74, p < 0.001 (transformed: sqrt(x+0.0005)).

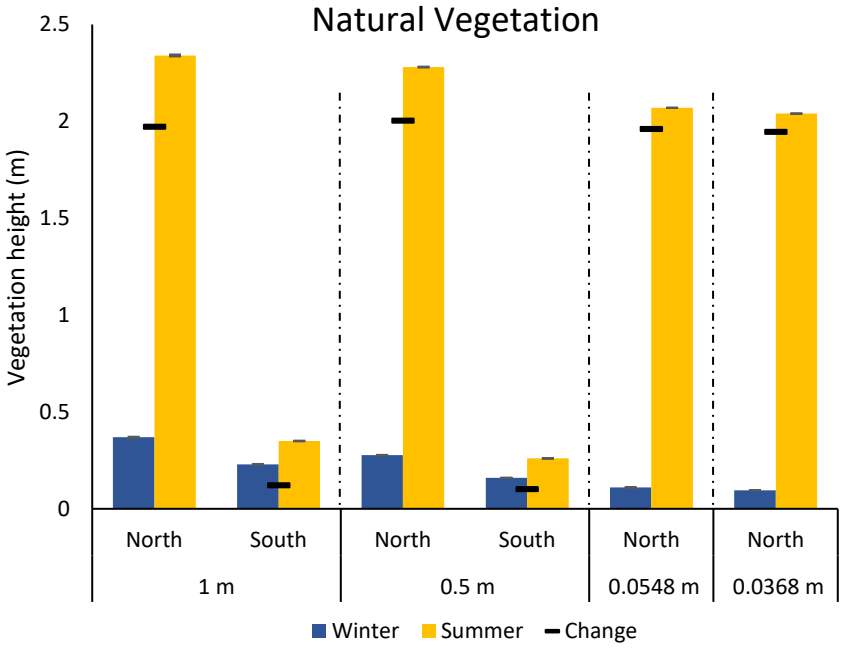


*Figure 2.15: Mean vegetation heights in natural extents of B. maritimus in the **north** and P. maritima in the **south**. Vegetation heights were calculated from different raster scale data. Also showing the change between winter and summer.*

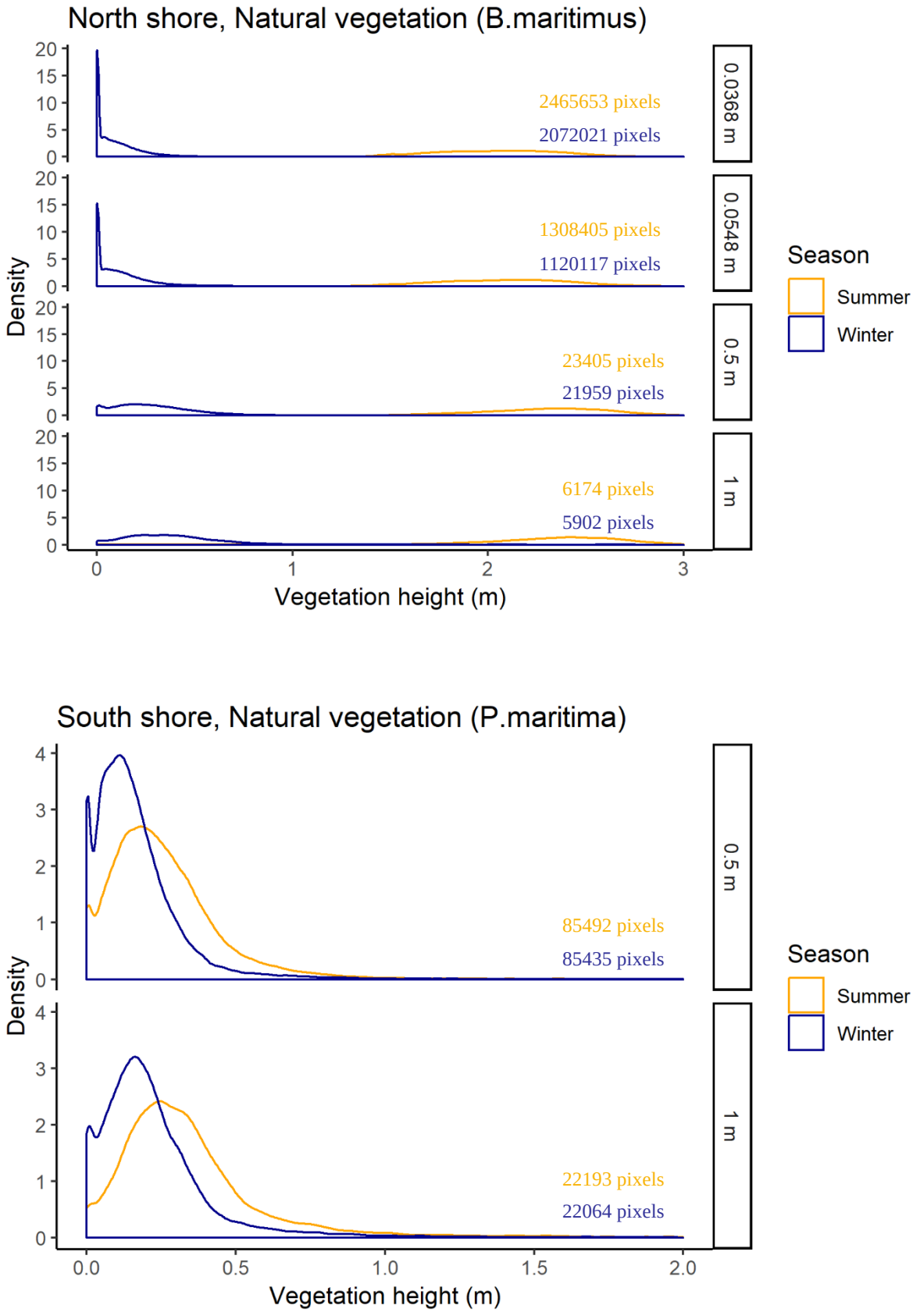


*Figure 2.16: Seasonal density curves for both natural areas (top = <u>B.maritimus</u> on the **north shore**, bottom = <u>P.maritima</u> on the **south shore**) plotting the frequency of pixels within vegetation height (cm) bins; where widths are defined by the 'height range'/30. Each season data was extracted using different scales - 1 m, 0.5 m, 0.0548 m and 0.0368 m (1 m and 0.5 m only for the south shore); the number of pixels present in each raster are also shown.*

### *2.11.1.3 Comparison of B. maritimus height between restored sites*

The two restored sites, on the north and south shores of the estuary, experience different abiotic conditions. For example, due to their respective place in the tidal frame or the prevailing topography of the area. For the northern site, an immediate vertical stone façade confines the marsh area while in the south, a small stepped natural saltmarsh platform has been formed. These differences are extended through to their respective vegetative extent and quantities.

As evident in the comparison of seasonal difference within restored sites, both across scales and at each scale, the north and south shore appear to display different vegetative characteristics; whereby the north shore vegetation is consistently shorter in stature. This difference is further extended to the quantity of vegetative material which cycles (growth) through the seasons.

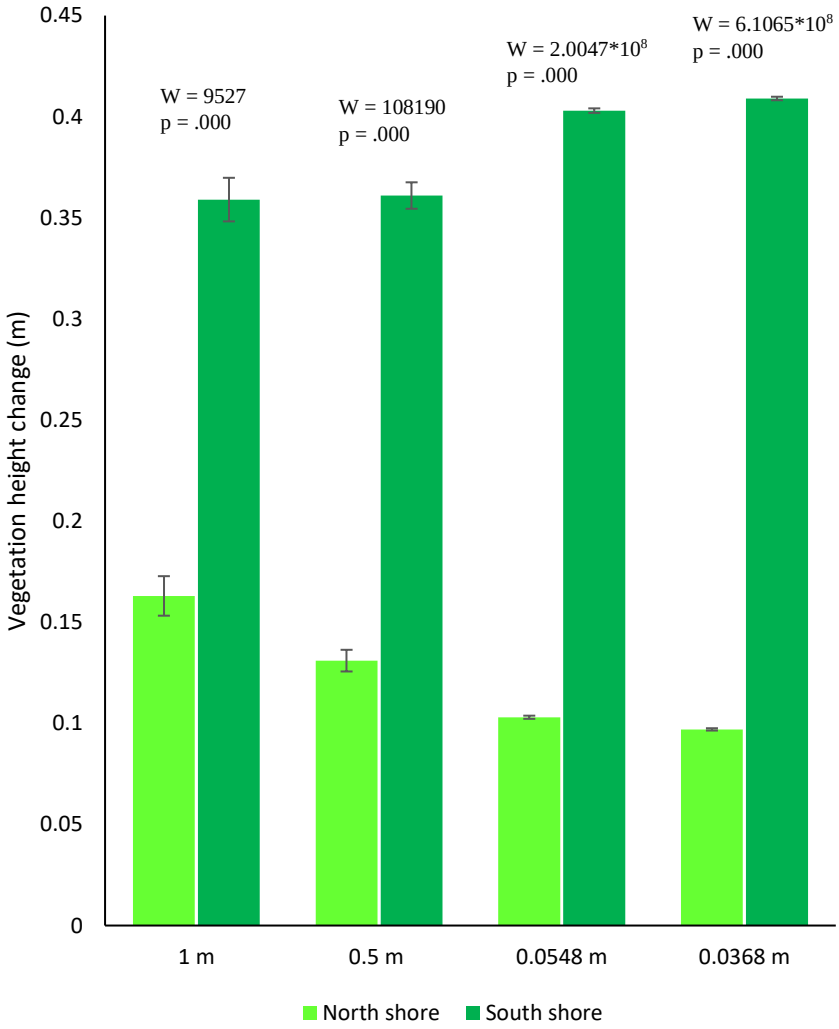


*Figure 2.17: Mean changes in vegetation height between winter and summer for the **north** and **south shore** sites, calculated from four raster scales created from point cloud data. Showing standard error bars and Wilcoxon rank sum test which compared between sites at each scale.*

The average increase between winter and summer was a growth of 0.124 m for the north shore site and 0.383 m for the south shore. At all scales used to calculated change in vegetation height (Figure 2.17) there was as a significant difference between sites, with the south shore showing significantly more growth than during the period than the north shore vegetation.

When assessing the respective proportional changes with season at the north and south shore there was a more similar trend between the two sites, specifically when assessing at coarse scale raster data level (Figure 2.18). At both the 1 m and 0.5 m resolution, the data show that, proportionally, vegetation of the north shore had more growth than that of the south shore. There was no significant difference in this proportional change when assessing data from the 1 m raster layer, however this difference becomes significant as the scale

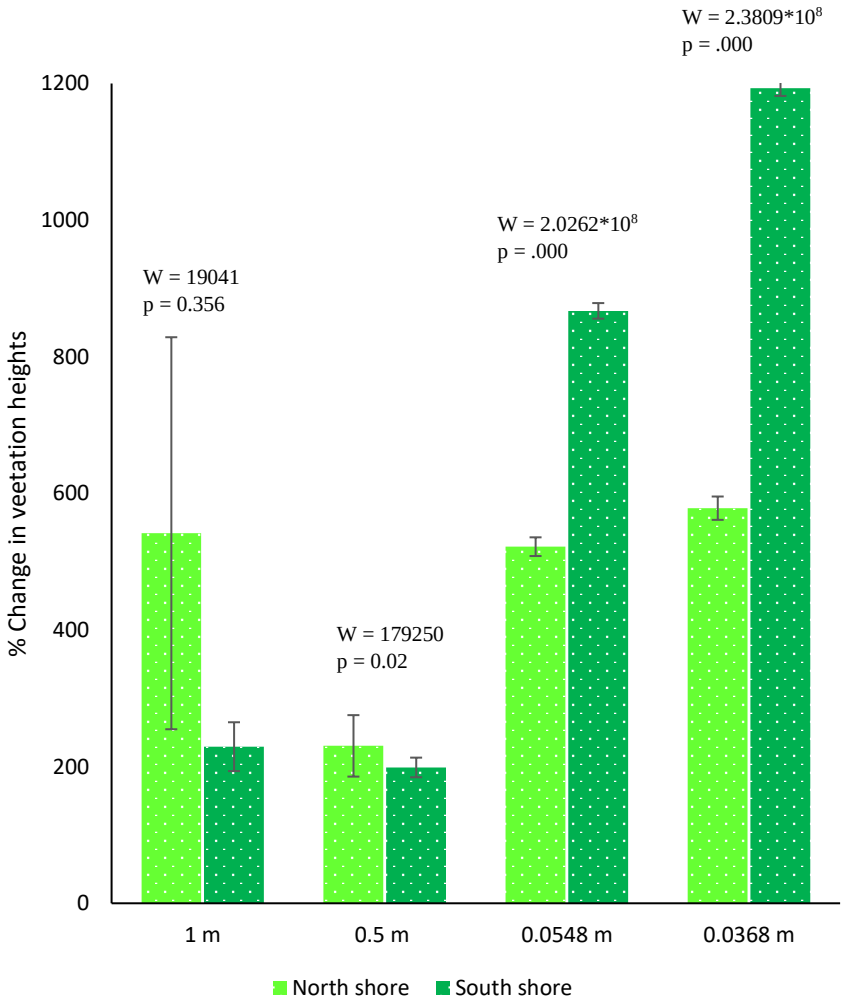


*Figure 2.18: Mean percentage increase of vegetation heights between winter and summer in restored sites on the **north** and **south shore** of the Eden Estuary, quantified at four different scale of raster data. Showing standard error bars and Wilcoxon rank sum test which compared between sites at each scale.*

decreases (Figure 2.18). In all instances, there was at least a four-fold increase in vegetation heights, signifying a large site-specific change with season and ultimately to the effective size of the biomass and carbon pools at any given time point.

The growth regimes of both restored areas were then compared to that of the large natural stand of *B. maritimus* on the north shore; no comparison was made with the *P. maritima* marsh of the south shore as an example of a very different vegetation type and not relevant to evaluating the current restored areas against a 'natural' example.

The average proportional change measured across the natural stand of *B. maritimus*, at all data scales; was 1016 % at 1 m, 1539 % at 0.5 m, 3994 % at 0.0548 m and 4709 % at 0.0368 m, an average of 2814 %. In a Wilcoxon rank sum pairwise comparison for all data scales at both restored sites and the natural stand all differences between restored vegetation and natural were significantly different. In all cases results indicate that the natural stand of vegetation exhibits significantly more growth during summer than does either restored site.

### *2.11.2 Seasonal change in carbon*

The seasonal change in vegetation comprises of both vertical growth and lateral expansion, both of which are evident at all sites, and are both important in the generation of biomass and carbon content quantity. Expansion is quantified using the returned raster pixel data extracted from the 3D point cloud data (see Table 6).

The area of vegetation along with its measured height at all sites (taken from raster data) is used in the quantification of biomass and carbon quantities, through the application of Equation 6 and Equation 9 for biomass and the subsequent conversion to carbon content, being 35 % for *B. maritimus* and 36 % for *P. maritima*.

#### *2.11.2.1 Seasonal change in carbon – Restored sites*

As presented in the previous sections, the restored sites of the estuary both present an expansion in their coverage and significantly increase in height. Hence, resulting in differences of the measured biomass and carbon store of *in situ* vegetation at different times of year.

There was an average expansion from winter to summer (across raster scales) of 24.7 $m^2$ and 44.3 $m^2$, at the north and south shore restored sites, respectively. Across scales (1 m to 0.0368 m) there was a range in expansion area of 12 $m^2$ to 34.13 $m^2$ in the north restored site and 39 $m^2$ to 48.89 $m^2$ in the south restored site. The data indicate that during summer there was possibly an increase in the number of shoots, shown by the increase in the total

number of pixels within the fine scale (0.0548 m and 0.0368 m) raster data (Figure 2.13); due to each pixel effectively representing a single stem (based on assumed vegetation density values). Taking the area being quantified from the number of pixels (Table 6), there was a larger difference between winter and summer for finer scale raster layers than coarser scales:

- The north shore site shows percentage increases of 8.9 %, 18.7 %, 61.3 % and 73.8 % for raster scales of 1 m, 0.5 m, 0.0548 m and 0.0368 m, respectively;
- The south shore site shows percentage increases of 10.6 %, 13.8 %, 21.6 % and 22.2 % for raster scales of 1 m, 0.5 m, 0.0548 m and 0.0368 m, respectively.

The effect of summer expansion is important to consider in determining carbon content, as mentioned both areas exhibit such a trend along with an increase in the height of vegetation; two factors which directly influence the amount of carbon being measured as stored (Figure 2.19, Figure 2.20). The north shore restoration site exhibits less absolute expansion than the south shore, however, there is still a large proportion of carbon 'growth' attributed to this new vegetation; ranging from 13 % of the total summer carbon stock when assessed at the coarse scale, rising to 42 % when considered at fine raster scales (Figure 2.19); these proportional increases in carbon present in the area do not correlate with the expansion in areal extent.

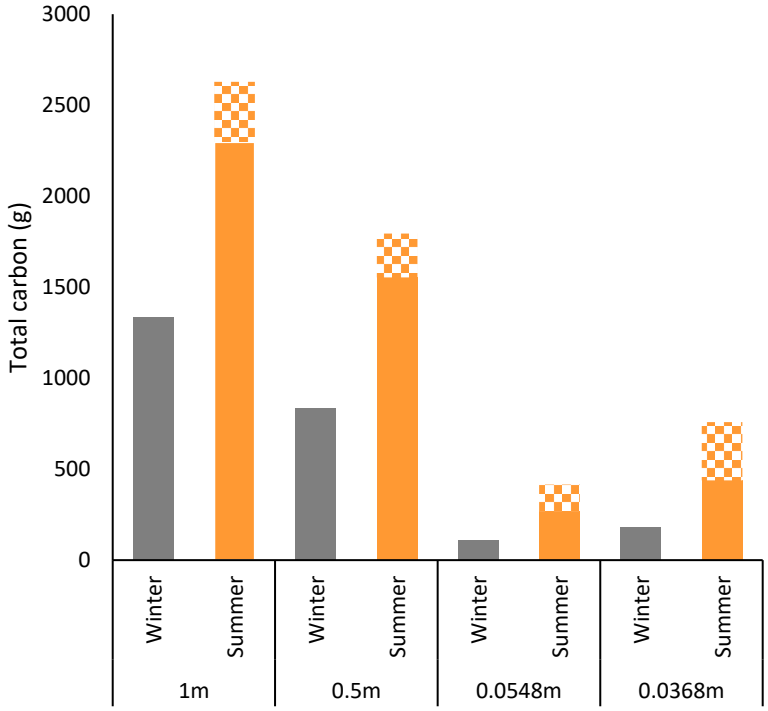


*Figure 2.19. Total vegetative carbon measured in restored vegetation on the **north shore** of the Eden Estuary. Displaying winter and summer totals - with summer broken down into original extent (solid) and area of expansion (checked); as calculated at each raster scale level.*

The south shore restored area displayed a larger absolute and proportional expansion than noted in the north shore site (Table 6). In terms of the total carbon store in restored vegetation of the south shore, there is a large quantity attributed to the area of expansion (Figure 2.20); accounting for between 1162 g and 5488 g (depending on raster scale used), far larger than those of the north shore, being between 145 g and 331 g (Figure 2.19). The largest proportional increases in carbon attributed to areal expansion, are found between fine scale raster data; with the south shore ranging between 24 % and 25 % and the north shore slightly a larger proportion of 35 % to 42 %.

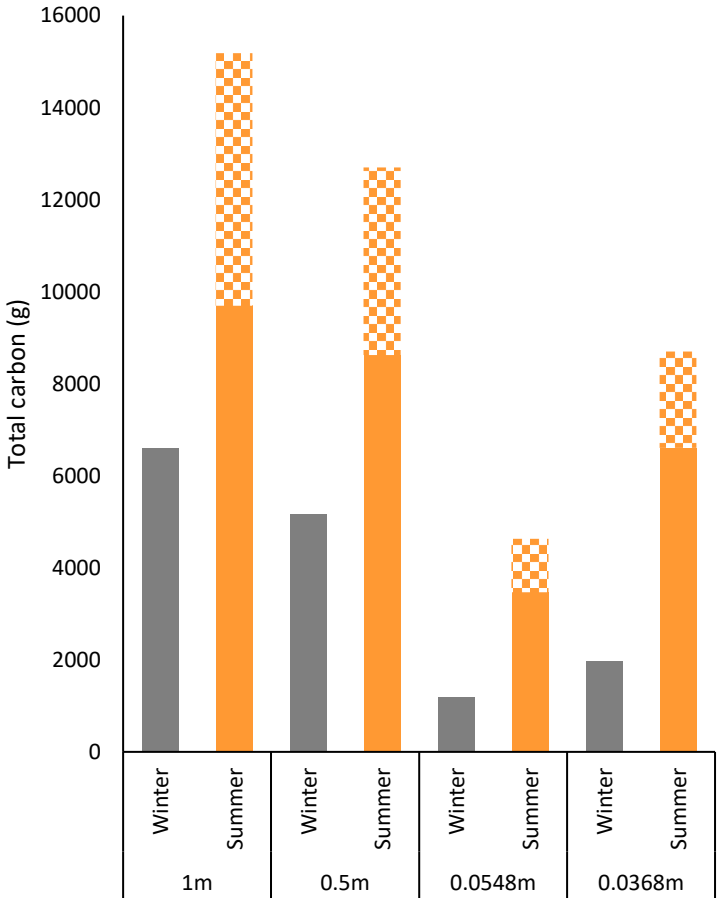


*Figure 2.20: Total vegetative carbon measured in restored vegetation on the **south shore** of the Eden Estuary. Displaying winter and summer totals - with summer broken down into original extent (solid) and area of expansion (checked); as calculated at each raster scale level.*

The significant differences between each site, season and scale shown in the vegetation height data remain true for biomass and carbon content, as these values are stem from those same height data with the same conversion factor applied across the entire dataset at the raster layer level; and thus, are directly related though each individual pixel value.

*Table 7: Summary table of the total carbon (grams) present in vegetation at each raster scale of each site in summer and winter. Values are calculated through a conversion factor of vegetation height to biomass (see Equation 6 and Equation 9) and assuming a 35 % carbon content. Also showing the proportional increase between seasons at each scale.*

| | **Restored vegetation - Total Carbon (g)** | | | | | | | |
|---|---|---|---|---|---|---|---|---|
| | **North shore** | | | | **South shore** | | | |
| **Scale (m)** | **0.0368** | **0.0548** | **0.5** | **1** | **0.0368** | **0.0548** | **0.5** | **1** |
| Winter | 177.5 | 109.1 | 833.7 | 1333.8 | 1972.1 | 1184.4 | 5161.8 | 6604.1 |
| Summer | 758.1 | 414.6 | 1794.2 | 2628 | 8701 | 4628.3 | 12701.3 | 15182.3 |
| *Change* | *580.6* | *305.6* | *960.5* | *1294.1* | *6728.9* | *3443.8* | *7539.5* | *8578.2* |
| ***Average change*** | ***785.2*** | | | | ***6572.6*** | | | |
| *Percentage increase* | 327 % | 280 % | 115 % | 97 % | 341 % | 291 % | 147 % | 130 % |

Carbon within vegetation is much greater in the south shore restored site than in the north (Table 7). During winter, within vegetation, there is an average of 613.5 g of carbon (gC) on the north shore and 3730.62 gC on the south shore; a six-fold difference. In summer these values increase to 1389.72 gC and 10,303.23 gC for the north and south shores respectively, a seven-fold difference. These values represent the total amount of carbon present at a discreet time point for the whole area studied. The proportional increases between seasons for each site are more similar than the absolute values, indicating the relative uniformity of growth during summer. This significant change in the size of the vegetative carbon stock between seasons is important to consider when reporting the possible carbon storage benefits of a system. The data suggest that depending upon measurement time there could be as much as a 6.6 kgC discrepancy, or 24.2 kgCO2e, in reported storage of a relatively small area of small estuary.

The data also highlight the influence of scale on the reported carbon storage quantity of a vegetated area. Large discrepancies can be driven by scale of measurement alone (Table 5), for example, there is more than an order of magnitude difference between the smallest and largest stock size reported at the north shore. This difference is partially to be expected as it compares values calculated from different densities, 324 stems/$m^2$ and 530 stems/$m^2$, however, this does not explain the large difference in total carbon stock.

Carbon content values corrected by area allow for a comparison of the efficacy of each shore's carbon storage potential per unit area. These data suggest that the application of coarse scale raster analysis is relatively robust, with very little change in the measured carbon per $m^2$ value at each scale (Figure 2.21). There is a clear difference between the two sites, with the south shore 'out-performing' the north shore. This is likely a product of the taller vegetation found within this site. Furthermore, there is a much higher increase in possible stem density as measured at the fine scale (Figure 2.21). This increase in stem density (number of pixels) will contribute to the increased total carbon content and per unit area content found at the south shore restored site.

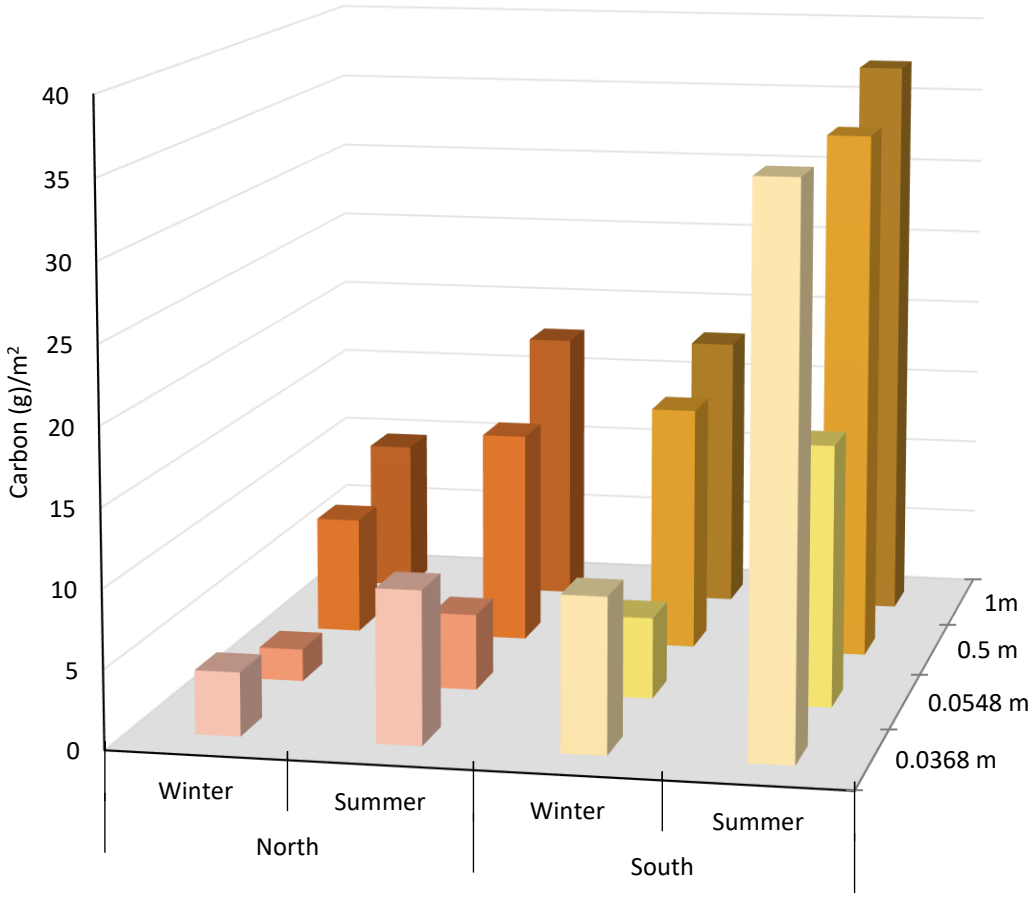


*Figure 2.21: Calculated carbon stock per $m^2$ for the north and south restored sites in winter and summer. Red shades are the north shore, yellow shades the south shore, shaded by different raster scale data.*

### *2.11.2.2 Seasonal change in carbon – natural areas*

As for restored vegetation, the stands of natural marsh, both *B. maritimus* and *P. maritima*, exhibit an expansion during summer and significant differences in the heights of vegetation within those extents.

The natural stand of *B. maritimus* expanded by an average of 432.96 $m^2$, with a range across scales of 272 $m^2$ to 565.43 $m^2$, the extent of *P. maritima* increased by 71.66 $m^2$, with a range of 14.25 $m^2$ to 129 $m^2$ across 1 m and 0.5 m raster layer data. Proportionally changes in *B. maritimus* were similar to those found in restored sites, with an average of 11.8 % increase in extent. Proportionally, *P. maritima* only expands an average of 0.3 % between winter and summer, illustrating the more conserved nature of the vegetation type.

*Table 8: Summary table of the total carbon (kilograms) at each scale of both natural sites in summer and winter. Values are calculated through a conversion factor of vegetation height to biomass (see Equation 6 and Equation 9) and assuming a 35 % carbon content for B. maritimus and 36 % for P. maritima. Also showing the proportional increase between seasons at each scale.*

| | **Natural vegetation - Total Carbon (kg)** | | | | | |
|---|---|---|---|---|---|---|
| | **North shore – *B. maritimus*** | | | | **South shore – *P. maritima*** | |
| **Scale (m)** | **0.0368** | **0.0548** | **0.5** | **1** | **0.5** | **1** |
| Winter | 20.60 | 12.90 | 85.34 | 123.03 | 426.41 | 603.24 |
| Summer | 572.12 | 308.87 | 810.71 | 884.71 | 667.97 | 924.27 |
| *Change* | *551.52* | *295.97* | *725.36* | *761.83* | *241.55* | *321.03* |
| ***Average change*** | ***583.67*** | | | | ***281.29*** | |
| *Percentage increase* | 2677 % | 2295 % | 850 % | 619 % | 57 % | 53 % |

The differences in vegetation growth mode, both of height and expansion, were reflected in the cycle of carbon stock within each area. At each site and at all scales there was a significant difference in the carbon storage of vegetation between winter and summer. *B. maritimus* exhibits a much enhanced carbon stock in summer compared to its winter state, increasing by as much as 2677 %, or a maximum actual increase of 761.83 kg (Table 8). The significant change between the seasons in the *P. maritima* area are far smaller, with only little over a 50 % increase from winter to summer (Table 8). Indicating the more stable and conserved dynamic present in the *P. maritima* complex system. However, the 'base'

winter stock is far larger than its *B. maritimus* counterpart, 426.41 kg – 603.24 kg compared to 85.34 kg – 123.03 kg when assessing across equal scales. When assessing their per unit area contribution both vegetation types provide similar values in the winter (Figure 2.22). In summer, these similarities do not hold true, with *B. maritimus* becoming a much greater carbon store per $m^2$ than *P. maritima* (Figure 2.22).

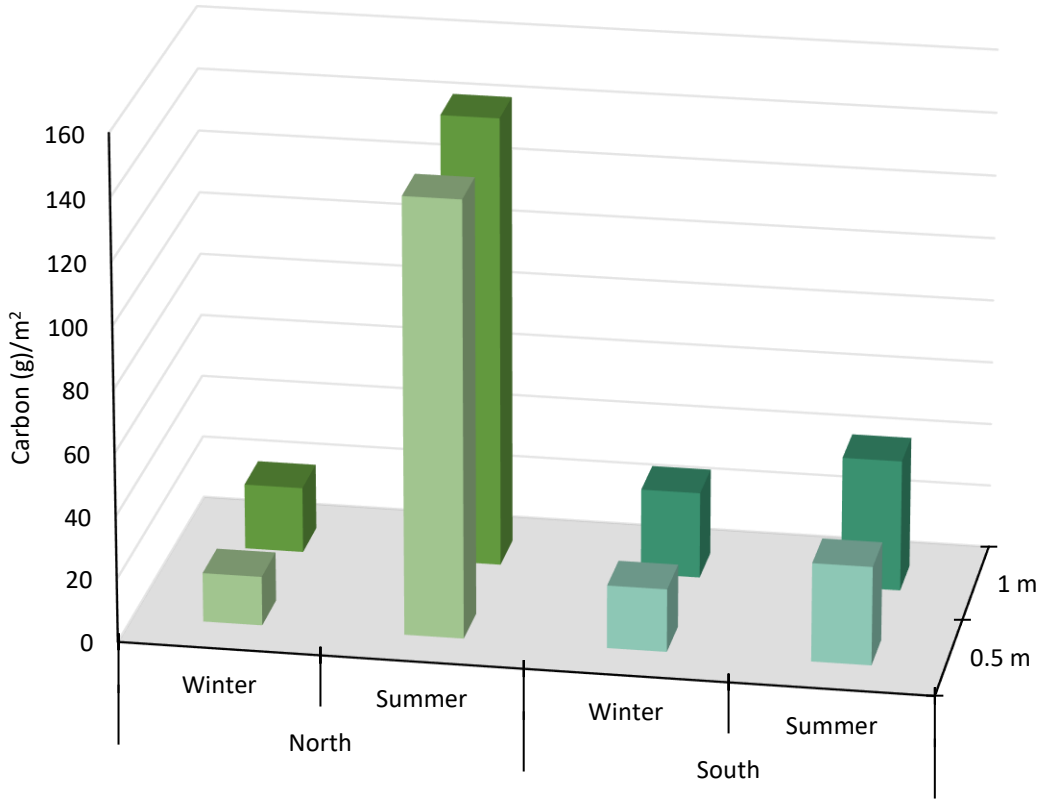


*Figure 2.22: Carbon stock per $m^2$ for the north and south natural vegetation areas in winter and summer. Green shades are the north shore, turquoise shades are the south shore, shaded by different raster scales (North only showing 1 m and 0.5 m for comparison with the South data), grey dashed lines indicating changes at different scales between seasons.*

### *2.11.2.3 Differences between natural and restored area carbon storage*

The vegetative carbon storage potential of the natural and restored area types were compared to assess the 'efficacy' of the restored area to potentially deliver equivalent ecosystem services are their natural counterparts. There is shown to be similarly low valus across the area types in winter per unit area, though the natural *P. maritima* marsh is shown to have the highest satanding carbon stock at this greatest point of die-back (Figure 2.23). The greatest carbon increase is found in the natural are of *B. maritimus* and is substantially more than found in all other areas. The two vegtation types of the south shore, though structurally different, display similar carbon stock fluctuations through between seasons (Figure 2.23).

## 2.12 Discussion – Vegetation carbon storage

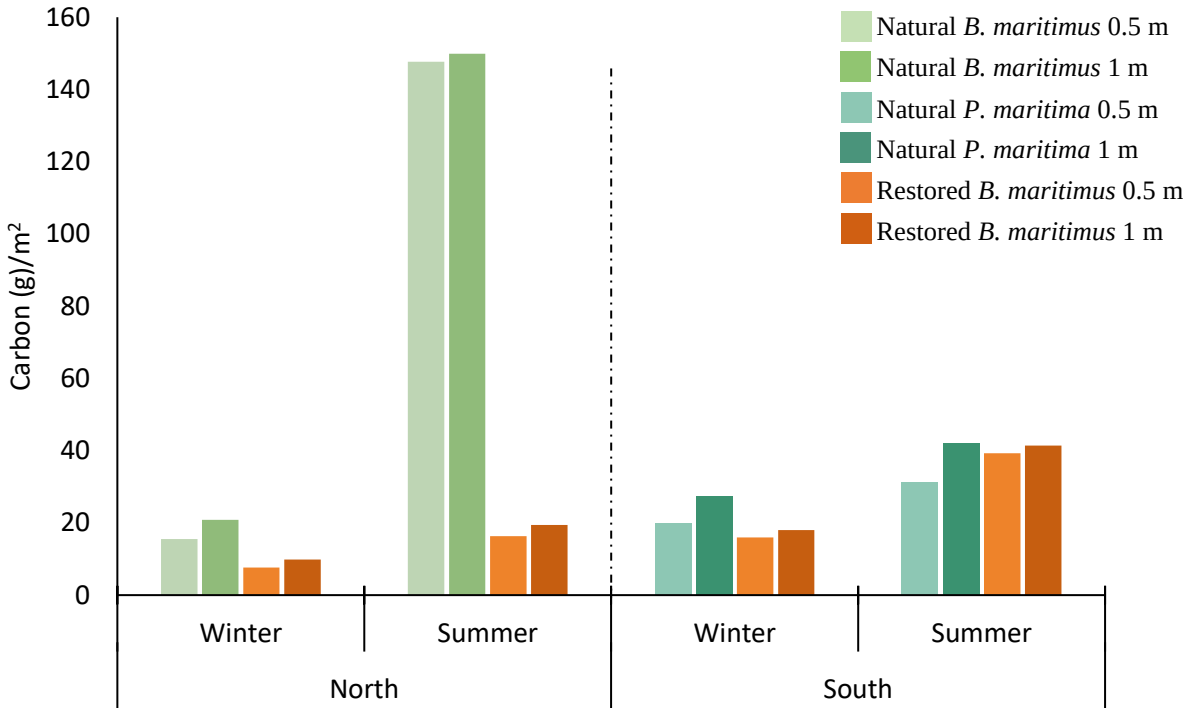


*Figure 2.23: Seasonal comparison of grams of carbon per $m^2$ in vegetation of the natural and restored areas of the estuary. Values shown use 1 m (dark shades) and 0.5 m (light shades) scale raster data. Bar colours indicate area type.*

The application of a TLS survey approach to assess saltmarsh vegetation across a relatively large area was tested and has been shown to be useful in the gathering of accurate data on vegetative structures and their respective contribution to the carbon pool. However, there are limitations to consider in both the surveying phase and analysing of the data.

Restored saltmarshes of the Eden Estuary contribute towards the total vegetative carbon budget of the system, which has been shown to differ greatly between winter and summer; due to both vertical growth and lateral expansion. Furthermore, natural extents of saltmarsh vegetation have been shown to exhibit similar functional changes regarding season. However, they display different carbon storage characteristics.

### *2.12.1 TLS considerations*

Working with laser scanning technology in the intertidal environment is restricted predominantly by its accessibility. The time limiting factor of tides coupled with the large amounts of equipment required restricts deployment to areas with suitable characteristics; such as ease of access, total extent, topographic complexity and vegetation type.

The Eden Estuary served as an ideal model site as it is highly accessible, allowing rapid deployment and retreat from the shore with the tides, and relatively small in extent; total area scanned was approximately 22,500 $m^2$, of which the north shore covered 6000 $m^2$ and the south shore 16,500 $m^2$. However, these still took multiple days to complete with the necessary coverage to capture the complexity of the vegetation. On a larger marsh this would introduce issues with accuracy, requiring registering of multiple scan-days together, due to probable lack of registration surfaces. A major allocation of time is the capture of multiple overlapping scans at different angles to all areas of the marsh, thus ensuring data is captured that will allow, for example, separation of vegetation from sediment surfaces. These requirements make TLS a labour-intensive exercise typically over an extended period, which maybe restrict its deployment in certain instances.

The tide-limited accessibility is further exacerbated with the requirement of fine weather for scanning; primarily dry and calm. Such weather conditions can be limited in exposed intertidal environments, particularly for surveys conducted in autumn and winter.

Promising advancements in laser scanning technology may mitigate some of these limitations through the deployment of drone-mounted units. Such an approach would allow more rapid data collection over a wider area, whilst also supporting multiple scan angles to be acquired through management of the survey flight. Furthermore, the effective 'single-scan' approach should reduce post-processing as it removes the user involvement of assigning and registering tie points between individual scans. Scanning from an elevated birds-eye view reduces any given angle of incidence to the marsh surface, improving penetration through dense vegetation (reducing shadowing), so increasing the capacity to extract accurate surfaces from the data; an issue which was recognised where insufficient data were collected to generate an accurate surface model. Though the lack of a summer specific sediment surface model is was not considered to have overly affected the data (as elevation changes were no more than a couple of mm), dedicated DTM and DSM would serve to further refine the accuracy and robustness of this approach. The unrestricted height of a drone also allows for data acquisition at all vegetation heights, again a limiting factor encountered in the project where vegetation height obscured the scanner view-field, increasing shadowing and discounting surveying in some areas. Further advantage to the additional height afforded by a drone could be the reduced need for such high-resolution scanning, as vegetation penetration becomes less of a limiting factor; thus, increasing scanning speed and reducing the size of the resulting datafile.

A major limitation encountered during data processing at this site was the generation of false returns from the atmosphere, which had to be manually removed from each scan. Errors were found across sites, days and season, with all returns of uniformly low intensity. When tested in other coastal environments (intertidal beach) no such errors were encountered, possibly attributing them to humidity around vegetated coastal systems. Such issues require further investigation and solutions integrated into the scanning process if possible; so minimising post-processing involvement and reducing possible accuracy loss through manual manipulation.

### *2.12.2 Data processing considerations and opportunities*

The remote sensing approach using laser scanning technology generates very large datasets, containing many millions of points. As this technology advances, the size of datasets will further increase. This brings with it associated issues with computing power to manipulate such large data sets. The approach employed here, to classify points by their 3D neighbourhood proved effective and vastly reduces the size of any given dataset containing information relating to specific criteria. This could further be advanced with the application of additional filters, either within the classification process or in pre-filtering, such as by intensity.

### *2.12.3 Carbon stocks of vegetation*

The current study has shown that it is possible to extract the required data from TLS survey points to generate an estimate of vegetative carbon stock. All data suggest that there is a large amount of carbon stored in vegetation of the areas surveyed in the Eden Estuary. In summer the total vegetative carbon store of surveyed areas reaches a maximum of 1.83 tonnes/carbon (6.7 tonnes/CO2e) or 0.63 tC $ha^{-1}$, down to a winter minimum of 0.44 tonnes/carbon (1.6 tonnes/ CO2e) or 0.18 tC $ha^{-1}$. These large discrepancies in stock estimates indicate the importance of when and how accounting measurements are taken. There is a clear risk of over-counting the total carbon sequestration contribution of an area if surveyed in summer as, depending upon vegetation type, a large proportion of this stock is cyclic and not retained year-round.

#### *2.12.3.1 Additional carbon storage through restoration*

Sites of restoration have been shown to contribute a substantial amount of carbon, relative to their size; 4.3 ± 0.8 kgC in winter up to 11.7 ± 2.0 kgC in summer, accounting for 1.8 % of the area studied. However, there are differences in their relative contributions, with the

south shore per unit area (winter = 12.3 gC $m^2$, summer = 31.1 gC $m^2$) containing more than twice as much carbon as the north shore (winter = 5.9 gC $m^2$, summer = 11.6 gC $m^2$).

The relationship is rooted in the height of vegetation present at each shore, which may reflect the 'health' or robustness of the two sites. Although the north shore site is 3 years older than the south shore, it is the south which more closely aligns with the state of the natural *B. maritimus* stand which both exhibit similar proportional winter carbon storage capacity. Furthermore, the south shore site has exhibited far greater expansion than the north shore, expanding by 2594 % and 653 % respectively from their original planting area. This equates to an average annual increase of 20.7 $m^2$ for the south shore site, with just a 4.7 $m^2$ for the north shore. The south restored site and north natural stand are also more similar in their tidal frame position, at 1.67 m and 1.64 m above mean sea level respectively, whereas the restored site on the north shore is higher at 1.76 m; reducing inundation period and possibly leading to reduced biomass production (Janousek et al., 2016).These differences highlight the dynamic nature of intertidal vegetation and the difficulty of predicting possible future additionality of carbon storage attributed to vegetation from conservation efforts. However, taking the lowest 'rate-of-return' from the north shore, where expansion has been lowest and features shorter vegetation there is an additional 613 ± 290 gC present within the system; with the same amount again cycling within it during summer. As these sites continue to expand their contribution to the carbon store increases, providing further additional value through an enhanced vegetative 'stock' and increased 'cyclic' capacity; leading to greater carbon burial, within or exterior to the discreet system.

#### *2.12.3.2 Natural vegetative carbon sinks*

The two types of natural vegetation studied display different carbon storage benefits, with *B. maritimus* retaining less but having a higher cyclic component and *P. maritima* having a larger stock component with less cyclic increase during summer. From a carbon benefit perspective, *P. maritima* perhaps offers a more valuable service through its larger stable carbon stock, even though its actual total storage capacity during a year does not equal the extent of the *B. maritimus* marsh area.

#### *2.12.3.3 Comparison between natural and restored vegetative carbon*

The study has shown that different vegetation types exhibit different carbon storage potential. However, it is important to assess how the restored areas, in their current state, compare to their natural counterparts; their potential destination as development continues. The data indicate that compared to the same vegetation type, currently, restored sites are 'under-performing'. This is indicated by the substantially greater carbon accumulation

attributed to the natural area of *B. maritimus* during the summer months. Though this is not necessarily part of the vegetation store, rather a cyclic component, it maybe be contributing to additional carbon input which is retained within the system. The reduced growth of restored areas during summer could impact the capacity of the vegetation to contribute towards increasing the estuary's carbon storage ecosystem service. However, taking winter as the baseline, or retained carbon in the system, all areas are somewhat comparable per unit area. This trend suggests that though restored areas presently offer limited contribution to extra-system carbon, they are storing carbon within their extents as effectively as their natural comparator. Interestingly on the south shore the structurally different vegetation types of the restored *B. maritimus* stand and the natural *P. maritima* extent display similar relationships between carbon stock and season.

### *2.12.4 Vegetative carbon stock estimations*

The study applied allometric scaling relationships to link quantified vegetation heights to biomass and carbon content values. Further to this transformation, it was necessary to assign a specific density to act as a multiplier to the otherwise single-stem measurements. The effectiveness of this approach could be improved to minimise possible discrepancies in these data.

For example, when considering the application of an estimated vegetation density of 530 stems/$m^2$ to the coarse scale (1 m and 0.5 m) *B. maritimus* raster, the data suggests a constant over-estimation of density. Taking the total extent of vegetation from the coarse scale data, giving an uninterrupted 'plan' of the vegetation stand, and calculating the effective density across this area using the fine scale data (which effectively assigns a pixel to a stem) the calculated density is far lower than the 530 stem/$m^2$ estimate used. At the low-density fine scale (0.0548 m) there is a density of 130 – 226 stems/$m^2$ and at the upper-density fine scale (0.0368 m) there is a density of 240 – 445 stems/$m^2$. This assumes that all stems are captured by the laser scanner and are further retained when converting to the 2D raster format being analysed. Further study is required to develop this approach and ensure its accurate representation of the environment. For example, taking more specific sample vegetation density measures to apply during calculation of biomass or conversion to raster data. A more accurate approach to remove potential bias would be to develop the processing tools for complex 3D laser scan data which allow the automatic extraction of stem structures, providing direct information on the biomass and carbon content of a given area.

## 2.13 Conclusion

Overall the application of such high-resolution LiDAR technology holds promise in enhancing accurate assessment of the vegetative carbon stock of intertidal areas. The approach employed here to classify the point clouds and utilise analysis through their conversion to 2D raster data proved effective; allowing easy extraction of data and rapid manipulation of large amounts of data. As technology becomes more accessible and new processing techniques are developed to optimise and streamline workflows this discreet remote sensing approach will be highly useful and applied.

The environmental data gathered though TLS of the Eden Estuary has shown that currently restored areas of *B. maritimus* which had been planted 13 to 16 years previously are functionally comparable at long-term carbon storage within their vegetation as is the natural stand. Their winter storage by unit area is similar to the natural area, particularly in the restored area on the south shore, which contained 12.3 $gC/m^2$, compared to the natural stand which contained 11.9 $gC/m^2$. The restored sites currently store approximately 4.3 kgC, increasing to 11.7 kgC in summer, or 15.8 kgCO2e and 42.9 kgCO2e respectively.

The study highlights the importance of seasonal consideration when carrying out vegetative carbon accounting exercises in saltmarsh areas; especially for particular species, such as *B. maritimus* studied here. Such need is presented through the large differences seen between the conserved stock of retained vegetative structures during in winter and those cyclic growth components in the summer months. Although, during summer growth more carbon dioxide is fixed, and organic matter produced this does not translate into an increasing vegetative carbon stock.

# Chapter 3: Sedimentary dynamics of the upper inter-tidal system

## 3.1 Introduction

Sediments play a major structural role in estuaries, particularly in their interaction with the shoreline, including features such as saltmarshes, whose existence is the result of biogeomorphic feedback between vegetation and sediments. Furthermore, sediments provide the major mechanism of carbon storage within such inter-tidal vegetated ecosystems through their incorporation of organic matter into bed material and their subsequent long-term burial. A primary determinant of sedimentary burial is the balance between the opposing processes of deposition and erosion.

The influence of saltmarsh vegetation, both of 'natural' swards and 'restored' stands, on these processes were studied in the Eden Estuary, Scotland. The investigation assesses how sediment dynamics differ between types of vegetation, including species type, restored areas and bare adjacent mudflats; and between tidal height, across spring to neap states; and between seasons. The objective was to understand how restored areas within estuarine saltmarsh systems compared in function to natural areas. The study further assessed how these differences may alter carbon sequestration potential of those restored areas, as compared to 'business-as-usual' mudflats and how they compare to natural established areas in 'equilibrium' within the present site and setting. Seasonal-tidal variation in deposition and settlement rates, elevation changes and vegetative structural data were acquired from Summer 2015 (August) through to Spring 2016 (June).

### *3.1.1 Sediment and saltmarshes*

Salt marshes are biogeomorphic intertidal ecosystems (Baptist et al., 2016; Thorne et al., 2014), meaning their structure and existence are a function of the interaction between biological components of vegetation and geomorphological processes associated with sediment movement (Baptist, 2005). Saltmarsh systems are highly dynamic with their function being controlled by various abiotic (e.g. elevation, wave impact, sediment supply) and biotic (e.g. vegetation structure, stem density) factors (Boorman, 2003; van Proosdij et al., 2006). Vegetation alters the hydrodynamic situation of the immediate area (Bouma et al., 2005) and the rate of sediment accretion typically increases, rates of resuspension are reduced and there is an increase in organic matter input (Boorman, 2003). These interactions continue through development and evolution of the marsh through a process of

positive feedback (Nolte et al., 2013a). Thus differing sediment dynamics, such as accretion rates or stability, can develop between vegetated areas and bare mudflats (Brown et al., 1999), possible within a relatively small area.

Coastal vegetated systems are experiencing rapid annual losses in global extent of up to 7 % (McLeod et al., 2011), of which saltmarshes are shrinking by 1 – 2 % per year (Duarte et al., 2008). Drivers of loss include anthropogenic pressures, such as coastal development or altered sediment supply, these systems are also potentially vulnerable to sea-level rise due to drowning (Crosby et al., 2016; Thorne et al., 2014), unless accretion keeps pace (Craft et

*Figure 3.1: Illustrative images of restored vegetation levels, images were captured on the south shore of the Eden Estuary, in winter 2014/2015 prior to commencement of this study. (A) showing a stretch of 'young' restoration, which was planted in 2013; (B) showing stand of 'old' restoration, which was planted in 2003.*

al., 2009; Kirwan et al., 2016; Reed et al., 1999). Losses of such areas would lead to a loss in the valuable ecosystem services they provide, such as carbon sequestration and storage (blue carbon); estimated to be 0.02 – 0.24 $PgCO_2$ per year for current saltmarsh loss rates (Pendleton et al., 2012). As such restoration efforts are required to reduce or reverse these losses, to retain the diverse ecosystem and maintain the benefits it provides.

Sediment and vegetation interactions are key to the maintenance of saltmarsh ecosystems, and so the way in which sediment dynamics are altered post-restoration are important if such initiatives are to be a success. Whilst, there has been various direct and modelling research towards understanding the interaction of vegetation and sedimentation within saltmarsh ecosystems (e.g. Moskalski and Sommerfield, 2012; Mudd et al., 2009, 2010; van Proosdij et al., 2006; Woolnough et al., 1995), little focuses specifically on restored areas. Within studies of restoration, managed realignment processes typically receive most attention, with information on direct transplanted, as conducted here, lacking. It is also documented that relationships between vegetation and sediment are not always conserved and vary depending upon site specific factors (Belliard et al., 2017; J. Court Stevenson et al., 1988). The way in which restored vegetation changes sediment regimes is less targeted, which this study investigates, building on preliminary research carried out by Maynard et al. (2011).

Furthermore, in the context of quantifying the carbon storage benefit of saltmarsh environments, understanding the action of sedimentary components is crucial as these account for the major portion of stored carbon in these areas (Duarte et al., 2005).

The study assessed sediment deposition and settlement rates of different areas within an estuary, quantifying their potential contribution to the sedimentary pool of each area; both in absolute material and in carbon content. Further seasonal measurements of changes in sediment surface elevation and altered above-ground vegetative structures were taken. These data together provide a detailed assessment of the current state of sediment dynamics within the Eden Estuary, facilitate investigation of the functional capacity of restored areas compared to their natural counterparts and gives an indication of their potential carbon storage benefit service. Furthermore, the investigation evaluated the influence of season on sediment dynamics - both as a temporal function and as a physical manifestation through vegetative structural change, the influence of tide state or inundation period (Reed, 1989; Temmerman et al., 2003), and the balance between the processes of sediment settlement, deposition and erosion.

Improving and advancing our understanding of sediment dynamics within a restoration context will provide benefit to future conservation initiatives through possible new insight into establishment and evolution of vegetation. This knowledge is further linked through to potential carbon storage benefit, providing greater depth and valuable insight to the mechanisms at play leading to the significant sedimentary carbon store found in saltmarshes.

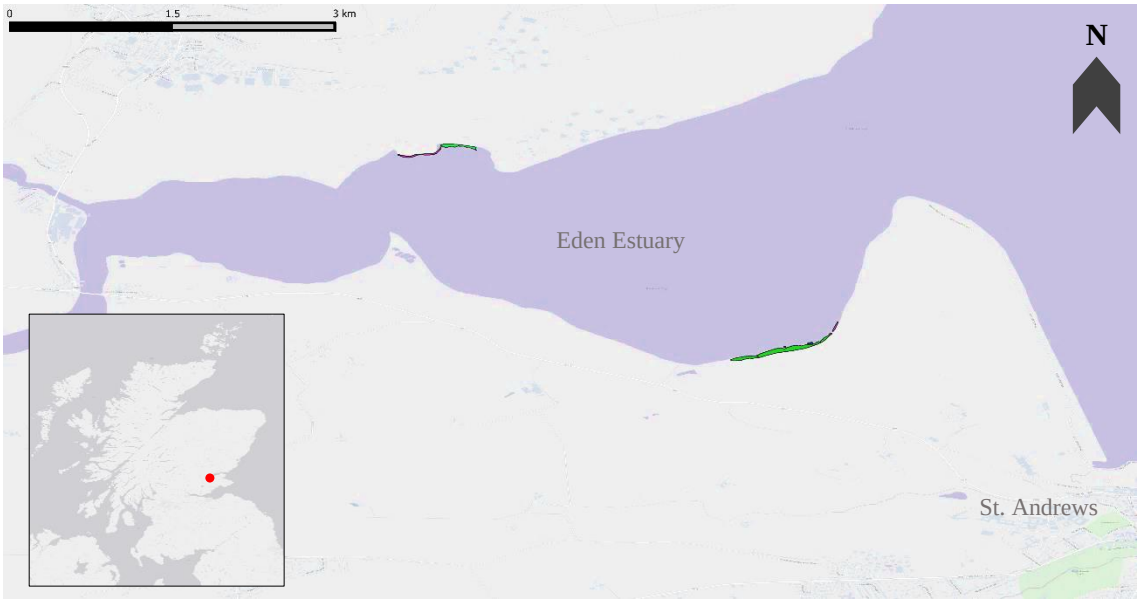


*Figure 3.2: Map showing location of study sites in relation to the whole Eden Estuary system. Polygons are visible on the north and south shores, for further detail see Figure 3.3 and Figure 3.4. Insert is a map of Scotland for larger spatial reference of site location; red dot indicates the Eden Estuary. Map image provide through ESRI Worldmap.*

## 3.2 Materials and methods

### *3.2.1 Study information*

The study was carried out on the Eden Estuary, Scotland (Figure 3.2) where significant efforts have been made in the field of saltmarsh conservation and restoration (Maynard, 2014). This site provided a model environment to investigate the sedimentary dynamics of restored areas of vegetation and draw comparisons with natural marshes and other unvegetated area within a spatially restricted extent of a small pocket estuary. The limited size of the estuary allows sampling to take place in different vegetation types/mudflat areas over a small area, acting to reduce possible confounding factors influencing the sedimentary dynamics within each focal site. Furthermore, the longitudinal nature, commencing in 2000

and continuing at present, of the restoration efforts allowed the study to assess how time and/or establishment success interact to influence sediment processes.

The study established 32 permanent sampling points, 16 on each of the north and south shores of the estuary (Figure 3.2), where three vegetation types were present – natural saltmarsh, "old" established restored marsh (cf 15 years) and "young" restored marsh (cf 5 years) and also on adjacent mudflats along each shore . In each of these distinct areas, four permanent sampling points were established in August 2015 (Figure 3.3 and Figure 3.4). The study was conducted over four consecutive seasons of Summer 2015, Autumn 2015, Winter 2015/2016 and Spring 2016. Sampling was designed to occur at the middle-to-end of each season to capture the effect of the given vegetative structure of that season, be that growth or senescence.

### *3.2.2 Survey details*

Sampling locations were selected through a stratified-random process which distributed points evenly along the longitudinal length of each target area using remote sensing software. Google aerial imagery, GPS data tracks and site knowledge were used in the placement of points. GPS tracks acted to delineate the target sites, being obtained by walking the circumference of each area type with a hand-held GPS unit (Garmin GPSMAP 64s). These were combined with aerial imagery to fully delineate all target areas, providing a restricted sampling zone and a measure of size for each. The shore-parallel length (east to west) of each area was determined and points equally distributed along this length. These provided primary reference points in the field, with final plots located along its shore-perpendicular axis to be best representative of the immediate areas site characteristics. At each point a permanent sampling plot was established, consisting of a Sediment Erosion Bar (SEB) (Nolte et al., 2013b) and a support tube for the sediment settlement trap (Figure 3.5); forming the focal points for the subsequent year-long study. Sampling centred on sediment dynamics, capturing data on deposition and settlement, with further data collected of sediment elevation change and vegetative structural change.

Sampling areas were located on the north and south shores, mirroring each other in the area types represented. The specific situation of the two shores differed in their respective elevations, with the north shore sitting lower in the tidal frame (Table 3.1).

On each shore two levels of restoration sites were selected, representing: younger -still establishing- marsh vegetation ('young') (Figure 3.1) which were planted between 2010 (north shore) and 2013 (south shore), (red in Figure 3.3 and Figure 3.4) and older

established marsh stands (old) (Figure 3.1) which were planted between 2000 (north shore) and 2003 (south shore), (blue in Figure 3.3 and Figure 3.4). On each shore an area of natural saltmarsh was also selected (green in Figure 3.3 and Figure 3.4). These areas consisted of *B. maritimus* on the north shore and *P. maritima* on the south shore. These two very different vegetation types were chosen as they were located adjacent to the restoration activity, and further, they represent two possible trajectories for those sites of restoration. That being, either reaching an equilibrium state lower in the tidal frame as a *B. maritimus* marsh or accrete vertically and transition to a low-mid *P. maritima* marsh. Finally, adjacent areas of mudflat were also studied, which spanned the entire longitudinal length of the vegetated areas on both the north and south shores.

*Table 3.1: Elevation of permanent sampling points. Obtained using relative GPS approaches, taken in September 2016, presented as height (m) above Ordinance Datum (mean sea level at Newlyn, Cornwall).*

| North shore | | South shore | |
|---|---|---|---|
| **Sampling point** | **Elevation (m)** | **Sampling point** | **Elevation (m)** |
| Natural 1 | 1.337 | Natural 1 | 2.280 |
| Natural 2 | 1.537 | Natural 2 | 2.391 |
| Natural 3 | 1.782 | Natural 3 | 2.403 |
| Natural 4 | 1.903 | Natural 4 | 2.365 |
| Old 1 | 1.846 | Old 1 | 1.654 |
| Old 2 | 1.848 | Old 2 | 1.652 |
| Old 3 | 1.726 | Old 3 | 1.731 |
| Old 4 | 1.637 | Old 4 | 1.651 |
| Young 1 | 1.567 | Young 1 | 1.734 |
| Young 2 | 1.278 | Young 2 | 1.558 |
| Young 3 | 1.185 | Young 3 | 1.536 |
| Young 4 | 1.591 | Young 4 | 1.549 |
| Mudflat 1 | 1.201 | Mudflat 1 | 1.526 |
| Mudflat 2 | 1.070 | Mudflat 2 | 1.581 |
| Mudflat 3 | 1.133 | Mudflat 3 | 1.360 |
| Mudflat 4 | 1.475 | Mudflat 4 | 1.244 |

### *3.2.3 Sample point information*

Sampling points were accurately geo-referenced through differential-GPS using a pair of Leica VIVA GS10 GNSS units. One unit was set as a 'Base' station within 3 miles of the study site taking position readings every 15 seconds. The Base station was established approximately 30 minutes prior to commencement of the survey and continued until approximately 30 minutes after survey completion. The second unit acted as a 'Rover' which was deployed over each point and collected data for approximately 10 minutes at each, on the same 15 second cycle as the Base unit. These provided millimetre accurate post-processed positioning in the horizontal (~5 mm) and the vertical (~10 mm). Processing was completed using Lecia *Geo Office 8.4* software. The position of the Base station was corrected using precise ephemeris data. The Rover points were subsequently processed against the Base station position; providing a 'correction' to each point determined by the absolute position of the Base and the Rovers readings over the given period for each position.


*Figure 3.3: Aerial imagery with geo-referenced polygons and points of specific study areas and sampling points (yellow) on the north shore; points are numbered 1 to 4 from west to east in each area. Image shows Leuchars MoD Army base which fringes the northern coast of the estuary. Polygon colours: green = natural vegetation (B. maritimus); blue = older restored vegetation of B. maritimus, planted in 2000; red = younger restored vegetation of B. maritimus, planted in 2010/2011; mudflat sampling was conducted at approximately 30 m perpendicular distance from vegetation fringe. Imagery taken from Bing VirtualEarth.*

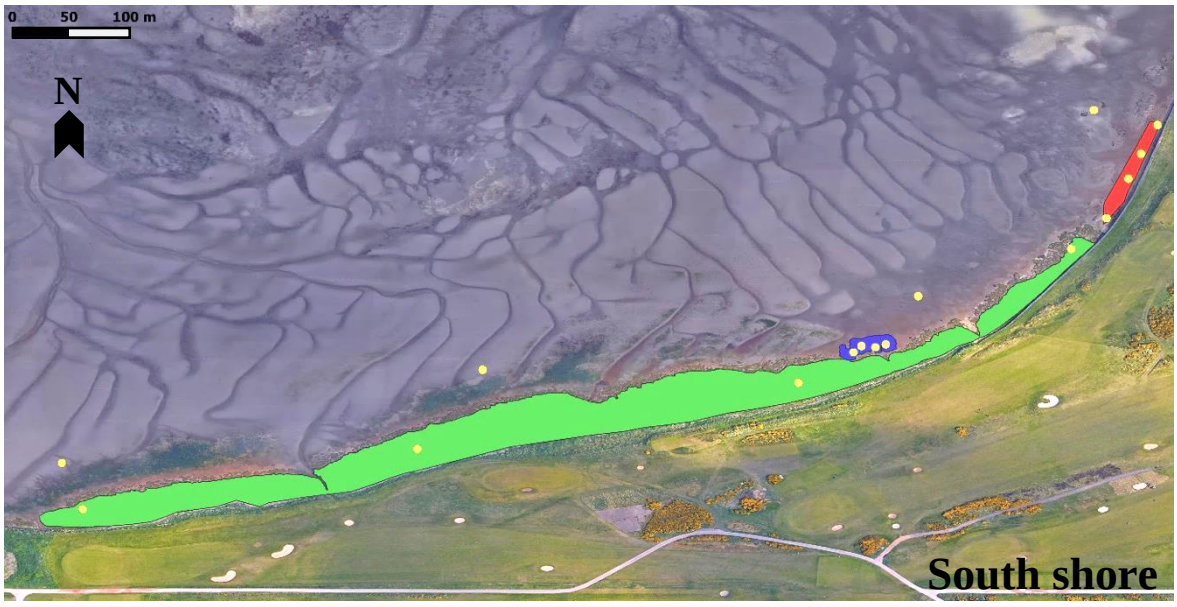


*Figure 3.4: Aerial imagery with geo-referenced polygons and points indicating study areas and sampling points (yellow) on the south shore; points are numbers 1 to 4 from west to east in each area. Image shows part of a Links Trust golf course complex which fringes the southern coast of the estuary. Polygon colours: green = natural vegetation (P. maritima); blue = older restored vegetation of B. maritimus, planted in 2003; red = younger restored vegetation of B. maritimus, planted in 2013; mudflat sampling was conducted at approximately 30 m perpendicular distance from vegetation fringe. Imagery taken from Google Satellite.*

### *3.2.4 Sampling approach*

In each season measurements of sediment deposition and settlement, quantification of vegetation structure and changes in sediment elevation were taken. Sampling was carried out at permanent points across the estuary within focal areas (Figure 3.3 & Figure 3.4). Sampling points consisted of a small plot with a Sediment Erosion Bar (SEB, Figure 3.5) established in a north-south orientation with a support tube for the sediment settlement trap sunk ~ 25 cm into the sediment approximately 1 m perpendicularly from the seaward most rod of the SEB (Figure 3.5).

*Figure 3.5: On the left a schematic diagram of the permanent sampling point set up. Solid black dots are the rods of the SEB, blue dashed rectangle and circles indicate the table of the SEB which is only present during measurement, unfilled black circle represents the support tube for sediment settlement trap, green dashed square and circle show placement location of the deposit trap. Image on the right show sampling plot set up with sampling units (deposit and settlement trap) in situ.*

### *3.2.5 Field - Sediment deposition and settlement*

Sampling of short-term discreet deposition and settlement events over two consecutive inundation periods were carried out, using deposit traps and settlement tubes. Measurements were taken across a spring to neap tide cycle during each season, taking place over an eight-day period, totalling four separate sample sets; a total of 1024 samples over the yearlong study (2 shores * 4 areas on each * 4 points in each area * 4 seasons * 4 samplings in each season * 2 sampling types). For each sampling event traps were deployed in the environment during the ebb tide (beginning on the ebb tide preceding a spring tide) and left for a period of two flood tides, after which samples were recovered and returned to the laboratory for processing. The following day (i.e. after a further two flood tides) traps were re-deployed, and the process repeated, with four samples spanning the spring-neap cycle.

#### *3.2.5.1 Deposit traps*

Deposition was measured using a modified 'sediment trap' as described by Reed (1989). The sampling unit was a custom-designed two-part plastic retention trap, consisting of a 5 mm thick PVC base and a 0.25 mm thick acrylic retention ring with a 90 mm diameter opening (Figure 3.6A). The trap held a pre-dried (24 hours at 60°C) and weighed filter paper (Figure 3.6B), 110 mm diameter, 3 – 5 µm pore sized, filter. Traps were set flush to the sediment surface and secured with 100 mm nails inserted through holes in each corner (Figure 3.6C). These were placed at low tide and remained in the environment over two consecutive flood tide events. When collected, care was taken to minimise disturbance of the deposited sediment, with traps transported horizontally.

#### *3.2.5.2 Sediment settlement tubes*

The tubes used to capture sediment settlement characteristics were initially designed to measure larval settlement (as described in Todd et al., 2006). The tubes are approximately 300 mm tall, of 30 mm diameter and internally baffled, to aid retention of settled material. Sediment was captured through the conical top which has a 10 mm aperture. Support units were permanently installed in the environment, being approximately 300 mm tall and 68 mm in diameter tubes. These were sunk 250 mm into the sediment, providing a hollow to allow insertion of the settlement tubes (Figure 3.7). Pre-deployment, traps were filled with filtered seawater and affixed into the support tubes in the environment, with opening approximately 100 mm above the sediment surface.

#### *3.2.5.3 Additional sampling*

It was found that there was not consistently enough sedimentary material available across traps in any given sampling to allow supporting analysis of carbon content. To address this, it was decided to take a secondary sample set to be produce a specific carbon conversion factor for application within this study. The secondary sampling took place on the spring tide following the eight-day sampling round. The single sampling event deployed 32 settlement traps and 64 deposit traps, doubling the number used previously to ensure that sufficient sample size to carryout out organic matter and carbon content analysis. This was of particular issue for points located in the *P. maritima* marsh, which are all higher in the tidal frame than the other study points.

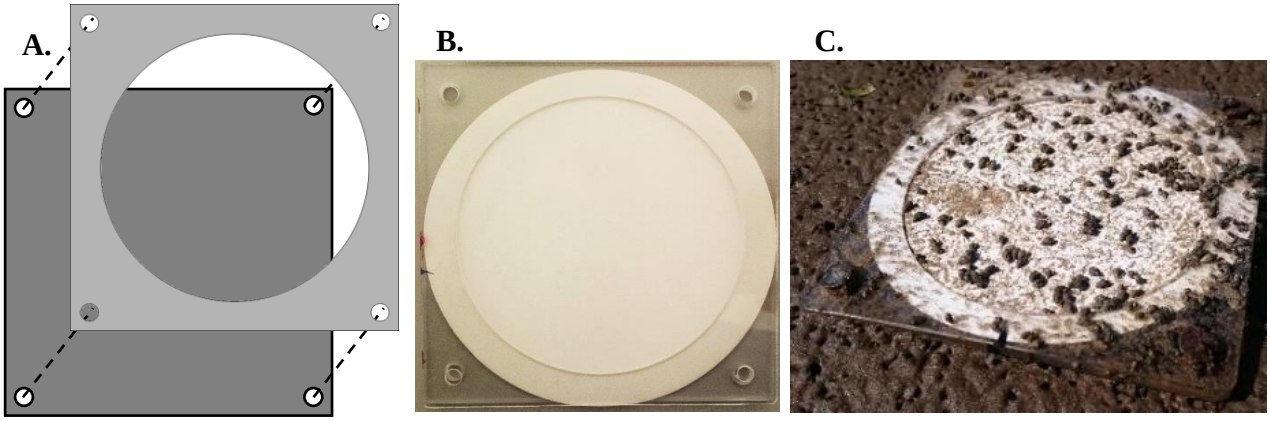


*Figure 3.6: (A) A diagram of a deposit trap showing the 110 mm x 110 mm x 5 mm PVC base (dark grey) with the acrylic retention ring top section above (light grey), with an 9 cm exposure area. Holes at each corner allow 10 cm nails to be pushed through both layers into the sediment, securing the trap. (B) A picture showing a prepped deposit trap pre-deployment, with filter paper in place. (C) A deposit trap in-situ prior to collection, after exposure to two flood tide events.*

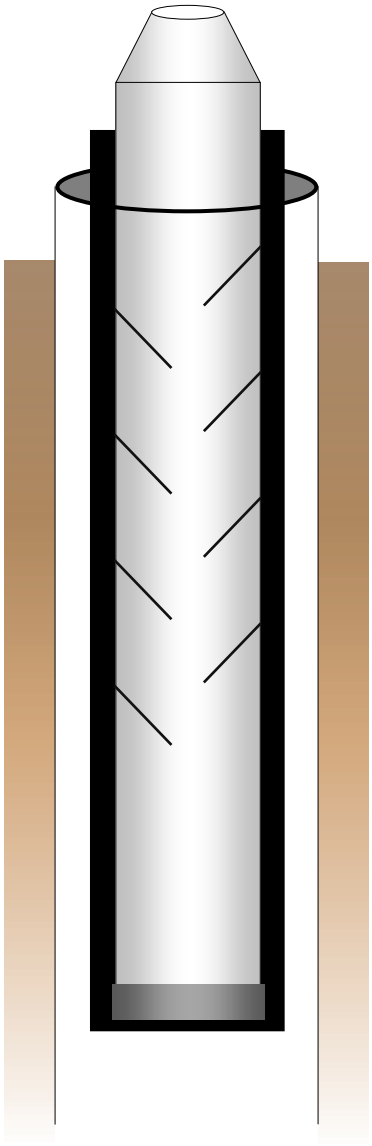

*Figure 3.7: Diagram of a settlement tube setup, shown sunk into the sediment. White area indicates the support tube which remains in the environment, sunk approximately 250 mm into the sediment. Black area is the tube support panel. Settlement tube shown in light grey with internal baffles, conical top and 10 mm aperture. Dark grey crew stopper allows easy retrieval of sample post-exposure.*

### *3.2.6 Field - Sediment elevation change*


*Figure 3.8: (A) Top of the 'table' bar, circular holes used as measurement points. (B) Underside of 'table' bar, right hole used to attach to rods. (C) Showing depth of attachment hole of the 'table'. (D) Showing SEB being used to measure sediment elevation in the environment.*

The long-term change in sediment accretion was quantified through an adapted version of the (rod) Sediment Elevation Table (SEB) (Figure 3.8 D, Figure 3.9) described by Cahoon et al. (2002), after Boumans and Day (1993). Two lengths of 10 mm reinforced steel bar were sunk vertically 1 m into the sediment 1.3 m apart, with approximately 300 mm proud of the surface. These support rods provide a permeant and stable measurement base onto which the ‘table’ sat for each measurement set. The ‘table’ was a 1.35 m long, 35 mm wide, 18 mm deep metal bar with partial holes aligned to fit the support rods (Figure 3.8, C). Along the length of the table, 11 equally spaced holes indicated the measurement points (Figure 3.9). A ‘mm’ graduated rod which fit snugly in guide holes allowed accurate measurements to be made of the distance between the top of the table to the sediment surface. Each seasonal measurement of a sample point is made up of 11 individual readings taken at whole mm integers, these data are averaged to provide a level surface which can be compared to previous and future measurements.

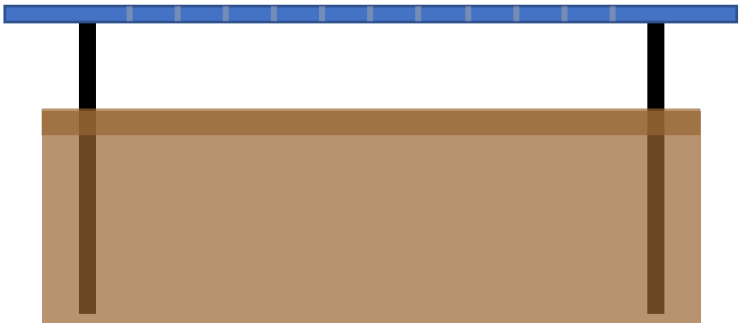

*Figure 3.9: Diagram of SEB. Reinforced 10 mm steel rods (black) are driven in the sediment to approximately 1 m with 30 cm proud of the surface and 1.3 m apart. The table (blue) is 1.35 m long, 35 mm wide, 18 mm deep aluminium bar. The end of the bar has holes which correspond to the rods allowing it to sit securely onto them. Along the length of the table are 11 equally spaced holes (grey lines) through which the distance from the sediment surface to table top are measured using a rod-ruler.*

### *3.2.7 Field – Vegetation characteristics*

Seasonal data were collected at each sampling point, capturing above -ground vegetative structure information through two images taken at each point; obtaining *cover* and *density* data. The two image types were captured as follows (Figure 3.10):

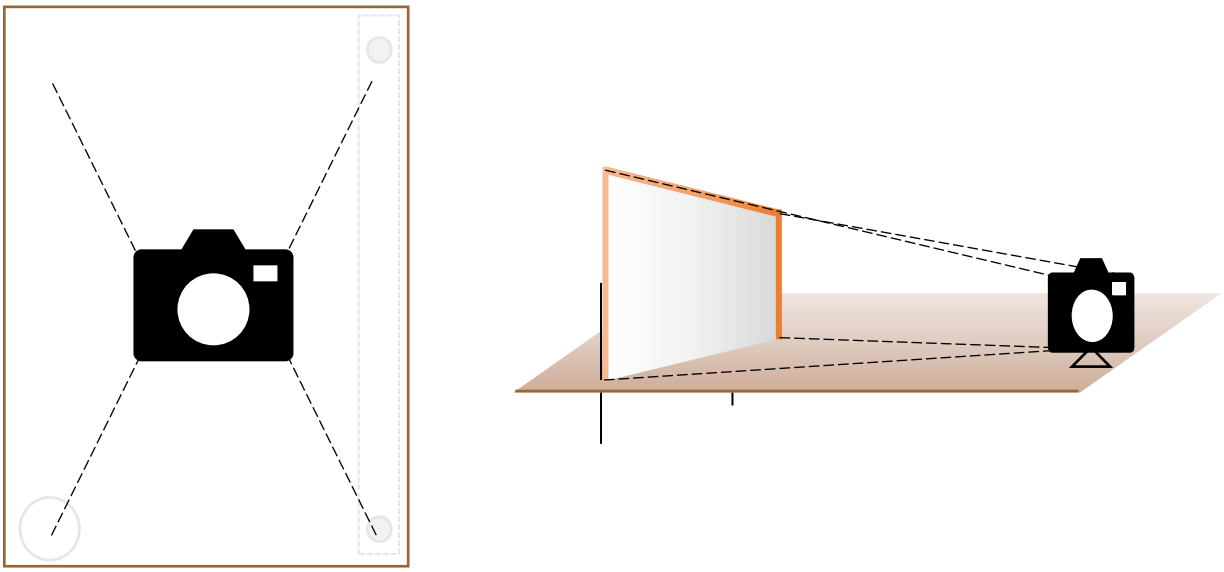

*Figure 3.10: Vegetation structure image capture approaches. The left shows camera position for vegetation 'cover' data, camera is held at approximately 1.5 m pointing directly downwards. The right shows setup for vegetation 'density' data image capture, camera is on tripod 15 cm above sediment surface, approximately 1 m perpendicular from white backing-board with orange boarder.*

- *Cover* image: camera was held 1.5 m above the sediment surface pointed directly downwards with the settlement support tube in the bottom corner of the image to provide a spatial calibration reference.

- *Density* image: camera was set on a tripod approximately 15 cm above the sediment surface and 1 m perpendicular distance from a backing-board (91 cm x 60.5 cm; with a 5 cm orange boarder along each side), the image being taken was taken transversely through the vegetation with a 1 m fixed focal distance. Vegetation within ≈ 20 cm of the camera lens was moved out of frame to prevent those foreground objects excreting an overly large influence on the images captured. The backing-board was held vertically, in a landscape orientation and spanned between the two SEB support rods and provided a plain white background to contrast the present vegetation against. The board was boarded with wide orange tape which provided a spatial calibration reference.

### *3.2.8 Laboratory – Deposit trap processing*

Deposit trap samples were processed on the day of collection from the estuary. The upper retention ring was carefully removed from the deposit trap, ensuring not to remove material held on the paper surface. The filter papers were removed from the trap, folded and placed in a large centrifuge beaker, to which 100 ml of distilled water was added. Samples were spun at 3000 rpm in a 150 mm radius centrifuge for 10 minutes, water was removed using a MORVAC filter pump. A further 50 ml of water was added, and sample centrifuged as before, water was removed, and sample transferred to a 50 mm diameter aluminium boat for further processing; distilled water was used to flush out entire sample. The washing steps were required as testing indicated that the 'ash-free' filter papers when exposed to saltwater left a small weight of residual material following combustion; washing helped prevent this occurring.

### *3.2.9 Laboratory – Settlement tube processing*

Full settlement tubes were emptied by carefully unscrewing the bottom lid, ensuring entire content were captured in a 200 ml pot. Distilled water was used to flush down through the tubes to ensure all material were removed. Once transferred samples were either processed on the same day or frozen for processing at a later date.

Samples were washed following a similar approach as detailed for deposit trap samples, however these required a prior step of an additional centrifuge spin and removal of the primarily saltwater; following this 100 ml distilled water was added and the steps followed as before.

### *3.2.10 Laboratory – Sediment dry weight*

The aluminium boats into which samples were transferred had been previously dried and weighed. Samples were then oven dried at 60°C for a minimum of 24 h, with fan driven warm airflow. Dried samples were removed from oven and placed into a desiccator to cool prior to being weighing. The weight of sediment was calculated according to Equation 10.

$$Sdw\ (grams) = Tdw - db$$

*Equation 10*

Where *Sdw* is the sediment dry weight, *Tdw* is the Total dry weight (g) of sediment and the aluminium boat and *db* is the dry weight of the aluminium boat (g). The processing of deposit samples included the filter paper used during sampling, as such the calculation was carried out as in Equation 11.

$$Sdw\ (deposit\ samples, grams) = Tdw\ - db\ - dp$$

*Equation 11*

Where *dp* is the dry weight of the filter paper (g).

### *3.2.11 Laboratory – Sediment organic content*

The organic content of sediments was calculated using a Loss-On-Ignition (LOI) approach. Once samples had been dried and weighed, aluminium boats were placed into a muffle furnace and combusted at 450°C for six hours (Craft et al., 1991; Kimble et al., 2000), ramped at 10°C per minute, this heating time was in addition to the six hour holding time. Post combustion samples were placed in a desiccator to cool prior to being weighed; providing a measure of weight loss through the removal of organic matter and retention of the mineral fraction. The organic content of the sample was calculated according to Equation 12 and the resulting organic content values according to Equation 13.

$$OM\ (grams) = Sdw - (CTdw - db)$$

*Equation 12*

Where *OM* is the organic matter content of the sample (g) and *CTdw* is the combusted Total dry weight of the sediment (g) and aluminium boat. It was assumed that the filter paper had been fully combusted and does not contribute to the resulting total weight.

$$\%OM = \left(\frac{OM}{Sdw}\right) \times 100$$

*Equation 13*

Where *%OM* is percentage organic matter content of the sample.

### *3.2.12 Laboratory – Sediment carbon content*

Organic carbon content of deposited sediment was obtained through gas chromatography via elemental analysis (EA). A sub-sample of sediment was prepared as follows. The sample was freeze-dried for a minimum of 12 h, then ground to a fine powder in a pestle and mortar and larger debris were removed - such as vegetative material, stones and shell fragments. Approximately 10 mg (±10 %) of milled sample was weighed into small (8 mm x 5 mm) silver capsules and 40 µl of 10 % HCl added to remove carbonates. Acidified samples were left over night in a fume hood, then placed in a drying oven to ensure all HCl had evaporated. Silver capsules were carefully folded and rolled, creating a sealed ball. These were analysed in an Elementar vario EL cube CHNS EA, with readings corrected back to doubled sulphanilamide standards every 10 samples. During analysis, samples were flash combusted at 1200°C, with an injection of oxygen, the resulting gaseous sample was separated and fed through three specific analysis columns (CO2, H2O, SO2; N2 is not absorbed by a column), carried in a flow of helium. Thermal conductivity across a detector quantifies sample components; with selective columns individually heated and gas production measured separately.

### *3.2.13 Filter paper error*

Testing of possible filter paper weighing error to total sediment dry weights and organic content values suggested that there was a consistent tendency to overestimate the amount of sediment present and to underestimate organic matter content. Tests were carried out on clean filter papers, which were exposed to saltwater and washed following the same protocol employed for sample processing.

Dry weight testing showed a significant difference [$t(19) = -8.804$, $p < 0.0001$] between the expected weight of paper and boat (mean = 1.6900 g, s.d = 0.0128) and the actual returned weights of filter papers (mean = 1.7032 g, s.d = 0.0127); an average discrepancy of 0.0132 ± 0.0015 g. This would produce an overestimation of total sediment quantity, as the 'heavier' filter paper post-deployment is effectively contributing to the recorded sediment weight. There was no significant correlation between the initial weight of the dried filter

paper and the resulting 'error' associated with it, p = 0.2, cor. = -0.30. This difference was applied as a correction to deposition dry weight measurements.

Organic matter content testing showed a significant difference [t(19) = -10.429, p < 0.0001] between the weight of the aluminium boat post combustion; where it is assumed the filter paper had fully ashed, and should be zero weight. The expected weight of the boat, was that measured prior to any input (mean = 0.9055 g, s.d = 0.0065) weighed less than its measured weight post-combustion (mean = 0.9159 g, s.d = 0.0096); an average difference of 0.0104 ± 0.0010 g. This would produce an underestimation of organic matter content of a sample, as the post-combusted weight is heavier than expected, which suggests 'less' organic matter had been lost. This difference was applied as a correction to combusted sediment weight.

### *3.2.14 Laboratory – Vegetation characterisation*

The seasonal images of vegetation in plan (*cover*) and transverse (*density*) views were processed to quantify vegetation present in a given frame using *ImageJ*. For each image *ImageJ* was provided with information of known distance (such as the width of tape on the board, or the diameter of the settlement support tube when visible), applying a unique spatial calibration to each and allowing more accurate evaluation of coverage.

Initially, each image was 'optimised', through adjustments of brightness and contrast, to maximise the visual distinction between vegetation and sediment (*cover*) or backing board (*density*) (Figure 3.11A). In each case the image was then converted to 8-bit (greyscale) and a threshold applied to select vegetation. Thresholding was carried out manually, aiming to set optimal limits which acquired maximum vegetation and minimum 'background by catch' (Figure 3.11B). Once thresholds were set, the image was analysed to give a measure of vegetation presence absolute area and percentage. Analysis of vegetation cover was carried out on a 75 x 75 cm area from the centre of the sampling plot. Analysis of vegetation density was carried out on a 50 x 50 cm area from the middle of the board with the bottom aligned along the sediment-board interface for the *density* images (Figure 3.10).

A *vegetation index* was created which combined *cover* and *density* values into a single metric. The index was calculated as per which bound values between zero and one.

$$Vegetation\ index = \frac{(Vegetation\ cover + Vegetation\ density)}{200}$$

*Equation 14*

**A.**

**B.**

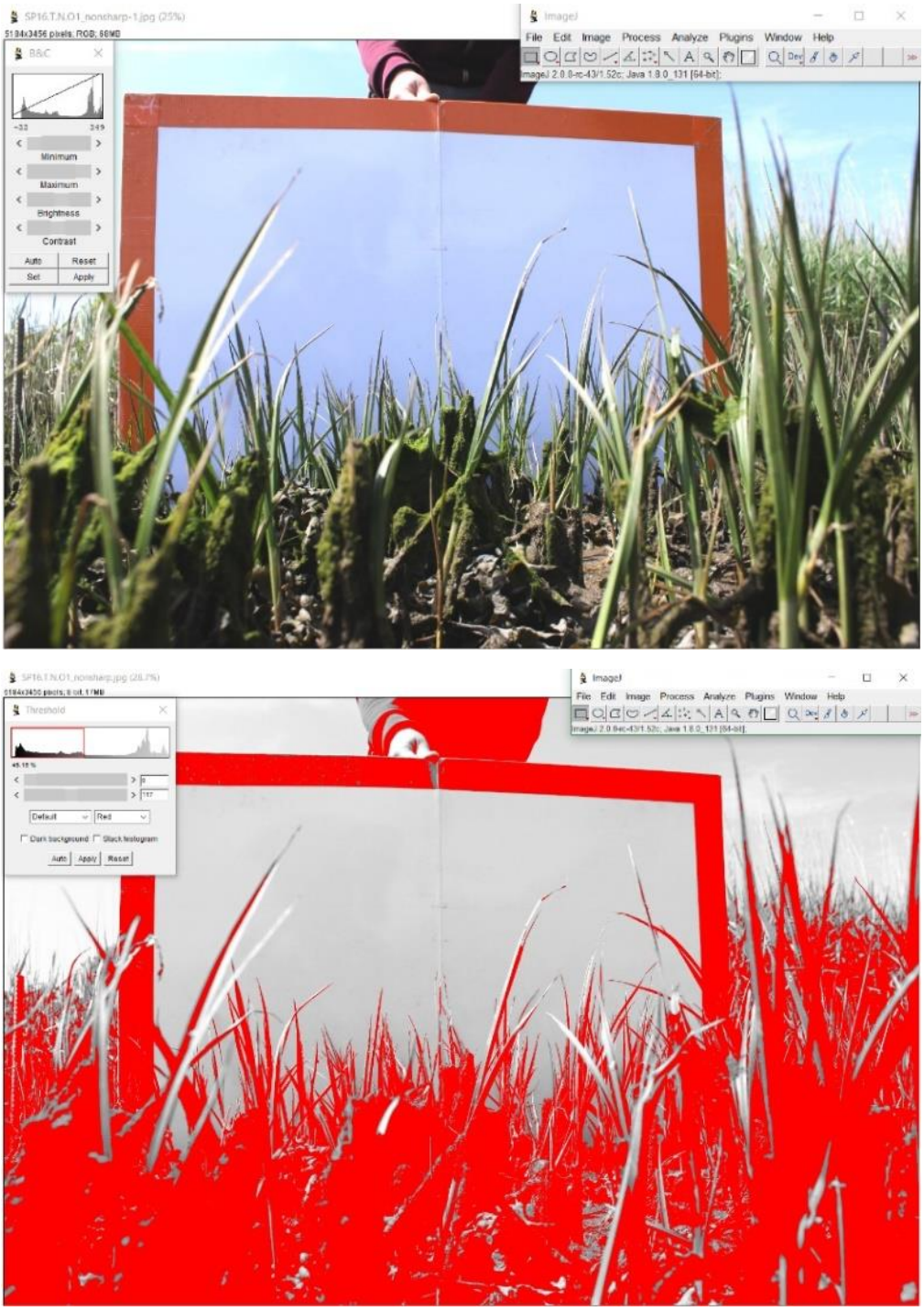


*Figure 3.11: Example of image processing carried out for vegetation density data collection. Image (A) shows the image being manipulated to enhance the distinction between vegetation and back-board, image (B) showing application of thresholds to the converted 8-bit greyscale image.*

## 3.3 Statistical analysis

Various assessments were made of deposition (rate, organic content, carbon content), settlement (rate, organic content, carbon content), vegetation structure and elevation change data.

Deposition and settlement rates were compared separately through the following. ANOVA was used to compare the rates of deposition or settlement found on each shore of the estuary, and further to compare these rates within each area type (i.e. natural, old planted, young planted and mudflat) located on each shore. When comparing between area types, data at each sampling point within a season were summed, giving a total amount of deposition or settlement occurring at a point during a season; removing issues associated with repeated measure type sampling which was conducted. The resulting dataset consisted of 128 points, 64 for each shore, from four season and four points in each area type. These data were also used to analyses the interactive influence of area type and season on each shore.

Correlation and linear regression were used to assess the relationship between amounts of sediment deposition and settlement occurring at each sampling point, where samples were paired within each sampling event.

Tidal inundation time experienced by all samples were assessed, comparing the differences between each shore, between area types within a shore and between similar areas n opposite shores.

Vegetation cover and density differences between areas were analysed and their influence on deposition and settlement rates (sediment dynamics) assessed. Beta regression was carried out with post-hoc Tukey's analysis to assess if vegetation cover and density were significantly different between area type. Beta regression was used as data was presented as a percentage. GLM was used to analyses the relationship between vegetation cover and density with season and area type, comparing the influence of season both with and without area type as a factor. Further analysis of these characteristics', and vegetation structure (vegetation index), influence on sediment deposition and settlement was completed using GLM.

Changes in sediment surface elevation were assessed using regression and ANOVA, to assess the relationship between elevation change and deposition (regression) and the influence of area type on resulting elevation change (ANOVA).

Finally, carbon content data were analysed. a series of GLM (which used a 'Gamma' family error distribution) assessed the relationship between organic matter content and organic carbon content and the influence of area type and season, comparing these GLM using ANOVA. One-way and two-way ANOVA was used to assess the relationships between carbon content and deposition and area type (and the interaction between these).

## 3.4 Hypotheses – sediment dynamics

Data in this chapter assess sediment dynamics over a year-long period (four seasons) within the area studied, comparing how the different area types influence, or experience, different sediment deposition, settlement and accretion. These data also assess the sedimentary carbon dynamics within the study area. The aim of which being to assess carbon sequestration differences and the influence of restoration activity on this process. The study held the following hypotheses:

- Vegetated areas will experience greater sediment deposition than bare mudflat.
- Vegetated areas will experience greater sediment accretion than bare mudflat.
- Vegetative structure will influence sediment dynamics.
- Different vegetative structure types (*P. maritima* and *B.maritimus*) will contribute to differing sediment dynamics.
- Restored areas will experience enhanced deposition than adjacent bare mudflats
- Carbon accretion will be greater in vegetated areas.
- Restored areas will experience enhanced carbon accretion than adjacent bare mudflats.

## 3.5 Results

The data collected towards this investigation allowed various assessments to be made around the sedimentary dynamics present within the Eden Estuary. The results are assessed in number of sections:

- A broad level evaluation of differences between the area types studied, focusing on how restoration areas differs from the mudflat and the natural vegetation.
- A finer scale investigation into the drivers of deposition; including settlement vs deposition rates, elevation/inundation period, vegetation structure, and season.
- An assessment of how sediment elevation changes differ between areas, and how these rates link with deposition measurements.
- An evaluation of how calculated carbon content differences in deposition relate to potential ecosystem service benefit of each area.

### 3.5.1 Deposition and settlement rates

In some instances, there was very little sediment deposition on filter papers (91 of 512 samples, 17.8 %), often resulting in "negative" sediment weights (typical <0.005 g discrepancy), likely resulting from subtraction of foil and paper weights and associated weighing error; these papers were assigned a zero value, as negative deposition is illogical. It was felt that these changes were acceptable as they serve to reflect the true situation of negligible, or in fact no, deposition.

#### 3.5.1.1 Deposition rate differences between area types and season

Rates of deposition showed marked differences between each area, both within shores (north and south) and across them; except for the old restored sites that exhibited similar total deposits during the study (Figure 3.12). There was a general trend of the natural and old restored sites exhibiting lower rates of deposition than found in the young restored and mudflat areas.

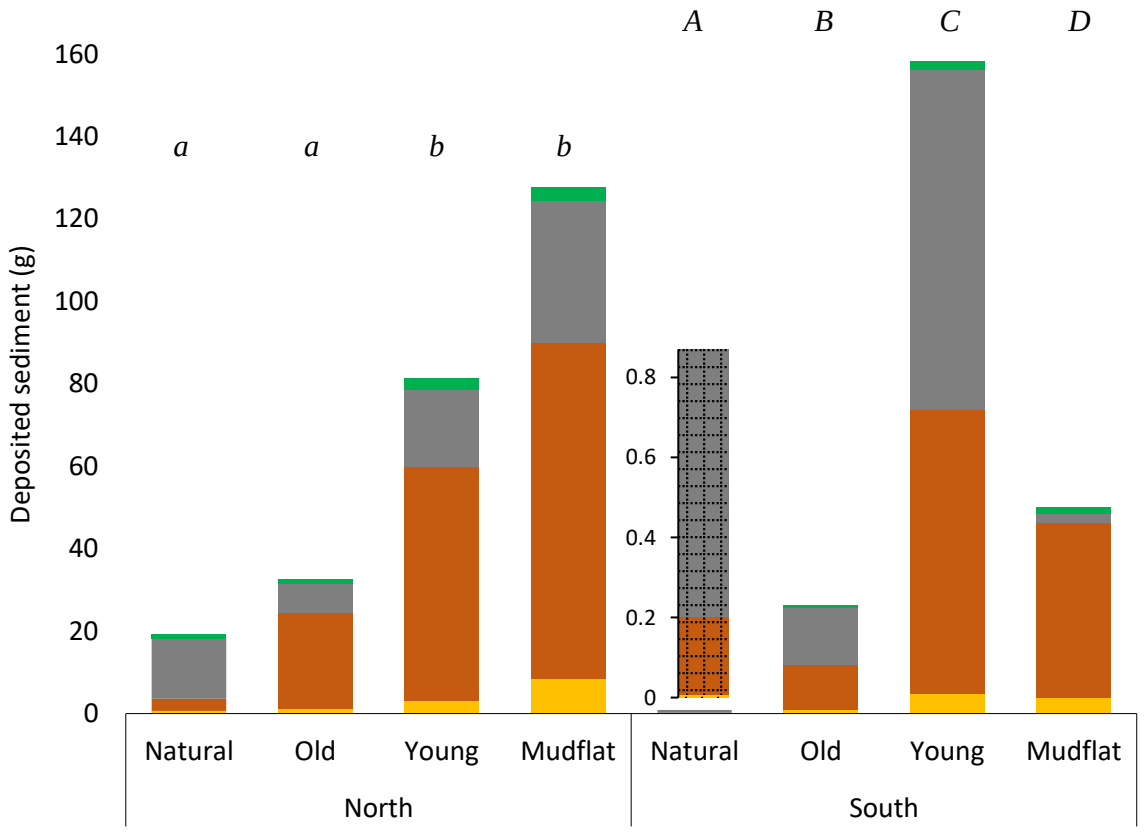


*Figure 3.12: Total dry weight of sediment deposition measured in each area on each shore in each season (n = 511). Bars are coloured by season, summer = yellow, dark orange = autumn, grey = winter, green = spring. Insert for the Natural area on the south shore (hatched fill) shown on different scale to view data. Letters indicate significant differences (p < 0.0001) within each shore of total deposition, lower case = north shore, upper case = south shore.*

There were significant differences between the amount of deposition measured on each shore (ANOVA: F(1, 509) = 14.35, p = 0.0002). Assessment of area type (within each shore, accounting for the determined significant difference between deposition on the north and south shores) influence on sediment deposition indicated the following. On the north shore there were significant differences between areas (ANOVA: F(3, 60) = 3.257, p = 0.0276). The south shore showed significant difference between areas (ANOVA: F(3, 60) =

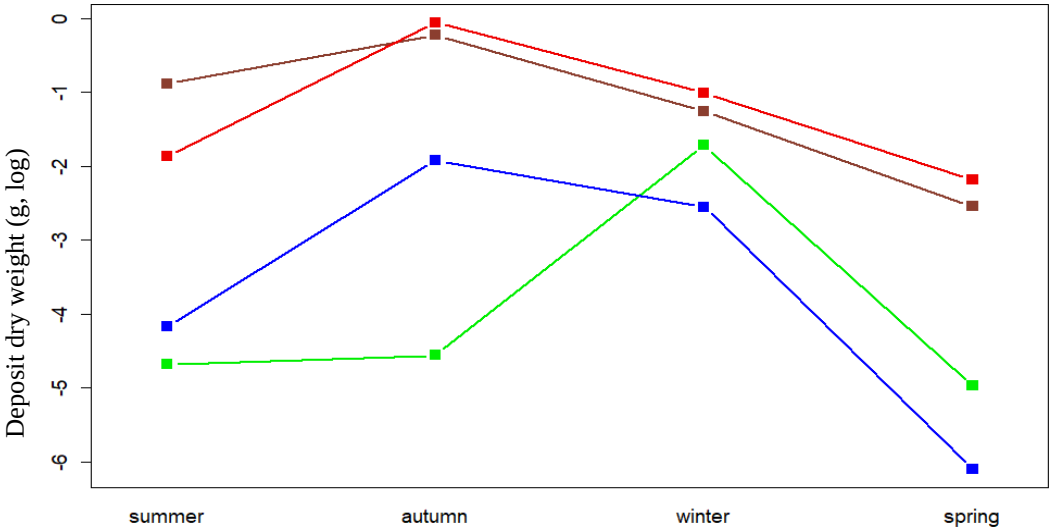


*Figure 3.14: Interactions between area type and season and the impact on observed sediment deposition during the study on the **north shore**. Plotted against the log of measured deposits dry weight (g), using the mean values of data. Line colour indicates area type: brown = mudflat, red = young restored saltmarsh, blue = old restored saltmarsh, and green = natural saltmarsh area (B. maritimus on the north shore).*

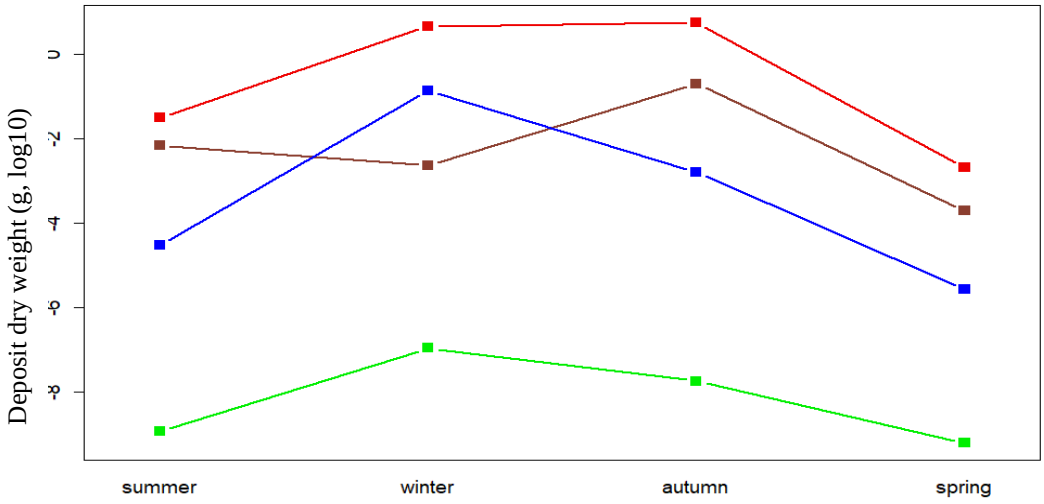


*Figure 3.13: Interactions between area type and season and the impact on observed sediment deposition during the study on the **south shore**. Plotted against the log of measured deposits dry weight (g), using the mean values of data. Line colour indicates area type: brown = mudflat, red = young restored saltmarsh, blue = old restored saltmarsh, and green = natural saltmarsh area (P. maritima on the north shore).*

40.44, $p < 0.0001$) and Tukey's HSD showed significant differences existed between the natural area and all other areas, no significant different was found between all other areas.

Investigation, with a two-way ANOVA, into the effects season plays on sediment deposition within each area on each shore indicates there is no significant interaction with season and area type on the north shore, ($F(9,48) = 1.376$, $p = 0.226$), where all areas interact similarly with changing season (Figure 3.14).

There was shown to be no significant interaction between season and area type in determined deposition rates on the south shore ($F(9, 48) = 1.202$, $p = 0.316$). However, there are shown to be slight differences in the relationships between the areas and season

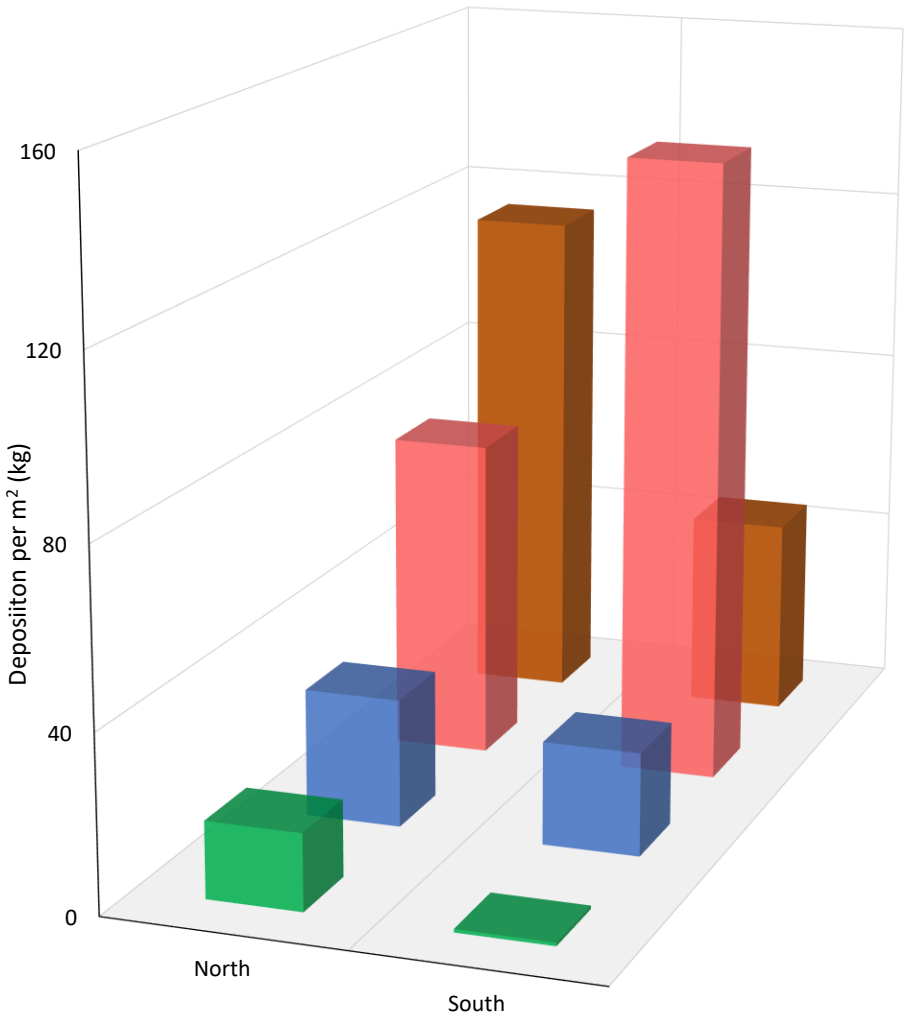


*Figure 3.15: Total sediment deposition estimated to occur within $1m^2$ in each area on each shore over one year. Colours indicate area type, where brown = mudflat, red = young restored, blue = old restored and green = natural saltmarsh (B. maritimus on the north shore and P. maritima on the south shore).*

than seen on the north shore (Figure 3.13), the natural area experienced markedly different deposition than all areas across all seasons.

Data were used to generate estimates of total deposition which could be expected to occur over a typical $1m^2$ area in each area over a single year (Figure 3.15). Figures are calculated based on average daily deposition over $1m^2$ in each area during each season, with each season then multiplied by a standard 91.25 days (one quarter of a year). The greatest and least sediment deposition are both expected to occur on the south shore, within the young restored area and natural saltmarsh respectively. On both sides of the estuary, the natural marsh area experienced the least deposition per unit area (17.39 $kg/m^2$ in the north and 0.78 $kg/m^2$ in the south), closely followed by the old restored sites (29.17 $kg/m^2$ in the north and 23.47 $kg/m^2$ in the south).

#### *3.5.1.2 Settlement rate between area type and season*

Sediment settlement rates (Figure 3.16), as measured just above the sediment surface adjacent to deposition measurements, did not display the same differences between shores as found with deposition rate. There was no significant difference between settlement rates measured found on each shore (ANOVA: $F(1, 509) = 0.6945$, $p = 0.405$).

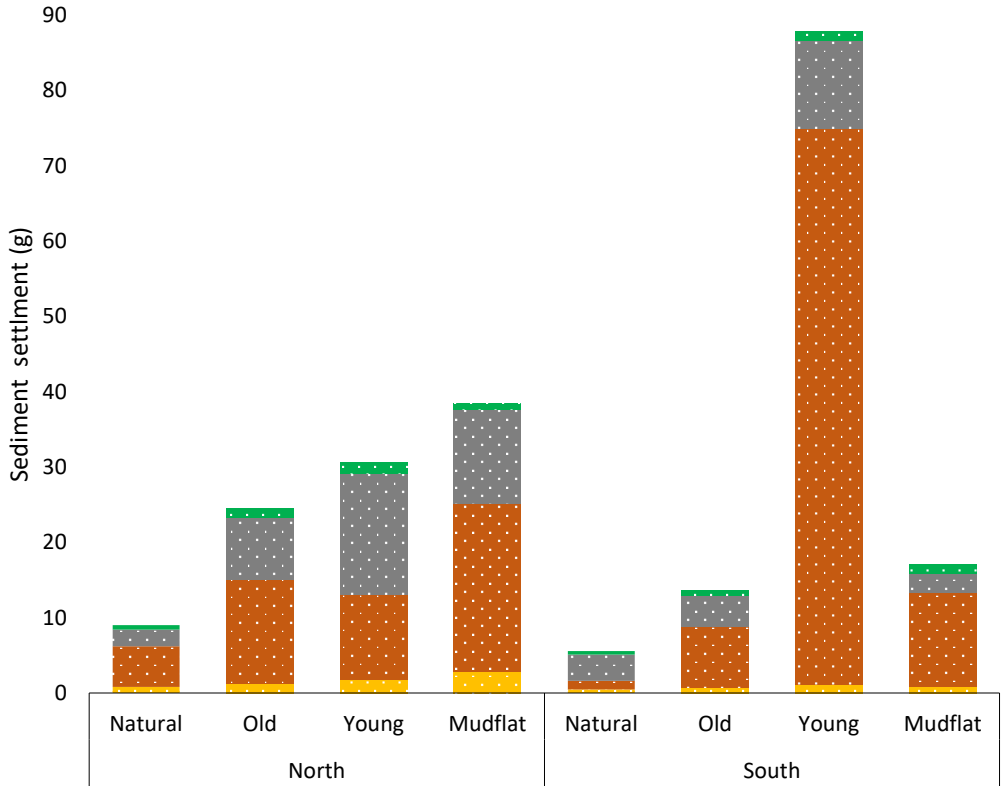


*Figure 3.16: Total dry weight of sediment settlement measured in each area on each shore in each season (n = 511). Bars are coloured by season, summer = yellow, dark orange = autumn, grey = winter, green = spring.*

Analysis of differences between area types on each shore shoed there were no significant difference between the areas on the north shore (ANOVA: $F(3, 60) = 2.315$, $p = 0.085$), however there were significant differences between the areas of the south shore (ANOVA: $F(3, 60) = 5.353$, $p = 0.333$). TukeysHSD post-hoc analysis showed that the only significant difference in sediment settlement rate on the south shore was found between the natural and young planted area ($p < 0.0001$).

Investigation of the interactive influence of area and season (two-way ANOVA) on each shore, showed there was no significant interaction on the north shore and a significant interaction on the south shore (ANOVA: $F(9, 48) = 6.916$, $p < 0.0001$).

#### *3.5.1.3 Relationship between deposition and settlement in different area types*

There was significant correlation ($r_s = 0.67$, $p < 0.0001$) between the rates of paired deposition and settlement measurements across the study area. Analysis within each area showed there were significant correlations between deposition and settlement in all areas (Table 3.2). All areas of *B. maritimus* vegetation display similar strengths in the relationship between deposition and settlement rates, specifically the area of old restoration on the north and south shore exhibit near equal relationship strengths with $r_s$ values of 0.78 and 0.79, respectively.

*Table 3.2: Summary of correlations between deposition and settlement rates measured in each area type across the full study, analysed using spearman's rank correlation to address non-normal distribution of the data.*

| Shore | Area type | rho | p |
|---|---|---|---|
| North | Natural | 0.72 | > 0.0001 |
| | Old Restored | 0.78 | > 0.0001 |
| | Young Restored | 0.64 | > 0.0001 |
| | Mudflat | 0.35 | 0.007 |
| South | Natural | 0.41 | 0.0008 |
| | Old Restored | 0.79 | > 0.0001 |
| | Young Restored | 0.71 | > 0.0001 |
| | Mudflat | 0.42 | 0.0007 |

Linear regression between ($log_{10} + 0.001$) deposition rate and settlement across the study, indicated a weak but significant relationship between them ($F(1, 509) = 78.69$), with an $R^2 = 0.13$. Assessment of the way in which settlement rate interacted with the specific area

type to influence the resultant deposition showed all areas, except the natural saltmarsh on the south shore, displayed a significant interaction with settlement. This relationship was evaluated in each area to determine the interaction of settlement and deposition within each of these defined areas; regressions used $log_{10} + 0.001$ transformed deposition data to produce normally distributed residuals. All areas showed a significant relationship between settlement and deposited material. Mudflat and young restored areas displayed similar relationships between settlement and deposition rates (Figure 3.17), with old restored areas and the natural stand of *B. maritimus* also displaying similar relationships; where the former showed a need for more sediment settlement to increase resulting deposition (Figure 3.17).

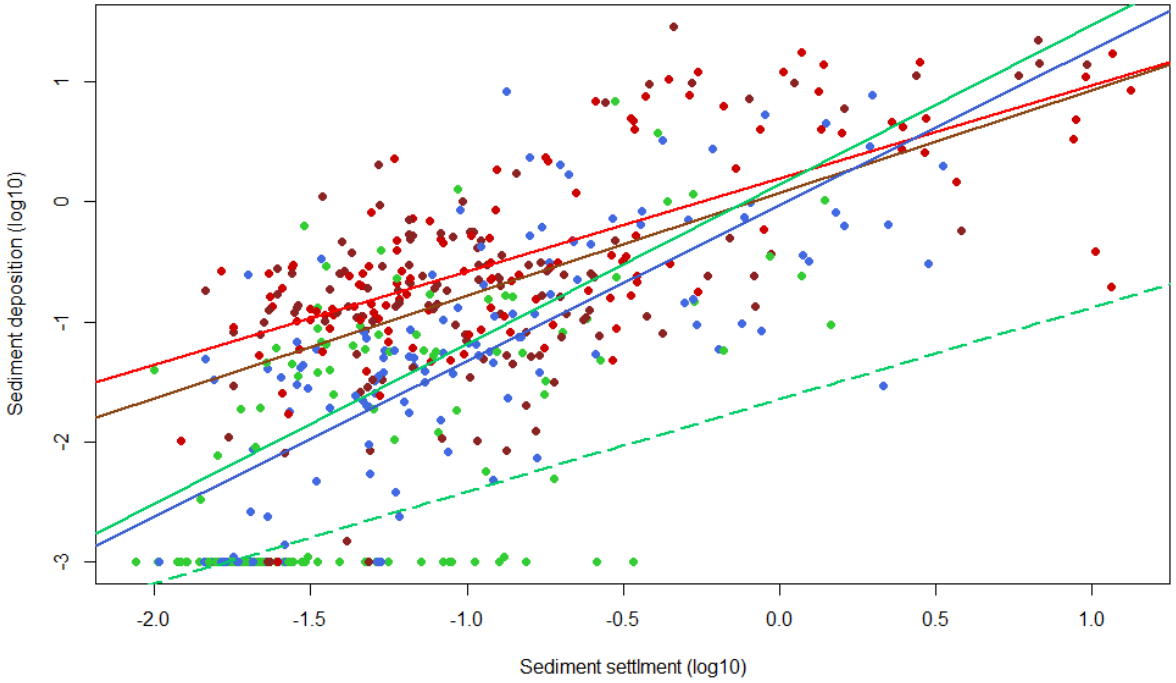


*Figure 3.17: Settlement and deposition data from across the study, plotted on log10 scale. Linear regression lines shown for each area type, one line each for the old restored, young restored and mudflat areas, with the natural area of the north (solid line) and south shore (dotted) plotted separately. Colours indicate area type, where brown = mudflat, red = young restored, blue = old restored and green = natural saltmarsh.*

The natural area of *P. maritima* saltmarsh displayed a substantially different relationship which indicate a lower rate of deposition in all circumstances and lower increase in deposition per unit of settlement increase (Figure 3.17).

#### *3.5.1.4 Relationship between deposition and elevation (inundation)*

Tidal inundation was calculated for each sample station from its known elevation (acquired by differential GPS) and tide gauge data, contributed by the British Oceanographic Data Centre (Leith). Inundation periods were determined over the course of each sampling

occasion for each point, providing immersion times experienced in each area type across seasons (Figure 3.18). Elevations were calculated using the known height, determined by high-accuracy differential GNSS in Summer 2016, as a baseline and applying collected SEB data to produce previous actual elevations values (Table 3.3). Geo-referenced elevations were converted to Admiralty Datum, applying a correction of 2.90 m to the Ordnance Datum, to match tide gauge data reference.

The two shores in the study were exposed to significantly different tidal inundation periods during the study ($F(1,510) = 39.95$, $p < 0.001$)), where the total inundation time across all sampling points were 1,800 hours on the north shore and 1,422 hours on the south shore.

On the north shore of the estuary, over the sampling period, there was a significant difference in inundation time between the sites ($F(3, 252) = 35.56$, $p < 0.001$); total inundation time, experienced by all sampling points, over the sampling period (i.e. the total time all samples at all points spent inundated) were, Natural = 420 hr, Old Restored = 373 hr, Young Restored = 516 hr and Mudflat = 579 hr. In a TukeysHSD test these differences were shown to be significant between all areas, except for between the natural and old restored area ($p = 0.15$).

*Table 3.3: Elevation above admiralty datum (m) of permeant sampling points through-out study period. Spring 2016 measured by high-accuracy GNSS, preceding months calculated as SEB changes from Spring 2016 reference.*

| Shore | Sample point | Summer 2015 (September) | Autumn 2015 (November) | Winter 2016 (February) | Spring 2016 (June) |
|---|---|---|---|---|---|
| North | Natural 1 | 5.174 | 5.180 | 5.179 | 5.181 |
| | Natural 2 | 5.287 | 5.286 | 5.286 | 5.289 |
| | Natural 3 | 5.301 | 5.304 | 5.303 | 5.307 |
| | Natural 4 | 5.256 | 5.264 | 5.263 | 5.266 |
| | Old 1 | 4.542 | 4.542 | 4.544 | 4.553 |
| | Old 2 | 4.544 | 4.547 | 4.546 | 4.551 |
| | Old 3 | 4.616 | 4.614 | 4.621 | 4.630 |
| | Old 4 | 4.539 | 4.540 | 4.540 | 4.546 |
| | Young 1 | 4.603 | 4.603 | 4.623 | 4.629 |
| | Young 2 | 4.463 | 4.463 | 4.453 | 4.456 |
| | Young 3 | 4.439 | 4.433 | 4.429 | 4.437 |
| | Young 4 | 4.443 | 4.437 | 4.438 | 4.442 |
| | Mudflat 1 | 4.421 | 4.422 | 4.422 | 4.426 |
| | Mudflat 2 | 4.482 | 4.481 | 4.482 | 4.485 |
| | Mudflat 3 | 4.246 | 4.240 | 4.242 | 4.243 |
| | Mudflat 4 | 4.141 | 4.133 | 4.142 | 4.141 |
| South | Natural 1 | 4.232 | 4.233 | 4.231 | 4.234 |
| | Natural 2 | 4.433 | 4.431 | 4.429 | 4.434 |
| | Natural 3 | 4.665 | 4.666 | 4.674 | 4.675 |
| | Natural 4 | 4.790 | 4.791 | 4.791 | 4.798 |
| | Old 1 | 4.742 | 4.744 | 4.742 | 4.741 |
| | Old 2 | 4.741 | 4.745 | 4.746 | 4.745 |
| | Old 3 | 4.624 | 4.620 | 4.624 | 4.623 |
| | Old 4 | 4.544 | 4.550 | 4.534 | 4.532 |
| | Young 1 | 4.473 | 4.477 | 4.466 | 4.467 |
| | Young 2 | 4.169 | 4.176 | 4.171 | 4.174 |
| | Young 3 | 4.099 | 4.099 | 4.084 | 4.086 |
| | Young 4 | 4.473 | 4.474 | 4.475 | 4.472 |
| | Mudflat 1 | 4.101 | 4.098 | 4.102 | 4.104 |
| | Mudflat 2 | 3.984 | 3.979 | 3.965 | 3.965 |
| | Mudflat 3 | 4.025 | 4.024 | 4.026 | 4.029 |
| | Mudflat 4 | 4.377 | 4.369 | 4.375 | 4.373 |

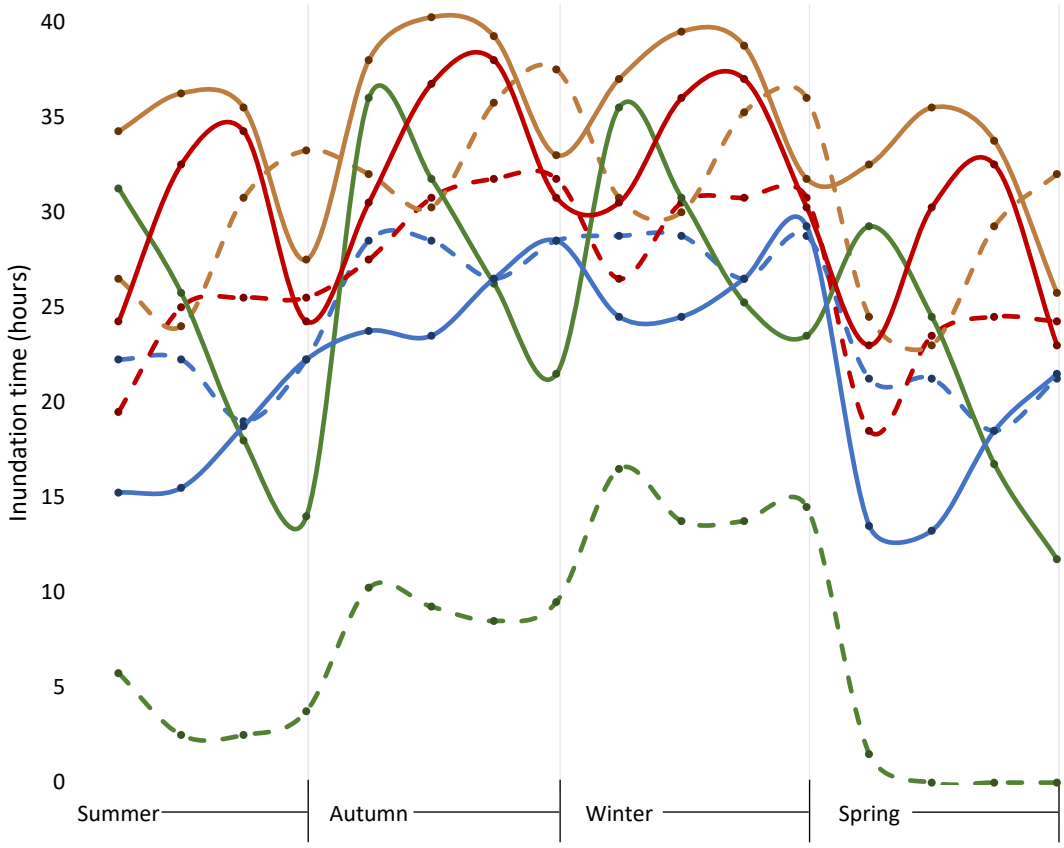


*Figure 3.18: Estimated inundation periods experienced by each sample point in each area on each shore throughout the study; calculated using the known elevation of sampling points and tidal data. Each point is a sampling location, four in each area, which are repeated in the same order in each season. Line colour indicates area type; green = Natural, blue = Old Restored, red = Young Restored and brown = Mudflat. Solid line is the north shore and dotted line the south shore.*

The different areas of the south shore were shown to experience significantly different immersion periods across the study ($F(3, 252) = 130.1$, $p < 0.001$), were Natural = 130 hr, Old Restored = 417 hr, Young Restored = 451 hr and Mudflat = 511 hrs. Tukey's HSD revealed that all areas of the south shore experience significantly different immersion periods, except between the between the old restored and young restored area. There was, however, a general trend of similar tidal inundation regimes experienced by the same area type on each shore, where older restored areas experience more inundation than the mudflat, which experience more than the young restored area (Figure 3.18). The two natural area types reflect their different situations in the study, with inundation being greatly different throughout the year (Figure 3.18). A comparison of area types across shores shows there to be no significant difference in experienced inundation for old restored areas ($p = 0.438$), young restored areas ($p = 0.051$), with the natural areas ($p < 0.0001$) and mudflats ($p = 0.035$) experiencing significantly different inundation regimes.

There was a large difference in the quantity of deposition which occurred per m2 per inundation period, where on average the bare mudflat and young restored area experiences significantly larger quantities of deposition (Table 3.4). The lowest average rate of deposition was found in the natural P. maritima marsh, being 0.66 g/m$^2$/hour inundation (Table 3.4); this area was also the highest in elevation (Table 3.3) and experienced the least amount of inundation during the study (Figure 3.18).

*Table 3.4: Average rates of deposition per m$^2$ with period of inundation in each area and season.*

| Shore | Area | Sediment deposition rate (g/m$^2$/hour inundation) | | | | |
|---|---|---|---|---|---|---|
| | | **Summer** | **Autumn** | **Winter** | **Spring** | **AVERAGE** |
| North | Natural | 0.91 | 4.03 | 19.96 | 2.32 | **6.80** |
| | Old | 1.80 | 35.81 | 10.39 | 2.78 | **12.70** |
| | Young | 3.49 | 65.84 | 21.82 | 3.97 | **23.78** |
| | Mudflat | 8.61 | 85.26 | 36.88 | 3.96 | **33.68** |
| South | Natural | 0.03 | 0.82 | 1.80 | 0.00 | **0.66** |
| | Old | 1.24 | 15.37 | 19.20 | 1.11 | **9.23** |
| | Young | 6.25 | 89.15 | 109.55 | 3.53 | **52.12** |
| | Mudflat | 4.32 | 49.45 | 2.48 | 2.40 | **14.67** |

#### *3.5.1.5 Relationship between deposition and vegetation structure*

Vegetation cover and density data were extracted from images captured at each sampling point once in each season during the study. The percentage of vegetation present in each sampling area was determined, providing 'cover %' against bare sediment and 'density %' against the white backing-board. These values were considered separately, investigating how these two broad aspects of vegetation structure interact with sediment processes. Furthermore, cover and density data were combined to generate a vegetation structure index, this was bound between 0 and 1.

Vegetation cover and density of each area type displayed similar trends between shores (Figure 3.19, Figure 3.20). The bare mudflat showed consistently low values for both measures, with the young restored area similarly low for most sampling points; one point on the north shore appears to be doing 'better' than its counterparts exhibiting much greater cover and density values (Figure 3.20). The natural areas of the north and south shore displayed clear differences in structural dynamics throughout the year. The *B. maritimus* of

the north shore was dominated by high density percentages and lower cover values, with the south shores *P. maritima* presenting with the opposite, being dominated by higher cover percentage and lower density values (Figure 3.19).

Beta regression was carried out with post-hoc Tukey's analysis to assess if vegetation cover and density were significantly different between area type. The analysis of vegetation cover indicated that across the data, there was no significant difference between the mudflat on the south shore and the two stands of young restored vegetation, there was also no significant difference between the two area of young restored vegetation (Table 3.5); all being similarly low in values (Figure 3.20). Furthermore, no significant difference was found between the old restored stand of vegetation of the south shore and the natural area of *B. maritimus* on the north shore (Table 3.5).

A similar analysis assessing vegetation density data showed there to be no significant differences between the two mudflat areas and the young restored area on the south shore or the north young restored area and its adjacent mudflat (Table 3.5). Furthermore, as was found for vegetation cover, there was no significant difference between the old restored stand of vegetation and the natural area of *B. maritimus* on the north shore, also no difference between vegetation in the natural area of the south shore and the old restored area on the north shore (Table 3.5).

Changes in vegetation characteristics across season and within area type were analysed used GLM, where *season* and *area type* were applied as a fixed effects were compared against a GLM without *area* type. Comparisons of the AIC values for the two models indicates that *area type* better explains the vegetation cover measured with seasons, suggesting it places a significant role in vegetation cover values. GLMs were also used to compare vegetation density, as with vegetation cover. Comparison of two models with and without *area type*, the lower AIC value of the model containing the *area type* suggest, as with vegetation cover, that *area type* has a significant influence on vegetation density values measured.

Differences in the cover-density balance found at each area were combined when calculated into the vegetation structure index, of particular relevance in the case of natural saltmarsh areas on each shore. Vegetation index values indicate that, cumulatively, natural vegetation cover and density produce the 'most' vegetation across the study (Figure 3.22), though the areas of old restoration were also suggested to contribute large amounts of vegetation. Furthermore, when evaluated by vegetation index, the natural areas from the north and south shore were similar and their different cover-density balances 'masked' (Figure 3.21

and Figure 3.22); indicated by the mixed nature of similar sized points for natural vegetation on the north (average of 0.596) and south shore (average of 0.597) (Figure 3.22). Old restored vegetation was also shown to be similar to its natural counterparts, having an average vegetation index value of 0.284 on the north shore and 0.526 on the south shore (Figure 3.22).

*Table 3.5: Summary of Tukey's adjusted contrasts from beta regression modelled vegetation cover and density against different area types, showing only non-significant differences between areas ($p > 0.05$).*

| Comparators | | P |
|---|---|---|
| **Vegetation cover** | | |
| North Natural | South Old Restored | 0.0518 |
| North Young Restored | South Young Restored | 1 |
| | South Mudflat | 1 |
| South Mudflat | South Young Restored | 1 |
| **Vegetation density** | | |
| North Natural | South Old Restored | 0.9909 |
| North Old Restored | South Natural | 0.1209 |
| North Young Restored | South Young Restored | 0.8871 |
| | South Mudflat | 0.6173 |
| North Mudflat | North Young Restored | 0.2005 |
| | South Young Restored | 0.9279 |
| | South Mudflat | 0.9960 |
| South Mudflat | South Young Restored | 0.9997 |

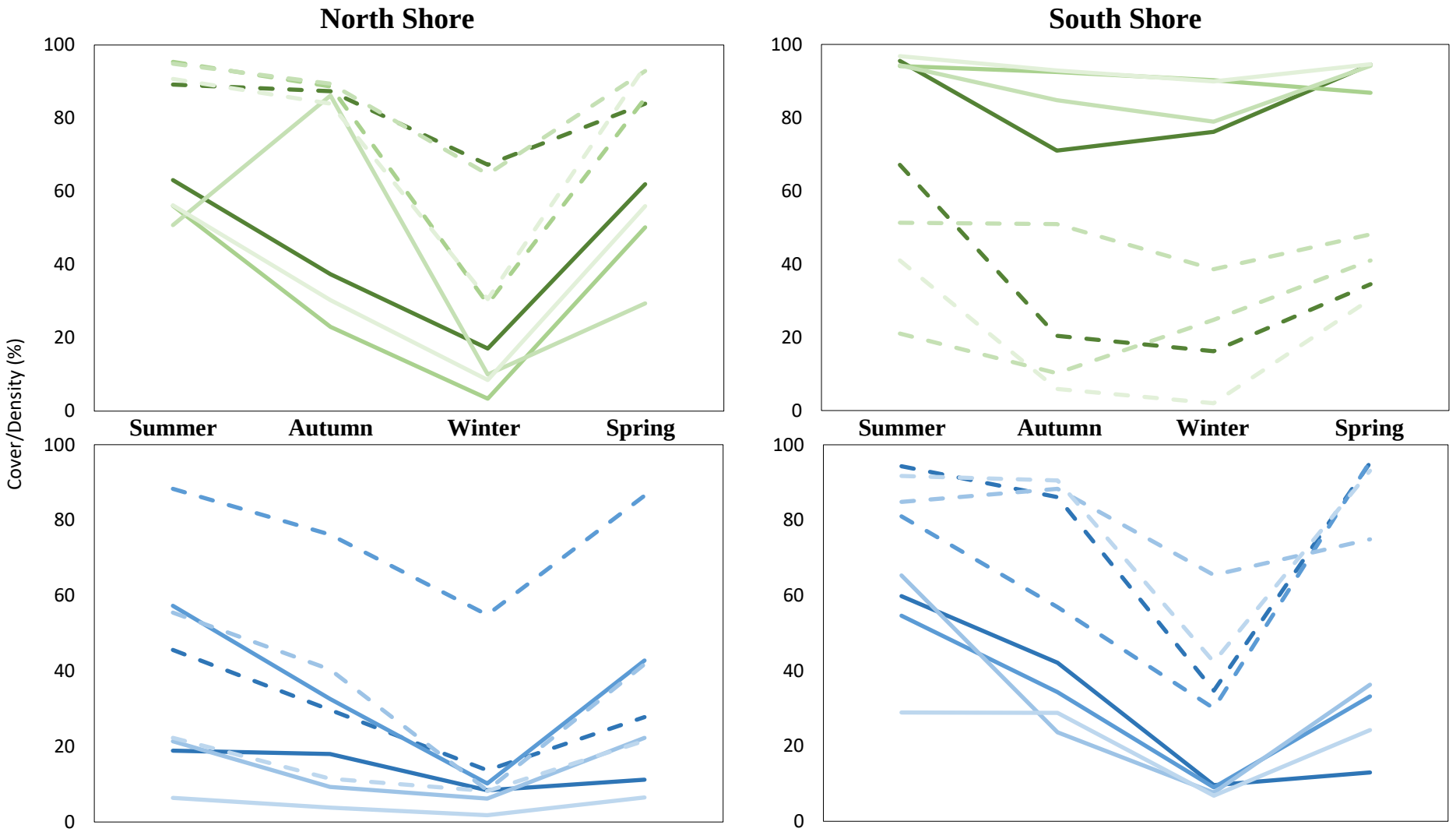


*Figure 3.19: Vegetation cover and density percentages measured across four seasons. Top row in green is natural saltmarsh and bottom row in blue is old restored vegetation. Solid lines show cover percentage and dotted lines show density percentage. Four line shades in each graph indicate four sample points used.*

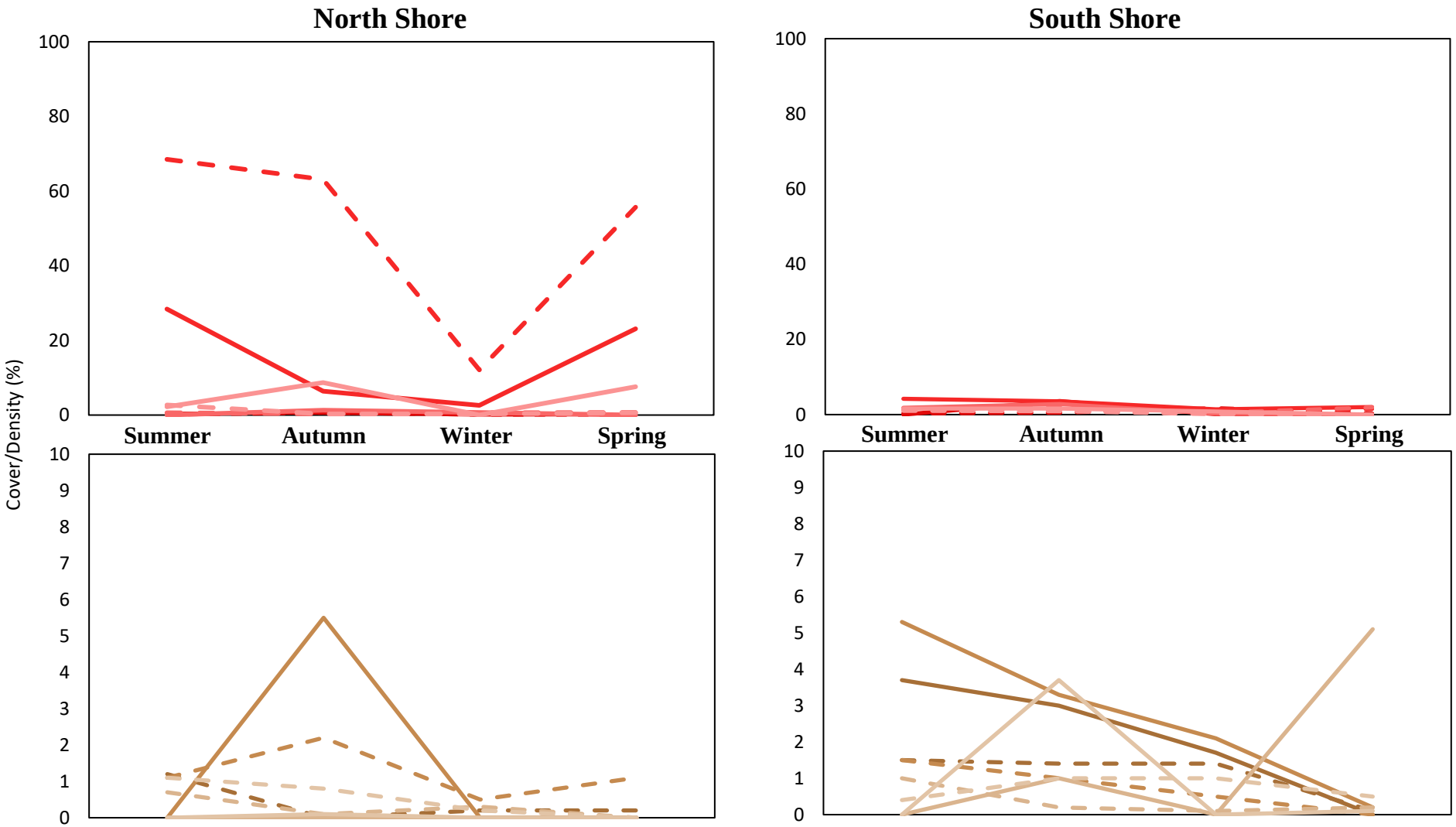


*Figure 3.20: Vegetation cover and density percentages measured across four seasons. Top row in red is young restored saltmarsh and bottom row in brown is mudflat. Solid lines show cover percentage and dotted lines show density percentage. Four line shades in each graph indicate four sample points used*

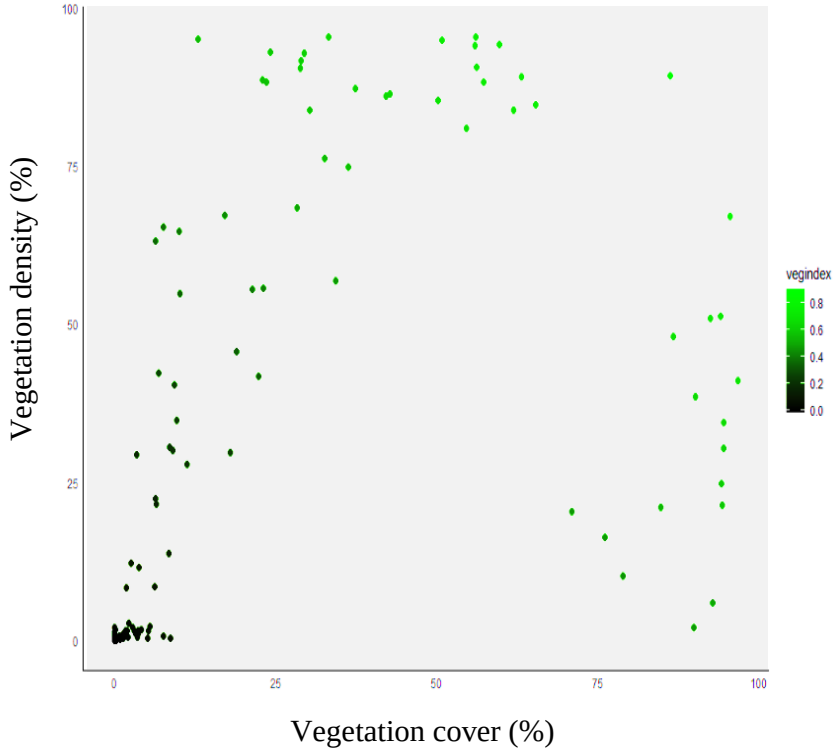


*Figure 3.21: Vegetation cover and density data for each sampling point in each season, coloured by the resulting assigned vegetation index value.*

The influence of vegetation structure on sediment deposition was investigated with a GLM taking $log_{10} + 0.001$ transformed sediment deposition values as a dependent variable with vegetation cover, density and their interaction as independent variables. The GLM ($F(3, 507) = 115.3$, $p < 0.001$), showed that the interaction of the two measures of vegetation characteristics significantly influenced deposition rates ($p = 0.0169$), fitted with the equation; Sediment deposition ($log_{10} + 0.001$) = -0.559 – (0.005*vegetation density) + (-0.026 + 0.0001*vegetation density)*vegetation cover, where the whole model explained 40 % of the variance in deposition quantity.

The influence of the calculated vegetation index on sediment deposition was assessed with a GLM taking $log_{10} + 0.001$ transformed sediment deposition values as a dependent variable. The GLM ($F(1, 509) = 225.6$, $p < 0.001$), showed that vegetation index had a significant relationship with the quantity of deposition which occurred, with the relationship defined as Sediment deposition ($log_{10} + 0.001$) = -0.057 – 0.146*vegetation index ($R^2 = 0.31$, $p < 0.001$).

A comparison of the two models suggest that the individual measures of vegetation characteristics and their interaction are more robust at explaining deposition rates, having a lower residual deviance than the modelled vegetation index, with a residual deviance difference of 65. However, both analyses express the same trend that with increased vegetation, however it is quantified, there is a slight reduction in the amount of sediment deposited.

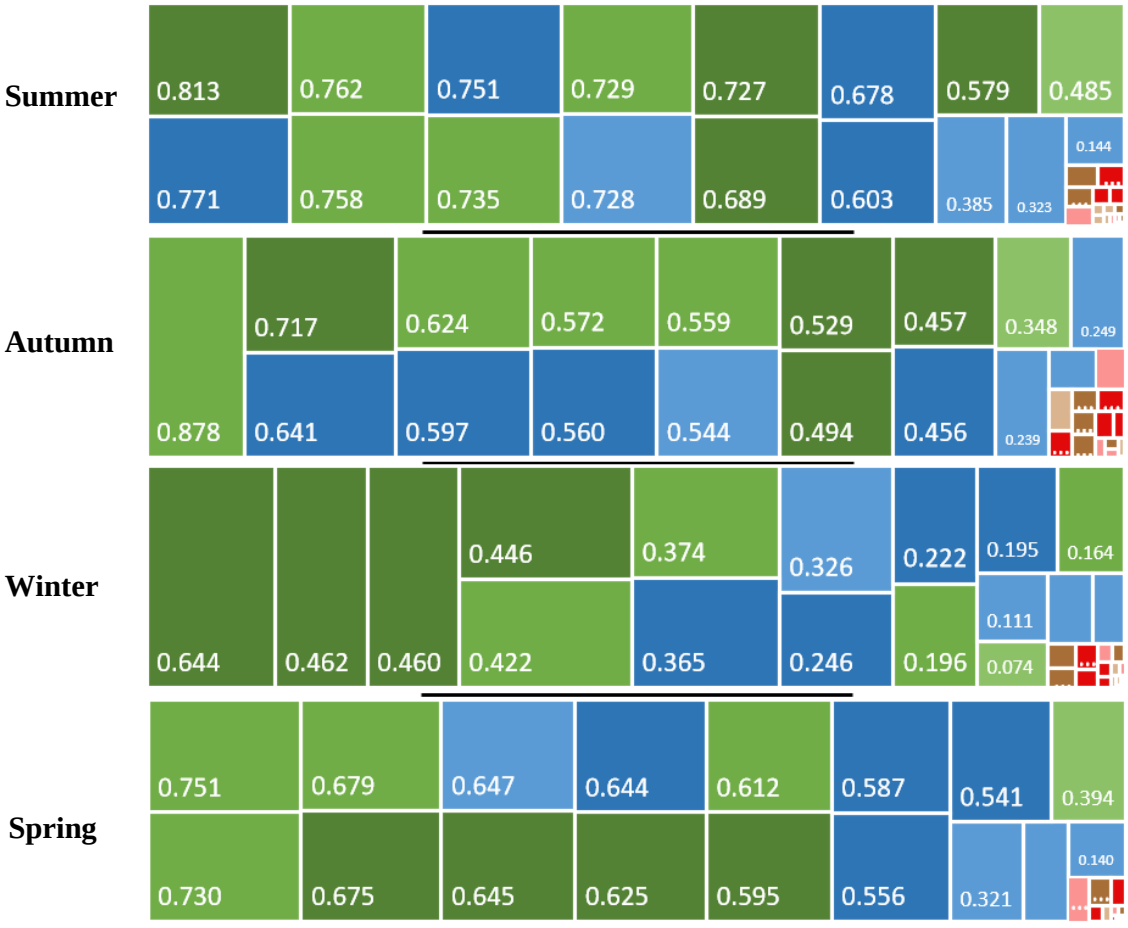


*Figure 3.22: Vegetation index for each season across the entire study area. The index is bounded between 0 and 1, and combines cover and density percentage data. The larger the box the greater the index value, arrnaged largest to smallest left to right. Colours indicate area type, light shades are the north shore, dark the south shore. Green = natural saltmarsh, blue = old restored area, red = young restored area, brown = mudflat.*

### *3.5.2 Elevation changes and deposition*

Changes in sediment elevation were determined from SEB measurements taken once per season. There were four SEBs in each area, each of which consisted of 11 measurements to determine the distance between the table and the sediment surface. Data from each SEB measurement (i.e. the 11 points) were averaged. Changes of elevation during the study were

calculated as the difference between the average SEB elevation of a season and its previous season, where the previous season acts as the reference data; the change during summer 2015, at the start of the study, was calculated from the spring reference, taken prior to the commencement of the study. These data were compared against the measured rates of deposition at each sampling point, assessing the relationship between 'potential accretion' as attributed to an assumed full-retention of deposits and actual accretion as measured by changed in sediment elevation.

#### *3.5.2.1 Comparison of elevation change between different area types and season*

During the study, the two shores display differing general trends (Figure 3.23) where on average across all areas in each seasons, the north shore was marginally erosional (-0.3 mm), and the south shore was accretional (1.5 mm); resulting in a respective total change of -1.2 mm and 5.8 mm respectively on each shore (Table 3.6).

On the north shore, the natural saltmarsh was shown to be a constantly accretional environment (Figure 3.23), with an average elevation change of 1.9 mm across the study. All other areas of the north shore experienced a net lowering of elevation (Table 3.6), assumed to be due to loss of material. The greatest loss across areas was recorded during winter, where there was a net lowering of 3 mm; only the natural saltmarsh accreted during this season. The 'lost' material during winter was mainly from the areas of restoration, with the old site lowered by 3 mm and the young site lowered by 7 mm.

On the south shore the greatest increase in sediment elevation was recorded by the old restored area of *B. maritimus* (Figure 3.23, Table 3.6), which constantly accreted and exhibited an average elevation increase across the area of 11.1 mm during the study period. As was found in the natural area on the north shore, this was the only area on the south shore to be constantly accreting (Figure 3.23); furthermore, these two areas had similar orthometric heights of 1.64 m and 1.67 m (see Table 3.3 for AD data), for the natural area of the north shore and the old restored area of the south shore, respectively. The areas of the south shore displayed more similar relationships than their counter-part of the north shore, with lower variation in each season between area types (Figure 3.23); suggesting, perhaps, a more conserved setting.

Across all areas, winter was the most dynamic season, which returned the largest variability of elevation change (Figure 3.23), a range of 35 mm across all areas. Over other seasons this range was smaller (17 mm in summer, 15 mm in autumn and 12 mm in spring). Both shores showed the natural saltmarsh to be the most conserved and stable site, with the

lowest variance in elevation change across the seasons (Table 3.6), this was followed by the old restored area. However, the young restored saltmarsh was shown to have the largest variance of sediment elevation changes on both shores, maximally being 49 mm (Table 3.6).

*Table 3.6: Summary elevation change data from SEB measurements for each area type studied. Data shows values taken across all SEB measurements in each area across the four seasonal sampling efforts.*

| Shore | Area type | Average change (mm) | Total change (mm) | Overall variance (mm) |
|---|---|---|---|---|
| North | Natural | 1.9 | 7.5 | 10.3 |
| | Old Restored | -0.4 | -1.6 | 24.1 |
| | Young Restored | -1.1 | -4.5 | 32.5 |
| | Mudflat | -1.5 | -6.0 | 24.6 |
| South | Natural | 0.7 | 2.9 | 8.2 |
| | Old Restored | 2.8 | 11.1 | 11.3 |
| | Young Restored | 1.4 | 5.4 | 48.8 |
| | Mudflat | 1.0 | 3.9 | 13.9 |

#### *3.5.2.2 Relationship between elevation change and deposition rate*

Changes in sediment elevation are, in part, a product of sediment deposition; being the net expression of deposition and erosion occurring over a given time period, other factors such as compaction and root growth can also have an influence. Assessment of the relationship between elevation and deposition measured during this study were investigated. The analysis used the calculated average change in elevation in each season at each sampling point (that is those points in Figure 3.23), and the average daily deposition per $m^2$ at each point in each season, calculated from the four measurements at each sampling point each season which collected sediment for 24 hours and spanned the spring-neap tidal range. Linear regression showed there was a significant relationship between elevation change and deposition rate across the all seasons and sampling points ($F(1,22) = 11.22$, $p = 0.001$); this, however, only explains 7.7 % of the variance in elevation change. Furthermore, the relationship structure is such that it indicates elevation change decreases with deposition at the rate of -0.004 $g/m^2/day$. The influence of area type interaction with deposition rates was assessed to discern how elevation may be affected differently within each area by

deposition. Only on the mudflat sites, of the north (ANOVA: p = 0.0003) and south (p = 0.04) shore, did the rates of deposition have a significant relationship to elevation changes.

#### *3.5.2.3 Elevation change and the deposition-erosion balance*

The role which vegetation plays in enabling the persistence of saltmarsh habitats centres largely around the resulting sedimentary dynamics it produces, namely the building of deposits to move or maintain its place within a tidal frame. The accretion or loss of these deposits is expressed through changing sediment surface elevations. Assessment was made of the difference between potential accretion experienced at each point and the actual measured change in sediment elevation, across $1m^2$ at each point. Potential accretion was calculated as the total seasonal deposition per $m^2$, where an average deposition quantity in each season provided a daily rate which was multiplied by 91.25 days (365 days / 4 seasons). The actual amount of sediment deposited was calculated from the measured change in height at each point, assumed as equal across a $1m^2$ area, and the use of site-specific surface bulk density values. Bulk density values were taken from sediment core data (Chapter 4), applying the following data from the surface sediments: *P. maritima* = 0.852 $g/cm^2$, *B. maritimus* = 1.663 $g/cm^3$, and bare mudflat = 1.512 $g/cm^3$.

*Table 3.7: Average sediment deposition and accretion values of each area type, measured over a year applied to $1m^2$. Percentage retention calculated from the average deposition and accretion data shown in the table.*

| Shore | Area type | Average deposition ($kg/m^2$) | Average accretion ($kg/m^2$) | Average % retention |
|---|---|---|---|---|
| North | Natural | 17 | 13 | 72 |
| | Old Restored | 115 | -2.6 | -2 |
| | Young Restored | 29 | -7.5 | -26 |
| | Mudflat | 73 | -9.1 | -13 |
| South | Natural | 0.14 | 0.35 | 258 |
| | Old Restored | 45 | 18 | 41 |
| | Young Restored | 24 | 9.0 | 38 |
| | Mudflat | 142 | 5.9 | 4 |

A comparison of the calculated potential deposition experienced in each area at each point indicated that, typically, the natural areas of vegetation function most positivity, 'retaining' the highest amount of sediment (Table 3.7). It was shown that the *P. maritima* vegetation of

the natural saltmarsh on the south shore retains over 100 % of the potential sedimentary deposits (Table 3.7), so accreting more sediment than estimated being input (Figure 3.23). The old restored areas displayed a higher rate of loss of deposited material than found in the young restored area; signified by their steeper slopes in Figure 3.23. However, these areas

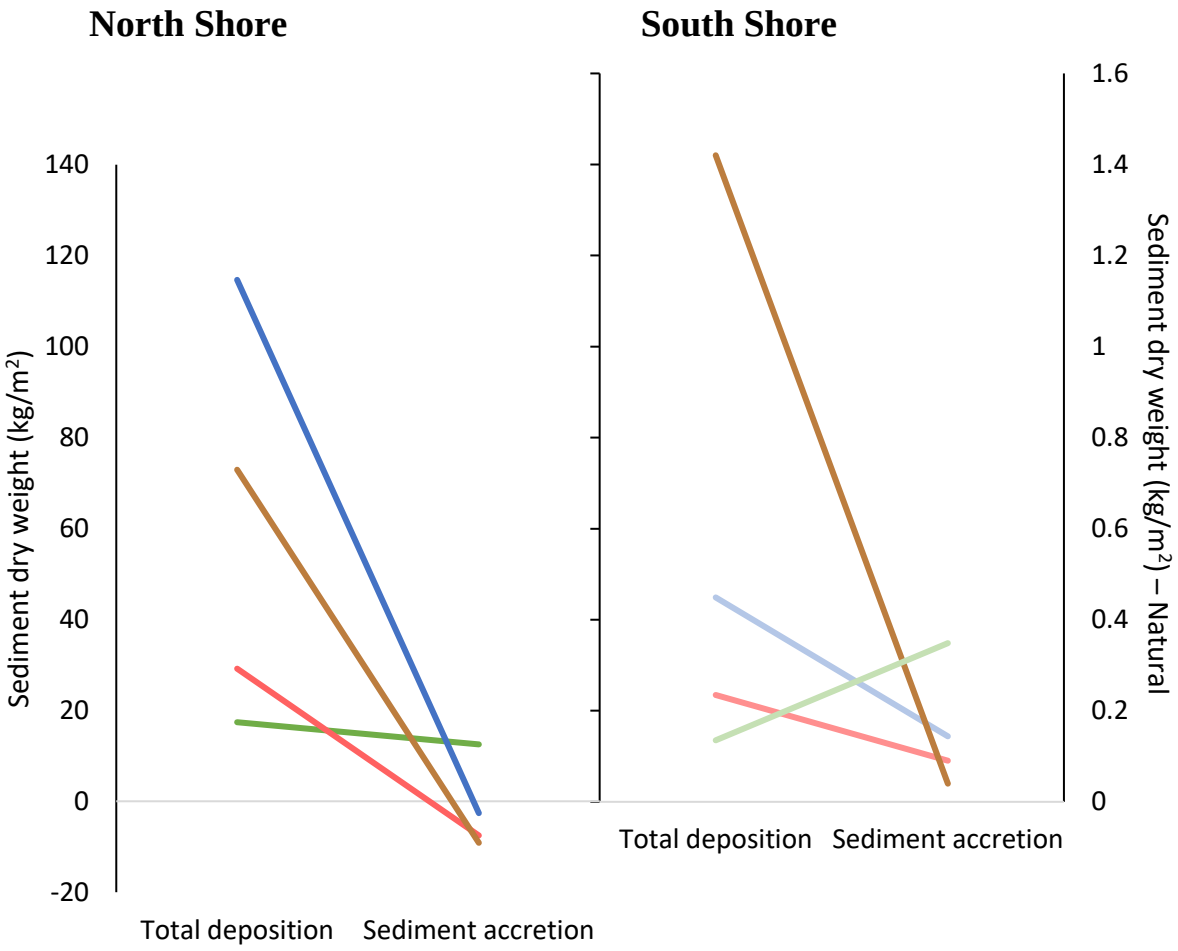


*Figure 3.23: Relationship between the estimated total amount of deposition over a year at each sampling point and the calculated amount of actual sediment accumulated at each point from measured elevation change and bulk density conversion factors. Sediment weights shown as kilogram dry weight per $m^2$ equivalent. Natural area on the south shore plotted on secondary axis. Colours indicate area type, green = natural saltmarsh, blue = old restored area, red = young restored area, brown = mudflat.*

experience considerably more deposition during the year and display either greater accretion rates or lower erosion rates, which culminate in them being the second most effective area type at retaining sediment deposits (Table 3.7). The north shore exhibited the greatest overall loss rates (Figure 3.23) and the lowest percentage rates of retention (Table 3.7). The lowest average actual retention was on the mudflat on the south shore, which did no retain an estimated 136 $kg/m^2$ (Table 3.7).

### *3.5.3 Carbon sequestration potential*

The contribution of sediment dynamics (i.e. the input characteristic and accretion) to the resulting carbon pool within the estuary was assessed. Investigating differences in carbon content of sediment in each area type and assessing possible drivers of the measured carbon content of those deposits. These data were also used to estimate possible carbon sequestration rates within each area, so informing on their possible ecosystem benefit.

#### *3.5.3.1 Relationship between organic content, carbon content and deposition rate*

Typically, when calculating organic content, there would be filter paper residue remaining (see 3.2.13), in the case of extreme low organic content this could result in 'negative' organic content, again as previous with deposition weight, these were assigned a zero value. It was felt that these changes were acceptable as they serve to reflect the true situation of negligible organic content of samples.

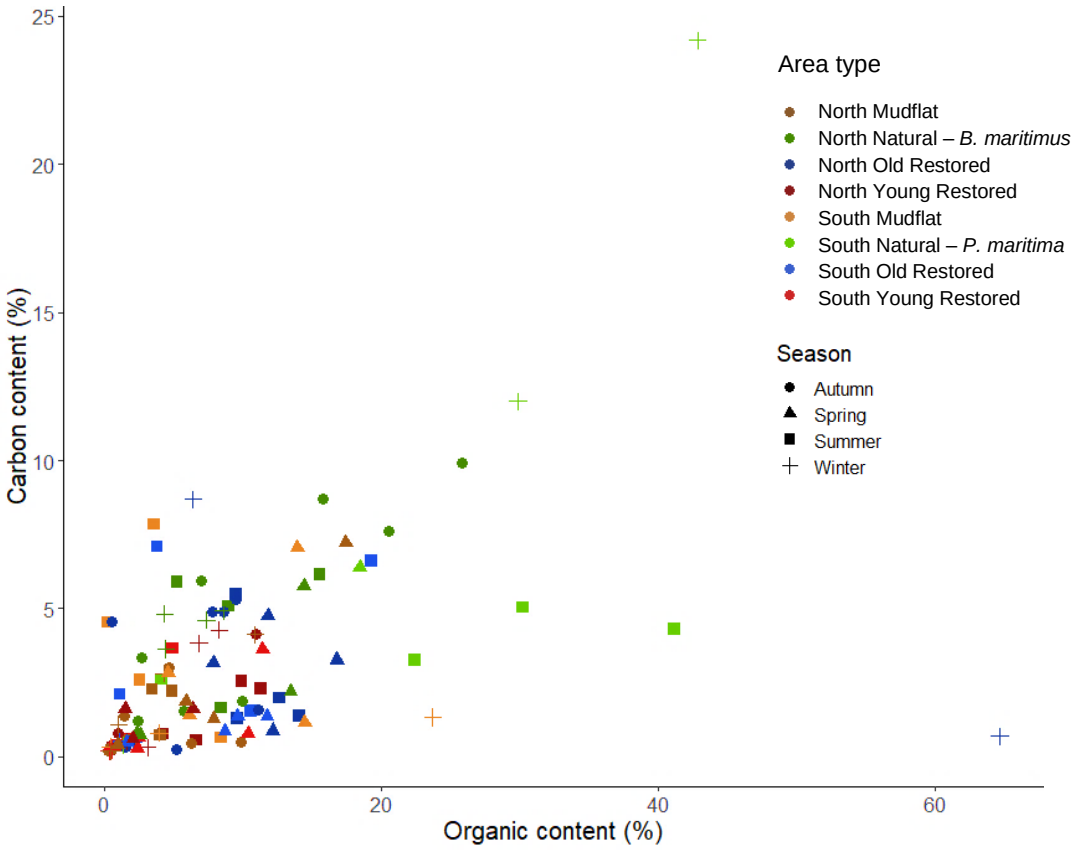


*Figure 3.24: Percentage organic content and carbon content of deposition samples collected in each season in each area during spring tide events. Points are coloured and shaped to indicate area type (colour) and season (shape).*

As detailed in section 3.2.5.3, a secondary set of samples was collected each season to provide enough material to conduct organic content and carbon content analysis on

sediment deposits. The relationship between these content values in this secondary sample set are used to apply site-specific conversion factors to the primary data set, for which only organic content values are held.

A GLM (which used a 'Gamma' family error distribution) taking the whole data set showed there was a significant relationship between organic content and carbon content ($F(1, 119) = 33.01$, $p < 0.001$) (Figure 3.24). Further analysis was conducted to assess the influence of area type on the relationship. A GLM, which used the interaction of organic content with area type, was compared with the basic model using ANOVA, which showed there was no significant difference in the variance explained by the two models ($p = 0.64$). Further analysis was done to assess if the relationship altered with season, again comparing the basic GLM with a GLM containing season as an interaction with organic content using ANOVA; the comparison showed there was no significant difference in the variance explained by the interaction with season ($p = 0.4$). Due to the lack of significant difference a single estuary-specific sediment conversion factor of *0.43 gC/g Organic matter* was applied across all organic content values (or 43 % of organic matter being carbon), from deposition samples collected in each season, across tide states within each area.

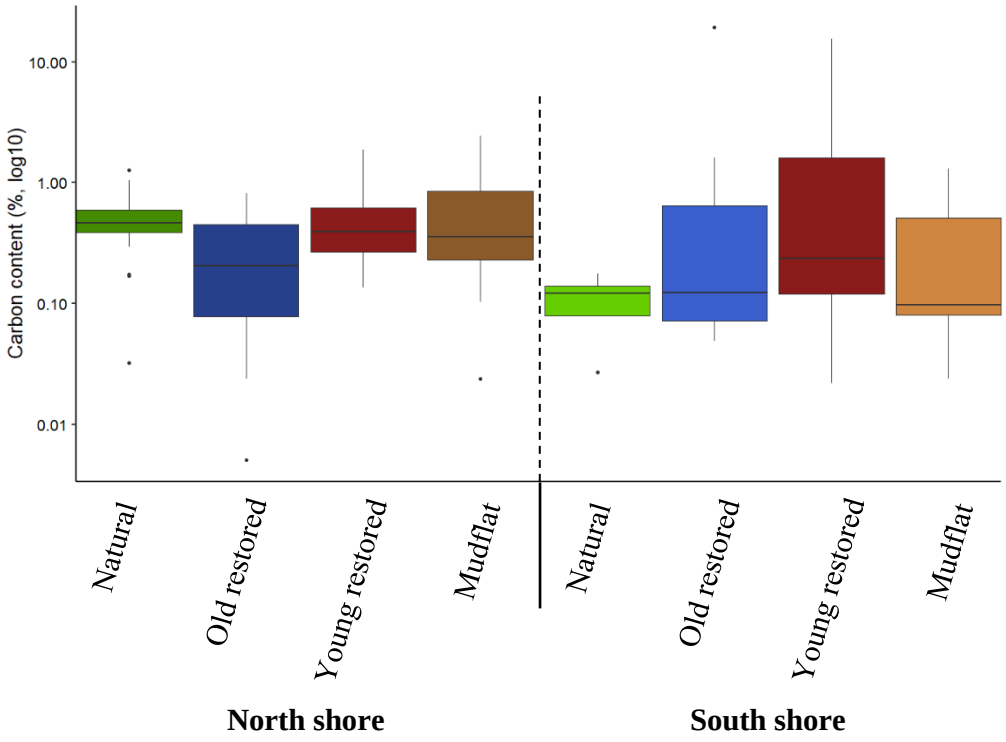


*Figure 3.25: Distribution of carbon content of deposit samples across the study period within each area type. Boxes show range between 25$^{th}$ and 75$^{th}$ percentile, thick black line is the median of the data and whiskers are 1.5 IQRs from the box. Data are plotted on a log axis.*

### *3.5.3.2 Relationship between carbon content and area type*

There was a broad range of carbon content found in deposited sediments during the study, with all areas experiencing a broad range of inputs. Generally, it was found that the north shore area had higher median rates of carbon input than the south (Figure 3.25), however, the south shore exhibits a higher average carbon deposition rate (Table 3.8). The south shore experienced the highest average rates of sedimentary carbon deposition overall (0.96 $gC/m^2/day$), it also is where the area of highest and lowest carbon deposition rates were recorded, in the young restored vegetation (1.98 $gC/m^2/day$) and natural *P. maritima* extent (0.03 $gC/m^2/day$), respectively. The carbon deposition rate on the mudflat of the north shore was shown to be the greatest on that shore, and over double of that recorded on the south shore, where it was the third lowest rate of carbon deposition (Table 3.9).

During the study, there were instances of zero (or quantities below level of detection) deposition and, further, similarly instances of zero or low organic matter content. These factors combine to generate a large number of zero instances across the dataset in terms of carbon content. Therefore, the average carbon content of deposits at each point in each season was calculated, providing a value of the seasonal state of carbon deposition at each point. Linear regression assessed the difference in carbon content deposition (*log*x+0.0001*) between shores and showed there was a significant difference between the rate of carbon deposition occurring on each ($F(1, 126) = 10.2$, $P = 0.002$), however this model only explained 8 % of the variance in carbon deposition. Further analysis assessed how carbon deposition altered with area type, this showed that there were significant differences between each area (ANOVA: $F(7, 120) = 8.917$, $p < 0.001$), and explained 30 % of the variance.

*Table 3.8: Annual average rate of carbon deposition (grams) per $m^2$ per day occurring in different study areas and on different shores of the estuary.*

| **Shore** | **Area type** | **Average carbon deposition ($gC/m^2/day$)** | |
|---|---|---|---|
| | | Area average | Shore average |
| North | Natural | 0.5271 | 0.5018 |
| | Old | 0.2538 | |
| | Young | 0.5665 | |
| | Mud | 0.6600 | |
| South | Natural | 0.0279 | 0.9564 |
| | Old | 1.5388 | |
| | Young | 1.9791 | |
| | Mud | 0.2798 | |

### *3.5.3.3 Relationship between carbon content and season*

The rate of carbon deposition was shown to vary between area types. There was also variation between seasons, with the south shore exhibiting greatest differences in carbon deposition rates between season and area type (Figure 3.26). As was done previously, analysis was conducted using the average carbon content of deposits at each point in each season. There were significant differences in rates of carbon deposition occurring across seasons (ANOVA: $F(3, 124) = 5.769$, $p = 0.001$).


*Figure 3.26: Average carbon deposition per $m^2$ per day (grams) in each area in each season. Seasonal values area stacked for each area type, lines are coloured by season, summer = yellow, dark orange = autumn, grey = winter, green = spring.*

There was no significant interaction between shore and season (two-way ANOVA: $F(3, 120) = 1.526$, $p = 0.2$). Comparison of seasonal differences between areas on each shore and

showed there were significant difference on both the north (two-way ANOVA: $p = 0.001$) and the south ($p = 0.014$). The influence of seasonal variation on each area was also assessed and showed there was no significant interaction ($p = 0.11$) between the two factors.

The data suggest that seasonality did not influence any area or shore significantly more than any other. However, the rates of carbon deposition which occurred in each area are considerably different (Table 3.9). The greatest rate of carbon deposition was recorded on the south shore during autumn, at 2.65 $gC/m^2/day$, and the lowest was found on the north shore during spring, with 0.33 $gC/m^2/day$. The largest difference within the same area season was during autumn with a difference between the average deposition rate of each shore being 1.8 $gC/m^2/day$, in winter this difference dropped to its lowest, displaying a difference of 0.08 $gC/m^2/day$ between the two shores.

*Table 3.9: Average rate of carbon deposition (grams) per $m^2$ per day occurring in each season on each shore.*

| Shore | Season | Average carbon deposition ($gC/m^2/day$) |
|---|---|---|
| North | Summer | 0.4072 |
| | Autumn | 0.8407 |
| | Winter | 0.4344 |
| | Spring | 0.3250 |
| South | Summer | 0.5935 |
| | Autumn | 2.6453 |
| | Winter | 0.5184 |
| | Spring | 0.9564 |

#### *3.5.3.4 Carbon sequestration in the study area*

The amount of carbon potentially being deposited into the estuary environment was calculated for each area type, considering the seasonal average carbon content of deposits and size of each area (Figure 3.27). The potential carbon sequestration from sediment deposition was calculated as a function of total estimated deposition during the study assuming there was no loss through erosion; representing the possible maximum benefit the area affords. The size over which sediment deposits were calculated were taken from GPS track data collected in the field, with the 'extent' of mudflat on each shore taken as the fronting length along the areas and being 20 m wide.

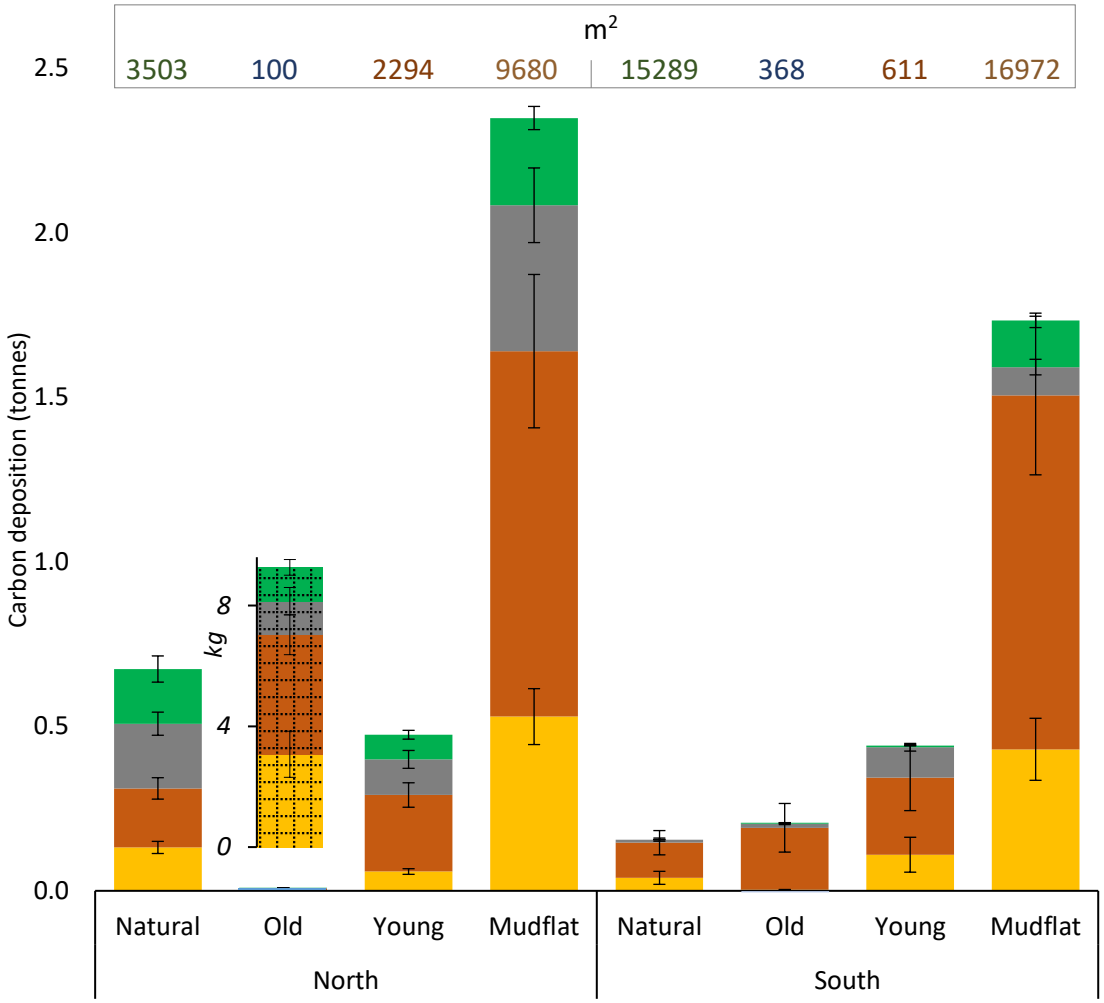


*Figure 3.27: Total amount of estimated carbon deposited in sediment (tonnes) during the year-long study period in each area type. Values calculated using area seasonal average carbon deposition rates. Bars are coloured by season, summer = yellow, dark orange = autumn, grey = winter, green = spring. Insert for the old area on the north shore (hatched fill) shown on different scale (kg) to view data. Showing standard error for each season. Data values above are the actual extent of each area.*

The actual carbon sequestration total of each area was also estimated, which linked the average carbon deposition rate in each area during each season to the measured average sediment elevation change (and so calculated sediment accretion quantity) in each season during the study period. In the instances of sediment loss (i.e. a lowering in sediment elevation) during a given season, the average carbon value of deposits for that season were used to estimate possible 'removal' of carbon from the area.

Overall the north shore was estimated to have received a greater amount of carbon deposits during the study, totalling 3.5 tC, opposed to the 2.5 tC received by the south shore areas. The mudflat areas of both shores were shown to be the sites of greatest potential carbon sequestration, totalling 2.35 tC and 1.7 tC on the north and south shores, respectively. This is a product of their greater extent, which compensates for the lower carbon content values of the deposits recorded in those areas (Table 3.8). In general, there was larger variation in

the carbon content of deposits located on mudflats in the study area, with vegetated areas displaying lower standard error of the mean across the seasons. The greatest variation in carbon content of deposits was during autumn and the lowest during spring. Although on average the north shore experienced deposits lower in carbon content than did the south (Table 3.8), the natural, young restored and mudflat areas all received greater carbon input than their southern counter-parts (Figure 3.27).

The lowest amount of carbon deposited within any of the vegetated area was found in the old restored area of *B.* maritimus on the north shore, which received a total of 9.26 kgC; this was also the smallest area, at 100 $m^2$. The second lowest quantity of carbon deposits in a vegetated area were found in the natural extent of *P. maritima* on the south shore, which received a total of 156 kgC; furthermore, this was the second largest area studied, being over 150 times larger than the old restored site on the north shore, at 15,298 $m^2$.

The restored areas of vegetation received deposits containing 1.1 tC during the study, with 216 kgC in the old established vegetation and 916 kgC in the young restored areas.

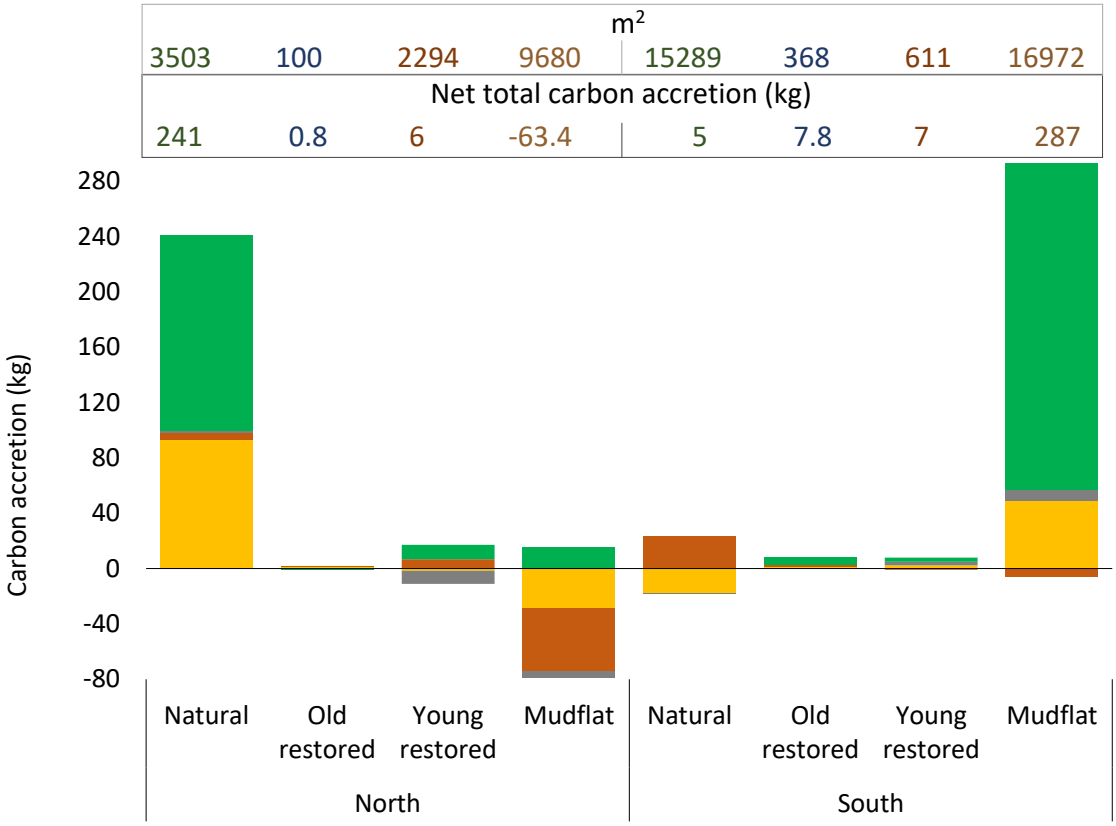


*Figure 3.28: Total estimated carbon accretion (kg) which occurred in each season in each area. Values calculated using area seasonal average carbon content and sediment elevation changes. Bars are coloured by area and shaded by season, which run from summer at the base (light shade) to spring at the top (dark shade). Data values above are the actual extent of each area and net total carbon accretion in each area.*

The actual amount of carbon sequestered through sedimentary deposition was also estimated (Figure 3.28), by combining seasonal carbon content values with the measured change in sediment elevation. The resulting trend in carbon quantity sequestration attributed to each area was substantially different from that found when only assessing carbon deposition rates (Figure 3.27). Estimates of the total amount of carbon expected to have been accreted into the system were far lower than those estimated when assuming constant deposition; 0.491 tC versus 6.3 tC. Furthermore, it was shown that, conversely to the carbon deposition estimates, the greatest amount of carbon accretion occurred on the south shore (307 kgC) not the north shore (184 kgC).

The greatest amount of carbon accretion was recorded as occurring in the mudflat area of the south shore, which gained 287 kgC, the lowest value (or greatest loss) was recorded on the mudflat of the north shore, which was estimated to have lost 63.4 kgC (Figure 3.28); displaying the largest difference in carbon accretion within an area type. The natural vegetation areas studied also displayed large differences in their resulting carbon accretion values, being 241 kgC and 5 kgC on the north and south shores, respectively (Figure 3.28). Furthermore, it was found the natural areas also displayed the largest difference in average carbon accretion rates per $m^2$; with the north shore (69 $gC/m^2$) being considerably greater than the south shore (0.3 $gC/m^2$) (Table 3.10).

*Table 3.10: Year averaged rates of carbon accretion per $m^2$ recorded in each area.*

| Shore | Area type | Carbon accretion ($gC/m^2$) |
|---|---|---|
| North | Natural | 68.8 |
| | Old | 8.1 |
| | Young | 2.6 |
| | Mud | -6.6 |
| South | Natural | 0.3 |
| | Old | 21.2 |
| | Young | 11.5 |
| | Mud | 16.9 |

The restored areas of *B. maritimus* vegetation were estimated to have accreted 21.6 kgC through sediment deposition during the study, over half of which occurred on the south shore (14.8 kgC). The greatest amount of carbon sequestration occurred in the vegetation of the old restored area, which also displayed the highest carbon accretion rate per unit area of all restored sites (second highest in the study area); being 21.2 $gC/m^2$ (Table 3.10). During

the course of the study the restored sites of the north shore were both shown to have sequestered carbon 0.8 kgC and 6 kgC, in the old and young restoration areas respectively (Figure 3.28); despite both having showed a net sediment loss (lowering in elevation) of 1.6 mm and 4.5 mm, respectively (Table 3.6).

*Table 3.11: Comparative values of carbon deposition and carbon accretion which occurred during the study at each area, and the differences between these and the effective retention efficiency of each area.*

| Shore | Area type | Deposited carbon (kg) | Accreted carbon (kg) | *Difference (kg)* | Retention efficiency (%) |
|---|---|---|---|---|---|
| North | Natural | 673.9 | 241.0 | *433* | 36 |
| | Old | 9.3 | 0.8 | *9* | 9 |
| | Young | 474.3 | 6.0 | *468* | 1 |
| | Mud | 2348.0 | -63.4 | *2411* | -3 |
| South | Natural | 155.7 | 5.0 | *151* | 3 |
| | Old | 206.7 | 7.8 | *199* | 4 |
| | Young | 441.4 | 7.0 | *434* | 2 |
| | Mud | 1733.3 | 286.9 | *1446* | 17 |

Carbon deposition and realised carbon accretion values were compared to evaluate each areas' efficacy in retaining potential carbon inputs within their confined area (Table 3.11). It was found that the natural extent of *B. maritimus* was most efficient at retaining sedimentary carbon deposits, where there was a difference of 433 kgC between the potential total and realised sequestration, an efficiency of 36 %. Sites of old restoration were shown to be more efficient than their less well-established younger counterparts, retaining 9 % and 4 % on the north and south shore respectively; making them the third and fourth most efficient areas. At the mudflat site of the south shore there was a difference of 1446 kgC, however this returned an efficiency of 17 % due to the large potential deposition value.

## 3.6 Discussion

The study considered various aspects of sedimentary dynamics within the Eden Estuary and how the restoration therein influences or alters such dynamics. Primarily, the study focused on the interaction between sediment deposition and settlement rates and the driving factors behind these; the vertical development of sediments in different areas; and the possible carbon sequestration benefit afforded by these different areas.

### *3.6.1 Issues during the study*

There were a few issues encountered during the study which are discussed below.

Firstly, issues arose around the low quantities of sediment being deposited onto sampling units and the occasionally low values of organic matter. These quantities were often below levels of detection or were lower than other introduced errors (such as from filter paper weight changes or scale error), producing illogical negative values of deposition or organic matter content. Although these were addressed during the analysis to assign such values as 'zero', it would be beneficial to ensure all data points were informative. Such issues could be addressed through the deployment of sampling units over a more prolonged period or the deployment of multiple sampling unit at each point to consolidate upon analysis, so increasing exposure, which may increase the amount of sediment deposition occurring; however, sampling over a prolonged period would reduce tidal range resolution data. Issues around organic content data may be addressed through the use of glass-fibre filter paper sampling units, which one could assume would not lose any weight during combustion (as appose to the assumption of full-combustion 'ash-less' papers); however, such papers are perhaps more fragile and may result in lost samples.

Issues were also encountered around area type classification, resulting from the young restored areas, of both the north and south shores, becoming persistently more degraded during the study; where by vegetation density across the entire extent became sparser and irregular. This culminated in much of the planted area lacking any visible live vegetation, though dead stems remained visible above the sediment; reducing its effectiveness to represent an 'establishing' area of vegetation, perhaps being more aligned with its previous mudflat condition. This was not accounted for in the analysis as it was deemed that restoration, once completed, is governed by natural processes and this may include the partial or full loss of planted vegetation and so reflect possible outcomes from conservation initiatives.

The growth of *Salicornia sp.* and *Ulva intestinalis* (Enteromorpha) in the study area on occasion could have had impacts on the study in the form of growth on supposedly 'bare mudflat' for the former and smothering in the case of the latter. The presence of *Salicornia sp.* was typically in low densities and comprised of small stature plants and typically not found at sites of direct study, so would likely have had minimal affect. Enteromorpha growth in some instances could be seen to cover large areas of the mudflat and vegetated areas. This coverage included established sampling points (Figure 3.29), which typically

was not interfered with as it was deemed a natural process which is occurring in the estuary; meaning algal mats may have been incorporated into the sediment bed or may be removed in subsequent tides. However, when carrying out sediment elevation data collection (SEB) the point of measurement was taken down to the sediment surface, so covering algae were carefully removed in these cases. Algae was occasionally was found to have partially or completely obscured the sampling unit placed the previous day (Figure 3.29). In the case of deposition this was carefully removed, ensuring the retention of all sediments on the trap, for the settlement tube the algae were simply removed. In both cases nothing could be done to interpret how these instances affected the data, however, serve to illustrate possible areas for sampling design improvements in the future.

### *3.6.2 Sediment deposition and settlement processes*

*Figure 3.29: Left image shows an established permanent sampling point mostly covered by a layer of U. intestinalis, also partially over the deposit trap placed the previous day. Right image shows an example of obscuring U. intestinalis obscuring the sampling aperture of a settlement trap installed the previous day.*

Deposition rates were shown to be particularly similar between the natural area of *B. maritimus* and old restored areas, all of which displayed lower rates of deposition than was found in areas of 'less' vegetation of the young restored sites and bare mudflat; which displayed statically similar levels of vegetation. It was expected that increased vegetation would increase deposition, however the opposite was found. Though vegetative structures are likely to create a depositionally encouraging environment through hydrodynamic friction reducing flow speeds, it is likely that this same process intercepts and removes sedimentary particles in suspension. In some instances, such as the natural *P. maritima* marsh, the significantly different elevation (and so inundation period), confounds the

influence of vegetation, however, there was no such distinction between other vegetated areas and mudflats, suggesting the primary driver behind reduced deposition is attributed to vegetative structures. It was shown that although these areas experienced less deposition, they were sites of greatest elevation increase.

Settlement measurements were designed to capture data which referred to the potential amounts of sediment which could be deposited at a given point in the study area. It is assumed that stronger links between settlement (i.e. potential deposits) and actual deposits indicate areas which exhibit higher efficiencies at sediment capture and retention. It was shown that settlement and deposition rates were most highly correlated in areas of *B. maritimus* vegetation, both in the natural stand and restored areas.

### *3.6.3 Changing elevation during the study*

Elevation changes in sediment were measured with SEBs during the study, which were assumed to reflect differences caused by accumulation or loss of surface sediment only and did not consider compaction or root growth expansion.

Data collected on changes in sediment elevation over the year long period suggest that vegetated areas display a greater tendency to accrete sediment, be that building at a greater rate or eroding at a lower rate than adjacent bare mudflat areas (Table 3.6). Furthermore, it was shown that there was limited relationship between rates of deposition and the resultant vertical accretion in vegetated area, which indicated that vegetation plays a role in the movement of those sediment after they have been deposited. It was shown that areas of vegetation generally exhibited higher rates of retention of potential total deposits during the study, with the natural area of the south shore retaining 258 % of estimated deposits. It is not possible to explain how the area retains over 100 % of potential deposited material, however likely drivers could be stochastic events, such as large spring tides bringing large amounts of sediment over a short period which were not sampled.

In the Eden Estuary it was indicated that the south shore is, perhaps, a more ‘nurturing’ environment, which facilitated the building in sediment elevation of all areas. Such characteristic may prove beneficial to the long-term longevity of vegetation, specifically to restored vegetation. It was shown that there was a large degree of variability in elevation change during the year. It is possible winter could play a key role in development and persistence of areas, as it was typical a season in which largest variation in elevation change was experienced. Such stochastic events of loss or gains could be of greater influence in a

given area than the underlying constant trends. For example, the north shore restored areas are accretionary then major loss during winter, 'undoes' the sedimentary development.

### *3.6.4 Influence on carbon sequestration*

The importance of understanding sediment accretion along with the given sedimentary carbon input was illustrated when assessing potential carbon deposition and realised carbon accretion in each area; between which there was a difference of 5.5 tC. It is interesting to note, for example, that in terms of total deposition more material was received by the north shore areas during the study, however it was also shown that the south shore received a greater amount of carbon deposits over the same period. Difference across such a relatively small spatial scale, perhaps highlight issues around predicting sedimentary carbon sequestration rates across larger extents with limited spatial sampling. Furthermore, it highlighted the influence of changing carbon content values when linked with elevation change. The discrepancy between elevation loss and increased quantity of retained carbon is a product of the 'value' of deposits occurring in each season and the response in sediment elevation change during the same period. In the case of the young restored area of the north shore, for example, the largest loss of sediment was found during winter (-0.72 cm), during which the sedimentary input was at the lowest in carbon content recorded throughout the study, resulting in a total loss of 9.6 kgC; as a comparison during spring there was an increase in elevation of 0.07 cm which equated to an addition of 10.5 kgC.

The study revealed that there was the potential for the sequestration of 6 tC across the study site from summer 2015 to summer 2016, with a realised sequestration of 491 kgC or 1.8 $tCO_2e$. The most efficient site of carbon sequestration was found to be the natural extent of *B. maritimus*, which retained 35 % of the estimated potential sedimentary carbon deposits it received. Restored areas of vegetation are suggested as being efficient sites of carbon accretion compared to other area types, particularly on the south shore of the estuary where there was an average accretion of 16.4 $gC/m^2$ over the study period. The restored areas of *B. maritimus* were shown to retain on average 4 %, with a maximum efficiency of 9 % in the old restored area on the north shore. The large difference between the efficiency rates of natural and restored stands of *B. maritimus* maybe a product of scale, where the restored sites were each an order of magnitude smaller, with no point in their extent being more than a few meters from the fringing edge of vegetation. The average efficiency retention on mudflats was also found to be 7 %, although this is due only to the south shore which retained 17 %, whereas the north shore displayed a loss in sedimentary carbon.

The additional ecosystem service afforded by restoration efforts in terms of carbon sequestration was calculated as the difference between what would have occurred under 'business-as-usual', which assumed data gathered on the mudflat is representative of the situation the restored sites would have experienced had no restoration taken place, and what occurred at those sites in their present condition during the study. On the north shore the data suggest that bare sediment areas would have experienced a net lowering in elevation and a loss of carbon during the study period. In the north shore restored sites there was calculated to be an additional 1.1 kgC and 18.8 kgC in the old and young restored sites, respectively. However, on the south shore, more carbon would have been retained had there been no vegetation, with an additional 26.4 kgC and 66 kgC being sequestered in the old and young restored areas, respectively. In total, there has been a net reduction in the quantity of sedimentary carbon sequestered into the system due to restoration, with an estimated 70.7 kgC less under restoration initiatives.

These data represent sediment accretion trends over a year period, which cannot inform on possible long-term trends of sediment elevation change. However, it is likely that typical biogeomorphic processes of sediment accretion will occur within areas of vegetation as the site develops and expands; such processes would serve to provide additional benefit above bare mudflats whose changes in elevation are governed by broadscale physical processes over-which the areas itself has limited influence. Furthermore, it was shown that restored areas of vegetation, specifically on the south shore, received the greatest rate of carbon deposition per unit area within the study. Such characteristics are indicative of strong potential for these areas to be sites of prolific carbon burial, with increased areal extent and vertical sediment development.

# Chapter 4: The sedimentary carbon store of the Eden Estuary

Intertidal vegetated systems, such as saltmarshes, have been suggested to confer valuable ecosystem services in the form of climate change mitigation through the long-term storage of, so called, 'blue carbon' (Burden et al., 2013; Duarte et al., 2013, 2008; Macreadie et al., 2017; Sousa et al., 2017; Van de Broek et al., 2018). This benefit predominantly results from the continued accumulation of organic matter which is buried into deep, stable sediments (Chmura et al., 2003).

The total sedimentary carbon storage in a given area is determined by many factors including, the past and present sediment supply, the elevation in relation to tidal influence and vegetative structures; all being broadly driven by ecosystem engineering processes (Kirwan and Mudd, 2012). It is often difficult to accurately estimate the total amount of carbon stored in sediments without direct reference measurements from a site due to the large variability between – and within – areas (Bai et al., 2016; Chmura et al., 2003). The prolonged nature of sediment burial means various changes could have occurred that influenced past burial and sequestration rates (Brevik and Homburg, 2004), which are unrealised in the displayed sediment-dynamic characteristics of the present.

The importance of accurate sedimentary carbon stock accounting is two-fold. First, from a preservation perspective it is necessary to know the quantity of carbon at risk of removal from the system should the saltmarsh be lost through degradation, so risk and extent of emission (Macreadie et al., 2013; Pendleton et al., 2012). Secondly, in assessing the accumulation or stock of sedimentary carbon in an area it is beneficial to have the most accurate specific estimation of an area possible to best illustrate the 'value' of, for example, restoration efforts (Andrews et al., 2006). To attain the most accurate carbon stock estimation it is also necessary to sample as deep into the sediment as is practicably possible, ideally a depth of 1 m should be collected (Howard et al., 2014 - The Blue Carbon Initiative). A deep core provides a more robust foundation on which to base stock calculations, reducing the need for extrapolation from shallow measurements and avoiding possible error introduction (Macreadie et al., 2017).

This research was focussed on improving understanding of the current sedimentary carbon stock within the Eden Estuary (Figure 4.1). Sampling of the sediment bed through the extraction of cores down to a refusal depth, reaching a maximum 65 cm was conducted. Cores were obtained from three focal areas within the Eden Estuary – natural stands of

*Puccinellia maritima*, well-established restored stands of *Bolboschoenus maritimus*, and un-vegetated adjacent mudflats. These samples were used to generate various depth profiles of carbon, organic matter bulk density and particle size composition. These data facilitated a thorough assessment of the current sedimentary carbon stocks within the estuary, how these differ depending upon vegetation and depth, how restoration may offer additional carbon storage benefit, and what factors might affect the given carbon content within these sediments.

## 4.1 Sediment carbon store sampling on the Eden Estuary

Sediment coring was conducted on the Eden Estuary in August and September 2017, with samples collected from the south shore of the estuary in the vicinity of the 'Kincaple marshes'. The cores were taken from the mudflat, restored sites and natural vegetation. The areas chosen provided a logical ecological spread across unvegetated mudflats to revegetated planted areas of *B. maritimus* (planted in 2003) to a mid-upper marsh *P.*

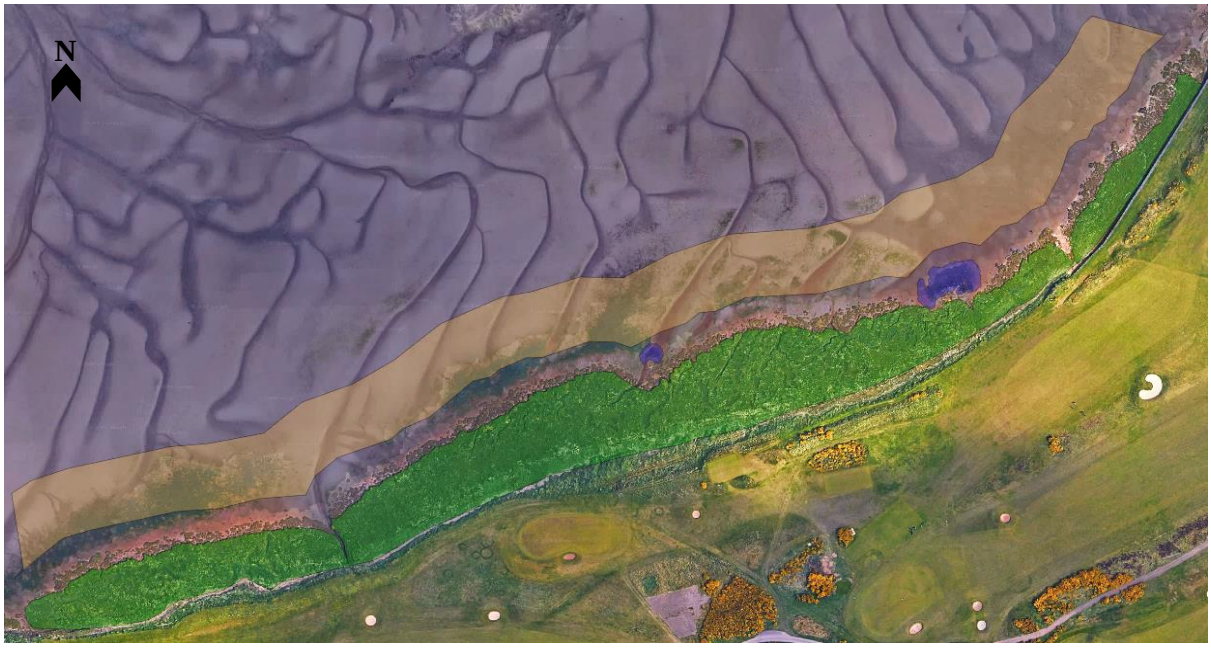


*Figure 4.1: Aerial image of south shore of the Eden Estuary where sediment core sampling was conducted. Bottom right corner shows the edge of the Links Trust golf course. Semi-transparent polygons define the extents of each area type sampled. Brown is the mudflat; blue is the restored area of B. maritimus and green is the natural P. maritima marsh.*

*maritima* complex (Figure 4.1). These eco-types are present across an increasing elevation and are used to represent the different likely states of saltmarsh vegetation (or lack thereof) on the Eden estuary. A total of 15 cores were taken, five in each area, to evaluate and

estimate current carbon stocks in this discreet estuary. The number was chosen as a balance between practical restrictions (e.g. sampling opportunity and processing availability) and effectively representing the study area; recently Young et al. (2018) suggested a sampling density of 40 cores are required to represent areas in the size region of 100 – 200 km, suggesting 15 cores spread over the < 1 km is robust.

## 4.2 Core sampling methodology

### *4.2.1 Sampling location*

Cores samples were acquired from the three focal areas - mudflat, restored and natural saltmarsh - on the south shore of the Eden Estuary. Samples were randomly distributed within each area, with their locations determined though the application of *QGIS 2.18.2*. The boundary of each area was acquired using a combination of field-collected GPS track data and remote-sensed polygon creation.

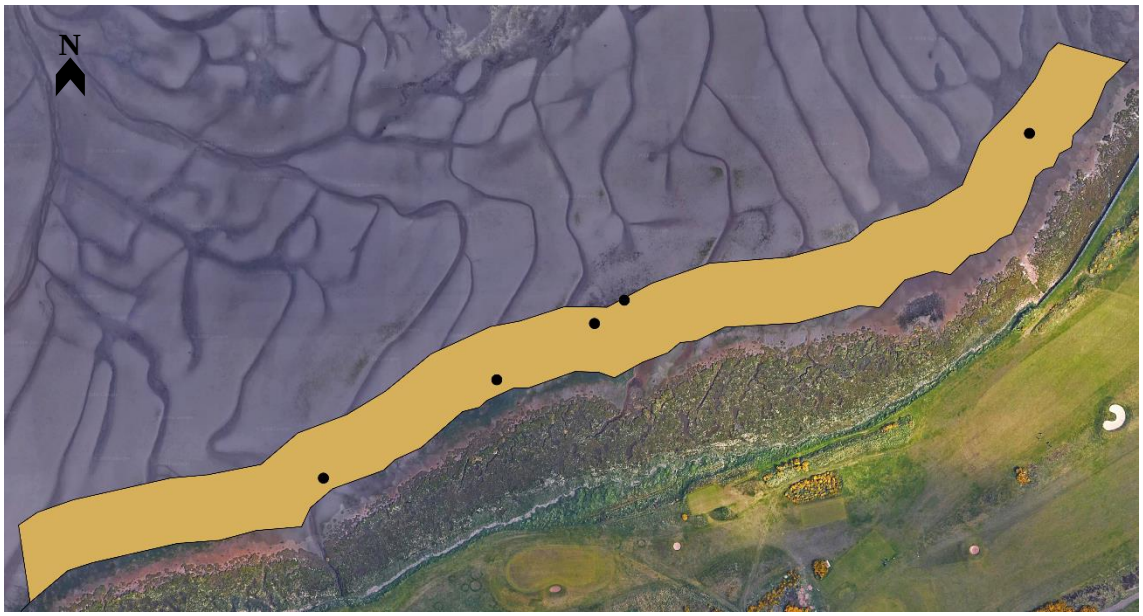


*Figure 4.2: Aerial image of estuary showing polygon of mudflat area studied in brown. Black dots are location of core samples, located through random selection by QGIS.*

The mudflat focal area was established using the fringing edge of the natural marsh's outer limit as a base line. From the base line a buffer zone of 10 m and 30 m was created, where these two zones overlapped was taken as the area of adjacent mudflat (Figure 4.2). These limits were put in place to focus sampling of mudflat areas under similar environmental influence (e.g. tide) whilst minimising possible overlap into vegetated areas due to imagery

or polygon error. The mudflat area sits at an average elevation of 1.220 m above ordnance-datum (OD).

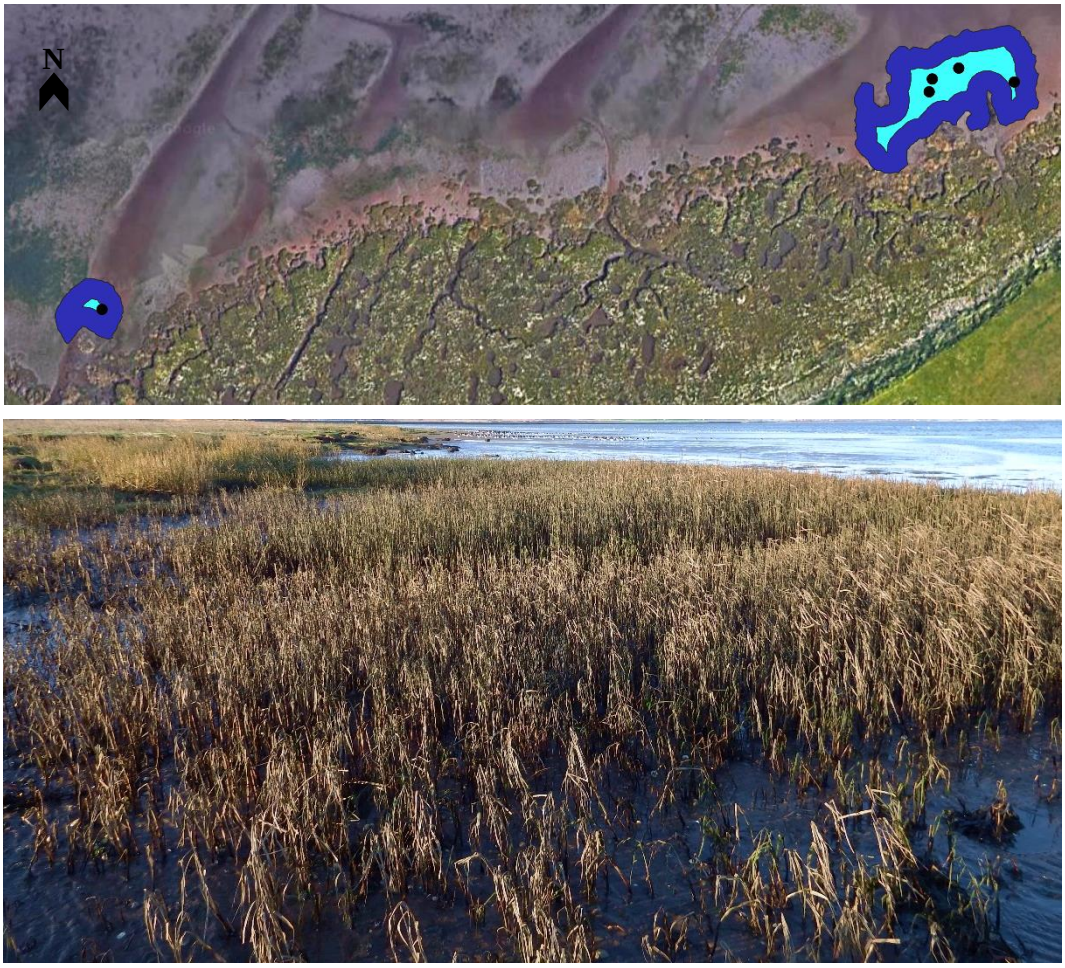


*Figure 4.3: Top - aerial image of restored sites studied. Dark blue polygon defines the outer limits of the vegetation determined through walked GPS track data, light blue polygon is a 3-meter buffered area, showing the area of interest for the study in which core sampling took place. Black dots are location of core samples, located through random selection by QGIS. Bottom image is the larger restored area taken during winter die-back phase.*

The restored area absolute limits were determined from GPS tracks generated in the field whilst walking their exterior, there were two stands of the same age and structure which were used in this study. These tracks defined the outer-limits for the area, from this a 'buffer' of 3 m was applied in *QGIS*, to produce the actual area which would be targeted during sampling (Figure 4.3). The buffer area was used to direct sampling effort towards those longer established areas of vegetation and reduce the measurement of the more dynamic edge region, whose presence could be relatively new (due to expansion). These

restored areas comprised of well-established mono-culture *B. maritimus* stands, having an average elevation of 1.471 m above OD.

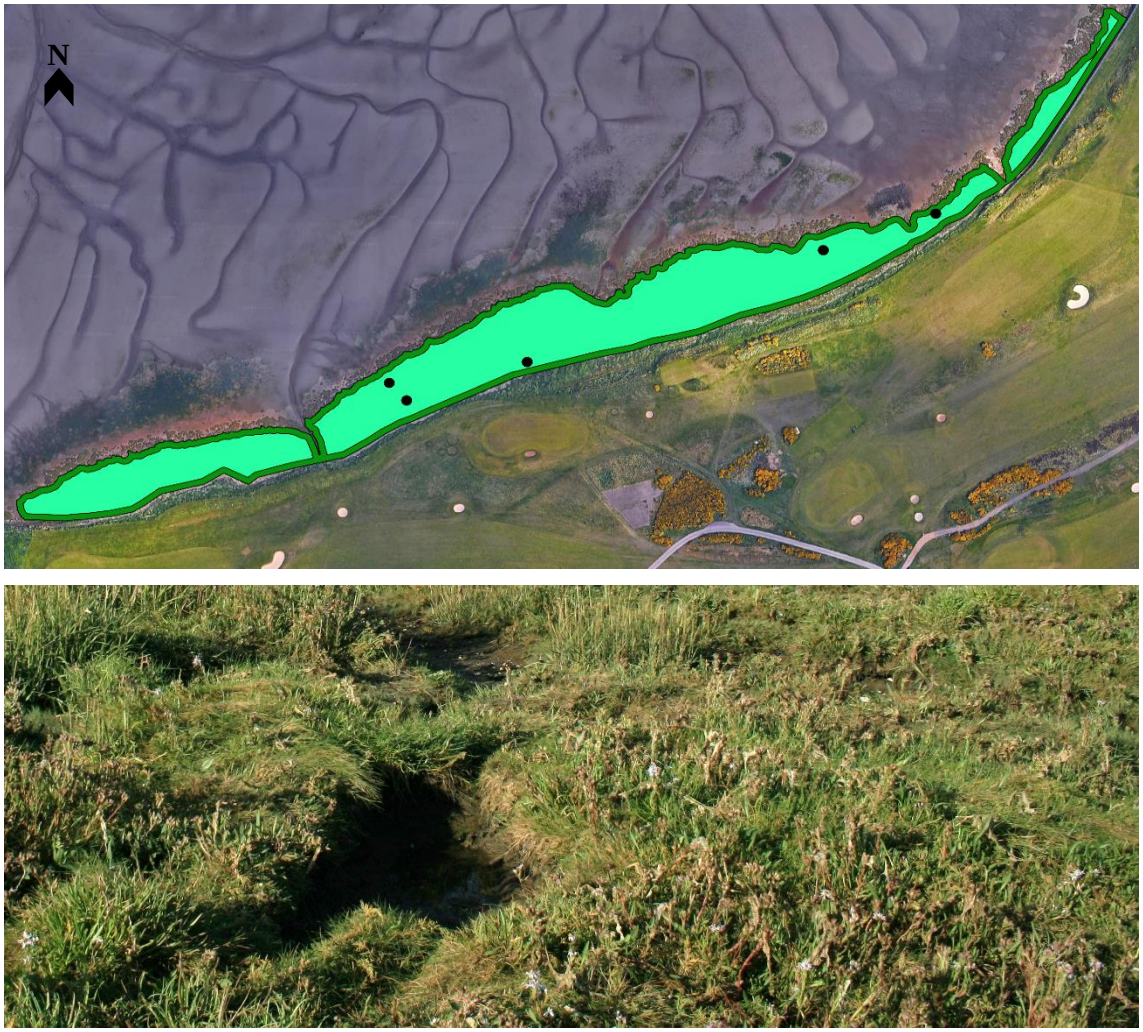


*Figure 4.4: Top: aerial image of estuary showing polygon of natural area of P. maritima studied. Dark green polygon defines the outer limits of the vegetation determined from remote imagery, light green polygon is a 3-meter buffered area of the total extent, showing the area of interest for the study in which core sampling took place. Black dots are location of core samples, located through random selection by QGIS. Bottom: Typical P. maritima community of the saltmarsh area studied.*

The extent of the natural area was determined with *Google Earth* imagery, which was used to create a polygon, delineated along the fringing edge of the *P. maritima* marsh (usually a clear distinguishable line where the saltmarsh platform ends in a small cliff down to bare mud) and using the visible strand line to determine the upper boundary. As with the restored are, a 3 m buffer was applied to this outer-limit shape (Figure 4.4). This ensured sampling points were within the saltmarsh extent – i.e. within the *P. maritima* community - and accounted for error introduced from manually creating the polygon. The vegetation community sampled was represented under SM13 of the National Vegetation Classification

(Pigott et al., 2000) called SM13a in the Scottish Saltmarsh Survey (Haynes, 2016). This mid-marsh area sits at an average elevation of 2.138 m above OD.

These buffered extents of the restored and natural areas and the calculated extent for the mudflat were used to define sampling locations. Inside each area QGIS randomly distributed five points, whose locations were used in the field as sampling points, navigated to by a hand-held GPS unit (Garmin GPS 64s).

### *4.2.2 Sediment coring of intertidal sediments*

Sub-surface samples of sediment were retrieved using a coring device, which takes the general form of a vertical cylinder that is inserted into the sediment and retains a column of sediment when removed (Skilbeck et al., 2017). Various corers are available, typically in the form of a Russian corer or Gouge corer. These designs are widely used and can facilitate the extraction sediment samples. However, there are risks associated with core deformation during collection. Such as the potential to 'squash' the sample if the sediment is particularly dense and requires high amounts of percussive force to progress downwards. Although such issues can be mitigated, such as through the application of compaction corrections (Morton et al., 1997), it is beneficial to minimise its affects during collection in the first place.

Sediment core distortion can be reduced through the use of larger diameter core tubes, which reduce the effect of fiction build up during penetration, (Skilbeck et al., 2017) or the use of high-frequency vibrations in place of discreet percussive force to facilitate the corers progress into the sediment. In this study, coring was carried out using a handheld vibrating core tube; specifically, a Speciality Devices Inc. Vibecore-Mini (Figure 4.5). Such corers produce high-frequency vibrations in the x-y plane, which are directed down the core tube. These vibrations aid passage of the core down through the sediment by effectively liquifying the immediate boundary layer, so reducing the friction along the core length. The Vibecore-Mini vibrates at 83 – 100 Hz and was fitted with 3-inch diameter core tubes. The head unit of the device generated the vibration and housed an attachment ring and a one-way valve. The valve allowed displaced air and water to pass up out of the core tube, which created a seal upon retrieval through the development of a vacuum in the tube.

### *4.2.3 Sediment core retrieval*


*Figure 4.5: A hand-held Vibecore-Mini unit with a 4-inch core tube attached. Along with additional core tubes and accessories.*

Sediment core samples were collected by area, extracting 5 cores from each. Each sediment core was collected in a different core tube allowing multiple cores to be extracted in one visit with samples remaining contained, protected and undisturbed; core tubes were simply affixed and removed from the head attachment ring as required. Where the core tubes were affixed to the head unit of the corer there is a one-way valve which acts to create a vacuum within the tube as it progresses through the sediment. This design works most efficiently when used in saturated, or ideally flooded, sediment; so, reducing the air space within the tube or interstitial spaces and enhancing the creation of a vacuum. The vacuum aided the retrieval of the core sample, reducing loss through slippage of the sediment out of the bottom of the tube.

Samples from the natural marsh area were collected during spring tide events, immediately following high tide. Cores in the restored area and on the mudflat were taken at any tide state which inundated them, with sampling being carried out following high tide as soon as area was accessible by wading.

Initial testing suggested that some loss of sediment occurred from the bottom of the tube, in certain sediment types within the target areas. However, it was decided to not add a core catcher to the tubes. Core catchers are flexible metal toothed collars which attach internally to the bottom of core. As the corer progresses through the sediment the teeth are pushed aside, upon retrieval the pressure of the sediment stack forces the teeth to close sealing the core tube and retaining the sample. However, there is potential for the teeth of the catcher to disturb the sample during collection. Furthermore, not all sediments were prone to loss from the bottom of the tube, thus it was decided to accept possible loss of sample and minimise disturbance to the core.

During sampling, each area was sampled on separate days, for logistical ease with removal from site, storage and initial processing. All cores were taken down to refusal; considered to be reached when the corer made no more progress at full vibration and with considerable downward pressure applied. Coring effort was ceased after a few seconds upon reaching this to minimise possible disturbance down the core length with excessive continual vibration. Most cores reached refusal within 20 seconds. In mudflat and restored saltmarsh sediments the corer made relatively easy progress, sampling the *P. maritima* marsh was more difficult, with initial resistance in the root/vegetation layer and increased resistance down the core.

*Figure 4.6: Thick walled pipe section which was filled with hot water and used to rapidly heat frozen core tubes, facilitating the removal of the sediment core.*

Once taken all cores were capped at both ends with tight fitting plastic ends. Capping ensured no loss of sediment occurred and that there could be no input onto the lower or upper sediment surfaces. The capped core tubes were labelled and stored upright during transport from the estuary to the laboratory.

### *4.2.4 Sediment core storage and removal*

Cores were placed vertically into a freezer immediately following collection, where they were left to fully freeze; helping to preserve the sample and facilitating the sample removal processes.

To remove the core with minimal disturbance a novel solution was designed (Figure 4.6). A tall thick-walled plastic pipe was secured upright and sealed at its base, where the height of the pipe was at least a cores length. This pipe was filled with very hot water and a

frozen and sealed core tube plunged into it whilst attached to the vibrating head unit. The core tube remained immersed for a period of approximately 30 seconds and was then removed. The cap was immediately removed and holding the corer at a shallow angle, the intact sediment core was gently vibrated out into a length of half pipe; this approach facilitated the removal of the sample whole with minimal streaking along its length.

### *4.2.5 Sediment core processing*

*Figure 4.7: Frozen sediment core after extraction from core tube into half-pipe capture device. Showing retained head of excess water (right, whitish block) held above the sediment during collection.*

The whole frozen sediment core was left to defrost in the half-pipe capture device at room temperature for approximately 4 h. Precise timing was dependent upon individual cores, but all were processed as soon as possible (i.e. once defrosted). Whilst defrosting cores were slightly elevated at one end to ensure excess water (Figure 4.7) drained away from the sample, so as to not interfere with the core.

Once defrosted the cores were sliced using a sharp flat disc (Figure 4.8) in a single motion, minimising loss or transfer of material between sections. Cores were sectioned intensively at shallow depths becoming less frequent with depth. The sampling regime aimed to be effective and efficient; capturing the likely variation in near surface, less conserved region of the sediment bed, through to the stable deeper deposits. Sampling took place as follows:

- Surface to 10 cm: sliced into 1 cm sections, giving a total of 10 sections.
- 10 cm – 30 cm: sliced into 5 cm sections; giving 4 sections.
- 30 – 50 cm: sliced into 10 cm sections; giving 2 sections.
- > 50 cm: every 25 cm.

The final section of a core was measured and noted for use in future analysis. Each core section was individually bagged and re-frozen, preserving the sample – including water content and organic matter.

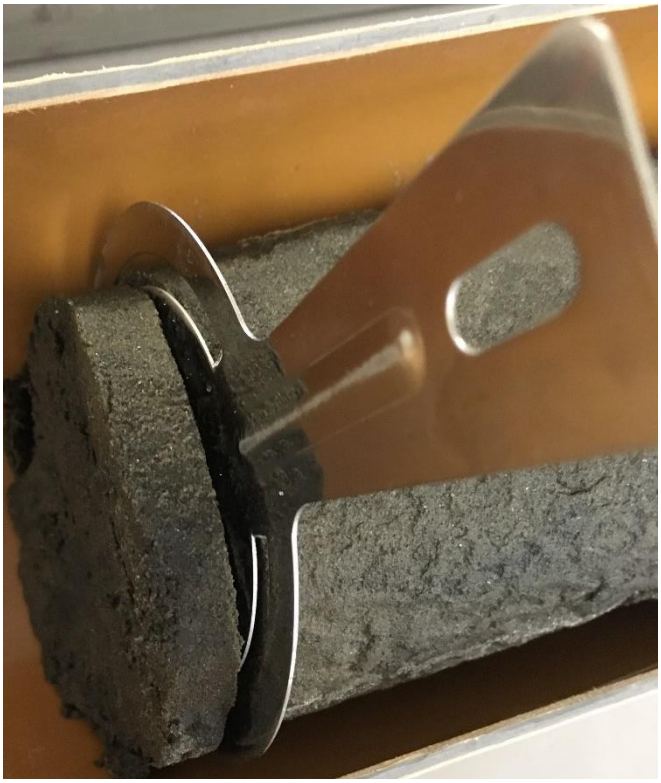

*Figure 4.8: Sediment core being sliced with the sharpened disc core slicer. Showing a 1 cm section being removed.*

### *4.2.6 Sediment core analysis*

#### *4.2.6.1 Sediment dry weight and water content*

Core sample sections were defrosted in their sealed sample bags and weighed at room temperature. Samples were then dried in a drying oven at 60°C for a minimum of 48 h, with fan driven warm airflow. Samples were repeatedly checked and re-arranged in the oven to ensure all were thoroughly dried. If sediment was still wet after time period samples were left until no water droplets or condensation on the bag were visible. Fully dried samples were cooled in a desiccator and re-weighed. This provided the dry weight of the sample and allowed the calculation of its water content – shown in Equation 15.

$$Water\ content\ (\%) = \left(\frac{Tw - Td}{Tw}\right) \times 100$$

*Equation 15*

Where *Tw* is the total wet weight of the sample (g) and *Td* is the total dry weight of the sample (g).

#### *4.2.6.2 Sediment bulk density*

The sediment dry bulk density of core sections was calculated (Equation 16) using the volume of sample from the known dimensions of the core tube (ID = 7.4 cm), the length of the section (*l*) and the total dry weight of the sample. It was assumed that the core tube was a perfect cylinder and the inner diameter does not change. The length of each section was as described above, in the case of the final section the actual measured length was used. The dry bulk density was calculated according to Equation 16.

$$Dry\ Bulk\ Density\ (grams\ per\ cm^3) = \frac{Td}{\left(\pi\ \times\ (ID/2)^2\right) \times l}$$

*Equation 16*

#### *4.2.6.3 Sediment particle size analysis*

Sub-samples of each core section were used to analyse sediment particle size composition (Coulter counter) using a 'wet' methodology. Pre-analysis preparation removed organics and calcium carbonate, allowing the analysis to be conducted on primary particle sizes. First organics were removed, samples were placed into 25 ml falcon tubes and 4 ml of hydrogen peroxide (30 % vol) added to each. Sample were vortexed thoroughly, until mixed, and sonicated for 15 min. These were re-mixed by vortex and sonicated for a further 15 min. Samples were placed in warm water (60 °C) for five hours, after which an additional 1.5 ml of hydrogen peroxide was added, samples vortexed and re-placed in the bath for a further hour; ensuring the reaction had completed. During the organic breakdown reaction care was taken to minimise crossing of samples from the production of 'organic foam' (a result of the exothermic reaction) spilling out and between sample tubes by ensuring spacing between

tubes and removing any significant ‘foam’. Once reaction was complete samples were spun at 2000 rpm in a 150 mm radius centrifuge for 10 min and supernatant removed.

Following the removal of organics, a second step was conducted to removed carbonates (e.g. shell fragments). A 1.5 ml volume of 20 % hydrochloric acid was added to the samples and the tube contents mixed. These were placed in a 60 °C oven for two hours, being re-mixed after one hour. The samples were centrifuged as described previously and supernatant removed. The final step ensured the removal of chemicals through the addition of 2 ml distilled water, mixing, centrifuge and removal of supernatant; twice repeated.

A 5 % solution of sodium hexametaphosphate (Calgon) was added to the samples to act as a dispersing agent. Prior to laser granulometry analysis, samples were thoroughly mixed to ensure particles were homogenised and dispersed throughout. Each sample was added to the Coulter counter through a 2 mm sieve into approximately 2 L of water.

The resulting particle size composition was assessed variously using both the Wentworth (Wentworth, 1922) and Folk (1954) classifications. The Wentworth Scale was initially conceived in the early 1900s with the intention of producing an applicable geological universal classification of sediments which specified terms for given size breakdowns of particles (Table 4.1). Folk (1954) created ‘textural groups’ of sediment based upon their ratios of size classes as described by Wentworth (1992) (Table 4.1). The ‘Textural group’ classification applies a coarse representation of the sediment based around gravel, sand and mud and is more practical than groupings based on the Wentworth Scale (Chotiros, 2017), and of particular use in initial assessment of sediments. Both approaches are useful in describing sedimentary composition and provide complimentary information from which to investigate the influence of particle sizes on carbon storage.

*Table 4.1: Sedimentary particle diameter classifications as described by Wentworth (1922) and the textural groupings of Folk (1954).*

| **Wentworth Scale** | **Particle diameter** | **Textural groups** |
|---|---|---|
| Boulder | **> 256 mm** | Gravel |
| Cobble | **64 – 256 mm** | |
| Pebble | **4 – 64 mm** | |
| Granule | **2 – 4mm** | |
| Very coarse sand grain | **1 – 2 mm** | |
| Coarse sand grain | **500 µm – 1 mm** | Sand |
| Medium sand grain | **250 – 500 µm** | |
| Fine sand grain | **125 – 250 µm** | |
| Very fine sand grain | **62.5 – 125 µm** | |
| Silt particle | **3.9 – 62.5 µm** | Mud |
| Clay particle | **< 3.9 µm** | |

#### *4.2.6.4 Sediment organic content*

The organic content of sediments was calculated using a Loss-On-Ignition (LOI) approach. In some instances, post-dried sections were solid, assumed to be due to high clay content, so core sections were thoroughly unconsolidated down to their constitutional parts before analysis. Once samples had been homogenised a sub-sample of approximately 4 g was placed into weighed aluminium boats. Samples were placed into a muffle furnace and combusted at 450°C for six hours, ramped at 10°C per minute. Post-combustion samples were placed into a desiccator to cool prior to being re-weighed; providing a measure of weight loss through the conversion of organic matter to gaseous $CO_2$. The organic content of the sample was calculated according to Equation 12 and the resulting percentage organic content values according to Equation 13.

$$OM\ (grams) = Sdw - (CSdw - aluminium\ boat)$$

*Equation 17*

Where *OM* is the organic matter content of the sample (g), *Sdw* is the sediment dry weight of the sub-sample and *CSdw* is the combusted sub-sample weight of the sediment (g).

$$\%OM = \left(\frac{OM}{Sdw}\right) \times 100$$

*Equation 18*

Where *%OM* is percentage organic matter content of the sample.

#### *4.2.6.5 Sediment organic carbon content*

Organic carbon content of sediment was obtained through gas chromatography via elemental analysis (EA). A sub-sample of each homogenised core section sediment was prepared as follows. First the sample was ground to a fine powder in a pestle and mortar and larger debris were removed - such as vegetative material, stones and shell fragments. Approximately 10 mg (±10 %) of milled sample was weighed into small (8 mm x 5 mm) silver capsules and 40 µl of 10 % HCl added to remove carbonates. Acidified samples were left over night in a fume hood, then placed in a drying oven to ensure all HCl had evaporated. Silver capsules were carefully folded and rolled, creating a sealed ball. These were analysed in an Elementar vario EL cube CHNS EA, with readings corrected back to doubled sulphanilamide standards every 10 samples. During analysis, samples were flash combusted at 1200°C, with an injection of oxygen, the resulting gaseous sample was separated and passed through three specific analysis columns ($CO_2$, $H_2O$, $SO_2$; $N_2$ is not absorbed by a column), carried in a flow of helium. Thermal conductivity across a detector quantifies sample components; with selective columns individually heated and gas production measured separately.

#### *4.2.6.6 Sediment carbon density*

The actual amount of carbon present in a given amount of sediment is determined by the carbon density of those sediments. Carbon density is a product of the sediment dry bulk density and its carbon content, being calculated as shown in Equation 19.

$$Carbon\ density\ (grams\ Carbon\ per\ cm^3) = Dry\ bulk\ density\ \times carbon\ content\ \%$$

*Equation 19*

Where Dry bulk density ($g/cm^3$) is calculated by Equation 16.

### *4.2.7 Sediment core analysis summary*

The vertical analyses of sediment from the cores provide insight into changes in carbon distribution with time, generating data profiles for each analysis. These depth profiles allow investigation into changing carbon storage with depth and possible factors affecting this value.

Some sediment appeared to be "lost" during core preparation. Loss was defined as the difference between the measured penetration depth of the core tube in the field and the total length of sediment core retrieved from the tube. It was noted that there was an average loss of 94 mm across the areas; specifically, being 104 mm, 69 mm and 110 mm for the mudflat, restored and natural areas respectively. It is unclear as to the cause of this loss. On inspection of the emptied core tubes there were possible signs of 'slippage', where material had possibly entered the tube then upon retrieval had slipped back down until enough vacuum was created to hold the sediment column in place. It is possible there was a degree of compaction, however, due to the nature of the sampling technique - which minimises such effects - and the considered approach to remove any excessive downward force it is assumed that compaction has not influenced these cores and were processed without corrections applied and the former error is more likely.

## 4.3 Statistical analysis

The analysis of sediment core samples provided a range of data on its properties to assess; including water content, bulk density, particle size, organic content, carbon (organic) content and carbon density. Analysis was conducted on each data type (water content, bulk density, organic content, carbon content and carbon density), ANOVA assessed the difference between the profiles of the five cores taken within each area, investigating the variation of these data types within a similar area. Post-hoc (TukeysHSD) was used to assess the ANOVA and investigate any significant differences between cores which were found. ANOVA was used to assess the differences in the profile data between areas using the mean averaged data of the fives cores taken in each, with TukeysHSD post-hoc analysis applied to interrogate differences found. ANOVA was also used to assess down core variation in values of the different data types, comparing within area individually. Spearman's rank analysis was used to assess the relationship between organic content and carbon content of profiles in each area, determining if these relationships differ.

## 4.4 Hypotheses – Sediment cores

Data in this chapter assess the sedimentary depth profile of different area types within the study, to investigate differences between natural and restored areas and how these influence sedimentary carbon storage. The study held the following hypotheses:

- Within area sediment profile properties will display low amounts of variation.
- Vegetated areas would exhibit more similar sedimentary characteristics than bare mudflat.
- Carbon content of vegetated areas will be greater than bare mudflat.
- Natural areas of vegetation will display greater sedimentary carbon store than restored areas.
- Carbon content will decrease with depth.
- Carbon storage will be greatest in the area of natural vegetation.

## 4.5 Sediment coring results

### *4.5.1 Sediment water content depth profile*

The water content of sediment cores showed a general trend of increased water content with 'increased vegetation'; whereby mudflat was the lowest followed by restored vegetation and the highest found in the natural area of *P. maritima* (Figure 4.9). 'Increased vegetation' is meant as the amount of visible above ground structure, extant below ground rooting structure and historical below ground vegetative matter from previous growth.

Water content of sediments became more similar with depth, declining towards the lower limits defined by the mudflat; particularly in restored and mudflat areas (Figure 4.9). Sediment water content within the restored area, on average, converge, to approximately 21 %, with those found on the mudflat below 40 cm (Figure 4.9). Natural marsh sediments reflected the same 21 % water content at depths > 50 cm

An ANOVA (which assumed unequal variance of residuals) of the mudflat cores water content indicates a significant difference of means in each profile ($F(4, 31.8) = 2.7246$, $p = 0.046$), affected by the values out with one standard deviation of the mean (Figure 4.9). The means of each core (Table 4.2) show that 'mudflat core 1' had a higher average water content than was found in the other four cores. An ANOVA of restored area core water content showed there was no significant difference between the cores ($F(4, 65) = 1.447$, $p =$

0.2287, Figure 4.9). An ANOVA of natural area core water content profiles showed there was a significant difference between the cores ($F(4, 65) = 3.762$, $p = 0.008$, Figure 4.9). Investigation of the data shows that mean water content of 'natural core 2' was less than all other cores and was different from the general trend of the other four cores (Table 4.2). Assessment of the model using TukeysHSD showed that significant differences were only present between core 2 and 3 (diff. = 10.315, $p = 0.0327$) and core 2 and 4 (diff. = 12.1914, $p = 0.007$).

*Table 4.2: Summary data of average percentage water content in each of the five cores taken from the mudflat, the restored area and the natural saltmarsh extent.*

| **Area** | **Cores** | | | | |
|---|---|---|---|---|---|
| | 1 | 2 | 3 | 4 | 5 |
| Mudflat | 24.9 | 21.5 | 21.8 | 21.5 | 21.6 |
| Restored | 26.4 | 24.4 | 24.7 | 24.9 | 24.3 |
| Natural | 46.7 | 37.4 | 47.7 | 49.6 | 43.8 |

Comparing the average water content of each area type showed a significant difference between them (ANOVA; $F(2, 48) = 60.46$, $p < 0.0001$). Further analysis using TukeysHSD shows that the only the natural area was significantly different ($p < 0.0001$), with the restored and mudflat area not being statistically different from one another ($p = 0.5141$).

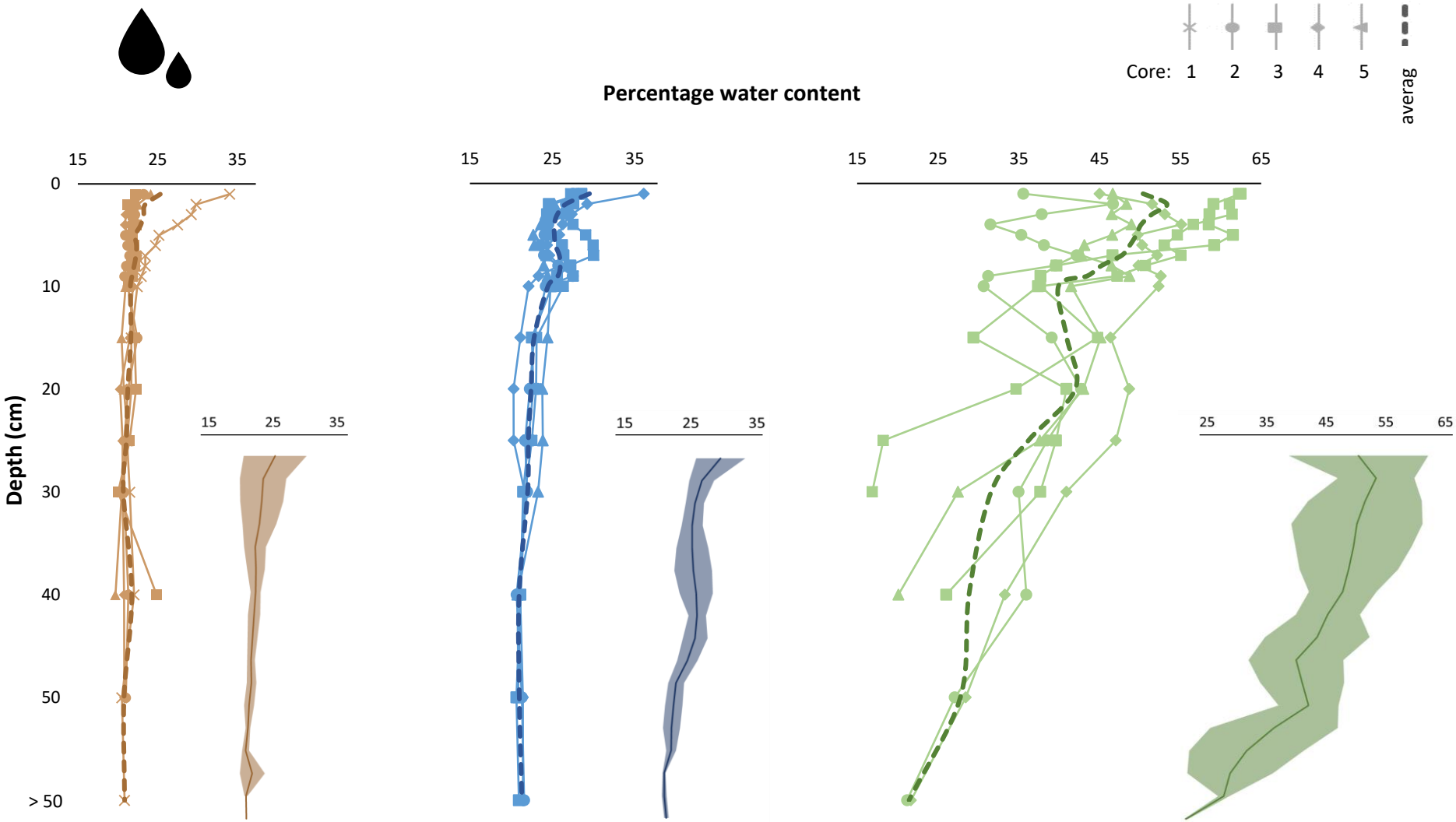


*Figure 4.9: Down core water content percentage profiles for mudflat (brown), restored (blue) and natural marsh (green) areas. Main plots showing individual profiles for each core (solid lines) and averaged profiles (dotted line). Smaller insert plots representative of average core profile (line) and one standard deviation (shaded area), not to same depth scale as main plots.*

### *4.5.2 Sediment bulk density profiles*

Sediment dry bulk density plays an import direct role in evaluating the carbon storage of sediments and can have a large influence on the total stock of any given area. The current study shows that sediments from the mudflat and restored areas, generally, have a higher bulk density through their depth than does sediment of the natural saltmarsh (Figure 4.10).

An ANOVA comparing the bulk density values with depth of cores taken on the mudflat show no significant differences between the cores ($F(4, 74) = 1.481$, $p = 0.216$). An ANOVA comparing the bulk density values with depth of cores taken in the restored area of *B. maritimus* show no significant differences between the cores ($F(4, 78) = 0.4818$, $p = 0.749$). The bulk density profiles of the cores in the mudflat and restored areas tend to lie within one standard deviation of their mean profile, highlighting the lack of variation between cores (Figure 4.10); however, all areas displayed relatively narrow standard deviation profiles. An ANOVA comparing the bulk density values with depth of cores taken in the natural extent of *P. maritima* saltmarsh shows there were significant differences between the cores ($F(4, 73) = 3.842$, $p = 0.0069$). Further analysis with TukeysHSD showed that significant differences were found between natural core 2 and core 1 (diff. = 0.2639, $p = 0.0368$), and core 3 (diff. = 0.3101, $p = 0.007$), and core 4 (diff. = 0.2513, $p = 0.0362$).

An ANOVA of the average down core bulk densities of each area showed there were significant differences between the sites ($F(2, 48) = 56.22$, $p < 0.0001$). A TukeysHSD demonstrated that statistical differences were only present between the natural area and restored area (diff. = 0.4595, $p < 0.0001$) and the mudflat (diff. = 0.5486, $p < 0.0001$); no significant difference was found between the restored area and mudflat (diff. = 0.0891, $p = 0.2757$).

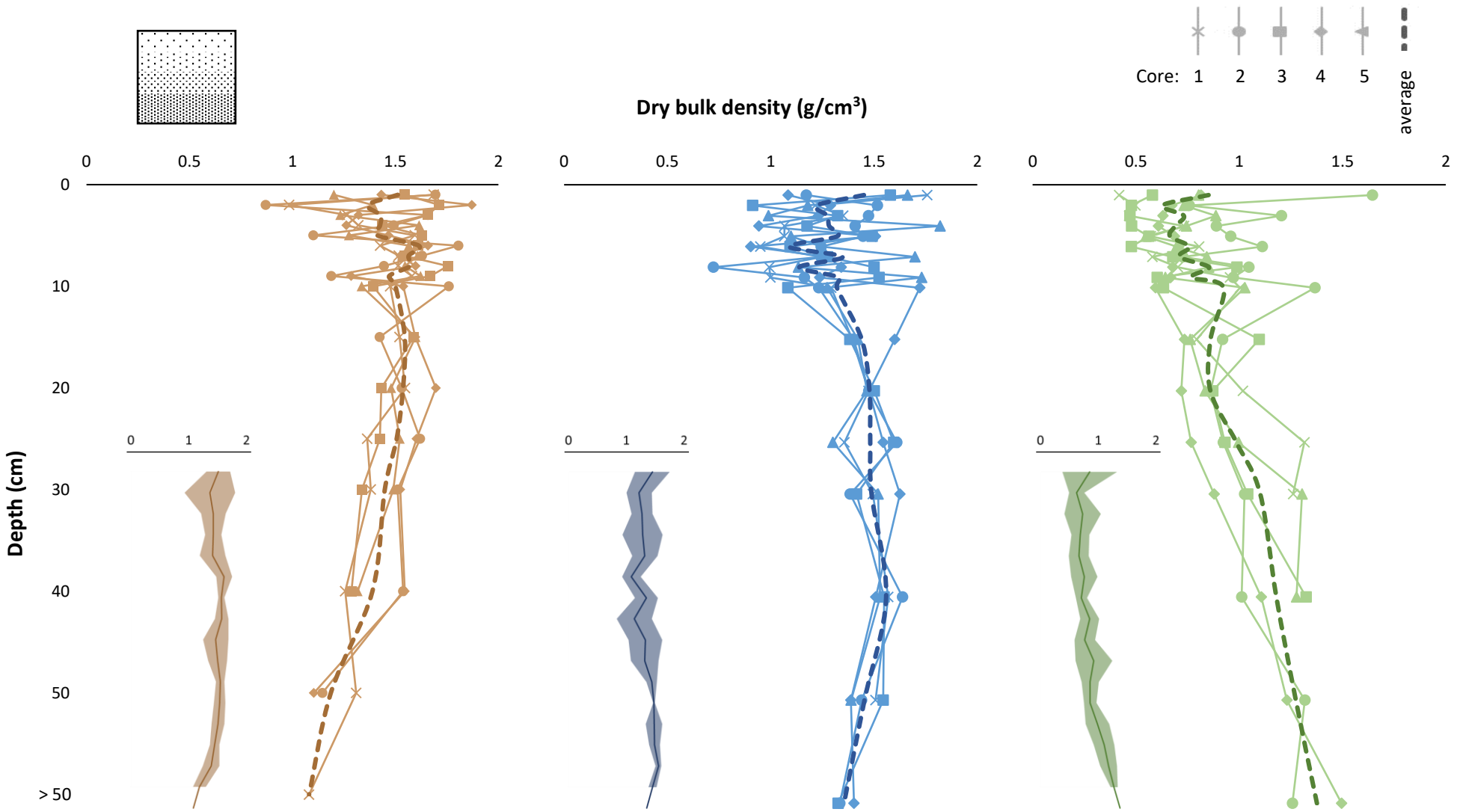


*Figure 4.10: Down core dry bulk density (g/cm$^3$) profiles for mudflat (brown), restored (blue) and natural marsh (green) areas. Main plots showing individual profiles for each core (solid lines) and averaged profiles (dotted line). Smaller insert plots representative of average core profile (line) and one standard deviation (shaded area), not to same depth scale as main plots.*

### *4.5.3 Sediment particle size composition profile*

The particle size composition profile of each core was determined with a coulter counter, acquiring primary particle sizes. Triplicate analysis of each sample gave percentage composition values over 31 size ranges, from 4 µm to 2000 µm; the maximum particle size measured was 1750 µm. These triplicate data were averaged for each depth sample (layer), then averaged across each layer in each area, providing a representative core value for each area type (Table 4.3, Table 4.4,Table 4.5). Sediment from the natural saltmarsh comprise smaller average size particles down the entire depth of the core than those from the mudflat or restored areas (Figure 4.11 and Table 4.3, Table 4.4, Table 4.5). Generally, mean particle sizes were similar at the surface (> 10 cm); being an average of 148 µm in sediments of natural saltmarsh, 203 µm in the restored saltmarsh and 202 µm on the mudflat – a difference of 55 µm. At mid-depths these size differences were more pronounced, 88 µm difference, with the natural saltmarsh sediments tending to smaller average sizes. Towards the bottom of the cores, sediment sizes appear to be converging for all areas sampled, resulting in a difference of only 28 µm.

The skewness of the samples was also determined, where 0 indicates an equal distribution around the mean. A skewness vales of > 0 indicates a 'right-skewed' distribution whose mainly larger values increase the mean but do not affect the mode and a value < 0 indicated a 'left-skewed' distribution the mainly smaller particles reduce the mean value but do not affect the modal value (Beckman-Coulter, 2011). Both the restored (Table 4.4) and mudflat (Table 4.3) areas exhibit near equal size distributions (skewness close to zero) down the length of their cores; as such the mean values obtained can be considered representative of the sample. The sediments from the natural saltmarsh extent show higher positive skew (Table 4.5), suggesting the mean values were being influenced by the presence of larger particles in the sample. The different particle size distribution shapes, as indicated by their skewness, illustrates the likely differing sedimentary processes of these areas, which could directly influence other factors, such as organic content and carbon storage.

The median particle size of sediments were similarly distinguished as their mean size, where by the sediment of the natural saltmarsh were consistently smaller and sizes began to converge at the bottom of the core towards the median size of the sediment found in the restored and mudflat areas (Figure 4.11).

*Table 4.3: Sediment particle size (µm) data at each depth section averaged across five cores from the mudflat. Output taken from coulter counter output.*

| Depth (cm) | Mudflat | | | | | |
|---|---|---|---|---|---|---|
| | Mean | Median | Skewness | D10 | D90 | D90-d10 |
| 1 | 184.2 | 193.0 | -0.1 | 22.9 | 296.7 | 273.8 |
| 2 | 191.2 | 198.0 | 0.0 | 34.4 | 306.8 | 272.4 |
| 3 | 191.6 | 198.9 | 0.0 | 22.6 | 308.6 | 286.0 |
| 4 | 190.2 | 197.3 | 0.0 | 25.1 | 304.4 | 279.4 |
| 5 | 248.0 | 201.9 | 0.3 | 39.9 | 577.7 | 537.8 |
| 6 | 189.1 | 197.2 | 0.0 | 25.4 | 305.2 | 279.8 |
| 7 | 192.7 | 199.2 | -0.1 | 28.6 | 305.5 | 276.9 |
| 8 | 209.3 | 200.7 | 0.8 | 39.5 | 316.8 | 277.4 |
| 9 | 194.7 | 200.4 | -0.1 | 35.6 | 307.1 | 271.5 |
| 10 | 225.3 | 202.0 | 0.3 | 37.9 | 489.5 | 451.7 |
| 15 | 205.5 | 208.3 | 0.0 | 39.8 | 325.8 | 286.0 |
| 20 | 220.0 | 215.7 | 0.3 | 103.3 | 338.3 | 235.0 |
| 25 | 220.4 | 214.1 | 0.5 | 127.6 | 327.6 | 200.0 |
| 30 | 221.1 | 213.1 | 0.5 | 138.8 | 324.6 | 185.8 |
| 40 | 219.1 | 212.1 | 0.5 | 138.0 | 317.7 | 179.7 |
| 50 | 222.3 | 213.6 | 0.6 | 138.9 | 324.5 | 185.6 |
| >50 | 245.1 | 235.5 | 0.4 | 150.7 | 364.1 | 213.5 |

*Table 4.4: Sediment particle size (µm) data at each depth section averaged across five cores from the restored saltmarsh area. Output taken from coulter counter output.*

| Depth (cm) | Restored area | | | | | |
|---|---|---|---|---|---|---|
| | Mean | Median | Skewness | D10 | D90 | D90-d10 |
| 1 | 192.0 | 192.7 | 0.2 | 70.0 | 299.5 | 229.4 |
| 2 | 204.7 | 201.6 | 0.2 | 96.6 | 312.3 | 215.7 |
| 3 | 207.1 | 204.7 | 0.2 | 94.9 | 316.1 | 221.2 |
| 4 | 206.4 | 204.2 | 0.2 | 91.3 | 315.4 | 224.1 |
| 5 | 202.2 | 201.9 | 0.1 | 71.1 | 312.1 | 241.1 |
| 6 | 200.7 | 201.3 | 0.0 | 51.8 | 312.7 | 261.0 |
| 7 | 198.5 | 201.0 | 0.1 | 41.2 | 310.8 | 269.5 |
| 8 | 200.7 | 202.0 | 0.1 | 46.9 | 316.4 | 269.4 |
| 9 | 199.0 | 201.5 | 0.0 | 34.6 | 316.2 | 281.6 |
| 10 | 219.5 | 203.1 | 0.7 | 36.5 | 333.4 | 296.9 |
| 15 | 208.9 | 207.8 | 0.1 | 60.3 | 329.8 | 269.5 |
| 20 | 211.2 | 203.2 | 0.8 | 83.3 | 337.6 | 254.2 |
| 25 | 205.2 | 198.5 | 0.5 | 92.4 | 320.0 | 227.6 |
| 30 | 207.2 | 202.4 | 0.4 | 83.3 | 327.5 | 244.2 |
| 40 | 224.0 | 217.1 | 0.7 | 106.4 | 348.7 | 242.3 |
| 50 | 232.1 | 222.4 | 0.5 | 131.7 | 355.1 | 223.4 |
| >50 | 247.3 | 234.3 | 1.1 | 142.2 | 375.5 | 233.3 |

*Table 4.5: Sediment particle size (µm) data at each depth section averaged across five cores from the natural saltmarsh area. Output taken from coulter counter output.*

| Depth (cm) | Natural marsh | | | | | |
|---|---|---|---|---|---|---|
| | Mean | Median | Skewness | D10 | D90 | D90-d10 |
| 1 | 153.4 | 87.4 | 2.7 | 3.5 | 372.6 | 369.1 |
| 2 | 151.5 | 48.9 | 3.0 | 2.9 | 408.7 | 405.8 |
| 3 | 138.1 | 53.0 | 3.6 | 2.7 | 352.4 | 349.7 |
| 4 | 155.6 | 60.7 | 2.5 | 3.0 | 431.0 | 428.1 |
| 5 | 136.9 | 53.3 | 2.8 | 2.4 | 385.7 | 383.3 |
| 6 | 134.8 | 40.0 | 3.0 | 2.4 | 356.2 | 353.8 |
| 7 | 146.4 | 33.7 | 3.1 | 2.3 | 475.9 | 473.6 |
| 8 | 146.8 | 41.0 | 2.6 | 2.3 | 446.3 | 444.0 |
| 9 | 174.0 | 60.2 | 2.5 | 2.5 | 525.1 | 522.6 |
| 10 | 150.8 | 46.3 | 2.3 | 2.2 | 459.2 | 457.0 |
| 15 | 125.4 | 81.3 | 1.9 | 3.3 | 285.9 | 282.6 |
| 20 | 116.7 | 32.2 | 2.5 | 2.4 | 293.4 | 291.0 |
| 25 | 121.7 | 61.9 | 2.1 | 3.4 | 271.2 | 267.8 |
| 30 | 131.3 | 95.3 | 1.2 | 6.7 | 285.2 | 278.5 |
| 40 | 137.6 | 121.9 | 1.4 | 32.4 | 237.4 | 205.0 |
| 50 | 148.9 | 152.6 | 0.6 | 6.3 | 289.5 | 283.2 |
| >50 | 218.0 | 212.0 | 0.9 | 36.2 | 349.9 | 313.7 |

Assessment of the ‘d10’ profile showed natural saltmarsh sediments to the dominated by finer particles (Figure 4.11), with average d10 = 7 µm and a maximum of 134 µm at a depth of 40 cm. Restored sediments were characterised by a larger d10 then mudflat sediments at the surface, down to approximately 10 cm depth. This separation was more pronounced than when assessed by mean or median, with an average difference of 41 µm down to 10 cm and a maximum of 72 µm at 3 cm.

The descriptive values of sediment particle size composition illustrate slightly differing relationships between each area. Generally, the natural saltmarsh sediments comprised of smaller sediments (Figure 4.11) with those of the restored and mudflat being typically similarly larger. However, it is important to note that these relationships were not consistent across evaluation types (Folk 1954), indicating differing actual compositions beyond strict ‘size’ defined descriptors; such as the application of type classification.

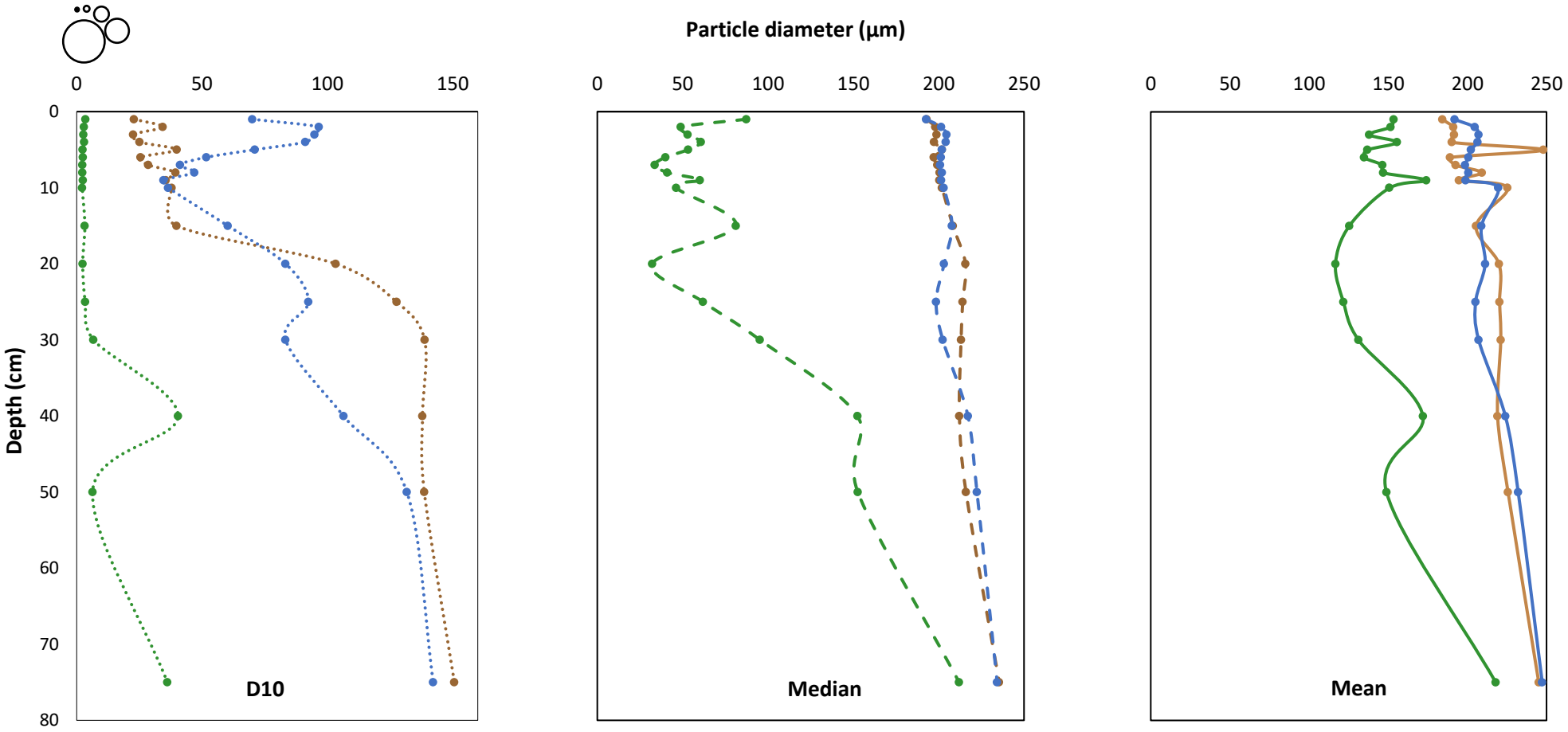


*Figure 4.11: Depth profiles of particle size averaged across five cores in each area at each depth. Left panel showing d10 values (i.e. the diameter of particle at which 10 % of the given sample sits below), middle panel showing the median sediment particle diameter of the sample and right panel showing the average diameter of sediments. Colours represent the different area type - mudflat = brown, restored = blue and natural marsh = green.*

Sediment types were determined using GRADISTAT v8 (Blott and Pye, 2001), which uses the percentage sediment volumes of the defined size classes of the coulter counter analysis to generate 'textural group' categorisation and provide a 'sediment name' after Folk (1954). Data used to generate sediment type profiles was the product of first averaged triplicate output of proportional composition of each section of each core, then secondly a subsequent average of each depth section across cores to generating a single composition for each depth in all the areas; each of which were then analysed in GRADISTAT v8.

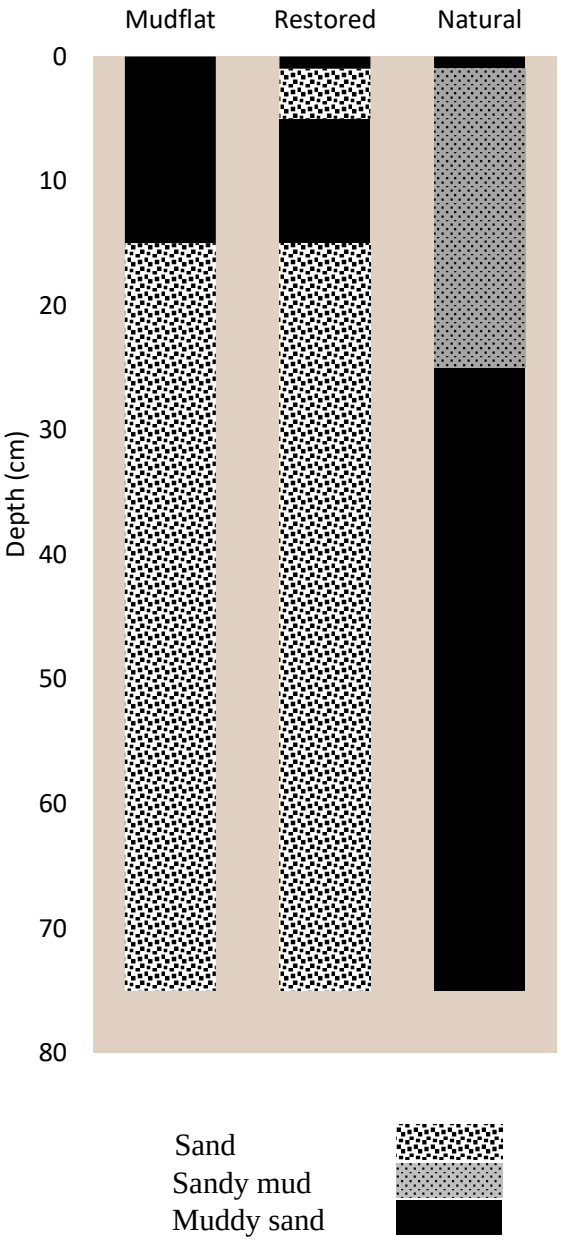


*Figure 4.12: Sediment composition 'Textural group' profiles for each area, averaged across the five cores taken in each area. Sediment type was determined using GRADISTAT v8, using proportional size composition data from coulter counter analysis.*

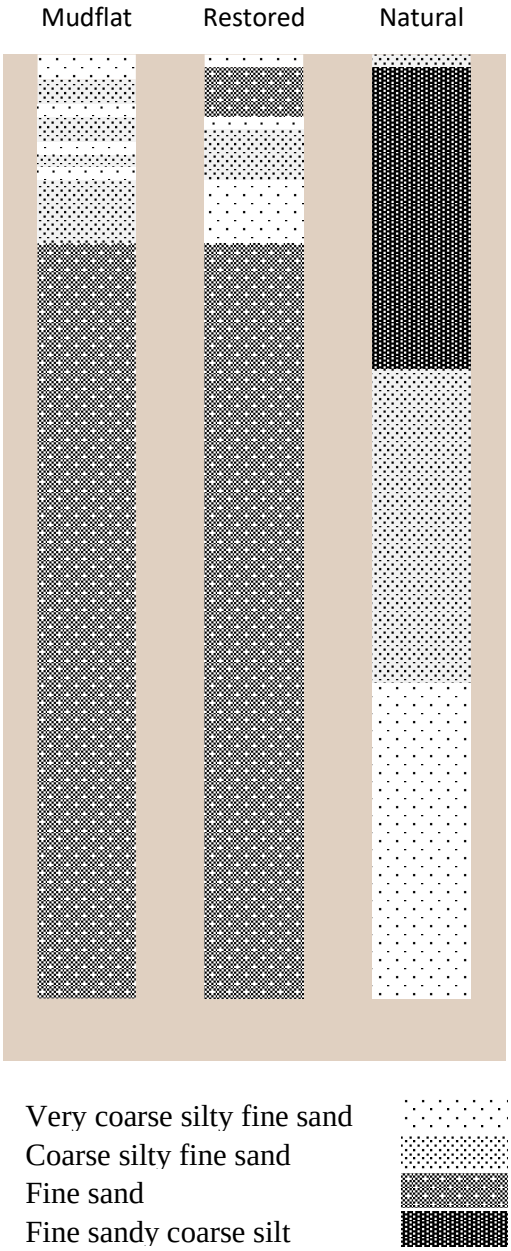


*Figure 4.13: Sediment name composition depth profiles for each area, averaged across the fives core samples of each. Sediment names are those provided by GRADISTAT v8. using proportional size composition data from coulter counter analysis.*

All depths from the three areas fall on the spectrum of mud and sand, with gravel unrepresented. The surface sediments of all areas were labelled as the textural group ‘muddy sand’ (Figure 4.12), that is sediments dominated by particles smaller than 62.5 µm with a component of those particles falling between 62.5 µm and 2 mm (Flemming, 2000; Folk, 1954 - Table 1). Down to a depth of 15 cm, the sediments of the mudflat and restored area are predominantly muddy sand, below which was solely classed as sand (Figure 4.12). The textural classification of sediments in the natural area exhibit a different profile, being classed as sandy mud at shallow depths (< 25 cm), and then muddy sand down to the bottom of the core. The sedimentary classification of the average core data displays a clear separation of the mudflat and restored cores from the natural saltmarsh sediments (Figure 4.14). The sediment ‘name’ is generated from its composition of size classes (Table 4.1). The fine particles found within all the sediment samples analysed fall within the ‘silt’ size family (Figure 4.14), with the very fine clay particles not, or insignificantly, represented.

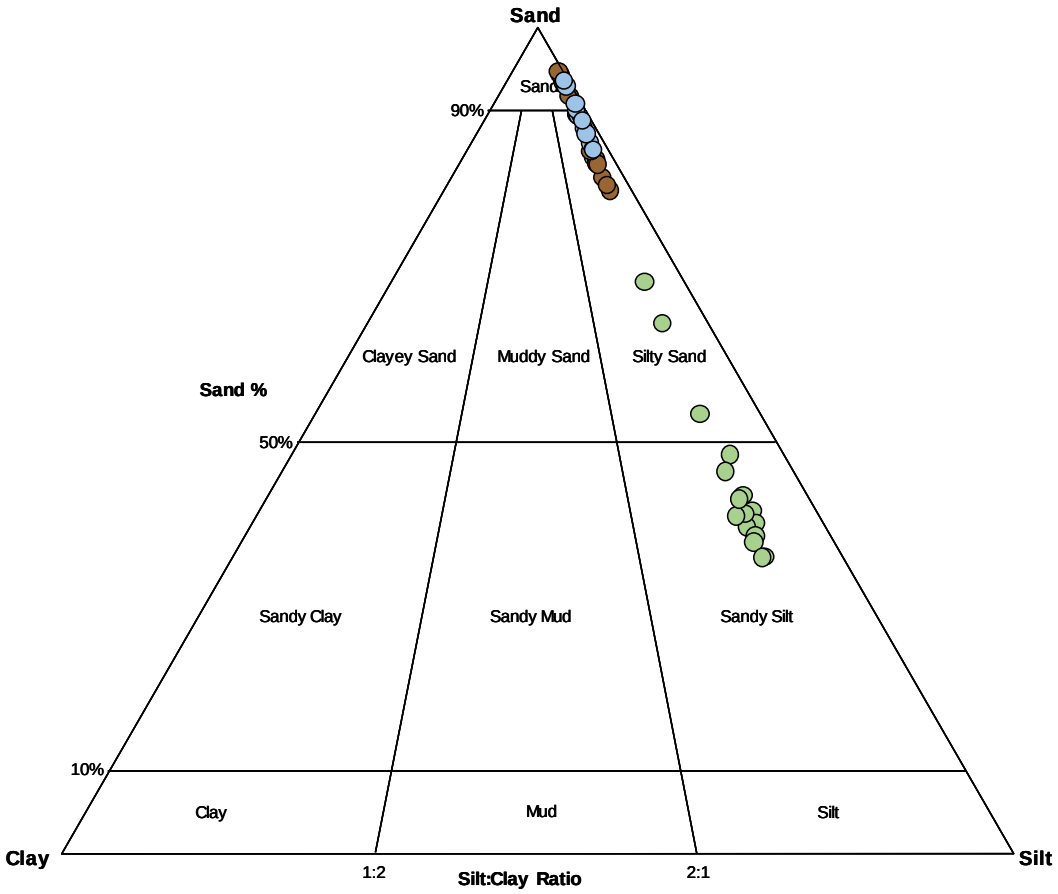


*Figure 4.14: Average sedimentary composition ternary plot showing individual points for each depth layer of the three areas studied. Green = Natural, Blue = Resorted and Brown = Mudflat.*

### *4.5.4 Sediment organic content depth profile*

There were large differences in organic matter content profiles between the natural area and the restored and mudflat area (Figure 4.15). The upper 10 cm of the natural area was approximately an order of magnitude greater in organic content than mudflats or restored areas (Table 4.6). The organic content of sediment from the mudflat and the restored area followed very similar trajectories, both of whose content values decrease with depth (Figure 4.15). Values go from a maximum of 2.07 % and 2.45 % down to a minimum 0.38 % and 0.39 % at a depths below 50 cm for the mudflat and restored area, respectively (Table 4.6). The organic content of sediment in all areas declined from the surface to their base, the lowest content for the natural area being similar to the highest content for the other two areas.

Within areas the profiles of the mudflat and restored display similar trends, with relatively narrow standard deviations for each (Figure 4.15). The natural area displayed a larger variation in organic content values between the five cores taken, with a larger standard deviation found down the whole profile than the mudflat and restored areas (Figure 4.15).

*Table 4.6: Average percentage organic content by depth of cores from each study areas. Depth values signify the bottom of each core section, e.g. 1 cm is the value for the core section from 0 cm to 1 cm.*

| **Depth (cm)** | **Organic content (%)** | | |
|---|---|---|---|
| | Mudflat | Restored | Natural |
| 1 | 1.82 | 2.05 | 18.04 |
| 2 | 1.65 | 1.70 | 19.60 |
| 3 | 1.79 | 1.55 | 18.62 |
| 4 | 1.80 | 1.44 | 16.99 |
| 5 | 1.67 | 1.53 | 16.10 |
| 6 | 1.62 | 1.59 | 15.10 |
| 7 | 1.56 | 1.60 | 14.57 |
| 8 | 1.51 | 1.59 | 11.18 |
| 9 | 1.52 | 1.53 | 12.31 |
| 10 | 1.44 | 1.48 | 9.85 |
| 15 | 1.50 | 1.07 | 8.03 |
| 20 | 1.14 | 1.09 | 7.84 |
| 25 | 0.82 | 1.04 | 7.09 |
| 30 | 0.62 | 0.91 | 4.74 |
| 40 | 0.54 | 0.72 | 3.73 |
| 50 | 0.50 | 0.66 | 2.58 |
| >50 | 0.38 | 0.54 | 1.16 |

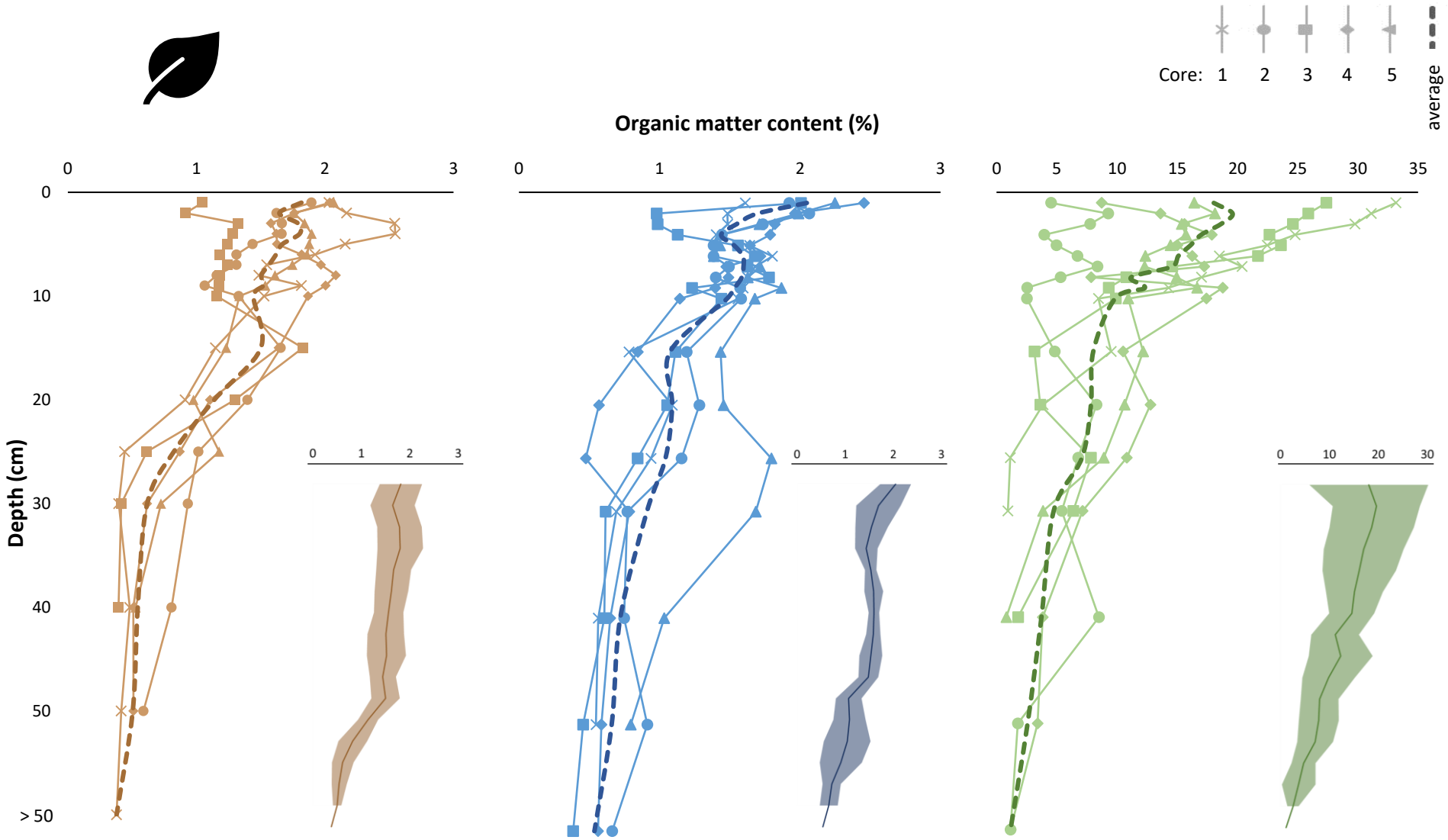


*Figure 4.15: Depth profiles of percentage organic matter content, calculated by loss-on-ignition, of each core for mudflat (brown), restored (blue) and natural (green) areas. Main plots showing individual profiles for each core (solid lines) and averaged profiles (dotted line). Note that data for the natural core (green) organic matter content is shown on a different scale. Smaller insert plots representative of average core profile (line) and one standard deviation (shaded area), not to same depth scale as main plots.*

An ANOVA of organic content of cores taken on the mudflat presented no significant difference between them ($F(4, 74) = 1.409$, $p = 0.2395$). An ANOVA of the organic content values from the cores taken within the restored area showed there were no significant differences ($F(4, 78) = 1.969$, $p = 0.1075$). An ANOVA for the organic content of cores from the natural area show there were significant differences between the cores ($F(4, 73) = 5.65$, $p = 0.0005$). A TukeysHSD show that these significant differences were found between core 2 and core 1 (diff. = 11.36, $p = 0.0003$) and core 2 and core 3 (diff. = 8.76, $p = 0.0069$).

### *4.5.5 Sediment carbon content depth profile*

Carbon content values within each area were assessed with ANOVA, which revealed significant differences between the mudflat cores - $F(4, 74) = 12.44$, $p < 0.0001$ – and natural cores - $F(4, 74) = 7.002$, $p < 0.0001$; no significant difference was found between sediment cores from the restored saltmarsh area (Figure 4.16 illustrates the standard deviation spread and actual profile data, illustrating the differences within areas). TukeysHSD indicated significant differences were predominantly between core 4 and 5 and the other three on the mudflat and for sediments of the natural saltmarsh only core 2 was significantly different from the other cores (Table 4.7). Though significant, the differences within the cores of the mudflat are relatively small, being 0.4 % on average, the natural saltmarsh sediments, however, show a larger variance across the cores (Figure 4.16).

*Table 4.7: Post-hoc TukeysHSD test of ANOVA model for the carbon content values of the five cores taken in mudflat sediments and natural saltmarsh sediments.*

| Area type | Cores | Difference | P |
|---|---|---|---|
| Mudflat | 4-1 | 0.41 | 0.0001 |
| | 5-1 | 0.53 | < 0.0001 |
| | 4-2 | 0.34 | 0.0023 |
| | 5-2 | 0.46 | < 0.0001 |
| | 5-3 | 0.29 | 0.0193 |
| Natural | 2-1 | -3.29 | 0.0104 |
| | 3-2 | 4.55 | 0.0001 |
| | 4-2 | 3.14 | 0.0101 |
| | 5-2 | 4.02 | 0.0007 |

The carbon content profiles of sediments measured in each area suggest a general trend of increasing percentage carbon from mudflat to restored to natural areas (Figure 4.16, Table 4.8). In the mudflat sediments there was little trend with depth, however, both the restored and natural area display a trend of decreasing carbon content with depth; with a marked higher percentage in near surface (~ < 10 cm) sediments (Figure 4.16). Between the areas there were three "breaks" with depth where the relationship to each other alters; from 0 – 10 cm, 10 – 40 cm and > 40 cm (Figure 4.16). ANOVA of all core carbon content data comparing the areas presented significant differences between all areas ($F(2, 237) = 53.35$, $p < 0.0001$), which explained 31 % of the variance in carbon content. For most of its depth, the natural saltmarsh holds a higher carbon content than both restored and mudflat area, until all three being to converge at 40 cm depth with values between 1.36 and 2.27 % (Table 4.8). At the surface (< 10cm) there was a marked separation between the average carbon content found in the three areas (Figure 4.16), presenting the largest differences from the whole profile; with a range of 5.87 % between mudflat and the natural area (Table 4.8). The total range in carbon content reduces with depth, between 10 and 30 cm there was a difference of 3.05 % between the restored and natural area and below 40 cm a 1.24 % difference between the mudflat and restored area (Table 4.8).

The organic carbon content profiles within and between areas displayed different relationships the organic content of those sediments (Figure 4.17), which suggests that organic matter alone does not sufficiently explain the carbon content of sediments. A Spearman's rank correlation assessment showed that that there was no significant relationship between the mudflat data ($p = 0.322$), however, there were significant correlations between the restored ($p < 0.0001$) and the natural area ($p < 0.0001$), with rho scores of 0.50 and 0.87, respectively. There is a clear difference in the relationship between organic and carbon content, specifically between the restored and natural areas (Figure 4.17), which exhibited significant correlations. The natural area has a larger organic matter content to carbon content ratio than does the restored area; whereby a greater increase in organic matter was required to result in each increase in carbon content than was needed in the restored area. This indicates a 'higher-value' organic content within the restored saltmarsh areas, from a carbon storage perspective.

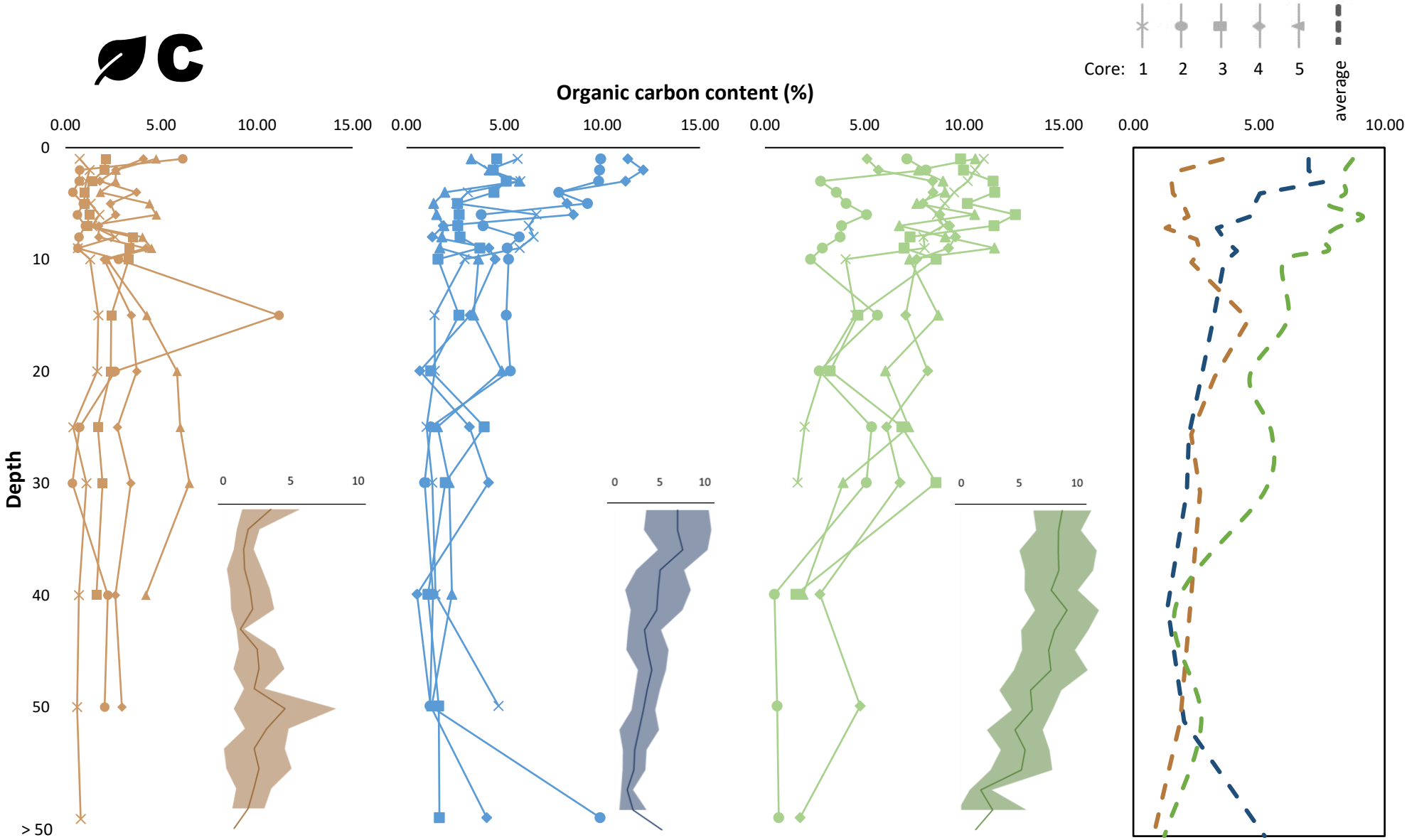


*Figure 4.16: Depth profiles of percentage organic carbon content, calculated by elemental analysis, of each core for mudflat (brown), restored (blue) and natural (green) areas. Main plots show individual profiles for each core (solid lines), and separate panel of averaged profiles (dotted line). Smaller insert plots representative of average core profile (line) and one standard deviation (shaded area), not to same depth scale as main plots.*

*Table 4.8: Average percentage organic carbon content, from LOI, by depth of cores from each study areas. Average data from 0 to 10 cm, 10 to 40 cm and > 40 cm are also shown. Depth values signify the bottom of each core section, e.g. 1 cm is the value for the core section from 0 cm to 1 cm.*

| Depth (cm) | Organic carbon content (%) | | | | | |
|---|---|---|---|---|---|---|
| | Mudflat | | Restored | | Natural | |
| 1 | 3.55 | 2.15 | 6.97 | 5.07 | 8.73 | 8.02 |
| 2 | 1.86 | | 6.97 | | 8.41 | |
| 3 | 1.52 | | 7.55 | | 8.37 | |
| 4 | 1.58 | | 5.03 | | 8.43 | |
| 5 | 1.99 | | 4.80 | | 7.77 | |
| 6 | 2.20 | | 4.65 | | 9.13 | |
| 7 | 1.29 | | 3.32 | | 8.07 | |
| 8 | 2.51 | | 3.63 | | 7.54 | |
| 9 | 2.66 | | 4.12 | | 7.74 | |
| 10 | 2.31 | | 3.61 | | 5.97 | |
| 15 | 4.59 | 3.19 | 3.18 | 2.32 | 6.13 | 5.37 |
| 20 | 3.23 | | 2.71 | | 4.63 | |
| 25 | 2.30 | | 2.21 | | 5.52 | |
| 30 | 2.65 | | 2.13 | | 5.21 | |
| 40 | 2.27 | 1.64 | 1.36 | 2.87 | 1.69 | 1.88 |
| 50 | 1.86 | | 2.02 | | 2.71 | |
| >50 | 0.80 | | 5.23 | | 1.24 | |

### *4.5.6 Carbon density profiles*

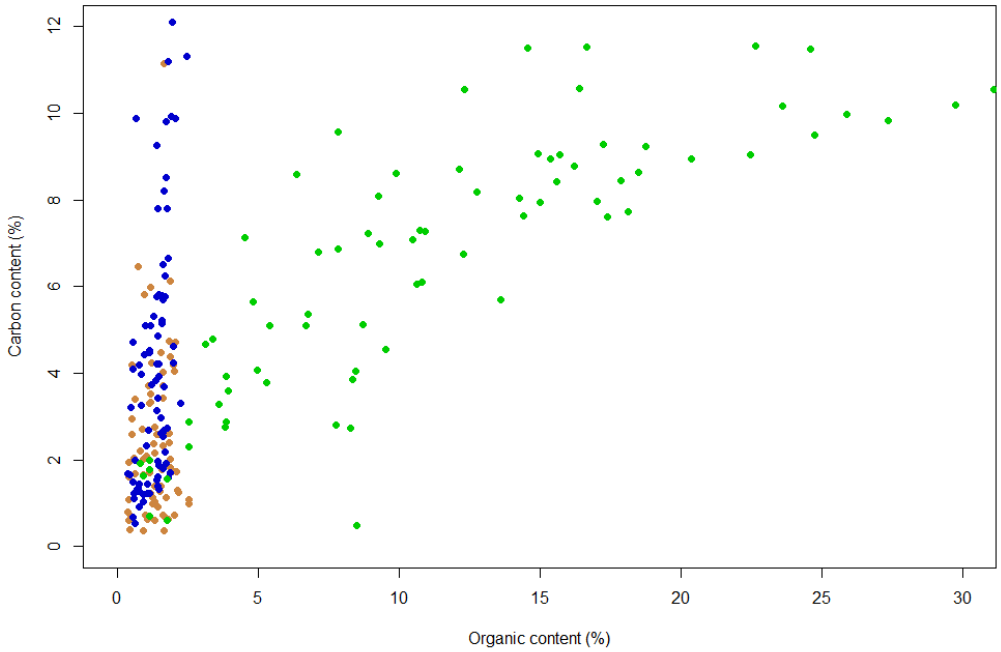


*Figure 4.17: Percentage organic content, from LOI, against percentage carbon content of all depth sections from all cores. Colours indicate areas to which the point relates; mudflat = brown, restored area = blue, and natural area = green.*

In order to calculate the amount of carbon stored within the sediments of the study area it was necessary to evaluate the sediment bulk density and carbon content (see appendices) to acquire the respective carbon density of sediments – gC/cm3. The carbon density of sediment was, on average, highest in the restored saltmarsh area (Figure 4.18). However, below 10 cm depth there was no consistent trend separating the three areas (Figure 4.18, Table 4.9). ANOVA showed that carbon density profiles from the mudflat were significantly different from one another ($F(4, 74) = 12.19$, $p < 0.0001$) and the same was found for the natural area ($F(4, 73) = 3.739$, $p = 0.008$). TukeyHSD showed the only significant difference in the natural area was between core 2 and 5 (Table 4.10), within the mudflat area there were more significant difference between the cores (Table 4.10). No significant difference was found within the restored area sediment carbon density profiles ($F(4, 78) = 1.937$, $p = 0.1125$). The general trend of average carbon density diverges from the previous relationships found between all other sediment data. At the surface rather than the natural area being skewed right or left of both the mudflat and restored area sediments, it now sits between them, with the carbon density of the restored area being greatest; a result of the greater bulk density in these sediments, even though their actual carbon content is relatively low compared with that found in the natural area.

*Table 4.9: Average carbon density (grams of carbon per $cm^3$) by depth of cores from each study areas. Average data from 0 to 10 cm, 10 to 40 cm and > 40 cm are also shown. Depth values signify the bottom of each core section, e.g. 1 cm is the value for the core section from 0 cm to 1 cm*

| **Depth (cm)** | **Carbon density ($gC/cm^3$)** | | | | | |
|---|---|---|---|---|---|---|
| | **Mudflat** | | **Restored** | | **Natural** | |
| 1 | 0.0527 | 0.0320 | 0.0934 | 0.0637 | 0.0694 | 0.0567 |
| 2 | 0.0279 | | 0.0895 | | 0.0513 | |
| 3 | 0.0209 | | 0.0972 | | 0.0536 | |
| 4 | 0.0218 | | 0.0610 | | 0.0551 | |
| 5 | 0.0275 | | 0.0678 | | 0.0489 | |
| 6 | 0.0348 | | 0.0474 | | 0.0644 | |
| 7 | 0.0200 | | 0.0434 | | 0.0564 | |
| 8 | 0.0402 | | 0.0372 | | 0.0620 | |
| 9 | 0.0400 | | 0.0514 | | 0.0565 | |
| 10 | 0.0347 | | 0.0491 | | 0.0493 | |
| 15 | 0.0691 | 0.0482 | 0.0459 | 0.0380 | 0.0516 | 0.0490 |
| 20 | 0.0497 | | 0.0400 | | 0.0382 | |
| 25 | 0.0352 | | 0.0335 | | 0.0518 | |
| 30 | 0.0389 | | 0.0325 | | 0.0547 | |
| 40 | 0.0318 | 0.0206 | 0.0213 | 0.0406 | 0.0202 | 0.0238 |
| 50 | 0.0213 | | 0.0298 | | 0.0336 | |
| >50 | 0.0086 | | 0.0707 | | 0.0176 | |

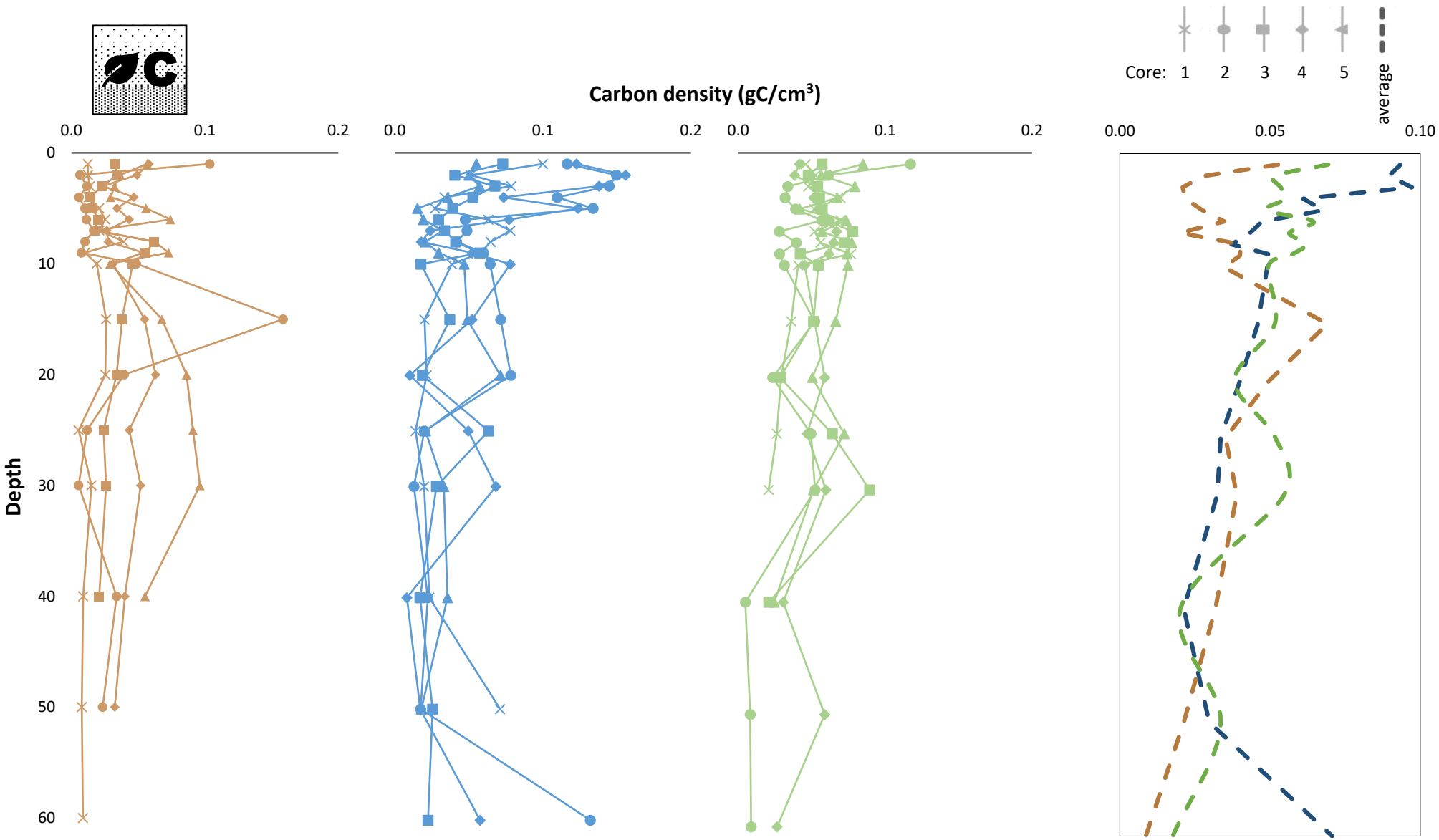


*Figure 4.18: Depth profiles of carbon density, calculated by from dry bulk density and carbon content values, of each core for mudflat (brown), restored (blue) and natural marsh (green) areas. Showing individual profiles for each core (solid lines) and separate panel of averaged profiles (dotted line).*

*Table 4.10: Post-hoc TukeysHSD test of ANOVA model for the carbon content values of the five cores taken in mudflat sediments and natural saltmarsh sediments.*

| Area type | Cores | Difference | P |
|---|---|---|---|
| Mudflat | 3-1 | 0.6462 | 0.0305 |
| | 4-1 | 1.0180 | 0.0001 |
| | 5-1 | 1.2616 | < 0.0001 |
| | 4-2 | 0.8285 | 0.0024 |
| | 5-2 | 1.0721 | 0.0001 |
| Natural | 5-2 | 0.0242 | 0.0036 |

An ANOVA comparing the carbon density profiles of each area demonstrated a significant difference ($F(2, 237) = 14.62$, $p < 0.0001$). A post-hoc TukeyHSD revealed that there was no significant difference between the natural and restored area ($p = 0.69$), however, there were significant differences between the mudflat and natural area (difference = 0.5366, $p < 0.0001$) and the mudflat and restored area (difference = 0.4494, $p < 0.0001$).

The differences between the areas was greatest in surface sediments down to 10 cm, with a difference of 0.0317 $gC/cm^3$, almost double that of the lower (mudflat) value (Table 4.9). The average carbon density differences decrease with depth, with a difference of 0.011 $gC/cm^3$ between 10 and 40 cm and a difference of 0.02 $gC/cm^3$ below 40 cm depth. ANOVA of carbon density changes with depth returned no significant difference down the cores from the mudflat ($p = 0.41$). However, there were significant differences in the carbon density profiles within the restored ($F(16, 66) = 2.639$, $p = 0.003$) and the natural areas ($F(16, 61) = 2.268$, $p = 0.011$). The changing carbon density with depth values facilitates an estimation of the carbon present (stored) in sediments, taking consideration of the changing 'value' of store with depth.

### *4.5.7 Sedimentary carbon store*

The total volumetric amount of sediment found within the study area were calculated for each depth section sampled down the collected cores. The carbon content of an 'average' core was calculated using the carbon density value of each depth section multiplied by the volume of that section; assuming sections were cut accurately and that each core was a perfect cylinder with a cross-sectional area of 43.01 $cm^2$ ($\pi * 3.72cm^2$). The volume of

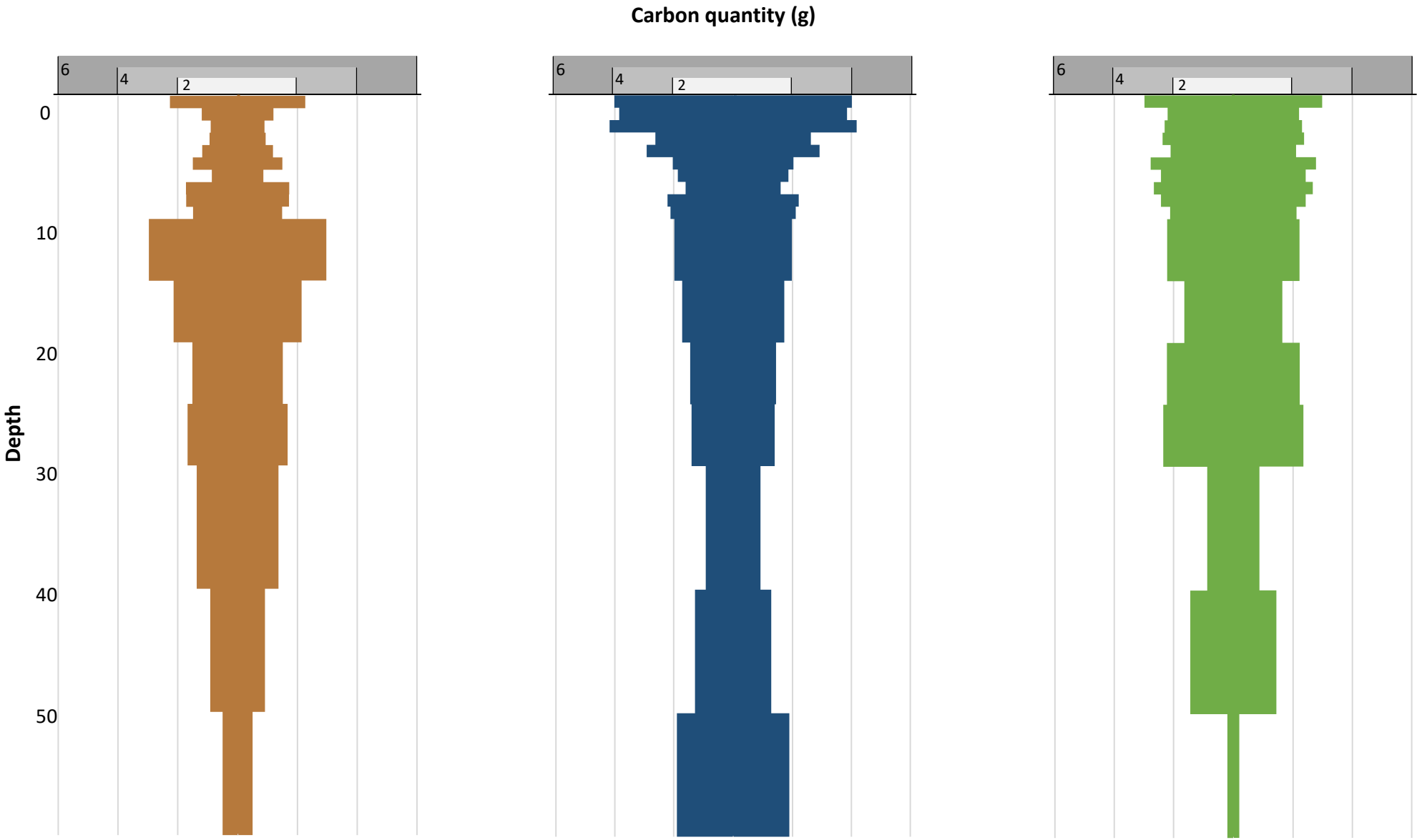


*Figure 4.19: Carbon quantities within an average core (43 cm$^2$ surface area) in each of the areas sampled; mudflat = brown, restored saltmarsh = blue, natural saltmarsh = green.*

the final depth section was an average of all cores sections in that area that reached below 50 cm. It was necessary to generate values for each depth layer measured in the case of sediments from the restored and natural areas due to the significant changes that occur with depth. Although the difference in carbon density with depth were not significant it was deemed more appropriate to generate total stock values in the same sectioned fashion to provide equally 'accurate' storage values across areas.

Total organic carbon (TOC) of sediment per core showed the restored saltmarsh area to contain the most carbon (100.99 gC), followed by the natural saltmarsh area (91.55 gC), with the mudflat containing the least (83.07 gC); based upon achieved core retrieval depths. The distribution, with depth, of this carbon differs between each area (Figure 4.19). The natural saltmarsh displays a relatively uniform distribution of carbon down to 30 cm where

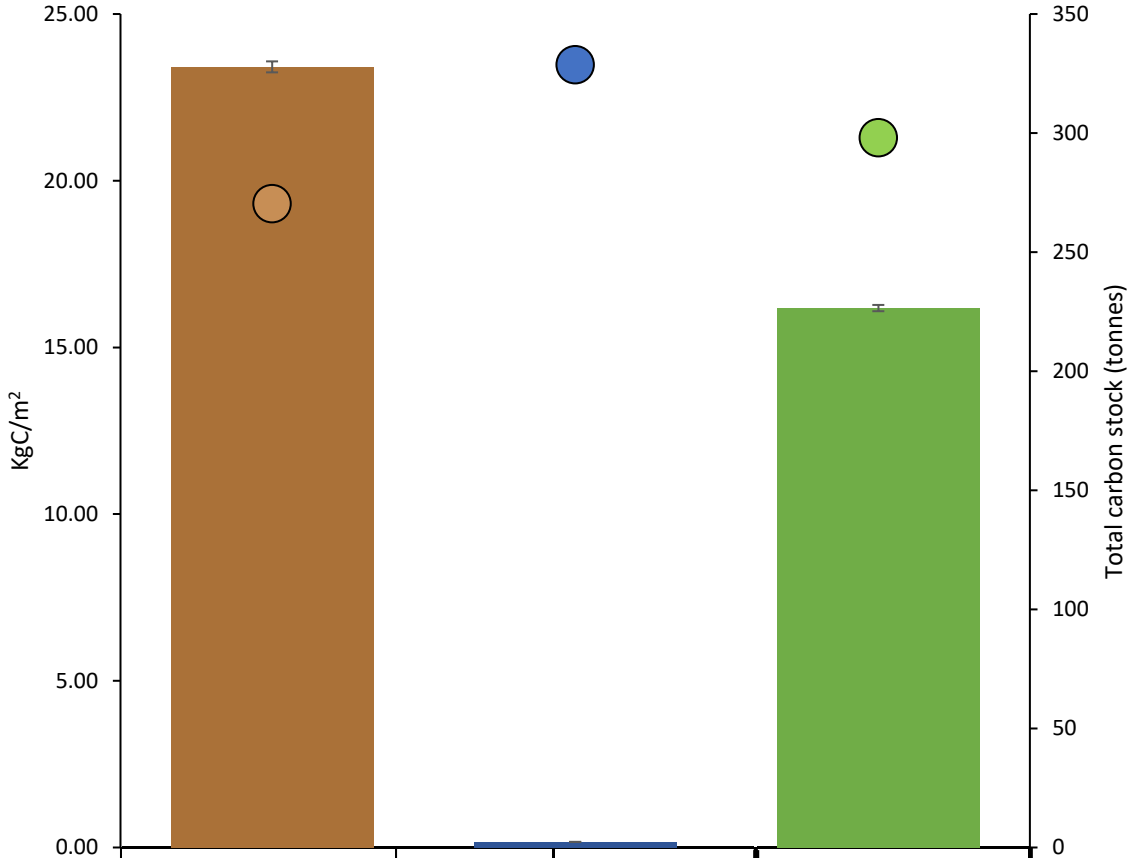


| Area | Size ($m^2$) | Kg Carbon $m^2$ | Total Carbon (Tonnes) |
|---|---|---|---|
| Mudflat | 16,972 | 19.315 | **327.81** |
| Restored | 100 | 23.481 | **2.35** |
| Natural | 10,641 | 21.287 | **226.52** |

*Figure 4.20: The carbon per metre square ($kgC/m^2$; points) and sedimentary carbon storage total (Tonnes; bars) of the studied mudflat, restored saltmarsh and natural saltmarsh areas. Size of area determined from calculated mapped extent; carbon stocks are product of down core sediment totals. Area carbon totals display standard error.*

there is a marked reduction, with a dramatic reduction below 50 cm (Figure 4.19). Both the mudflat and the restored area were less uniform in their carbon distribution with depth, being similar in trend down to 40 cm, however, below this the mudflat continues to lose carbon whereas the sediment in the restored area displays an increase.

These data were used to estimate the total sedimentary carbon store within the studied areas. A total stock was calculated using the coverage of each area used in the initial determination of core placement, the 'buffered' extent was used in the vegetated areas (Figure 4.2, Figure 4.3 & Figure 4.4). The greatest amount of carbon was found in mudflat sediments (328 ± 4.62 tC), followed by the natural saltmarsh (227 ± 2.63 tC) and then the restored area of saltmarsh (2.4 ± 0.03 tC) (Figure 4.20). However, proportionally the highest concentration of carbon is found within sediments of the restored saltmarsh, which hold over 4 kg of carbon per $m^2$ than mudflat sediments, and over 2 kg of carbon per $m^2$ than the natural saltmarsh (Figure 4.20).

*Table 4.11: Summary data of all sedimentary descriptors, showing average core values for each depth section in each area. Overall average of each descriptor in each area also shown.*

| Depth (cm) | Water content (%) | | | Bulk Density (g/cm$^3$) | | | Mean particle size (µm) | | | Median particle size (µm) | | | d10 particle size (µm) | | | Organic content (%) | | | Carbon content (%) | | |
|---|---|---|---|---|---|---|---|---|---|---|---|---|---|---|---|---|---|---|---|---|---|
| | Mudflat | Restored | Natural | Mudflat | Restored | Natural | Mudflat | Restored | Natural | Mudflat | Restored | Natural | Mudflat | Restored | Natural | Mudflat | Restored | Natural | Mudflat | Restored | Natural |
| 1 | 25.3 | 29.5 | 50.4 | 1.5 | 1.5 | 0.9 | 184.2 | 192.0 | 153.4 | 193.0 | 192.7 | 87.4 | 22.9 | 70.0 | 3.5 | 1.8 | 2.0 | 18.0 | 3.5 | 7.0 | 8.7 |
| 2 | 23.5 | 26.7 | 53.3 | 1.4 | 1.2 | 0.6 | 191.2 | 204.7 | 151.5 | 198.0 | 201.6 | 48.9 | 34.4 | 96.6 | 2.9 | 1.6 | 1.7 | 19.6 | 1.9 | 7.0 | 8.4 |
| 3 | 23.2 | 25.6 | 51.5 | 1.4 | 1.3 | 0.7 | 191.6 | 207.1 | 138.1 | 198.9 | 204.7 | 53.0 | 22.6 | 94.9 | 2.7 | 1.8 | 1.5 | 18.6 | 1.5 | 7.5 | 8.4 |
| 4 | 22.9 | 25.2 | 50.1 | 1.4 | 1.3 | 0.7 | 190.2 | 206.4 | 155.6 | 197.3 | 204.2 | 60.7 | 25.1 | 91.3 | 3.0 | 1.8 | 1.4 | 17.0 | 1.6 | 5.0 | 8.4 |
| 5 | 22.2 | 25.2 | 49.6 | 1.4 | 1.3 | 0.7 | 248.0 | 202.2 | 136.9 | 201.9 | 201.9 | 53.3 | 39.9 | 71.1 | 2.4 | 1.7 | 1.5 | 16.1 | 2.0 | 4.8 | 7.8 |
| 6 | 22.4 | 25.4 | 48.8 | 1.6 | 1.1 | 0.8 | 189.1 | 200.7 | 134.8 | 197.2 | 201.3 | 40.0 | 25.4 | 51.8 | 2.4 | 1.6 | 1.6 | 15.1 | 2.2 | 4.7 | 9.1 |
| 7 | 22.3 | 25.8 | 47.7 | 1.6 | 1.3 | 0.7 | 192.7 | 198.5 | 146.4 | 199.2 | 201.0 | 33.7 | 28.6 | 41.2 | 2.3 | 1.6 | 1.6 | 14.6 | 1.3 | 3.3 | 8.1 |
| 8 | 22.0 | 26.0 | 45.2 | 1.6 | 1.1 | 0.9 | 209.3 | 200.7 | 146.8 | 200.7 | 202.0 | 41.0 | 39.5 | 46.9 | 2.3 | 1.5 | 1.6 | 11.2 | 2.5 | 3.6 | 7.5 |
| 9 | 21.8 | 25.7 | 43.5 | 1.5 | 1.3 | 0.8 | 194.7 | 199.0 | 174.0 | 200.4 | 201.5 | 60.2 | 35.6 | 34.6 | 2.5 | 1.5 | 1.5 | 12.3 | 2.7 | 4.1 | 7.7 |
| 10 | 21.6 | 24.5 | 39.9 | 1.5 | 1.3 | 0.9 | 225.3 | 219.5 | 150.8 | 202.0 | 203.1 | 46.3 | 37.9 | 36.5 | 2.2 | 1.4 | 1.5 | 9.8 | 2.3 | 3.6 | 6.0 |
| 15 | 21.7 | 22.8 | 40.9 | 1.5 | 1.4 | 0.9 | 205.6 | 208.9 | 125.4 | 208.3 | 207.8 | 81.3 | 39.8 | 60.3 | 3.3 | 1.5 | 1.1 | 8.0 | 4.6 | 3.2 | 6.1 |
| 20 | 21.3 | 22.4 | 42.0 | 1.5 | 1.5 | 0.9 | 220.0 | 211.2 | 116.7 | 215.7 | 203.2 | 32.2 | 103.3 | 83.3 | 2.4 | 1.1 | 1.1 | 7.8 | 3.2 | 2.7 | 4.6 |
| 25 | 21.1 | 22.1 | 36.2 | 1.5 | 1.5 | 1.0 | 220.4 | 205.2 | 121.7 | 214.1 | 198.5 | 61.9 | 127.6 | 92.4 | 3.4 | 0.8 | 1.0 | 7.1 | 2.3 | 2.2 | 5.5 |
| 30 | 20.7 | 22.0 | 31.6 | 1.4 | 1.5 | 1.1 | 221.1 | 207.2 | 131.3 | 213.1 | 202.4 | 95.3 | 138.8 | 83.3 | 6.7 | 0.6 | 0.9 | 4.7 | 2.7 | 2.1 | 5.2 |
| 40 | 21.8 | 21.0 | 28.8 | 1.4 | 1.6 | 1.2 | 219.1 | 224.0 | 172.0 | 212.1 | 217.1 | 152.4 | 138.0 | 106.4 | 40.5 | 0.5 | 0.7 | 3.7 | 2.3 | 1.4 | 1.7 |
| 50 | 20.8 | 21.0 | 27.8 | 1.2 | 1.5 | 1.3 | 225.7 | 232.1 | 148.9 | 216.0 | 222.4 | 152.6 | 138.7 | 131.7 | 6.3 | 0.5 | 0.7 | 2.6 | 1.9 | 2.0 | 2.7 |
| > 50 | 20.9 | 21.3 | 21.4 | 1.1 | 1.4 | 1.4 | 245.1 | 247.3 | 218.0 | 235.5 | 234.3 | 212.0 | 150.7 | 142.2 | 36.2 | 0.4 | 0.5 | 1.2 | 0.8 | 5.2 | 1.2 |
| **AVERAGE** | **22.1** | **24.2** | **41.7** | **1.4** | **1.4** | **0.9** | **210.2** | **209.8** | **148.4** | **206.1** | **205.9** | **77.2** | **67.6** | **78.5** | **7.4** | **1.3** | **1.3** | **11.0** | **2.3** | **4.1** | **6.3** |

## 4.6 Discussion of sediment profiles

The study of sediment cores taken from three areas of the estuary indicate that differing factors influence the characteristics of their sediments (Table 4.11), and ultimately are shown to enhance the carbon storage value within a restored *B. maritimus* above both its 'original' mudflat state and its natural saltmarsh comparator.

There was a consistent trend which separated the sediment characteristics of the natural saltmarsh area from the other sediments; excluding profiles of carbon density. Serving to illustrate the different environmental factors acting upon these areas, perhaps most influentially being their respective elevations. The restored area and mudflat lie at similar elevations, between approximately 1.2 m and 1.5 m above OD, thus are exposed to similar tidal and wave influence, whereas the natural saltmarsh sits higher at an average of 2.1 m above OD, dramatically altering the tidal and wave exposure. This alters factors such as sediment input, erosion potential, and immersion period, which combine with biotic factors such as vegetative structures influence the resulting sediment bed dynamics.

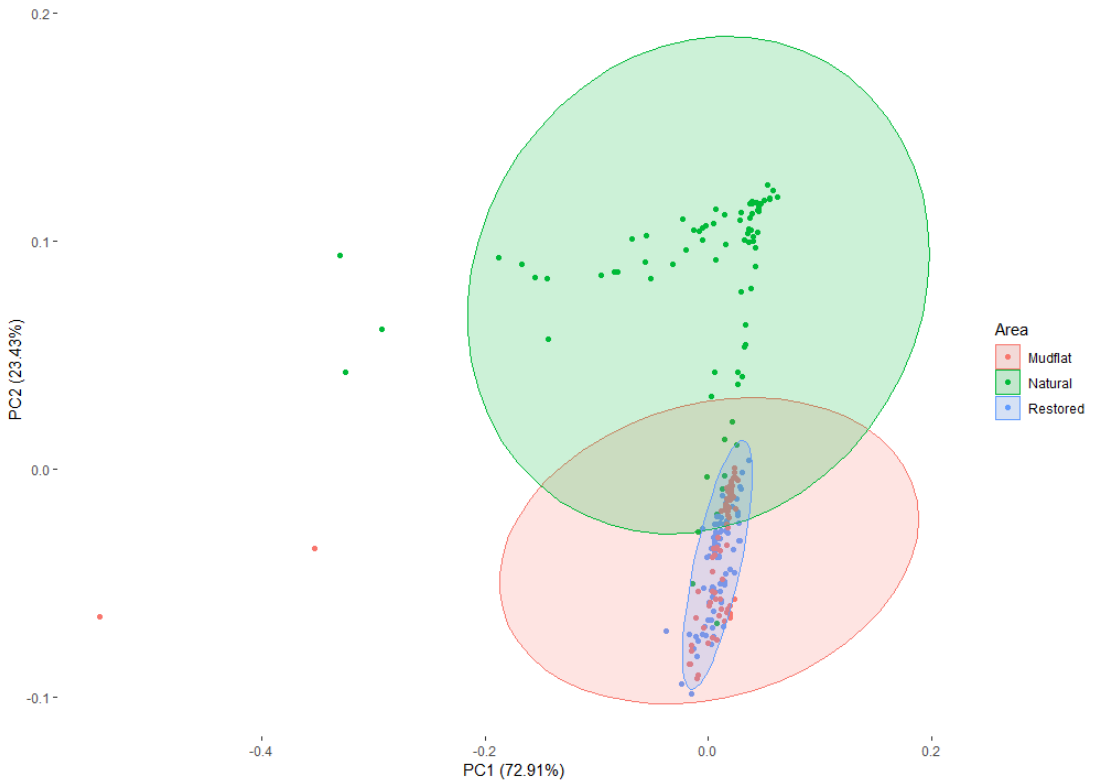


*Figure 4.21: PCA cluster plot using water content, bulk density, organic content, mean particle size, median particle size, particle d10 size and d90 size sediment descriptors of all sediments for each area. Cluster ellipses showing 0.95 confidence level.*

Each sites situation results in their sedimentary differentiation, which drives the separation of the natural saltmarsh sediments from the others, but also suggests that sediments of the restored area diverge from their mudflat reference point; being consistently skewed from the profiles of the mudflat. However, principle component analysis of all sedimentary descriptors (i.e. water content, bulk density, organic content, mean particle size, median particle size, particle d10 size and d90 size) indicates that the sediment characteristics of mudflat and restored area are at least 95 % similar (Figure 4.21). The similarity described by the PCA is likely reflective of the trend for sediment descriptor values to converge, relatively rapidly, with depth, perhaps highlighting the enhanced influence of vegetation to surface sediments.

Water content and bulk density profiles of the sediments indicate that the restored saltmarsh area still reflects the character of bare mudflat prior to the direct planting of *B. maritimus*; having, on average, equal bulk densities and a 2 % difference in water content (Table 4.11). The natural saltmarsh had significantly different water content and bulk density profiles. The similarity of restored and mudflat sediments suggests the process which alters these characteristics are relatively slow or perhaps that the presence of *B. maritimus* vegetation does not alter these factors to the same extent as a complex community of *P. maritima*. However, from a carbon sequestration and storage perspective the higher bulk density values in the restored area are an important feature in determined its carbon 'value' (Table 4.11).

Assessment of particle size composition across the areas suggests that, again, mudflat and restored saltmarsh sediments were similarly composed; having near equal mean and median values down their profiles (Table 4.11). There was a difference in d10 values in the surface sediments of these areas, which indicate that the mudflat is more dominated by finer particles (smaller d10 value). Though their d10 values become more similar with depth, the restored area sediments remain more dominated by larger particle sizes than the mudflat, grouping strongly towards a sand-dominated sediment (Figure 4.14). It would be expected that the presence of vegetation would encourage the capture and retention of fine particles due to the retardation of flow, however this is not reflected in this study. The particle size composition of the natural saltmarsh area is distinct from the other areas, being strongly dominated by finer particle; illustrated through its mean, median and d10 values (Table 4.11); as would be expected due to the abundant vegetation of the natural marsh.

The organic matter content of sediment profiles exhibited similar trends between the three areas as shown with the previously discussed characteristics. On average sediment from the mudflat and restored area have the same percentage of organic matter down their cores (Table 4.11). The organic content of the natural saltmarsh sediment is nearly an order of magnitude greater than the other areas and remains greater with depth; where only below 50 cm is a smaller value found than in the entirety of the other profiles (Table 4.11). Organic content values were considered important indictors for carbon content of sediments.

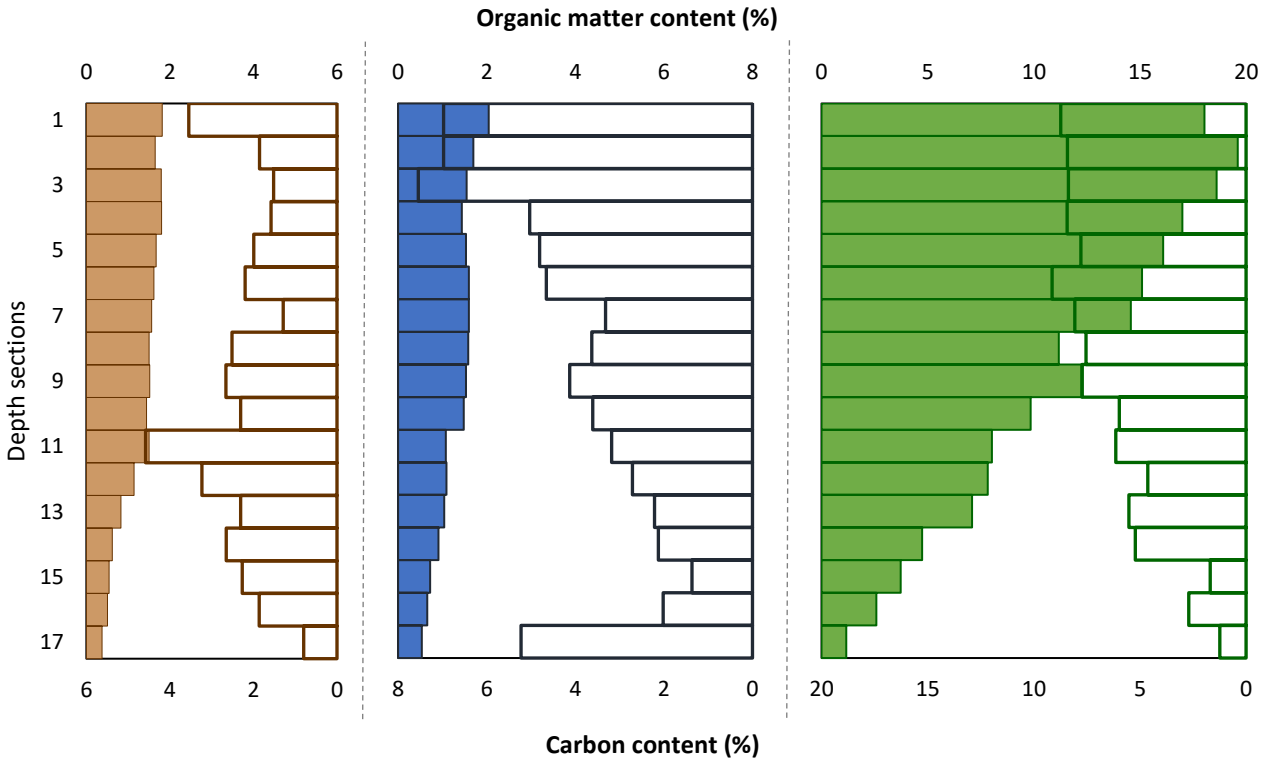


*Figure 4.22: Average percentage organic matter content (solid) and average percentage carbon content (non-filled) recorded from fives cores in each area down the sediment profile (depth sections represent 1 to 10 are 1cm each, 11 to 14 are 5cm each, 15 and 16 are 10cm each, 17 dependent on penetration depth). Average values taken from all cores. Colours indicate area type; mudflat = brown, restored saltmarsh = blue, natural saltmarsh = green. Scales differ between areas.*

However, the carbon content of sediments did not display the same trend as determined by organic matter content (Figure 4.22), exhibiting a different relationship between the areas than previously found. The amount of carbon within sediments previously been explained as being inversely proportional to bulk density (Avnimelech et al., 2001) or predicted through particle size composition data (Kelleway et al., 2016). In this study such predictors were not clearly available; for example particle size composition was shown to be extremely similar between the mudflat and restored area (Figure 4.11 to Figure 4.14), and other descriptors lacked significant differences between them. However, those sediments

held significantly different quantities of carbon, as such it would be difficult to apply an 'easy analyses' of sediment and accurately determine carbon content of those sediments. Generally, the process of saltmarsh development through the accumulation of sediments is considered to play an important role in their capacity to serve as high-value carbon sinks; through the constant burial of organic (carbon) matter. As was expected (due to its higher organic content) the older, higher-elevation natural saltmarsh exhibited the highest average carbon content profiles; being greatest in surface sediments. However, this higher carbon content was not as dissimilar to the restored saltmarsh sediments as expected (Figure 4.22), based on their organic matter contents (Figure 4.16 & Table 4.11). At the surface (< 10 cm) there was an average difference of 13.6 % in organic matter content between the natural and restored area, dropping to 3 % when assessing their respective carbon contents. This appears to be driven by contrasting organic matter to carbon content relationships between the areas. The sediment in the restored area returned a higher percentage carbon content than organic matter in all instances (i.e. all cores at all depths), in general the natural area showed the opposite relationship (Figure 4.22). This trend is possibly a product of the restored areas placement in the tidal frame, whereby the greater influence of tidal borne inorganic sediment serves to 'dilute' the organic matter (Chmura, 2013). This then influences the results obtained during analysis, with 'bulk' organic matter values (generated from a larger sample, and so more influenced by the possible 'dilution' factor) compared against 'fine' carbon content values (obtained from very small samples of sediment and so reducing the proportional influence of dilution). However, there was a clear indication that the organic matter found within restored area sediments were 'higher value' in terms of carbon storage than are those of the natural saltmarsh. This enhanced carbon content plays a key role in determining the TOC stock of the restored area versus the natural saltmarsh and the bare mudflat.

The sedimentary carbon density value was used to generate TOC stocks estimates for each of the areas. As was found with carbon content profiles, the relationship of average carbon densities between the areas differs from that of the other characteristics. The balance of bulk density and carbon content of the sediments serves to bring the average profiles of carbon density into closer alignment (Figure 4.18). This interaction is crucial to the resultant TOC value of each area, serving to move the restored area from 'second' to the natural area in terms of sedimentary carbon content to having the highest carbon quantity per unit area of the three areas. Again, there was a general trend of reducing carbon density with depth as reflected in the organic and carbon content profiles. The restored area profile displays the same increase at the base of the core, a product of the same increase in carbon content

shown at this depth (Figure 4.16). This increase at depths below 40 cm serve to increase the value of restored saltmarsh area, whereas in both the natural and mudflat sediments, display the expected decrease with depth (Bai et al., 2016; Kelleway et al., 2016), and their 'value' decreases.

Generally, carbon densities of sediments in this study were greater than other reported figures within saltmarsh systems, such as the data of Chmura et al (2003) giving an average $0.039 \pm 0.003$ g $cm^3$. The greater density in this system could be a product of factors such as its cool temperate climate reducing organic matter breakdown (Chmura et al., 2003; Kirwan and Blum, 2011). The higher carbon density recorded in these sediments than noted by other studies perhaps offers greater opportunity for carbon storage driven saltmarsh conservation activates in the future within Scotland.

Carbon density values of mudflat sediments were significantly less than those of the vegetated areas studied. Furthermore, their carbon density values were shown to be highly variable, where there were significant differences between the profiles of all the cores within the area. The vegetated areas were more conserved, with no significant difference found within the restored area and a significant difference only between two cores of the natural area. This higher variation in carbon density makes the mudflat data potentially less robust when calculating a carbon stock, than for those of the more conserved vegetated areas.

These data were finally used to provide an estimate of the total amount of organic carbon presently stored within the sediments of the studied areas in the Eden Estuary. This suggested a grand total of $556.7 \pm 2.1$ tC located within the limits of the Kincaple marshes area (delineated in Figure 4.1), a total area of 9,238 $m^2$. Broken down by area type there was $327.8 \pm 4.62$ tC in mudflat sediment, $2.35 \pm 0.03$ tC in restored saltmarsh sediments and $226.5 \pm 2.63$ tC in natural saltmarsh sediment (Figure 4.23). Normalised by area, allowing for direct comparison of each area, gave values of 19.3 $kgC/m^2$ for the mudflat, 23.5 $kgC/m^2$ for the restored saltmarsh and 21.3 $kgC/m^2$ for the natural sites (Figure 4.23).

The 'additionality' of the restored saltmarsh area to carbon storage was calculated with the assumption that prior to conservation action, the sediment aligned with the current situation found on the mudflat. Following this assumption, if no restoration had existed there would be an estimated 1.93 tC stored, presently, with restoration, there is 2.35 tC stored in the sediment, an extra 0.4 tC or a 22 % increase. This modest increase in carbon stored is the equivalent to 1.5 $tCO_2$ or driving over 5,000 miles in a typical car achieving 40 mpg.

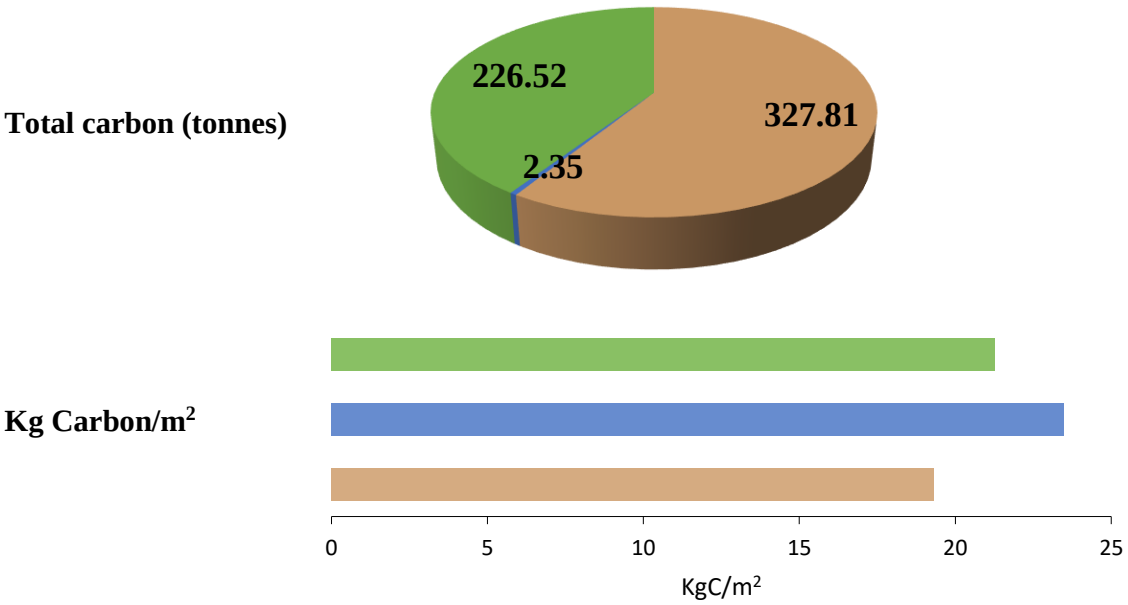


*Figure 4.23: Top shows total carbon storage (tonnes) and bottom is relative carbon storage (per $m^2$) of the three area types studied. Colours indicate area type; mudflat = brown, restored saltmarsh = blue, natural saltmarsh = green.*

Although there was little discernible difference between the sediments of these two areas, the results show opposing carbon values, with the mudflat being of lowest value and the restored saltmarsh being the most valuable carbon storage. A comparison of the restored saltmarsh carbon stock to that of the natural saltmarsh area indicates that more carbon is currently stored within the recently restored vegetation. The driver of this functionality of the restored site is likely due to the differing tidal influence. The restored area currently sits lower in the tidal frame, so having greater potential to accrete organic rich allochthonous material which could be more influential than autochthonous production (Van de Broek et al., 2018). However, this does not suggest that the restored area will remain 'more valuable'. Currently this area is dynamically adjusting, expanding and accreting towards some, yet undefined, equilibrium state. Typically, this will entail its movement vertically within the tidal frame as the interaction between water, sediment and vegetation act to continually accrete sediments; which could in the future mirror the studied natural marsh situation.

There is strong potential for the lateral expansion of the planted *B. maritimus* marsh; which has already expanded 4,700 % since planting, in the specific area studied here. The continued expansion and subsequent additionality afforded beyond the current mudflat mode could offer large carbon storage benefits. If we assume that expansion will continue within the current ecological limits governed by the tide; taking the length of 'available'

habitat as the length of the current natural marsh extent (640 m) and the width as the current width of the restored area (11 m), giving a potential expansion area of 7,040 $m^2$. Applying calculated carbon storage value to this area would result in a total of 165.3 tC, an additional 29 tC (106.4 $tCO_2e$) above the 'business as usual' situation upon reaching the equivalent state as the studied restoration, which had been growing for 16 years when sampled. It is likely that it takes shorter time period to reach the measured storage size, as much of the present resorted area is a product of expansion and so younger than 16 years old. This assumes that development of the new expansion follows that of the area studied, further, this does not consider probably continued future sequestration which could occur in within these new vegetated areas. Therefore, although at present the carbon store of restored areas are small, they have the potential to store substantial amounts in their sediments as their extent coverage increases.

# Chapter 5: General discussion

The research in the preceding chapters have considered the vegetative components, sedimentary dynamic behaviour and the characteristics of buried sediments in natural and restored areas of the Eden Estuary. Ultimately these data help evaluate the carbon sequestration and storage capacity of each area and, specifically, quantified the influence that restoration activities have on this capacity. These data are now compiled to assess the total carbon sequestration and storage potential of different areas types in the Eden Estuary and assess the possible 'value' of these ecosystem service benefits.

## 5.1 Carbon sequestration rates

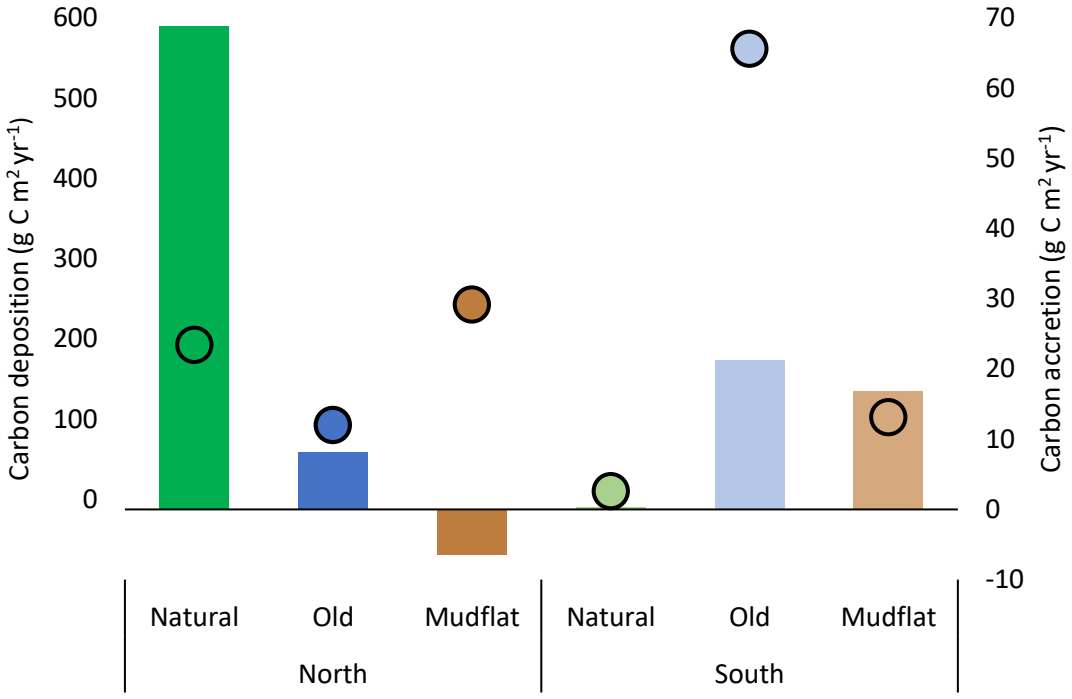


*Figure 5.1: Predicted sedimentary carbon deposition rate (points) and actual carbon accretion rate (bars) rates per m$^2$ averaged over the year period of the study.*

The carbon sequestration rates measured within the Eden Estuary are predominantly associated with sediment dynamics. There was a significant cyclic component of vegetative carbon, whose fate is unknown and is possibly transported offshore. The rates of carbon sequestration were only considered in the natural vegetation stands, mudflat and successfully established areas of restoration (i.e. old restored areas). The variation in success and fragmentation displayed by areas of young restoration meant they did not provide representative data of a re-vegetated area. This section focuses on the possible

benefits realised from restoration activities which have successfully produced healthy stands of saltmarsh vegetation. The issues around success rate of restoration are considered apart from this and therefore data from the young restored areas, which displayed limited success, are not used here.

### *5.1.1 Sedimentary carbon sequestration*

The rates of, and relationships between, sedimentary carbon deposition and accretion were shown to vary (Figure 5.1). The efficiency of retaining carbon deposits was highest in the natural vegetated area of *B. maritimus* (36 %). On average the restored areas of vegetation displayed a 6 % efficiency at retaining carbon deposits, greater than that displayed by the natural area of *P. maritima* (3 %). The rate of carbon accretion was shown to be greatest in the natural area of *B. maritimus* (Table 5.1). The rates of accretion were relatively high in restored areas, being greater than their adjacent mudflat areas on each shore, thus offering higher value per meter square than if no restoration had occurred. However, all measured carbon accretion rates sit at the lower end of other reported data which span from 18 to 1713 gC $m^{-2}$ $yr^{-1}$ (Chmura et al., 2003; Duarte et al., 2005; McLeod et al., 2011).

*Table 5.1: Yearly sedimentary carbon accretion rates*

| Shore | Area type | Carbon accretion rate (gC $m^2$ yr) | Total carbon accretion (kg per year) |
|---|---|---|---|
| North | Natural | 68.8 | 241.0 |
| | Old Restored | 8.1 | 0.8 |
| | Mudflat | -6.6 | -63.4 |
| South | Natural | 0.3 | 5.0 |
| | Old Restored | 21.2 | 7.8 |
| | Mudflat | 16.9 | 286.9 |

The study demonstrated there were significant cyclic variation in vegetative components across the area types studied. This component could play an important role in carbon sequestration into the saltmarsh ecosystem through enhanced fixing of $CO_2$ and subsequent incorporation into their sediments, however this organic material may be transported elsewhere (Cai, 2011). It is therefore difficult to quantify the value of this cyclic component, as its fate it unknown, but it may represent possible additional beneficial carbon sequestration; leading to storage in the estuarine pool or elsewhere. This benefit depends on

both the destination of the material and how labile this material is likely to be, and this would be worth further investigation.

### *5.1.2 Vegetation carbon sequestration*

There was a much greater cyclic component associated with *B. maritimus* vegetation, be that in the natural or restored stands (Figure 5.2). The restored areas exhibited similar 'cyclic rates', with 56 % and 64 % of the total vegetation on the north and south shore

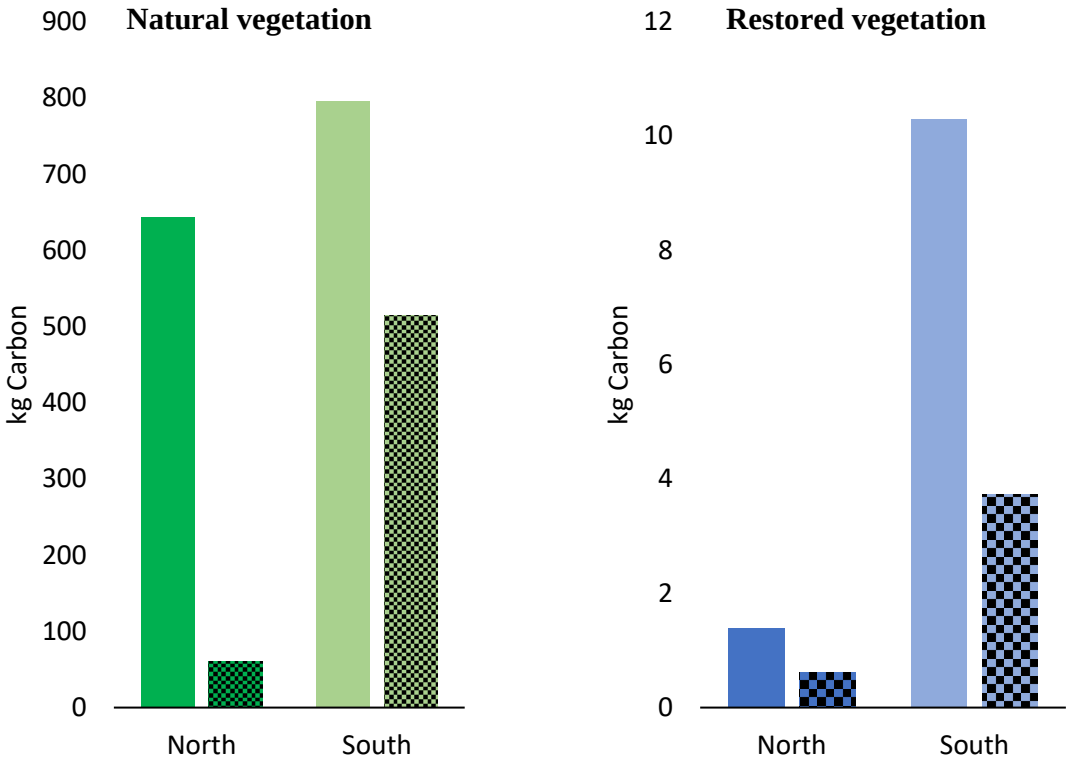


*Figure 5.2: Total amount of carbon present in vegetation of the studied areas in winter (checked) and summer (solid). Left panel showing data from natural areas, B. maritimus on the north shore and P. maritima on the south shore. Right panel show data for restored areas of B. maritimus.*

respectively being made up of a cyclic component; or those parts which are not retained perpetually by vegetation. Such large differences between the seasons are important to consider from a carbon sequestration valuation perspective.

The information available from this study only allows the determination of how much extra carbon is present within restored vegetation which is retained during winter, it is not possible to determine if the extra growth during summer contributes to broader-site scale increases in carbon sequestration and storage. However, it is possible to determine the rate of carbon sequestration occurring in vegetated areas. Within the two restored areas there was an average yearly sequestration of 12.2 $gC/m^2$, this returns a total rate of an additional

4.89 kgC cycling per year inside restored vegetation, above that which would occur in its previous bare mudflat condition.

## 5.2 Carbon storage

The current total carbon storage in each area studied in the Eden Estuary is defined as the current amount of carbon presently stored in each area. It is a product of that stored in sediments down to the depth sampled through core sampling (typically between 50 and 70 cm deep), and that found in retained vegetation throughout the year, as revealed though remote-sensing analysis (Figure 5.3).

The carbon benefit of restoration reflects successfully established areas only (i.e. old restored areas), the variation in success and fragmentation displayed by areas of young restoration meant they did not provide representative data of a re-vegetated area. Total carbon values were calculated using the winter values (content and extent) for vegetation

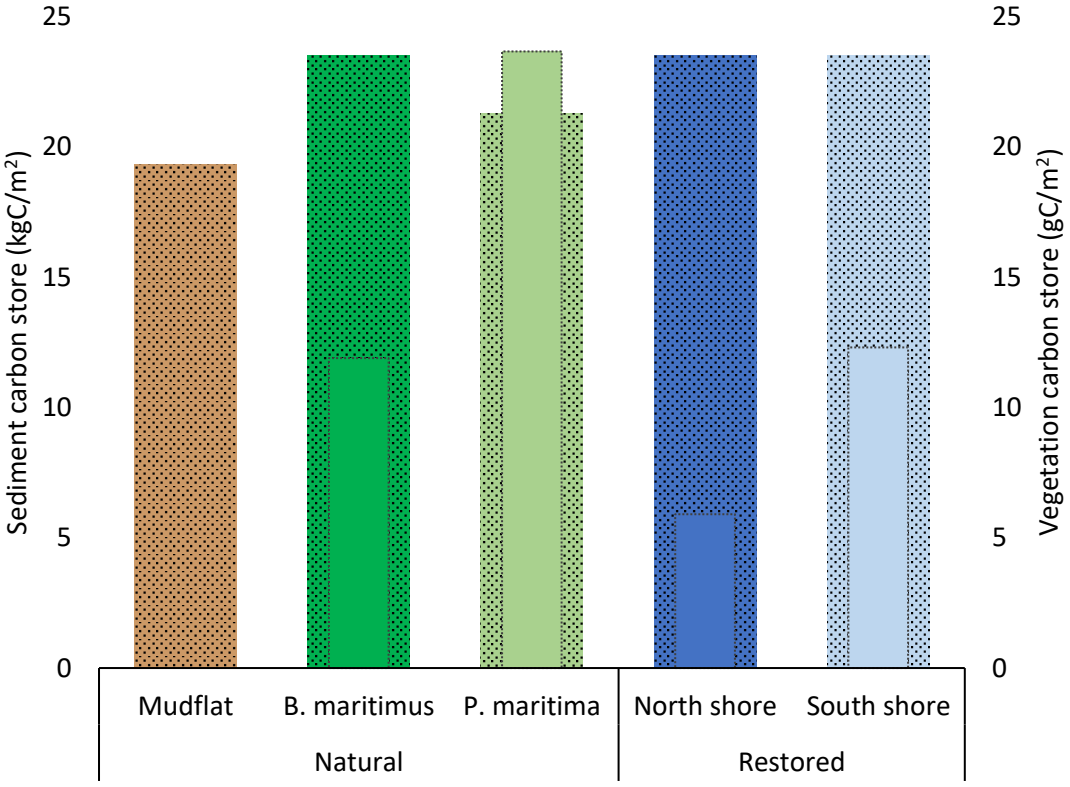


*Figure 5.3: Sedimentary and vegetative carbon storage capacity of different area types in the Eden Estuary. Sediment store is the dotted section, vegetation is solid. Vegetation values calculated from winter state.*

total stock and the 3 m buffered extent of each area type for sedimentary storage. This represents the relevant area over which vegetation influence is likely taking place.

The relative carbon store of natural vegetated areas of *P. maritima* was the greatest (Figure 5.3). Restored stands of *B. maritimus* displayed similarity to the natural area from which they were harvested, with the example on the south shore being slightly greater than its natural counterpart; 35.8 gC/m$^2$ against the 35.4 gC/m$^2$ of the natural extent. The average total carbon storage of restored sites was 32.6 gC/m$^2$.

*Table 5.2: Carbon stock values of each area investigated on the Eden Estuary.*

| Area type | | Sediment store (tC) | Vegetation store (kgC) | TOTAL STORE (tC) | |
|---|---|---|---|---|---|
| Natural | Mudflat | 514.8 | 0.0 | | **514.8** |
| | *B. maritimus* | 71.2 | 60.5 | | **71.2** |
| | *P. maritima* | 226.5 | 514.8 | | **227** |
| Restored *B. maritimus* | North shore | 0.5 | 0.6 | 0.47 | **2.8** |
| | South shore | 2.3 | 3.7 | 2.35 | |

The total amount of carbon stored within the areas studied on the Eden estuary was 816 tonnes (Table 5.2). The total amount of carbon currently stored in sites of restoration was small compared to that found elsewhere (Table 5.2). This is due to their small extent, making up just 0.3 % of the area studied. The current extent of restored areas (120 m$^2$) has currently resulted in an additional carbon storage of 504 kgC since its initial planting, attributed to its vegetation and sediments; assuming that prior to restoration activities the sediments of those areas reflected that found on the mudflat area.

These data indicate that through restoration, the unit area carbon storage value of the Eden Estuary is increased. Though at present the value is relatively low when taken within the entire intertidal system, it is likely that the restored stands of vegetation will continue to expand, as they have done previously. It is predicated that this will lead to the continuation of additional carbon storage over a larger extent, thus increasing the value of the initially small restoration project.

## 5.3 Blue carbon value

The monetary value of the carbon sequestration and storage capacity of restoration on the Eden Estuary can be applied to the relative amount of effective carbon-dioxide ($CO_2e$). This is obtained through the application of a conversion factor of 3.67. Being the weight ratio between the atomic mass of carbon (12) and that of carbon dioxide (12 + (oxygen) 16 + 16 = 44). The current UK Carbon Floor Price (CFP, January 2019) value of £18 $tCO_2$ was used to monetise the carbon benefits in the Eden Estuary, though it is expected this price will rise to £30 $tCO_2$ by 2030 (Hirst and Keep, 2018).

The average rate of sequestration in sediments of the restored areas were between 8.1 gC $m^2$ $yr^{-1}$ and 21.2 gC $m^2$ $yr^{-1}$; or between 29.7 gCO2e $m^2$ $yr^{-1}$ and 77.8 gCO2e $m^2$ $yr^{-1}$. At their present extent this returned a total of 8.6 kgC $yr^{-1}$, or 31.6 $kgCO_2e$ $yr^{-1}$. This has a value of between £0.15 and £0.57 per year.

Current additional carbon storage capacity is taken as the difference in the total amount of carbon stored in vegetation and sediments of restored (2.8 tC) and what would be expected if they had remained as mudflat (2.3 tC). This gave an additional 0.5 tC stored over the present life of the restored sites, or 1.8 tCO2e. Appling the CFP this additional portion of carbon sink capacity is valued at £32.40.

The values relating to current restoration activities are low, and likely to be of limited use from a subsidisation perspective. This is perhaps due to their small area and at present relatively low carbon sequestration and storage capacity. However, their rate of expansion has been rapid, especially on the south shore. Considering the possible future extent of *B. maritimus* as fronting the current *P. maritima* marsh, being an area of 7,040 $m^2$ (640 m long and 11 m wide, the current width of the restored vegetation), could result in an additional 29 tC stored in sediment. At such a point it value would be £1,916, being 106 tCO2e. Furthermore, their value could be considered from an avoided emissions perspective. For example, it could be assumed they do, or will, convey erosion protection to the large carbon stock of the *P. maritima* marsh thus avoided the possible removal of up to 227 tC, or 833 tCO2e, which is valued at £14,996.

## 5.4 Subsidisation possibility

Much of the saltmarsh restoration activity in the Eden Estuary has been driven by Dr C. Maynard and a degree of reliance upon volunteers; from the general public, family and

friends, and from stakeholders, such as the RAF/Army, Links Trust golf course, and Fife Coast and Countryside. As such costs have, out of necessity, have been kept relatively low. However, such a model is not necessarily sustainable, especially given the type of work required. Where it is often time-restrictive (due to tide), physical, wet, cold and generally dirty; such characteristics are not always conducive to gathering the support of volunteers.

Currently costs associated with restoration activities on the Eden Estuary are difficult to estimate. As the figure must consider capital value of investment in equipment and staff time on the project through-out a number of years, it also relies on assigning a 'value in kind' for the time given by volunteers. Furthermore, the time given by vested interest stakeholders, could be deemed to be 'investing' their time to possibly 'buying' them something; be that increased coastal protection from saltmarshes reducing sea-defence maintenance costs or the requirement to enhance the habitats and ecosystem of the estuary in general. This effective return on their volunteered time makes it difficult to accurately quantify that time cost.

Presently, research is being carried out to improve the feasibility and robustness of restoration activities through the development of a 'supply chain', which will grow planting stock from estuarine vegetation. This production of large stock quantities, if successful, will reduce the labour cost of any given planting campaign and, further, may serve as an alternative revenue stream through the provision of vegetation to other such projects beyond the Eden Estuary. Ultimately it is hoped this will reduce the net cost of saltmarsh restoration, thus increasing the proportional subsidisation worth of *Blue carbon* payments.

It has been shown that there is limited value to be gained through the sale of the addition carbon sequestration and storage benefit afforded by saltmarsh restoration actives directly at the current scale, but possible large values through indirect emission avoidance roles. However, the rate at which this return is paid could reduce its effectiveness/usefulness, especially on the typically 'small scale' project structure examined here, with perhaps minimal capital funds for initial investment. This could be overcome with upfront investment in future increased natural capital value; however, this adds to the, possibly already perceived, risks of such payments. There is a requirement to understand and address the 'permanence' of the sale of the carbon being (or to be) sequestered and stored (Chmura, 2013). This could be addressed through a discounting approach, which reduces the amount (value) or carbon which is expected to be sequestered during a project to minimise the likelihood of not meeting those targets.

## 5.5 Issues to consider from this study

### *5.5.1 Vegetation cycle*

The degree to which the stock of carbon found within vegetation was shown to vary between vegetation types, where *B. maritimus* displayed a far greater fluctuation between its summer and winter structures. This seasonal cycle is to be expected, however, the degree to which carbon is retained throughout the year is important for determining the value of its store. Furthermore, although the data applied relatively specific allometric scaling relationships from examples within the estuary, it would be advisable to improve such estimates through the application of site and season specific conversion factors. This will facilitate accurate vegetative carbon accounting for that stored and that cycling within the system.

### *5.5.2 Remote sensing application*

The data gathered through Terrestrial Laser Scanning (TLS) proved to be relatively effective to enable the extraction of vegetation structure information across the entire study area. However, a few issues arose during deployment; namely the effort required to gather data, weather sensitivity, processing time and missing data. Firstly, the acquisition of TLS data is labour intensive, and progress was slow, which restricts the effective area over which it can be realistically deployed, due to tidal and weather impacts over longer time periods. Furthermore, even with careful and considered surveying which ensured significant overlap of scans and multiple scan angles of the entire site there were missing data (shadowing) from the sediment surface. Shadowing is mostly driven due to the complexity of vegetation and the increasingly oblique scans angles away from the scanning unit, typically resulting in a reduced laser returns from the sediment. This limited data makes the extraction of DTMs (digital terrain model) difficult, due to the 'holes' in the surface making it necessary to interpolate from surrounding data, thus reducing the accuracy of the DTM.

Much of these issues may be addressed with the development of drone mounted laser scanning technology, which allows for the collection of similarly high-resolution data in a short time-frame, over a larger area and from increasingly acute angles. Such technology will allow rapid collection of site wide vegetation structure data which can inform on the carbon store and cycle therein.

### *5.5.3 Restoration success rate*

#### *5.5.3.1 Establishment success and persistence*

During the study it was noted that there are possible issues around the degrees of success which were achieved from restoration activities; as revealed by the limited establishment of vegetation in the young restored area. These areas appeared to display reduced vegetation cover at the conclusion of the research, with minimal to no live vegetation present. Such uncertainty reduces the value of restoration initiatives as it increases the risks of achieving predicted additional carbon storage in a given area. The major risk being that success could lead to long-lived large increases in carbon storage, however failure, does not have any associated benefit beyond the 'business as usual' functionality, thus negated all predicted added value.

As understanding of drivers behind restoration success increases it may be possible to combine it with other data to guide their future placement and so maximise ecosystem service output and increased natural capital value. Information gathered through highly accurate TLS (or equivalent drone mounted systems) could, for example, guide placement based upon current sediment elevation.

#### *5.5.3.2 Expansion*

The vegetative expansion from successfully established restoration areas suggest that this rate is not uniform. Currently the area of old restoration on the south shore is over three times larger than that on the north shore, despite being three years younger. Although rapid expansion is beneficial to carbon sequestration and storage, being able to predict this rate is necessary for forecasting the possible value of a restoration activity.

The continued development of understanding and adaptation of restoration approaches will help resolve these two issues around restoration success, for example improving their placement and design through increased understanding of drivers behind success or lack of. Additional information and data better our capacity to project the state of restoration initiatives, thus improving our capacity to predict the its value and facilitate access to their full subsidisation potential.

## 5.6 Broader context and considerations

### *5.6.1 Wider applicability*

This study has highlighted the degree to which these dynamic saltmarsh environments exhibit large variation in carbon sequestration and storage, even across the relatively limited spatial scale of a small pocket estuary on the east coast of Scotland. Precise carbon dynamics of an area are crucial to best understand the likely 'benefit' which may be offered by saltmarshes, or their restoration. Furthermore, the risks around restoration success play a key role in determining the 'value' which they generate. It would therefore be difficult to apply the findings from the study of the Eden Estuary to similar activity on other estuaries. However, it has served to highlight the effectiveness of saltmarsh restoration, through transplantation onto existing intertidal areas, to deliver a degree of beneficial climate change mitigation ecosystem services when successful. Thus, it serves as an additional positive factor in the discussion around the restoration of these threatened ecosystems.

An improved awareness of benefits attributed to saltmarsh areas results in a greater perceived loss at their degradation and an increased desire for their restoration or conservation.

### *5.6.2 External additional benefits*

The current study sought to investigate the carbon benefits afforded by restoration activities and compare them with those of natural areas. Some of the process by which restoration enhances carbon sequestration and storage, such as encouraging sediment deposition by decreasing water flow, are likely to influence the environment out with the vegetation directly. Such external influence could serve to increase the realised benefit of restoration beyond its bounds. It was noted, for example, there appeared to be a shallowing of the *P. maritima* vegetation 'cliff edge' behind restoration on the south shore. This could be driven by the creation of a benign environment between the planted *B. maritimus* and the natural mid-marsh vegetation, encouraging deposition and reducing erosion. Such benefits may be of high value as they reduce the risks of emission through saltmarsh disturbance and likely increase carbon storage through the increased spread of other vegetation.

### *5.6.3 Whole ecosystem value*

It has been illustrated that the saltmarsh restoration leads to an enhanced carbon sequestration and storage capacity. This value should be appreciated as contributing to the total economic value of the restored saltmarsh area. The consideration of all additional

benefits arising from saltmarsh restoration, provides an understanding of their true value, thus increasing the economic feasibility of restoration. Of relevance on the Eden Estuary is perhaps the possible coastal protection benefit afforded by saltmarshes, particularly of the invaluable land of the Links Trust Old Course, the world famous 'home of golf'. This value could be defined through possible avoided or reduced cost of hard sea defences incurred by the Link Trust. However, a 'total ecosystem value' maybe difficult to access through typical market approaches, therefore, opportunities could be sort through local scale payment vehicles such as incorporation into local authority budgets and council tax payments.

### *5.6.4 Sources and fate of carbon*

Saltmarshes are generally thought of as being net carbon sinks, predominantly through the continual accretion of organic matter into their sediments. The composition of carbon found buried within saltmarsh sediments is largely governed by prevailing environmental condition at the time of their burial; be that dominated by autochthonous or allochthonous inputs. This balance may shift with altered environmental condition, such as terrestrial farming practices or changing sea levels. However, this balance may play a key part in the resultant long-term carbon store of a saltmarsh, or determine if they are a new source of carbon to the atmosphere (Borges, 2005). Allochthonous material being longer-lived and autochthonous material decomposing over decadal timescales (Van de Broek et al., 2018), and the majority of emissions resulting from the breakdown of marsh biomass (Cai, 2011). This being the case it is necessary to understand the broader site and setting, at a catchment scale, to appreciate possible drivers of change to carbon inputs available to be deposited and stored within a saltmarsh.

The question of carbon emission rate and its relation to sequestration within saltmarshes is important (Ullman et al., 2013), further, when this is coupled with understanding the balance of carbon input sources, direct us towards another question. That is, what would occur if the saltmarsh area were to become degraded, drowned, or eroded? It is suggested that the degradation of saltmarsh areas lead to between 25 % and 100 % of carbon stored with sediments to be returned (oxidised) into the atmosphere, depending upon disturbance type (Pendleton et al., 2012). Such approaches lead to estimated carbon emissions of between 0.02 and 0.24 Pg $CO_2$ $yr^{-1}$ (1 Pg = 1 billion tonnes) (Pendleton et al., 2012). However, it is perhaps not a straight forward release of a certain percentage of carbon back to the atmosphere depending upon disturbance type, there is the possibility for the relocation of carbon to another sink; such as being exported to oceanic carbon sinks.

If saltmarsh wasn't there it is likely terrestrial inputs would pass through the estuarine zone relatively un-processed due to typically short transit times (Cai, 2011). Once incorporated into the oceanic carbon cycle, the fate of carbon may be more or less secure depending upon the environmental factors of a given area. However, there are extremely large sedimentary carbon sinks found in near shelf areas; for example, in the Scottish fjordic system there is an estimated 295.6 ± 52 Mt OC currently stored which accumulate 0.017 – 0.022 Mt OC $yr^{-1}$ (Smeaton et al., 2017); greater than the 0.014 Mt C $yr^{-1}$ that estimated to be sequestered in Scottish saltmarshes (Burrows et al., 2014). If such trends were confirmed it may bring into question the 'effectiveness' of certain intertidal areas as carbon sinks, particularly those smaller saltmarsh extents found fringing estuaries where intercepted terrestrial carbon is likely to have continued its journey into the oceanic carbon cycle (and sink). Such issues will require consideration in a policy and economic setting to ensure correct accounting is taking place, to avoid double-counting carbon storage or over-estimating carbon emissions from degradation.

## 5.7 Conclusion

The process of saltmarsh restoration through transplantation in the Eden Estuary on the east coast of Scotland is shown to result in the increased carbon sequestration and burial capacity if successfully established. At present the value of this additional ecosystem service is relatively small, primarily a result of their limited spatial extent.

However, the degree to which this benefit is realised per unit area of restoration is perhaps difficult to estimate. There was shown to be large variation in carbon sequestration and storage within and between areas, and the factors influencing this unclear. Furthermore, and perhaps of greatest issue, centres around the success rates of restoration; where project 'failure' would result in no returned additional benefits. This varying degree of success perhaps also reduces confidence in the permanence of those existing areas and could impact on their future value.

If the natural capital value of saltmarsh restoration is to be leveraged, the potential unknowns will require further scrutiny, especially under the predicted changes resulting from climate change which are likely to directly influence these areas. This will enable the effective delivery of climate change mitigating ecosystem services and their accurate valuation; hopefully facilitating funding of conservation initiatives and so the maintenance of these vulnerable ecosystems in the future.

# References

Adam, P., 2002. Saltmarshes in a time of change. Environ. Conserv. 29, 39–61.

Allen, J.R.L., Pye, K., 1992. Coastal saltmarshes: their nature and importance. In: Allen, J.R.L., Pye, K. (Eds.), Saltmarshes: Morphodynamics, Conservation and Engineering Significance. Cambridge University Press, pp. 1–18.

Andersen, H.-E., Reutebuch, S.E., McGaughey, R.J., 2006. A rigorous assessment of tree height measurements obtained using airborne lidar and conventional field methods. Can. J. Remote Sens. 32, 355–366.

Andrews, J.E., Burgess, D., Cave, R.R., Coombes, E.G., Jickells, T.D., Parkes, D.J., Turner, R.K., 2006. Biogeochemical value of managed realignment, Humber estuary, UK. Sci. Total Environ. 371, 19–30.

Approved VCS Methodology: Methodology for Coastal Wetland Creation, 2014.

Avnimelech, Y., Ritvo, G., Meijer, L.E., Kochba, M., 2001. Water content, organic carbon and dry bulk density in flooded sediments. Aquac. Eng. 25, 25–33.

Bai, J., Zhang, G., Zhao, Q., Lu, Q., Jia, J., Cui, B., Liu, X., 2016. Depth-distribution patterns and control of soil organic carbon in coastal salt marshes with different plant covers. Sci. Rep. 6, 34835.

Baptist, M.J., 2005. Biogeomorphology. In: Schwartz, M.L. (Ed.), Encyclopedia of Coastal Science. Springer Netherlands, Dordrecht, pp. 192–194.

Baptist, M.J., de Groot, A. V., van Duin, W.E., 2016. Contrasting biogeomorphic processes affecting salt-marsh development of the Mokbaai, Texel, The Netherlands. Earth Surf. Process. Landforms 41, 1241–1249.

Barbier, E.B., Hacker, S.D., Kennedy, C., Koch, E.W., Stier, A.C., 2013. Wyoming Scholars Repository The Value of Estuarine and Coastal Ecosystem Services Publication Information. PLoS One 8, 169–193.

Bartlett, K.B., Bartlett, D.S., Harriss, R.C., Sebacher, D.I., 1987. Methane Emissions along a Salt Marsh Salinity Gradient. Biogeochemistry.

Bauwens, S., Bartholomeus, H., Calders, K., Lejeune, P., 2016. Forest inventory with

terrestrial LiDAR: A comparison of static and hand-held mobile laser scanning. Forests 7.

Beaumont, N.J., Jones, L., Garbutt, A., Hansom, J.D., Toberman, M., 2014. The value of carbon sequestration and storage in coastal habitats. Estuar. Coast. Shelf Sci. 137, 32–40.

Beckman-Coulter, 2011. Coulter LS Series: Product Manual.

Belliard, J.-P., Temmerman, S., Toffolon, M., 2017. Ecogeomorphic relations between marsh surface elevation and vegetation properties in a temperate multi-species salt marsh. Earth Surf. Process. Landforms 42, 855–865.

Belluco, E., Camuffo, M., Ferrari, S., Modenese, L., Silvestri, S., Marani, A., Marani, M., 2006. Mapping salt-marsh vegetation by multispectral and hyperspectral remote sensing. Remote Sens. Environ. 105, 54–67.

Bienert, A., Maas, H., Scheller, S., 2006. Analysis of the information content of terrestrial laserscanner point clouds for the automatic determination of forest inventory parameters. In: Workshop on 3D Remote Sensing in Forestry. pp. 1–7.

Blott, S.J., Pye, K., 2001. GRADISTAT: a grain size distribution and statistics package for the analysis of unconsolidated sediments. Earth Surf. Process. Landforms 26, 1237–1248.

Boorman, L., 1999. Salt marshes–present functioning and future change. Mangroves Salt Marshes 227–241.

Boorman, L., 2003. Saltmarsh Review. An overview of coastal saltmarshes, their dynamic and sensitivity characteristics for conservation and management.

Boorman, L.A., Garbutt, A., Barratt, D., 1998. The Role of Vegetation in Determining Patterns of the Accretion of Salt Marsh Sediment. Sediment. Process. INtertidal Zo. 139, 389–399.

Borges, A.A. V., 2005. Do we have enough pieces of the jigsaw to integrate CO2 fluxes in the coastal ocean? Estuaries 28, 3–27.

Bos, D., Loonen, M.J.J.E., Stock, M., Hofeditz, F., van der Graaf, A.J., Bakker, J.P., 2005. Utilisation of Wadden Sea salt marshes by geese in relation to livestock

grazing. J. Nat. Conserv. 13, 1–15.

Bouma, T.J., De Vries, M.B., Low, E., Kusters, L., Herman, P.M.J., Tánczos, I.C., Temmerman, S., Hesselink, A., Meire, P., Van Regenmortel, S., 2005. Flow hydrodynamics on a mudflat and in salt marsh vegetation: Identifying general relationships for habitat characterisations. Hydrobiologia 540, 259–274.

Bouma, T.J., van Belzen, J., Balke, T., van Dalen, J., Klaassen, P., Hartog, A.M., Callaghan, D.P., Hu, Z., Stive, M.J.F., Temmerman, S., Herman, P.M.J., 2016. Short-term mudflat dynamics drive long-term cyclic salt marsh dynamics. Limnol. Oceanogr. 61, 2261–2275.

Boumans, R., Day, J.W., 1993. High precision measurements of sediment elevation in shallow coastal areas using a sedimentation-erosion table. Estuaries 16, 375–380.

Brevik, E.C., Homburg, J. a., 2004. A 5000 year record of carbon sequestration from a coastal lagoon and wetland complex, southern California, USA. Catena 57, 221–232.

Brodu, N., Lague, D., 2011. 3D Terrestrial lidar data classiffcation of complex natural scenes using a multi-scale dimensionality criterion: applications in geomorphology. 1–18.

Broome, S.W., Seneca, E.D., Woodhouse, W.W., 1986. Long-Term Growth and Development of Transplants of the Salt-Marsh Grass Spartina alterniflora. Estuaries 9, 63.

Brown, S.L., Warman, E.A., McGrorty, S., Yates, M., Pakeman, R.J., Boorman, L.A., Goss-Custard, J.D., Gray, A.J., 1999. Sediment Fluxes in Intertidal Biotopes: BIOTA II. Mar. Pollut. Bull. 37, 173–181.

Burd, F., 1989. The saltmarsh survey of Great Britain. Nat. Conserv. Counc. Peterbrgh.

Burden, A., Garbutt, R. a., Evans, C.D., Jones, D.L., Cooper, D.M., 2013. Carbon sequestration and biogeochemical cycling in a saltmarsh subject to coastal managed realignment. Estuar. Coast. Shelf Sci. 120, 12–20.

Burrows, M., Kamenos, N., Hughes, D., Stahl, H., Howe, J.., Tett, P., 2014. Assessment of carbon budgets and potential blue carbon stores in Scotland's coastal and marine environment.

Cahoon, D., French, Spencer, T., Reed, D., Moller, I., 2000. Vertical accretion versus elevational adjustment in UK saltmarshes: an evaluation of alternative methodologies 223–238.

Cahoon, D.R., Lynch, J.C., Hensel, P.F., Boumans, R., Perez, B.C., Segura, B., Day, J.W., 2002. High-precision measurements of sediment elevation: I. Recent improvements to the sediment-erosion table. J. Sediment. Res. 72, 730–733.

Cahoon, D.R., Reed, D.J., Day, J.W., 1995. Estimating shallow subsidence in microtidal salt marshes of the southeastern United States: Kaye and Barghoorn revisited. Mar. Geol.

Cai, W.-J., 2011. Estuarine and coastal ocean carbon paradox: CO2 sinks or sites of terrestrial carbon incineration? Ann. Rev. Mar. Sci. 3, 123–45.

Cavagnini, G., Scalvenzi, M., Trebeschi, M., Sansoni, G., 2007. Reverse engineering from 3D optical acquisition: application to Crime Scene Investigation. In: da Silva Bartolo, P.J., Jorge, M.A., da Conceicao Batista, F., Almeida, H.A., Matias, J.M., Vasco, J.C., Gaspar, J.B., Correia, M.A., Andre, N.C., Alves, N.F., Novo, P.P., Martinho, P.G., Carvalho, R.A. (Eds.), Virtual and Rapid Manufacturing: Advanced Research in Virtual and Rapid Prototyping. Taylor and Francis Group: London, pp. 195–201.

Childers, D.., Day, J.W., McKellar, H.N., 2000. Twenty more years of marsh and esturine flux studies: revisting Nixon (1980). In: Weinstein, M.., Kreeger, D.. (Eds.), Concepts and Controversies in Tidal Marsh Ecology. pp. 391–424.

Chmura, G., Anisfeld, S., Cahoon, D.R., Lynch, J., 2003. Global carbon sequestration in tidal, saline wetland soils. Global Biogeochem. Cycles 17.

Chmura, G.L., 2013. What do we need to assess the sustainability of the tidal salt marsh carbon sink? Ocean Coast. Manag. 83, 25–31.

Chotiros, N., 2017. Acoustics of the Seabed as a Poroelastic Medium. In: Acoustics of the Seabed as a Poroelastic Medium.

Christiansen, T., Wiberg, P., Milligan, T., 2000. Flow and sediment transport on a tidal salt marsh surface. Estuarine, Coast. Shelf ….

Christie, M., Remoundou, K., Siwicka, E., Wainwright, W., 2014. Valuing marine and

coastal ecosystem service benefits: Case study of St Vincent and the Grenadines' proposed marine protected areas. Ecosyst. Serv. 11, 1–13.

Costanza, R., Arge, R., Groot, R. De, Farberk, S., Grasso, M., Hannon, B., Limburg, K., Naeem, S., Neill, R.V.O., Paruelo, J., Raskin, R.G., Suttonkk, P., 1997. The value of the world ' s ecosystem services and natural capital. Nature 387, 253–260.

Craft, C., 2007. Freshwater input structures soil properties, vertical accretion, and nutrient accumulation of Georgia and U.S. tidal marshes. Limnol Ocean. 52, 1220–1230.

Craft, C., Clough, J., Ehman, J., Joye, S., Park, R., Pennings, S., Guo, H., Machmuller, M., 2009. Forecasting the effects of accelerated sea-level rise on tidal marsh ecosystem services. Front. Ecol. Environ. 7, 73–78.

Craft, C., Megonigal, P., Broome, S., Stevenson, J., Freese, R., Cornell, J., Zheng, L., Sacco, J., 2003. The pace of ecosystem development of constructed Spartina alterniflora marshes. Ecol. Appl. 13, 1417–1432.

Craft, C., Seneca, E., Broome, S., 1991. Loss on ignition and Kjeldahl digestion for estimating organic carbon and total nitrogen in estuarine marsh soils: calibration with dry combustion. Estuaries 14, 175–179.

Crooks, S., Rybczyk, J., O'Connell, K., Devier, D.L., Poppe, K., Emmett-Mattox, S., 2014. Coastal Blue Carbon Opportunity Assessment for the Snohomish Estuary - The Climate Benefits of Estuary Restoration.

Crosby, S.C., Sax, D.F., Palmer, M.E., Booth, H.S., Deegan, L.A., Bertness, M.D., Leslie, H.M., 2016. Salt marsh persistence is threatened by predicted sea-level rise. Estuar. Coast. Shelf Sci. 181, 93–99.

Dale, J., Burgess, H.M., Cundy, A.B., 2017. Sedimentation rhythms and hydrodynamics in two engineered environments in an open coast managed realignment site. Mar. Geol. 383, 120–131.

Dame, R.F., Spurrier, J.D., Williams, T.M., Kjerfve, B., Zingmark, R.G., Wolaver, T.G., Chrzanowski, T.H., McKellar, H.N., Vernberg, F.J., 1991. Annual material processing by a salt marsh-estuarine basin in South Carolina, USA. Mar. Ecol. Prog. Ser. 72, 153–166.

Dassot, M., Constant, T., Fournier, M., 2011. The use of terrestrial LiDAR technology in forest science: Application fields, benefits and challenges. Ann. For. Sci. 68, 959–974.

David, J., 2012. The application of allometric relationships and the importance of primary production when assessing the value of a salt marsh. University of St Andrews.

Davidson, K.E., Fowler, M.S., Skov, M.W., Doerr, S.H., Beaumont, N., Griffin, J.N., 2017. Livestock grazing alters multiple ecosystem properties and services in salt marshes: a meta-analysis. J. Appl. Ecol. 54, 1395–1405.

Davidson, N.C., 2014. How much wetland has the world lost? Long-term and recent trends in global wetland area. Mar. Freshw. Res. 65, 934.

Davy, A.J., 2000. Development and structure of Saltmarshes: Community patterns in time and space. In: Weinstein, M.., Kreeger, D.. (Eds.), Concepts and Controversies in Tidal Marsh Ecology. pp. 137–156.

Doody, J., 2004. 'Coastal squeeze'—an historical perspective. J. Coast. Conserv.

Duarte, C., Middelburg, J., Caraco, N., 2005. Major role of marine vegetation on the oceanic carbon cycle. Biogeosciences.

Duarte, C.M., Dennison, W.C., Orth, R.J.W., Carruthers, T.J.B., 2008. The charisma of coastal ecosystems: Addressing the imbalance. Estuaries and Coasts 31, 233–238.

Duarte, C.M., Losada, I.J., Hendriks, I.E., Mazarrasa, I., Marbà, N., 2013. The role of coastal plant communities for climate change mitigation and adaptation. Nat. Publ. Gr. 3, 961–968.

Engels, J.G., Jensen, K., 2010. Role of biotic interactions and physical factors in determining the distribution of marsh species along an estuarine salinity gradient. Oikos 119, 679–685.

Fang, J.Y., Liu, G.H., Xu, S.L., 1996. Carbon Pools in Terrestrial Ecosystems in China. In: Wang, R.S., Fang, J.Y., Gao, L., Feng, Z.W. (Eds.), Hot Spots in Modern Ecology. China Science and Technology Press, Beijing, pp. 251–277.

Flemming, B.., 2000. A revised textural classification of gravel-free muddy sediments

on the basis of ternary diagrams. Cont. Shelf Res. 20, 1125–1137.

Folk, R.L., 1954. The Distinction between Grain Size and Mineral Composition in Sedimentary-Rock Nomenclature. J. Geol. 62, 344–359.

Garbutt, A., Wolters, M., 2008. The natural regeneration of salt marsh on formerly reclaimed land. Appl. Veg. Sci. 11, 335–344.

Gray, A.., 1992. Saltmarsh plant ecology: zonation and succession revisited. In: Allen, J.R.L., Pye, K. (Eds.), Saltmarshes: Morphodynamics, Conservation and Engineering Significance. Cambridge University Press, pp. 63–79.

Gray, A.J., Scott, R., 1977. Puccinellia maritima (Huds.) Parl.: (Poa Maritima Huds.; Glyceria Maritima (Huds.) Wahlb.). J. Ecol. 65, 699.

Grimsditch, G., Alder, J., Nakamura, T., Kenchington, R., Tamelander, J., 2013. The blue carbon special edition - Introduction and overview. Ocean Coast. Manag. 83, 1–4.

Hanley, N., Shogren, J., White, B., 2013. Introduction to environmental economics.

Hardisky, M.A., Daiber, F.C., Roman, C.T., Klemas, V., 1984. Remote sensing of biomass and annual net aerial primary productivity of a salt marsh. Remote Sens. Environ. 16, 91–106.

Haynes, T.A., 2016. Scottish saltmarsh survey national report, Scottish Natural Heritage Commissioned Report No. 786.

Herr, D., Pidgeon, E., Laffoley, D., 2012. Blue Carbon Policy Framework: Based on the discussion of the International Blue Carbon Policy Working Group. Gland.

Hijmans, R.J., Etten, J. van, 2012. raster: Geographic Data Analysis and Modeling with raster data. R package raster version 2.5-8.

Hirst, D., Keep, M., 2018. Carbon Price Floor (CPF) and the price support mechanism.

HM Government, 2018. A Green Future: Our 25 Year Plan to Improve the Environment.

Hollenbeck, J.P., Olsen, M.J., Haig, S.M., 2014. Using terrestrial laser scanning to support ecological research in the rocky intertidal zone. J. Coast. Conserv. 18, 701–714.

Howard, J., Hoyt, S., Isensee, K., Pidgeon, E., Telszewski, M. (Eds.), 2014. Coastal Blue Carbon - methods for assessing carbon stocks and emmission factors in mangroves, tidal salt marshes, and seagrass meadows. Conservation International, Intergovernmental Oceanographic Commission of UNESCO, International Union for Conservation of Nature, Arlington.

Howard, J., Sutton-Grier, A., Herr, D., Kleypas, J., Landis, E., Mcleod, E., Pidgeon, E., Simpson, S., 2017. Clarifying the role of coastal and marine systems in climate mitigation. Front. Ecol. Environ. 15, 42–50.

Hu, Z., van Belzen, J., van der Wal, D., Balke, T., Wang, Z.B., Stive, M., Bouma, T.J., 2015. Windows of Opportunity for saltmarsh vegetation establishment on bare tidal flats: the importance of temporal and spatial variability in hydrodynamic forcing. J. Geophys. Res. Biogeosciences n/a-n/a.

I. Möller, B.A., Spencer, T., French, J.R., Leggett, D.J., Dixon, M., 2001. The sea-defence value of salt marshes: Field evidence from north norfolk. Water Environ. J. 15, 109–116.

IFLI, 2018. Inner Forth Landscape Initiative End of Project Report A3.8 Skinflats Managed Realignment.

J. S. Pethick, J.S., 1981. Long-term Accretion Rates on Tidal Salt Marshes. SEPM J. Sediment. Res. Vol. 51, 571–577.

Janousek, C., Buffington, K., Thorne, K., Guntenspergen, G., Takekawa, J., Dugger, B., 2016. Potential effects of sea-level rise on plant productivity: species-specific responses in northeast Pacific tidal marshes. Mar. Ecol. Prog. Ser. 548, 111–125.

Jones, L., Angus, S., Cooper, A., Doody, P., Everard, M., Garbutt, A., Gilchrist, P., Hansom, J., Nicholls, R., Pye, K., Ravenscroft, N., Rees, S., Rhind, P., Whitehouse, A., 2011. Coastal Margins. In: The UK National Ecosystem Assessment Technical Report. UNEP-WCMC, Cambridge, pp. 411–458.

Jones, L., Garbutt, A., Hansom, J., Angus, S., 2013. Impacts of climate change on coastal habitats. Mar. Clim. Chang. IMPACTS Partnersh. Sci. Rev. 2013.

Kelleway, J.J., Saintilan, N., Macreadie, P.I., Ralph, P.J., 2016. Sedimentary Factors are Key Predictors of Carbon Storage in SE Australian Saltmarshes. Ecosystems 19,

865–880.

Kimble, J.M., Follett, R.F., Stewart, B.A., Follett, R.F., Stewart, B.A., 2000. Assessment Methods for Soil Carbon. CRC Press.

King, S.E., Lester, J.N., 1995. The value of salt marsh as a sea defence. Mar. Pollut. Bull. 30, 180–189.

Kirwan, M., Blum, L., 2011. Enhanced decomposition offsets enhanced productivity and soil carbon accumulation in coastal wetlands responding to climate change. Biogeosciences 8, 987–993.

Kirwan, M.L., Guntenspergen, G.R., D'Alpaos, A., Morris, J.T., Mudd, S.M., Temmerman, S., 2010. Limits on the adaptability of coastal marshes to rising sea level. Geophys. Res. Lett. 37.

Kirwan, M.L., Mudd, S.M., 2012. Response of salt-marsh carbon accumulation to climate change. Nature 489, 550–3.

Kirwan, M.L., Temmerman, S., Skeehan, E.E., Guntenspergen, G.R., Faghe, S., 2016. Overestimation of marsh vulnerability to sea level rise. Nat. Clim. Chang. 6, 253–260.

Koch, Wilhelm Daniel Joseph, Koch, Wilhelm Daniel Joseph, 1846. Synopsis der deutschen und schweizer Flora, enthaltend die genauer bekannten phanerogamischen Gewächse, so wie die cryptogamischen Gefäss-Pflanzen, welche in Deutschland, der Schweiz, in Preussen und Istrien wild wachsen und derjenigen ... na, 2. Aufl. ed. Gebhardt & Reisland, Leipzig,.

Lewis, P., 2013. Case study 6 Medmerry managed realignment-West Sussex.

Liang, X., Kankare, V., Hyyppä, J., Wang, Y., Kukko, A., Haggrén, H., Yu, X., Kaartinen, H., Jaakkola, A., Guan, F., Holopainen, M., Vastaranta, M., 2016. Terrestrial laser scanning in forest inventories. ISPRS J. Photogramm. Remote Sens. 115, 63–77.

Lillebø, A.I., Pardal, M.A., Neto, J.M., Marques, J.C., 2003. Salinity as the major factor affecting Scirpus maritimus annual dynamics: Evidence from field data and greenhouse experiment. Aquat. Bot. 77, 111–120.

Loudermilk, E.L., Hiers, J.K., O'Brien, J.J., Mitchell, R.J., Singhania, A., Fernandez, J.C., Cropper, W.P., Slatton, K.C., 2009. Ground-based LIDAR: A novel approach to quantify fine-scale fuelbed characteristics. Int. J. Wildl. Fire 18, 676–685.

Macreadie, P.I., Hughes, a. R., Kimbro, D.L., 2013. Loss of "Blue Carbon" from Coastal Salt Marshes Following Habitat Disturbance. PLoS One 8, 1–8.

Macreadie, P.I., Ollivier, Q.R., Kelleway, J.J., Serrano, O., Carnell, P.E., Ewers Lewis, C.J., Atwood, T.B., Sanderman, J., Baldock, J., Connolly, R.M., Duarte, C.M., Lavery, P.S., Steven, A., Lovelock, C.E., 2017. Carbon sequestration by Australian tidal marshes. Sci. Rep. 7, 44071.

Marhold, K., Ducháček, M., Hroudová, Z., 2006. Typification of Three Names in the Bolboschoenus maritimus Group (Cyperaceae) 103–113.

Maris, T., Cox, T., Temmerman, S., De Vleeschauwer, P., Van Damme, S., De Mulder, T., Van den Bergh, E., Meire, P., 2007. Tuning the tide: creating ecological conditions for tidal marsh development in a flood control area. Hydrobiologia 588, 31–43.

Masselink, G., Hanley, M.E., Halwyn, A.C., Blake, W., Kingston, K., Newton, T., Williams, M., 2017. Evaluation of salt marsh restoration by means of self-regulating tidal gate – Avon estuary, South Devon, UK. Ecol. Eng. 106, 174–190.

May, N.C., Toth, C.K., 2007. Point Positioning Accuracy of Airborne LIDAR Systems: A Rigorous Analysis. In: Stilla, U., Mayer, H., Rottensteiner, F., Heipke, C., Hinz, S. (Eds.), Photogrammetric Image Analysis 2007 (PIA07), International Archives of Photogrammetry, Remote Sensing and Spatial Information Sciences, 36, (3/W49B). pp. 107–111.

Maynard, C., 2014. Restoring the degraded shoreline. University of St Andrews.

Maynard, C., McManus, J.. J., Crawford, R.M.M.. R.M.M., Paterson, D.D.., 2011. A comparison of short-term sediment deposition between natural and transplanted saltmarsh after saltmarsh restoration in the Eden Estuary (Scotland). Plant Ecol. Divers. 4, 103–113.

McLeod, E., Chmura, G., Bouillon, S., 2011. A blueprint for blue carbon: toward an improved understanding of the role of vegetated coastal habitats in sequestering

CO2. Front. Ecol.

Mcowen, C., Weatherdon, L., Bochove, J.-W., Sullivan, E., Blyth, S., Zockler, C., Stanwell-Smith, D., Kingston, N., Martin, C., Spalding, M., Fletcher, S., 2017. A global map of saltmarshes. Biodivers. Data J. 5, e11764.

Morgan, P.A., Burdick, D.M., Short, F.T., 2009. The Functions and Values of Fringing Salt Marshes in Northern New England, USA. Estuaries and Coasts 32, 483–495.

Morton, R.A., White, W.A., Summer, F., 1997. of Coastal Characteristics of and Corrections for Core Shortening in Unconsolidated Sediments. J. Coast. Res. 13, 761–769.

Moskalski, S.M., Sommerfield, C.K., 2012. Suspended sediment deposition and trapping efficiency in a Delaware salt marsh. Geomorphology 139–140, 195–204.

Mudd, S.M., D'Alpaos, A., Morris, J.T., 2010. How does vegetation affect sedimentation on tidal marshes? Investigating particle capture and hydrodynamic controls on biologically mediated sedimentation. J. Geophys. Res. Earth Surf. 115.

Mudd, S.S.M., Howell, S.S.M., Morris, J.J.T., 2009. Impact of dynamic feedbacks between sedimentation, sea-level rise, and biomass production on near-surface marsh stratigraphy and carbon accumulation. Estuar. Coast. Shelf Sci. 82, 377–389.

Mukupa, W., Roberts, G.W., Hancock, C.M., Mukupa, W., Roberts, G.W., Hancock, C.M., 2016. A review of the use of terrestrial laser scanning application for change detection and deformation monitoring of structures A review of the use of terrestrial laser scanning application for change detection and deformation monitoring of structures. Surv. Rev. 0, 1–18.

Murray, B., Vegh, T., 2012. Incorporating Blue Carbon as a Mitigation Action under the United Nations Framework Convention on Climate Change: Technical Issues to Address. Duke University - Nicholas Institute for Environmental Policy Soluitons, Durham, NC.

Murray, B.C., Jenkins, W.A., Sifleet, S., Pendleton, L., Baldera, A., 2010. Policy brief - Payments for Blue Carbon; Potential for Protecting Threatened Coastal Habitats. Durham, NC.

Nolte, S., Koppenaal, E.C., Esselink, P., Dijkema, K.S., Schuerch, M., De Groot, A. V., Bakker, J.P., Temmerman, S., 2013a. Measuring sedimentation in tidal marshes: A review on methods and their applicability in biogeomorphological studies. J. Coast. Conserv. 17, 301–325.

Nolte, S., Koppenaal, E.C., Esselink, P., Dijkema, K.S., Schuerch, M., De Groot, A. V., Bakker, J.P., Temmerman, S., 2013b. Measuring sedimentation in tidal marshes: a review on methods and their applicability in biogeomorphological studies. J. Coast. Conserv. 17, 301–325.

Owers, C.J., Rogers, K., Woodroffe, C.D., 2018. Terrestrial laser scanning to quantify above-ground biomass of structurally complex coastal wetland vegetation. Estuar. Coast. Shelf Sci. 204, 164–176.

Pendleton, L., Donato, D., Murray, B., Crooks, S., Jenkins, W.A., Sifleet, S., Craft, C., Fourqurean, J., Kauffman, J.B., Marba, N., Megonigal, P., Pidgeon, E., Herr, D., Gordon, D., Baldera, A., 2012. Estimating global "blue carbon" emissions from conversion and degradation of vegetated coastal ecosystems. PLoS One 7.

Peters-Stanley, M., Hamilton, K., Marcello, T., Sjardin, M., 2011. Back to the Future: State of Voluntary Carbon Markets 2011. Washington DC.

Pethick, J.S., 1992. Saltmarsh geomorphology. In: Allen, J.R.., Pye, K. (Eds.), Saltmarshes: Morphodynamics, Conservation and Engineering Significance1. Cambridge University Press, pp. 41–62.

Pigott, C., Ratcliffe, D., Malloch, A., Birks, H., 2000. British Plant Communities: Volume 5, Maritime Communities and Vegetation of Open Habitats. Cambridge University Press.

Radabaugh, K.R., Powell, C.E., Bociu, I., Clark, B.C., Moyer, R.P., 2017. Plant size metrics and organic carbon content of Florida salt marsh vegetation. Wetl. Ecol. Manag. 25, 443–455.

Ranwell, D.S., 1972. Ecology of Salt Marshes and Sand Dunes, Ecology of Salt Marshes and Sand Dunes. Chapman and Hall.

Reed, D.J., 1989. Patterns of sediment deposition in subsiding coastal salt marshes, Terrebonne Bay, Louisiana: The role of winter storms. Estuaries 12, 222–227.

Reed, D.J., Spencer, T., Murray, A.L., French, J.R., Journal, S., 1999. Marsh surface sediment deposition and the role of tidal creeks: Implications for created and managed coastal marshes. J. Coast. Conserv. 5, 81–90.

Reid, W. V., Mooney, H.A., Cropper, A., Capistrano, D., Carpenter, S.R., Chopra, K., Dasgupta, P., Dietz, T., Duraiappah, A.K., Hassan, R., Kasperson, R., Leemans, R., Robert M. May, T. (A. J.. M., Pingali, P., Samper, C., Scholes, R., Watson, R.T., Zakri, A.H., Shidong, Z., Ash, N.J., Bennett, E., Kumar, P., Lee, M.J., Raudsepp-Hearne, C., Simons, H., Thonell, J., Zurek, M.B., 2005. Ecosystems and Human Well-being: Synthesis. In: Sarukhán, J., Whyte, A. (Eds.), Millennium Ecosystem Assessment. Island Press, Washington DC.

Rodwell, J.S., 1995. British Plant Communities, Volume 4. Aquatic Communities, Swamps and Tall-fen Herbs. Cambridge University Press.

Rogers, K., Macreadie, P., Kelleway, J., Saintilan, N., 2018. Blue carbon in coastal landscapes : a spatial framework for assessment of stocks and additionality. Sustain. Sci. 0, 0.

Saintilan, N., Rogers, K., Mazumder, D., Woodroffe, C., 2013. Allochthonous and autochthonous contributions to carbon accumulation and carbon store in southeastern Australian coastal wetlands. Estuar. Coast. Shelf Sci. 128, 84–92.

Saintilan, N., Wilson, N.C., Rogers, K., Rajkaran, A., Krauss, K.W., 2014. Mangrove expansion and salt marsh decline at mangrove poleward limits. Glob. Chang. Biol. 20, 147–157.

Schrift, A.M., Mendelssohn, I.A., Materne, M.D., 2008. Salt marsh restoration with sediment-slurry amendments following a drought-induced large-scale disturbance. Wetlands 28, 1071–1085.

Shepard, C.C., Crain, C.M., Beck, M.W., 2011. The protective role of coastal marshes: A systematic review and meta-analysis. PLoS One 6.

Silvestri, S., Defina, A., Marani, M., 2005. Tidal regime, salinity and salt marsh plant zonation. Estuar. Coast. Shelf Sci. 62, 119–130.

Skilbeck, C.G., Trevathan-Tackett, S., Apichanangkool, P., Macreadie, P.I., 2017. Sediment Sampling in Estuaries: Site Selection and Sampling Techniques. pp. 89–

120.

Smeaton, C., Austin, W.E.N., Davies, A.L., Baltzer, A., Howe, J.A., Baxter, J.M., 2017. Scotland's forgotten carbon: a national assessment of mid-latitude fjord sedimentary carbon stocks. Biogeosciences 14, 5663–5674.

SNH, 2011. Eden Estuary Site of Special Scientific Interest: Site Management Statement. Cupar.

Sousa, A.I., Santos, D.B., da Silva, E.F., Sousa, L.P., Cleary, D.F.R., Soares, A.M.V.M., Lillebø, A.I., 2017. 'Blue Carbon' and Nutrient Stocks of Salt Marshes at a Temperate Coastal Lagoon (Ria de Aveiro, Portugal). Sci. Rep. 7, 41225.

Stevenson, J.Court, Ward, L.G., Kearney, M.S., 1988. Sediment transport and trapping in marsh systems: Implications of tidal flux studies. Mar. Geol. 80, 37–59.

Stevenson, J. Court, Ward, L.G., Kearney, M.S., 1988. Sediment transport and trapping in marsh systems: Implications of tidal flux studies. Mar. Geol. 80, 37–59.

Sullivan, G., 2001. Establishing vegetation in restored and created coastal wetlands. In: Zedler, B. (Ed.), Handbook for Restoring Tidal Wetlands. CRC Press, pp. 119–156.

Teasdale, P.A., Collins, P.E.F., Firth, C.R., Cundy, A.B., 2011. Recent estuarine sedimentation rates from shallow inter-tidal environments in western Scotland: implications for future sea-level trends and coastal wetland development. Quat. Sci. Rev. 30, 109–129.

Temmerman, S., Govers, G., Wartel, S., Meire, P., 2003. Spatial and temporal factors controlling short-term sedimentation in a salt and freshwater tidal marsh, scheldt estuary, Belgium, SW Netherlands. Earth Surf. Process. Landforms 28, 739–755.

Thies, M., Spiecker, H., 2004. Evaluation and future prospects of terrestrial laser scanning for standardized forest inventories. In: International Archives of Photogrammetry, Remote Sensing and Spatial Information Sciences. pp. 192–197.

Thorne, K.M., Elliott-Fisk, D.L., Wylie, G.D., Perry, W.M., Takekawa, J.Y., 2014. Importance of Biogeomorphic and Spatial Properties in Assessing a Tidal Salt Marsh Vulnerability to Sea-level Rise. Estuaries and Coasts 37, 941–951.

Todd, C.D., Phelan, P.J.C., Weinmann, B.E., Gude, A.R., Andrews, C., Paterson, D.M., Lonergan, M.E., Miron, G., 2006. Improvements to a passive trap for quantifying barnacle larval supply to semi-exposed rocky shores. J. Exp. Mar. Bio. Ecol. 332, 135–150.

Trilla, G.G., Borro, M.M., Morandeira, N.S., Schivo, F., Kandus, P., Marcovecchio, J., 2013. Allometric Scaling of Dry Weight and Leaf Area for *Spartina densiflora* and *Spartina alterniflora* in Two Southwest Atlantic Saltmarshes. J. Coast. Res. 292, 1373–1381.

Tyler-Walters, H., 2004. Puccinellia maritima salt-marsh community. In: Tyler-Walters, H., Hiscock, K. (Eds.), Marine Life Information Network: Biology and Sensitivity Key Information Reviews, [on-Line]. Plymouth: Marine Biological Association of the United Kingdom.

Ullman, R., Bilbao-Bastida, V., Grimsditch, G., 2013. Including Blue Carbon in climate market mechanisms. Ocean Coast. Manag. 83, 15–18.

Van de Broek, M., Vandendriessche, C., Poppelmonde, D., Merckx, R., Temmerman, S., Govers, G., 2018. Long-term organic carbon sequestration in tidal marsh sediments is dominated by old-aged allochthonous inputs in a macrotidal estuary. Glob. Chang. Biol. 2498–2512.

van Proosdij, D., Davidson-Arnott, R.G.D., Ollerhead, J., 2006. Controls on spatial patterns of sediment deposition across a macro-tidal salt marsh surface over single tidal cycles. Estuar. Coast. Shelf Sci. 69, 64–86.

Van Proosdij, D., Davidson-Arnott, R.G.D., Ollerhead, J., 2006. Controls on spatial patterns of sediment deposition across a macro-tidal salt marsh surface over single tidal cycles.

van Wijnen, H.J., Bakker, J.P., 2001. Long-term Surface Elevation Change in Salt Marshes: a Prediction of Marsh Response to Future Sea-Level Rise. Estuar. Coast. Shelf Sci. 52, 381–390.

Wentworth, C.K., 1922. A Scale of Grade and Class Terms for Clastic Sediments. J. Geol. 30, 377–392.

Weston, N.B., Dixon, R.E., Joye, S.B., 2006. Ramifications of increased salinity in tidal

freshwater sediments: Geochemistry and microbial pathways of organic matter mineralization. J. Geophys. Res. 111, G01009.

Wickham, H., 2016. ggplot2: Elegant Graphics for Data Analysis.

Wickham, H., Francois, R., Henry, L., Muller, K., 2017. dplyr: A Grammar of Data Manipulation.

Woolnough, S.., Allen, J.R.., Wood, W.., 1995. An exploratory numerical model of sediment deposition over tidal salt marshes. Estuar. Coast. Shelf Sci. 41, 515–543.

Young, M.A., Macreadie, P.I., Duncan, C., Carnell, P.E., Nicholson, E., Serrano, O., Duarte, C.M., Shiell, G., Baldock, J., Ierodiaconou, D., 2018. Optimal soil carbon sampling designs to achieve cost-effectiveness: a case study in blue carbon ecosystems. Biol. Lett. 14, 20180416.

Zeff, M.L., 1999. Salt marsh tidal channel morphometry: Applications for wetland creation and restoration. Restor. Ecol. 7, 205–211.

Zhang, W., Qi, J., Wan, P., Wang, H., Xie, D., Wang, X., Yan, G., 2016. An easy-to-use airborne LiDAR data filtering method based on cloth simulation. Remote Sens. 8, 501.

Zhu, Z., Bouma, T.J., Ysebaert, T., Zhang, L., Herman, P.M.J., 2014. Seed arrival and persistence at the tidal mudflat: identifying key processes for pioneer seedling establishment in salt marshes. Mar. Ecol. Prog. Ser. 513, 97–109.